Hepatitis C Virus Induced Changes to the Host Cell Phosphoproteome

by

Julie Boutilier

A Thesis submitted to the Faculty of Graduate Studies of

The University of Manitoba

in partial fulfilment of the requirements of the degree of

DOCTORATE OF PHILOSOPHY

Department of Medical Microbiology

University of Manitoba

Winnipeg

THE UNIVERSITY OF MANITOBA

FACULTY OF GRADUATE STUDIES

*****

COPYRIGHT PERMISSION

Hepatitis C Virus Induced Changes to the Host Cell Phosphoproteome

BY

Julie Boutilier

A Thesis/Practicum submitted to the Faculty of Graduate Studies of The University of Manitoba in partial fulfillment of the requirement of the degree

Of

Doctor of Philosophy

for Mum

Acknowledgements

Where to begin. The completion of a PhD program certainly requires extensive guidance, support and love of those who surround the candidate, and of course I was of no exception. There are too many people to mention, but of course a large part of gratitude deserves to be given to my supervisor, Mike Carpenter, my family members (Mum, Dad, Janet, Emmaline & Jasmine), lab associates and friends.

First, to Mike; although this may sound cliché, there are certainly not enough words, or maybe space, to tell you how much I am indebted to you for your supervision and more importantly friendship over the past 6 years. I am sure your were somewhat frightened in that first month after my arrival to your lab, I was a terrible mess having just moved away from Nova Scotia for the first time in my life. If it had not been for Sandra's and your support I am not sure I would have made it to the second month! I consistently voice that I could not have had a better, more suited supervisor for my PhD than what I found in you. I look forward to our continued scientific debates over the years to come, but remember, you bring the chocolate and I will bring the Scotch!

Now, to my family; only you know how crucial you all were to my success and sanity. Whether it was the multiple phone calls that lasted hours, the care packages that contained memories of home or the regular trips you made to visit me in the 'Peg, I never could have done it without your ever present love, support and faith. Mum, thanks for scrubbing the floors (three times), dropping my first Winnipeg Thanksgiving turkey on the floor, the hugs, kisses and tears and the ability to drop everything and come to my aid. You know how much I counted on you, so thanks for being the crutch I often needed. Dad, though you may have a hard time displaying emotions, I have always known how proud you are of me and that taught me that I could do anything I wanted because you believe in me. My big sis Janet, you have always been a surrogate mum to me, but over these past 6 years you have also become one of my best friends. I knew that if mum was not available you would be there for me. Thanks for all the care packages, the phone calls to check in on me (sorry for the long distance charges), the "vacations" you spent at 745 Wolseley Avenue, the emergency credit card and the ear to listen to all my woes, even when the phone calls came in the middle of the night. Emmaline, thanks for always understanding that choosing a profession should be based on your passion for the field and not necessarily the attached income. I am so proud of you and I can not wait to become friends first and Aunt and niece second. Finally, to my Grandparents, the Boutiliers and the Whitmans. You provided me the perseverance to make it through all of these years. Nannie Boutilier, you inspired in me the passion for learning. Granddad Boutilier, you were always my biggest fan, I hope I have done you proud this time. Nannie Whitman, your crafting abilities may have skipped a generation with Mum, but your creative abilities took hold in me and many, many lonely nights in Winnipeg were spent knitting, embroidering, painting or cross-stitching. Anne and Josh, thanks for visiting, listening to rants, giving me my needed space on occasion and treating me to the "good life".

To my friends, Candace, thanks for being like a second family to me, the car rides, the study sessions, the frustration rants, early morning workouts, and all the food!!!! Thanks to Yvon and Martyne (my French family), Lisa Baspaly (my Entomology guru with a talent for butt kicking and great taste in food!). All of my fellow lab mates; Todd, someone to always pick on, J-Lyn, my coffee connoisseur, Lady X, my Chinese Mum, and Aileen, my Newfoundland Grammie with a skill for thesis collating. Thank you all so much. Thanks to the Department of Medical Microbiology, especially Bevan, Charlene, Darryl, Saffron, Rae-Anne and Jamie for all the laughs. To Adam, thanks for the bi-weekly lunches and more importantly, for bringing me into the HIV research group.

To my old lab crew who believed in me and taught me how much fun research can be (Sam Dawe, Jenn Corcoran, Jayme Salsman, Deniz Top, Dave Mader, Ken Roy, Roberto DeAntueno and Jingyun Shou). A very special thanks to Roy Duncan and Don Stoltz who helped me through a busy honours research project and convinced Mike to take me a grad student (he blames you!).

Thank you to my graduate committee, Dr. Kevin Coombs, Dr. R. D. Gietz, Dr. Jingxin Cao and Dr. Mark Harris for providing me guidance and reading the beast of my thesis. Thanks to Dr. Charles Rice and Dr. Takaji Wakita for the generous reagent gifts that were crucial to my research.

Finally, thanks to Jasmine, my kitty for always being there for a much needed hug at the end of a hard day.

TABLE OF CONTENTS

List of Figures

List of Tables

List of Abbreviations

2DE	two-dimensional electrophoresis
BVA	biological variance analysis
BSA	bovine serum albumin
CHAPS	3-[(3-cholamidopropyl) dimethylammonio]-1-propanesulfonate
C-terminus	carboxy-terminus
DAPI	4'-6-diamidino-2-phenylindole, dilactate
DIA	difference in-gel analysis
DIGE	difference-in-gel electrophoresis
DMEM	Dulbecco's modified Eagle's medium
DNA	deoxyribonucleic acid
DTT	dithiothreitol
E1	envelope glycoprotein 1
E2	envelope glycoprotein 2
EF	elongation factor
eIF	eukaryotic translation initiation factor
EMCV	enchephalo mycocarditis virus
HCV	hepatitis C virus
IAA	iodoacetamide
IRES	internal ribosome entry site
NS2	non-structural 2
NS3	non-structural 3
NS4A	non-structural 4A
NS4B	non-structural 4B
NS5A	non-structural 5A
NS5B	non-structural 5B
N-terminus	amino-terminus
PAGE	polyacrylamide gel electrophoresis
PePHD	PKR eIF2α phosphorylation homology domain
pI	isoelectric point
PI3K	phosphatidylinositol-3-kinase
PKB	protein kinase B (also termed AKT)
PKC	protein kinase C
PKR	protein kinase R
PVDF	polyvinylidene fluoride
RNA	ribonucleic acid
SDS	sodium dodecyl sulphate
SH2	src homology 2 domain
SH3	src homology 3 domain

Abstract

Hepatitis C virus (HCV) is a leading global pathogen affecting over 3% of the world's population and at least 250 000 individuals in Canada alone. Infection with the (+) polarity RNA virus is often characterized by a chronic disease state that can ultimately culminate in liver cirrhosis, steatosis and hepatocellular carcinoma. HCV is the leading indicator for liver transplants in North America. In addition to the high incidence and persistent nature of HCV, current treatment regimens have limited efficacy and there is no vaccine available for prophylactic measures.

Viruses are obligate intracellular pathogens, ergo, they have to rely heavily on host cells in order to propagate. HCV is known to remodulate the cellular environment to create an intracellular milieu conducive to virus replication and propagation. Of the many cellular control mechanisms that viruses can take advantage of, protein phosphorylation is a key factor. Phosphorylation plays a key role in numerous cellular processes including antiviral signalling, protein expression, cell proliferation and cytoskeleton remodelling. Therefore, in an effort to better understand the pathogenic mechanisms of HCV infections; alterations to the host cell phosphoproteome were analyzed in Huh7.5 human hepatocytes containing a subgenomic replicon or in Huh7.5 cells infected with high titre HCVcc (cell cultured virus). Phosphoproteins were enriched from liver cell lines using phospho-serine, threonine and tyrosine antibody immunoaffinity. Phosphoprotein enriched fractions were analysed by high resolution, quantitative, 2D differential-in-gel electrophoresis (2D-DIGE) and phosphoproteins that exhibited statistically significant alterations between control and experimental cell lysates were deemed of interest and identified by mass spectrometry.

Subtle changes to the phosphoproteome were observed in subgenomic replicon Huh7.5 cell lines and included elevations in Hsp90 and amphiphysin II and decreases in tropomyosin 4 and calponin. More dramatic changes to the phosphoproteome were observed in Huh7.5 cells infected with live HCV. Increases in the poly-rC binding protein I and multiple tubulin and tropomyosin isoforms were obeserved. Very few changes were decreased in relation to mock infected cells but included two isoforms of calponin.

Despite the genotypic and genome coding differences between the subgenomic replicon and infectious HCV, similar protein families were altered when compared to control cell lines. These included cellular proteins associated with; cytoskeletal rearrangement, endoplasmic reticulum stress and protein translation. A number of proteins found to be altered using 2D-DIGE methodologies were confirmed by 2D immunoblotting. Of critical importance, the findings observed by 2D-DIGE were specific to both the phosphorylation status of the proteins as well as the specific isoform of each protein. In certain cases, total proteomic analysis by standard one dimensional separation methods would not have identified those changes discerned here.

CHAPTER I: INTRODUCTION

SECTION I – Hepatitis C Virus

Approximately 170 million people are infected with hepatitis C virus (HCV), corresponding to roughly 3% of the world's population (Poynard et al., 2003; Lauer and Walker, 2001). The main factors that contribute to the high incidence rate of HCV are; first the lack of effective treatment/preventative measures (McHutchison and Fried, 2003) and second the propensity of the virus to establish a persistent infection in upwards of 70% of cases. Chronic HCV infection ultimately culminates in progressive liver failure that is a result of liver inflammation (hepatitis), fibrosis, chirrosis and hepatocellular carcinoma (Hoofnagle, 2002) and as a result is the leading cause of liver transplantation in North America (Willems et al., 2002). Despite the many advances made pertaining to HCV since its description as the cause of non-A, non-B hepatitis in 1989 (Choo et al., 1989), many facets associated with infection including (but not limited to) the replication cycle of the virus, the mechanisms of virus pathogenesis and consequently the appropriate antiviral targets to both treat and prevent infection remain unclear.

HCV belongs to the family *Flaviviridae*, which contains three distinct genera; 1) *Flavivirus* whose members include Yellow fever virus and West Nile virus, 2) *Pestivirus* whose members include Bovine viral diarrhea virus (BVDV) and classical swine fever virus and 3) *Hepacivirus* of which HCV is the only member (Robertson et al., 1998). The classification of HCV into its own distinct genus is

based on differences between the prototypical human Flaviviruses. Unlike the other infectious agents, HCV is not transmitted by an arthropod vector, and secondarily genome structural differences account for variations in the mechanism of genome translation and replication (specifically the division of the NS5 coding region into two proteins, NS5A and NS5B in HCV) (Tanaka et al., 1995). With regards to the replication cycle of HCV, it is thought to most closely mimic that of BVDV (Ohba et al., 1996; Meyers and Thiel, 1996; Muerhoff et al., 1995) and therefore, BVDV continues to serve as a model for HCV studies.

Clinical

Initial infection with HCV often goes undiagnosed due to the absence of major observable symptoms during the acute phase of infection. In patients exhibiting a detectable phenotype, the presentation is often non-specific and includes general malaise, nausea and jaundice (Maheshwari et al., 2008). In very rare instances, acute HCV infection has been associated with fulminant hepatitis (Farci et al., 1996; Kato et al., 2001; Gordon et al., 1995). In a large proportion of cases, the virus persists at low levels in the liver and establishes a chronic infection which, over the course of decades, often results in hepatitis (liver inflammation), and in some cases fibrosis and hepatocellular carcinoma (Hoofnagle, 2002).

Although HCV replication occurs predominantly in the liver, persistent infection is associated with a number of extrahepatic diseases (Mayo, 2003) including acute cryoglobulinemia (Munoz-Fernandez et al., 1994), renal complications (Johnson et al., 1994), neuropathy (Authier et al., 2003; Morgello, 2005; Seifert et al., 2008)

and diabetes (Masarone et al., 2007; Mason and Nair, 2003). The extrahepatic manifestations can in part be explained due to liver associated changes, however, there is compeling evidence that HCV can replicate in non-hepatocyte cells including peripheral blood mononuclear cells (Bare et al., 2005) and epithelial cells (Deforges et al., 2004).

HCV is primarily transmitted through direct blood contamination, often through needle sharing between intravenous drug users and improper sterilization of tattoo needles (Yen et al., 2003; Ko et al., 1992). Prior to the discovery of HCV, a primary source of infections was the result of contaminated blood transfusions. With the advent of sensitive and specific screening tools, this form of transmission has essentially been eradicated in developed countries (Yen et al., 2003).

Current treatment regimens involve combination therapy of pegylated interferon alpha and the non-specific ribonucleoside antiviral Ribavirin (McHutchison and Fried, 2003). Treatment is often plagued with substantial side effects including nausea, malaise, influenza-like symptoms, anaemia and anorexia. There are contraindications to treatment that include hypertension, severe depression, old age and autoimmune disorders. Unfortunately, treatment efficiency is limited such that less than 50% of patients treated respond to therapy, some of whom subsequently develop chronic HCV infection. Interestingly, successful treatment

is often dictated by the genotype of the virus (Lauer and Walker, 2001; Bacon and McHutchison, 2007; Cross et al., 2008).

There are currently six commonly recognized HCV genotypes (1-6) which are further divided into subtypes (a, b, c, etc.), and quasi-species (1-100) (Simmonds et al., 1993; Robertson et al., 1998; Simmonds et al., 2005). Of the 6 predominant HCV genotypes, specific quantitative and geographical distribution exists. Genotypes 1a and 1b are highly prevalent and, along with genotypes 2 and 3 infections can be found worldwide. However types 1a and 1b are predominantly found in North America and Eastern Europe, while genotype 3 is endemic in Asia. Genotype 4 is localized within the Middle East, Egypt and middle Africa while genotype 5 is centralized to Southern Africa. The remaining genotypes are much less prevalent and can be found in Southern Asia (Nguyen and Keeffe, 2005). Genotype 1 has been the least responsive to current treatment regimens, while genotypes 2 and 3 have been the most successfully treated to date (McHutchison and Fried, 2003).

Genome

HCV contains a single stranded monopartite positive polarity RNA genome of approximately 9.6kb, that, when translated, produces a single polyprotein of ~3011 amino acids (Bartenschlager et al., 2004; Penin et al., 2004; Lindenbach and Rice, 2005; Moradpour et al., 2007; Appel et al., 2006). Shown in figure 1 is the full length genome that provides the coding sequence of the viral polyprotein and serves as a template for genome replication through a negative polarity RNA

Figure 1. **Hepatitis C virus (HCV) genome and polyprotein processing. (A)** HCV contains a single stranded 9.6kb RNA genome with positive polarity. The 5' and 3' ends of the genome contain highly structured non-translated regions (NTRS) which are necessary for genome replication and translation. The 5' NTR forms the internal ribosome entry site (IRES) that recruits the required cellular translation machinery in the absence of the 5' methylated cap present on most cellular mRNA transcripts. **(B)** Translation of the RNA genome produces a single polyprotein of ~3011 amino acids in length which is cleaved (see arrows) both co- and post-translationally by cellular and viral proteases to produce at least 10 proteins. **(C)** At the amino terminus of the polyprotein are the structural proteins (core-E1-E2) followed by the small ion channel p7 and the non-structural proteins (NS2-NS3-NS4A-NS4B-NS5A-NS5B). In addition to the above mentioned proteins, a ribosomal shift to an alternate reading frame in the core coding sequence results in the production of the F protein.

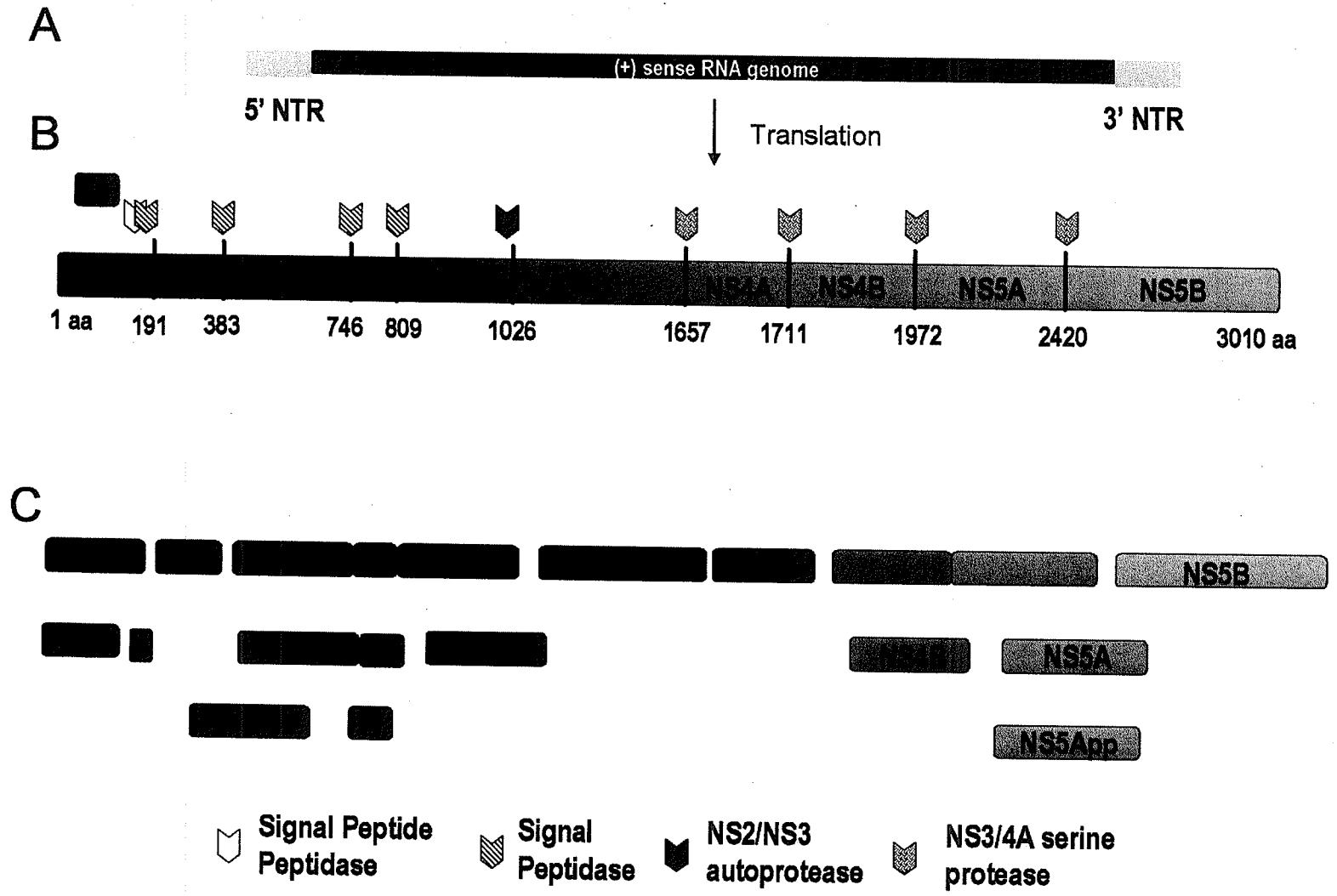
A
(+) sense RNA genome
5' NTR
3' NTR
B
Translation
NS4A
NS4B
NS5A
NS5B
1 aa
191
383
746
809
1026
1657
1711
1972
2420
3010 aa
C
NS5B
NS5A
NS5App
Signal Peptide Peptidase
Signal Peptidase
NS2/NS3 autoprotease
NS3/4A serine protease

intermediate. At the 5 prime (5') and 3 prime (3') ends of the genome are highly structured non-translated regions (NTR) that provide the necessary scaffolding to recruit both viral and cellular proteins that drive genome translation and replication. The 5' terminus contains an internal ribosome entry site (IRES). This structure recruits cellular translation proteins and ribosomes allowing translation of the viral polyprotein in the absence of cap-dependent mechanisms (Wang et al., 1993; Tsukiyama-Kohara et al., 1992). Other viruses, for example the *Picornaviridae*, have evolved similar mechanisms in order to override or augment the cellular translational machinery whereby the virus inhibits cap-dependent translation (necessary for most cellular transcripts) while maintaining the ability to translate viral proteins (Fig. 1) (He et al., 2001; Kou et al., 2006; Whitlow et al., 2006; Lyles, 2000). The 3' terminus of the genome contains a polypyrimidine/polyuridine tract which likely plays a role in translation termination (Yi and Lemon, 2003b) and may also provide the necessary interactions between the 5' and 3' ends to enable a more robust replication cycle whereby the genome forms a circle, thereby allowing the replication complexes to remain associated with the template and continue with subsequent rounds of replication (Friebe et al., 2005). Both the 5' and 3' NTRs are highly conserved between genotypes, likely due to their critical roles in genome replication and translation (Friebe et al., 2001; Kolykhalov et al., 1996; Kim et al., 2002; Tanaka et al., 1995; Tanaka et al., 1996; Yi and Lemon, 2003a; Yi and Lemon, 2003b).

The viral polyprotein is both co- and post-translationally cleaved by the cellular proteinases; signal peptidase (Hijikata et al., 1993a; Hijikata et al., 1993b) and signal peptide peptidase (McLauchlan et al., 2002; Okamoto et al., 2004) as well as the NS2/NS3 viral autoprotease and NS3/4A viral serine protease (Bartenschlager, 1999) to produce at least 10 unique viral proteins (Fig. 1) (Shimotohno et al., 1995).

At the amino terminus, the first coded protein is known as core. In its structural capacity, core can self associate and form icosahedral particles that encapsidate the viral genome to form the nucleocapsid structure (Lorenzo et al., 2001; Majeau et al., 2004; Blanchard et al., 2002; Shimizu et al., 1996). It is important to note that core is also implicated in altering many cellular processes (see section "Virus-Host Cell Interactions" below).

The two viral glycoproteins, E1 and E2 form heterodimers in ER membranes (Cocquerel et al., 2002) and upon virus maturation are incorporated into the virus particle, in conjunction with an envelope around the nucleocapsid. The viral envelope is then composed of E1E2 heterodimers and a cellular lipid bilayer. E1 and E2 are in large part responsible for virus-cell receptor interaction and subsequent entry of the virus into host cells, although details of this mechanism are only now becoming known. It is speculated that E2 serves as the primary recognition molecule on the virions thereby interacting with a number of cellular receptors and places E1 in close proximity to target cellular membranes, allowing

for E1 driven membrane-membrane fusion. Both glycoproteins demonstrate membrane fusion properties (Garry and Dash, 2003; Takikawa et al., 2000; Lavillette et al., 2007).

At the junction of the structural and non-structural proteins, lies a small protein termed p7. It is believed that p7 may also be a structural protein that acts as an ion channel in much the same fashion as the M2 protein of influenza (Griffin et al., 2003). The presence of p7 is thought to maintain an inactive glycoprotein complex during virus egress to ensure that assembled virus is released from cells in an intact state. This limits virus un-coating within infected cells due to potential membrane-membrane fusion of the virus envelope with membranous compartments of the cell (Steinmann et al., 2007; Moradpour et al., 2003). The remaining six proteins encompass the non-structural (NS) proteins, termed NS2-NS3-NS4A-NS4B-NS5A-NS5B. NS3-NS5B, are necessary and sufficient for translation and replication of the virus genome in cell culture models (Lohmann et al., 1999).

Apart from the autocatalysis of NS2 from the polyprotein in concert with NS3; little is known about the other potential roles of this protein. It has been implicated in the inhibition of both cellular and viral promoters (Dumoulin et al., 2003), inhibition of apoptosis via the liver specific CIDE-B pathway (Erdtmann et al., 2003) and inducing cell cycle arrest (Yang et al., 2006). Furthermore, along with p7, NS2 is necessary for proper virion formation (Jones et al., 2007a). The

following protein, NS3 is a multifunctional protein. Not only does the N-terminal portion of NS3 serve as a proteinase in complex with NS2, but it also associates with NS4A to cleave the remaining non-structural proteins from the polyprotein (Bartenschlager et al., 1995; Hijikata et al., 1993a; Hijikata et al., 1993b). The C-terminal region of NS3 contains an ATP-dependent helicase which is capable of unwinding highly ordered secondary structures (such as those found in the 5' and 3' NTRs) and is therefore thought to be involved in unwinding the viral genome for efficient replication (Bartenschlager, 1999). Due to the integral role NS3 plays in the propagation of HCV, it has been a prime target of antiviral research. NS3 has also been shown to alter many cellular processes resulting in immune modulation by inhibiting key immune signalling of the interferon inducible factor-3 (IRF3) and the retinoic-acid inducible gene I (RIG-I) (Foy et al., 2005; Foy et al., 2003). NS3 has also been associated with cellular transformation, a process that requires NS3 to be present in an active enzyme state (Zemel et al., 2001). Aside from functioning as a cofactor and membrane tethering agent for NS3, the NS4A protein has been shown to inhibit protein synthesis, at the level of transcription and translation, acting in concert with NS4B (Kato et al., 2002). The inhibition of translation may in part be due to the association of NS4A with the elongation initiation factor 1A (eIF1A) (Kou et al., 2006).

The remaining downstream proteins are highly involved in the formation of the replication complex associated within a membranous web (Egger et al., 2002; Gosert et al., 2003). The formation of membranous compartments containing the

non-structural proteins and viral genome appears to be predominately driven by NS4B (Elazar et al., 2004). It is speculated that the concentration and specific localization of the necessary factors for genome replication and protein production ensures an efficient means to replicate virus. Furthermore, NS4B contains a nucleotide binding motif (NBM) which has GTPase activity that is required for efficient genome replication (Einav et al., 2004). It has also been implicated in cellular transformation due to an interaction with Ha-Ras, both *in vitro* (Park et al., 2000) and *in vivo* (Einav et al., 2008).

NS5A, the penultimate non-structural protein has also been the focus of intense study, yet despite many efforts, the exact role of this protein in virus replication and pathogenesis remains elusive. It is likely that NS5A is a critical component of the replication complex as there have been many documented cell culture adaptive mutations which map to the NS5A coding sequence in tissue culture (Blight et al., 2000). NS5A becomes hyper-phosphorylated (Kaneko et al., 1994), in what appears to be a replication versus translation dependent manner (Neddermann et al., 1999; Kalliampakou et al., 2005; Evans et al., 2004) and the modification is also critical for efficient virion formation due to its interaction with core (Masaki et al., 2008). NS5A also contains what has been termed the interferon sensitivity determining region (ISDR) (Enomoto et al., 1996) a site that has been documented to be hypervariable. It is thought the the hypervariability of the ISDR may in part explain the differences in the success of antiviral therapies between different genotypes. Unfortunately, the predictive value of the ISDR

sequence for treatment response has been controversial (Murphy et al., 2002; Pawlotsky et al., 1998; Enomoto et al., 1995; Enomoto et al., 1996).

The final cleavage product from the carboxy-terminus of the polyprotein produces NS5B, the RNA-dependent RNA-polymerase (RdRp) which is the essential enzyme that catalyzes the production of both (+) and (-) polarity copies of the viral RNA genome (Lohmann et al., 2000). As with most other RdRps, these enzymes are highly processive but lack 3` - 5` exonuclease activity and therefore are prone to errors in copying (Lohmann et al., 2000). The increased error rate of RdRps can result in the production of defective genomes. However, certain mutations are not detrimental to the virus and may generate isolates with greater fitness. The high mutation rates associated with RNA viruses drives the generation of new quasispecies and genotypes of the virus, making the development of cross-protecting vaccines and antivirals difficult.

A frameshift product within the core coding sequence was recently discovered to be expressed during viral infection (Boulant et al., 2003; Varaklioti et al., 2002). Translation of the frameshift product initiates at the core start codon, however, the ribosome-protein complex shifts to an alternate reading frame (core ORF +1) somewhere near the 11^{th} codon to produce the F protein (F for frameshift, or ARF, for alternate reading frame). The F protein has not been ascribed a role in viral infection; however, it may serve as a decoy antigen to drive inappropriate neutralizing antibody responses in infected individuals and may also be involved

in the replication complex as it co-localizes with both core and NS5A (in co-transfections) (Xu et al., 2003). Furthermore, there is strong evidence that the F protein is produced during natural infection as infected patient serum contains F-specific antibodies (Walewski et al., 2001; Xu et al., 2001).

HCV Cell Culture

Until recently, the ability to robustly propagate HCV in tissue culture was not possible and alternative strategies were developed in order to study both the genome expression and replication in cells. The most predominantly used cell culture models are the subgenomic and full length replicon systems primarily developed in Dr. Ralf Bartenschlager's lab (Bartenschlager and Lohmann, 2001; Bartenschlager et al., 2003; Pietschmann and Bartenschlager, 2003). In this system, the sequence encoding the NS3-NS5B (subgenomic) or core-NS5B (full genomic) portion of the viral genome is cloned into an expression plasmid downstream of a T7 promoter. A drug resistance gene (neomycin/G418) is also incorporated into the replicon coding sequence, upstream of the viral genome providing the ability to select for cells containing the replicon. The resulting transcript encodes a bicistronic RNA that encompasses both the HCV 5' and 3' NTRs, a drug resistance gene, the enchepalomyocarditis virus (EMCV) IRES and a portion of the viral coding sequence (Fig. 2A). A representation of the subgenomic replicon used in this and other studies was developed by Lohmann *et al.* in 1999 (Lohmann et al., 1999).

Figure 2. **Generation of stable HCV replicon cell lines.** **(A)** The replicon construct used in this study was generated by Dr. V. Lohmann and kindly provided by Dr. Charlie Rice (New York) (Lohmann, Korner, Koch, Herian, Theilmann, & Bartenschlager, 1999). A portion of the HCV genotype 1b sequence is present in an expression vector containing a T7 promoter and drug resistance marker. Vector DNA was linearized and *in vitro* transcribed with T7 polymerase. **(B)** Schematic of the bicistronic subgenomic HCV replicon used in this study. The HCV internal ribosome entry site (IRES) at the 5' end of the RNA construct is followed by a small portion of the core coding region and a neomycin phosphotransferase II gene (NPTII/Neo^R). The HCV IRES recruits essential translation machinery to drive protein expression of the NPTII gene. The encephalomyocarditis virus IRES recruits the translation machinery for the remaining RNA sequence which includes the HCV non-structural proteins NS3-NS4A-NS4B-NS5A-NS5B. The HCV 3' non-translated region (NTR) is encoded by the remaining replicon sequence. **(C)** Upon replicon RNA transfection into permissive cells, three distinct outcomes are possible. I) If a cell does not receive a copy of the replicon RNA after transfection, then upon drug selection the cell will die, II) if a cell receives a copy of the replicon RNA following transfection but the replicon does not replicate, then the cell will die once drug selection is applied, or III) the replicon RNA is translated and replicated to sufficient levels allowing survival of the cell in the presence of drug. Upon drug selection the cells will continue to grow and subsequent clonal propagation of the cells will produce stable cell lines.

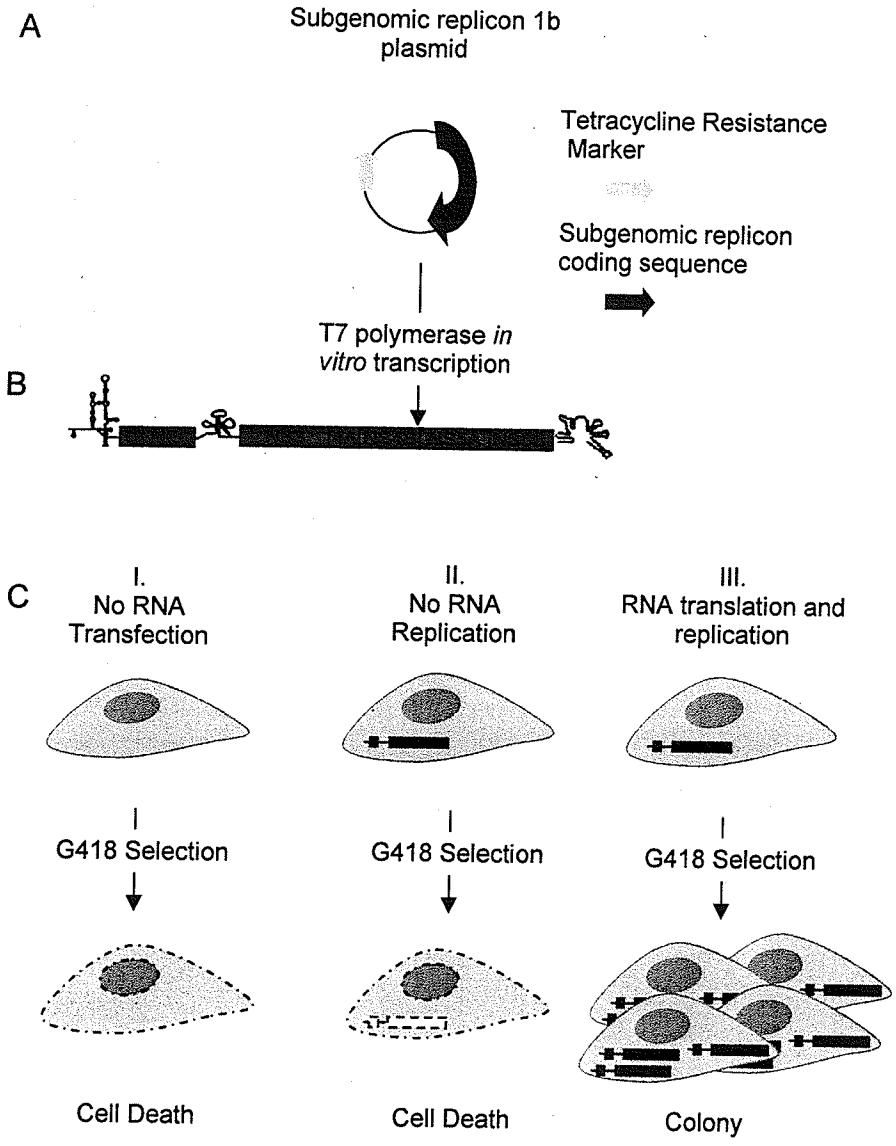
A
Subgenomic replicon 1b plasmid
Tetracycline Resistance Marker
Subgenomic replicon coding sequence
T7 polymerase *in vitro* transcription
B
C
I.
No RNA Transfection
II.
No RNA Replication
III.
RNA translation and replication
G418 Selection
G418 Selection
G418 Selection
Cell Death
Cell Death
Colony

Once the RNA transcript is transfected into a permissive cell line, translation of the first coding region is driven by the HCV IRES producing a drug resistance marker used for selection of cells harbouring the replicon. The second open reading frame is translated via the ECMV IRES and produces a polyprotein encoding the NS3-NS5B region (or full genome) of the HCV viral polyprotein. The subgenomic replicon construct contains all the necessary factors needed to translate and autonomously replicate the RNA genome, thereby recapitulating the molecular synthesis stages of the HCV life cycle (Fig. 2B).

Under drug selection, cell lines which continuously express high amounts of the viral proteins and replicating genome can be established. In the event that a cell is not successfully transfected with replicon RNA, or the replicon does not replicate once in the cytoplasm of the cell, G418 selection will eliminate those cells (Fig. 2C I and II respectively). However, when the replicon is both translated and replicated in the transfected cells, drug selection does not interfere with cell proliferation, thereby generating stable replicon cell lines (Fig. 2C III). For transient studies, the drug resistance marker has been replaced with more rapid screening markers such as luciferase or green fluorescent protein (Guo et al., 2001; Blight et al., 2000; Jones et al., 2007b). Furthermore, the NS5A coding region contains a flexible motif into which one of these markers can be inserted, without having obvious detrimental effect on virus replication in cell culture (Liu et al., 2006).

Aside from containing the full complement of virus coding region, full length replicons are in principal the same as the subgenomic replicons. However, it is of interest to note that despite the robust production of virus proteins and genome copies, no infectious virus is produced by cells containing these replicons (Blight et al., 2003; Ikeda et al., 2002; Pietschmann et al., 2002). It would therefore suggest that although the replication processes of the virus are recapitulated by the replicon system there still remains a defect in some aspect of virus assembly and/or release.

Not surprisingly, given the intimate relationship between the virus and host cell, numerous adaptive mutations have been mapped in the replicon system. One particular mutation that is highly conserved between replicons occurs at S2204I, within the NS5A coding region, a site known to undergo phosphorylation (Appel et al., 2005; Evans et al., 2004). Other regions of adaptive mutations lie within the NS3, NS4A and NS4B coding regions (Krieger et al., 2001; Lohmann et al., 2001). Interestingly, the enhanced replication observed in tissue culture due to these adaptive mutations is not typically paralleled in chimpanzees (Bukh et al., 2002; Kaul et al., 2007). This may in part be due to an enhanced immune response *in vivo* when higher levels of viral genome and protein are produced. It may also be due to the fact that in cell culture, adaptations are likely selected for based on efficient transcription and translation and not necessarily for other aspects of the virus replication cycle including genome packaging and virus release.

Although mutations within the viral genome enhance replication, the cellular environment also has an important role. A variety of cell lines and cell types have been tested for their ability to support HCV genome replication and/or infection, including HeLa and murine Hepa cells (Zhu et al., 2003b), 293T embryonic kidney (Ali et al., 2004), HepG2 (Date et al., 2004), peripheral blood mononucleocytes (PBMCS) and Raji B cell lines (Sung et al., 2003). When evaluating the efficiency of viral genome replication in these cell lines, typically only 10 viral RNA copies/cell were detected, while 1000-5000 viral RNA copies/cell are preferred. To date, only the human hepatoma liver cell line, Huh7, has proven to be highly permissive to HCV replicon propagation and infection. However it has been shown that only a subset of Huh7 cells support the replicon (~0.0005%), thereby implying that the state of the cell may be of importance to HCV replication (Lohmann et al., 2003; Nelson and Tang, 2006). Furthermore, if replicon permissive cells are "cured" of the replicon by IFNα treatment, the cells in turn support higher levels of HCV replication when the replicon is reintroduced although it is still only 0.005% of transfected cells (this number increases to 30% of transfected cells if the S2204I mutation is included in the viral RNA) (Blight et al., 2002). The phenomenon lead to the production of various Huh7 cell lines that exhibit increased support for HCV replication including Lunet (Friebe et al., 2001), Huh7.5 (Blight et al., 2002) and Huh7.5.1 (Zhong et al., 2005) cell lines. Upon closer investigation of the Huh7.5 cells, it was shown that the cells have a

deficiency in the RIG-I antiviral pathway which likely contributes to virus replication efficiency (Sumpter, Jr. et al., 2005; Foy et al., 2005).

The lack of infectious virus particle production with full length replicons limited studies involving virus packaging and infectivity. This has now been remedied following the discovery of an infectious genotype 2a virus (Kato et al., 2001; Wakita et al., 2005). This new strain, termed JFH1, for Japanese fulminant hepatitis 1 is infectious in cell culture and in chimpanzee models and does not appear to require adaptive mutations to efficiently propagate in either model system (Lindenbach et al., 2005; Wakita et al., 2005; Zhong et al., 2005). In 2005, electron micrographs of JFH1 purified virus (referred to as HCVcc for cell culture derived) were able to demonstrate the presence of spherical like particles with an electron dense core, in keeping with the speculated virion structure (Wakita et al., 2005).

Of course, with every advance there are caveats that must be considered during studies, JFH1 included. Previously mentioned, the most predominant genotype of HCV worldwide is genotype 1, which also happens to be highly non-responsive to antiviral efforts, while genotype 2 is typically more responsive to treatment (Andriulli et al., 2008). Furthermore, HCV infection is typically associated with liver complications such as liver cirrhosis, fibrosis and hepatocellular carcinoma, largely due to the persistence of the virus and chronic infection of the liver. The individual from which JFH1 was isolated suffered from only an acute infection,

and a rare complication of HCV infection, encephalitis (Kato et al., 2001). Therefore, it is not surprising that JFH1 behaves differently from the prototypical genotypes with regards to cell culture propagation as it behaves differently *in vivo*. Numerous groups have attempted to establish the specific regions within JFH1 which are responsible for its ability to propagate in tissue culture. Interestingly, the coding region spanning the core-NS2 can be replaced with alternative genotype sequence and the resulting chimera still produces infectious particles. However, the essential region must remain JFH1 sequence from a position termed C5 within the NS2 coding region to the remaining 3' coding region (Jones et al., 2007a; Kato et al., 2007; Pietschmann et al., 2006). Mutational analysis of the 3' region of JFH1 has provided little insight into the specific regions within JFH1 that are responsible for successful propagation. Essentially all of the regions appear to be important (Kaul et al., 2007; Sekine-Osajima et al., 2008; Murayama et al., 2007; Murray et al., 2007; Shavinskaya et al., 2007; Yi et al., 2007).

HCV lifecycle

Despite the recent discovery of *ex vivo* HCV models that demonstrate robust infection in cell lines, explicit details pertaining to the virus lifecycle remain incompletely understood. It is known that the main cellular targets of HCV are hepatocytes, however, there is evidence that other cell types are targeted by HCV, including B cells (Bare et al., 2005), peripheral blood mononuclear cells (Bare et al., 2005), intestinal epithelial cells (Deforges et al., 2004), and T lymphocytes (MacParland et al., 2006). In order to gain entry into target cells,

the virus E2 glycoprotein binds to a number of different cellular receptors including the tetraspanin CD81 (Wunschmann et al., 2000), human scavenger protein I (SR-BI) (Scarselli et al., 2002), DC-SIGN/L-SIGN (Lozach et al., 2003; Pohlmann et al., 2003) and claudin-1 (Evans et al., 2007) to name a few. CD81 interaction is necessary but not sufficient for virus entry; and furthermore, cells that co-express CD81, SR-BI and claudin-1 are not necessarily permissive for virus entry. It is likely that additional cellular factors are required for virus entry (Bartosch et al., 2003)reviewed in (Bartosch and Cosset, 2006; Cocquerel et al., 2006; Dubuisson et al., 2008).

Upon receptor recognition, the virus particle enters the cell via clathrin-dependent endocytosis (Codran et al., 2006; Blanchard et al., 2006) and therefore is contained within an endosome (Meertens et al., 2006). Upon acidification (Tscherne et al., 2006) of the endosome, and presumably E1 glycoprotein mediated fusion (Garry and Dash, 2003) of the endosomal membranes, the viral genome is released into the cytoplasm of the cell.

The genome is then translated by cellular machinery and processed into the 10 prototypical viral proteins (Shimotohno et al., 1995; Grakoui et al., 1993). Translation is known to occur on ER membranes, which results in the incorporation of all of the viral proteins into the membrane (Moradpour et al., 2003). The localization of the genome and viral proteins to the ER results in the formation of what is termed a membranous web. Presumably, the concentration

of the viral proteins to the membranous structures provides structural support for the replication complex (Lyle et al., 2002) and enhances the efficiency of virus propagation by facilitating the co-localization of all necessary factors (Schwartz et al., 2002) and most likely serves as the site of genome replication as well. It should be noted that upon viral translation, all of the viral proteins are expressed on the cytoplasmic side of the ER with the exception of the two glycoproteins. It is speculated that E1 and E2 enter the cellular retrograde transport pathway where they undergo glycosylation (Grakoui et al., 1993) and form heterodimers that are then incorporated into virions at the site of virus assembly (Lavie et al., 2007; Deleersnyder et al., 1997). Finally, through unknown mechanisms, the core protein oligomerizes to form particles which bind at least one copy of the positive polarity viral genome in positive polarity. The nucleocapsid is then enveloped by cellular membranes containing E1E2 heterodimers (postulated to be late Golgi endosome membranes) and subsequently released from the cell (Sandrin and Cosset, 2006; Gastaminza et al., 2008; Andre et al., 2005). Despite evidence that the F protein and p7 are also structural proteins critical to virus assembly and therefore present in intact virions, there has not yet been definitive proof these proteins are indeed incorporated (Murray et al., 2007; Jones et al., 2007a).

Virus-Host Cell interactions

The limited coding capacity of HCV mandates that virus propagation relies heavily on host cell machinery, the consequences of which drive the research presented herein.

HCV encoded proteins are multifunctional. In addition to the roles mentioned previously with regard to virion formation and genome processing, all of the viral proteins have also been shown to interact with a multitude of cellular proteins. Of particular interest to our lab group are alterations that affect host cell-signalling pathways which are predominantly governed by the post-translational modification, phosphorylation. Protein phosphorylation is a transient modification typical of serine, threonine and arginine amino acids and is regulated by protein kinases and phosphatases. The initiation of signalling cascades by phosphorylation often leads to alterations of gene transcription, cytoskeletal remodelling, antiviral responses, cell cycle progression and differentiation and therefore represents an attractive aspect of cell homeostasis that viruses can manipulate.

Precedence exists for HCV having a role in altering cellular phosphorylation. For example, the expression of HCV core has been shown to alter cell replication both *in vitro* and *in vivo*. Mechanistically, this phenomenon may in part be explained by the ability of core to bind the signal transducer and activator of transcription 3 (STAT3), which results in the activation and phosphorylation of STAT3. Phospho-STAT3 ultimately initiates an intracellular signal cascade that increases the proliferation and anchorage-independent growth of core-expressing NIH3T3 cells (Yoshida et al., 2002). Core has also been documented to inhibit the phosphorylation of extracellular regulated-signal kinase 1 (ERK1) and

mitogen-activated ERK kinase (MEK) which results in the inhibition of IL-2 expression and subsequent abrogation of T-cell proliferation (Yao et al., 2003; Yao et al., 2001). The ability to inhibit T-cell proliferation by HCV could be a significant determinant of HCV persistence, by suppressing a robust localized immune response.

The glycoproteins, in particular E2, have also been shown to alter signal cascades both intracellularly and extracellularly. As with core protein, E2 has been associated with alterations in the phosphorylation status of mitogen-activated protein kinases (MAPK) and ERK. Furthermore, the discovery of a protein kinase R (PKR) – eIF2 alpha (eukaryotic translation initiation factor) phosphorylation homology domain, termed PePHD (Taylor et al., 1999) lead to extensive studies with regards to the ability of E2 to bind PKR and block the induction of PKR through interferon alpha (IFNα) stimulation. The current treatment regimen for HCV is a combination therapy based on Ribavirin and IFNα. HCV genotypes 1a and 1b are particularily resistant to this treatment, and the ability of E2 to bind PKR and inhibit the IFNα treatment has been postulated to be one such mechanism of resistance. Interestingly, there does not appear to be any correlation with the sequence of the PePHD region and response to treatment or disease progression for most genotypes, including 1a and 1b (Boulestin et al., 2002; Bagaglio et al., 2005; Watanabe et al., 2003; Polyak et al., 2000; Cochrane et al., 2000; Puig-Basagoiti et al., 2001; Sarrazin et al., 2001; Berg et al., 2000; Chayama et al., 2000).

Phosphorylation events associated with NS3 have demonstrated the ability to block phosphorylation and thus activation of interferon responsive factor 3 (IRF3), a key antiviral factor (Foy et al., 2003). NS3 can also inhibit the function of cAMP-dependent protein kinase (PKA) (Borowski et al., 1997) and PKC (Borowski et al., 1999b) thereby affecting chromatin remodelling and cellular gene transcription. It is likely that the complex interactions of HCV mediated phosphorylation changes in the cell work in co-operation to maintain a homeostatic environment amendable to virus propagation and persistence.

An are of most intense study with regards to viral induced phosphorylation changes has been the phosphoprotein NS5A. Expression of NS5A leads to the activation of p85 phosphatidylinositol-3-kinase (PI3K) and subsequently AKT through phosphorylation (Street et al., 2004; Street et al., 2005). The activation of AKT by PI3K signalling cascades results in anti-apoptotic messaging that ensures the cells' survival. NS5A can also activate the Src family member Fyn kinase, while inhibiting other Src-kinase members, Hck, Lck, and Lyn (Macdonald et al., 2004). A complex network of NS5A phosphorylation activation and inhibition events seems to lead to the enhancement of viral persistence by promoting cell survival though p85 PI3K events, inhibiting the double stranded RNA response mediated by PKR and STAT3 and blocking apoptosis. Furthermore, cells that express NS5A have demonstrated transformed phenotypes and can form solid tumours *in vivo* (Gale, Jr. et al., 1999).

As detailed above, numerous studies have investigated the phosphorylation status of specific cellular proteins and/or pathways in the context of single virus protein expression, subgenomic/full length replicons and productive virus infection. However, to date no study has addressed the global phosphorylation changes in these settings. ***Therefore, the goal of this research project is to characterize the global phosphorylation changes of Huh7.5 liver cells that express HCV genes in the context of a subgenomic replicon or infectious HCV model system.***

SECTION II – Proteomics

Changes which occur in virus infected cells or in cells expressing specific viral genes have been assessed at both genomic and protein levels. Since the sequencing of the human, and many other model organism genomes, microarray technologies have been at the forefront of many genomic based studies including studies involving HCV infection and liver disease. Interestingly, there have been very few mRNA abundance changes detected in either *ex vivo* systems such as the replicon system (Scholle et al., 2004; Abe et al., 2005; Aizaki et al., 2002; Geiss et al., 2003; Hayashi et al., 2005; Zhu et al., 2003a), *in vivo* models of infected chimpanzees (Bigger et al., 2001; Bigger et al., 2004; Su et al., 2002) and liver biopsies of infected humans (Smith et al., 2003). Although limited changes in the transcriptome were detected, a general change to immune response genes (including LMP2, LMP7, serpin clade C, MHC class I and

cystatin) were found to have increased expression in replicon cell lines compared to naïve cell lines. In chimpanzee models, elevations in interferon stimulated genes (including STAT1α, STAT1β, IRF7, OAS1 and RIG-I) were found to be proportional to the level of viral load, persistence and clearance in infected chimpanzee models (Bigger et al., 2001). It bears mentioning that the samples used in both the chimpanzee models and HCV-infected individuals represent liver biopsies and therefore the presence of infiltrating immune cells and other non-infected cells may contribute to the sample material analysed. In *ex vivo* studies there has been a focus on studying the transcriptome changes that occur in subgenomic replicon cell lines treated with IFNα. Surprisingly, the number of altered genes was similar in naïve cells and replicon cells (Zhu et al., 2003a; Geiss et al., 2003). Furthermore, a study pertaining to the transcriptome changes induced in cell lines harbouring full length replicons revealed that gene expression changes were unique to each cell line and therefore not likely due to the expression of HCV RNA (Scholle et al., 2004).

One important fact that must be addressed is that genomic changes often do not correlate with changes in the protein levels and in part, results seen with cDNA microarrays may not reflect what is happening at the protein level. This is not surprising given the many levels of regulation from the point of gene transcription, alternative splicing, recruitment of essential transcription and translation factors, not to mention gene silencing mediated by small interfering RNAs (siRNA) and microRNAs (miRNA), reviewed in (Tang, 2005). In a variety of cell types (lung,

liver and prostate) and species (*homo sapiens, S. cervisiae*) the concordance between mRNA and protein abundances has been reported to be less than 50% (Anderson and Seilhamer, 1997; Chen et al., 2002; Gygi et al., 1999b). Therefore transcription changes can not always predict the functional changes within the cell. Moreover, transcription data alone can not provide information about the subcellular context or post-translational state of proteins. Therefore, proteomic assessments of HCV infection can provide an important understanding of the functional aspects intractable by a genomic approach.

There are numerous methods by which to investigate and compare the protein content of two cell populations, but regardless of the method used, there is the need to identify the proteins of interest and also quantify the changes in protein abundance incurred. The most efficient means to identify proteins is mass spectrometry; however, the cellular protein content is typically too complicated to evaluate by direct injection of a complex sample. Therefore, separation of these mixtures either by gel-based or chromatography-based methods are typically performed prior to injection into a mass spectrometer.

There are two modes of protein analysis, top down and bottom up. In a top down approach, intact proteins are analysed at the level of intact protein, while bottom up approaches rely on peptide information obtained from a mass spectrometer. Although dramatic improvements are occurring at the level of MS-based top-down experimentation, most current methodologies rely on digestion of proteins

prior to identification (Fig. 3). Following digestion (Fig. 3A and B), peptides are acidified and concentrated. Peptide samples enter the mass spectrometer following their soft ionization by a high voltage source. The mass of each peptide compared to its charge state (m/z) is determined by the mass spectrometer and the individual peaks of ion intensity correlate to individual peptides. The combination of a number of different peptides with known m/z values can be used to form a peptide mass fingerprint (PMF), that can be used in database searching to determine the best protein candidate that matches the PMF pattern (Fig. 3C). Alternatively, in order to obtain amino acid sequence information for a peptide, individual peptides can be selected by the mass spectrometer to undergo high-energy collision-induced dissociation which causes relatively random breaks on the peptide backbone spanning the peptide, a process known as tandem mass spectrometry (MS/MS). The separation distance between the individual peaks corresponds to amino acid residues within the peptide. This information is then used to generate the sequence order of amino acids in a given peptide (Fig. 3D). Given the large amount of spectral information for each MS experiment, software packages are available which select the peptides that will be processed for subsequent data analysis. The selection of these peptides is based on a variety of conditions including, but not limited to the intensity of the peptide compared to background signal and the presence of an appropriately balanced isotopic series (principally based on C12 and C13 isotopes). Both PMF and MS/MS generated spectra are processed by search engines that contain extensive databases of previously sequenced proteins or *in silico* generated

Figure 3. **Schematic of protein identification by mass spectrometry. (A)** Proteins of interest are cleaved into peptides by enzymatic digestion (depicted by different coloured lines in **(B)**. The commonly used enzyme, trypsin, cleaves the peptide bond on the carboxy side of arginine (R) or lysine (K) amino acids (with the exception of R/K that directly follow prolines). Consequently, each protein can be cleaved *in silico* to determine the sizes of all possible peptide fragments based on the enzyme used to digest the protein. The combination of the peptide fragments for any given protein observed by a mass spectrometer can then be compared to available peptide databases and used to assign an identification of the unknown protein according to the most likely candidate seen in the database queried. The pattern of peptides for each protein is known as the peptide mass fingerprint. It should be mentioned that for each mass spectrometry run, not all peptides injected into the mass spectrometer will be observed. This phenomenon is depicted in the MS trace shown in **(C)** which lacks the blue and orange coloured peptides. Standard MS peptide traces are plotted according to the ion intensity of each peptide versus the mass/charge (m/z) of each peptide. **(D)** In order to obtain actual amino acid sequence of peptides, the mass spectrometer must select a peptide of interest (in the case presented here, the second peptide, which is depicted in purple). The peptide is broken randomly into smaller peptides and individual amino acids via high energy collision induced dissociation (CID). Again, the data is presented according to the ion intensity versus the m/z for each peptide. Individual amino acid sequence can then be extrapolated from the difference mass between each peak which will correspond to the known m/z of an amino acid with or without post-translational modification.

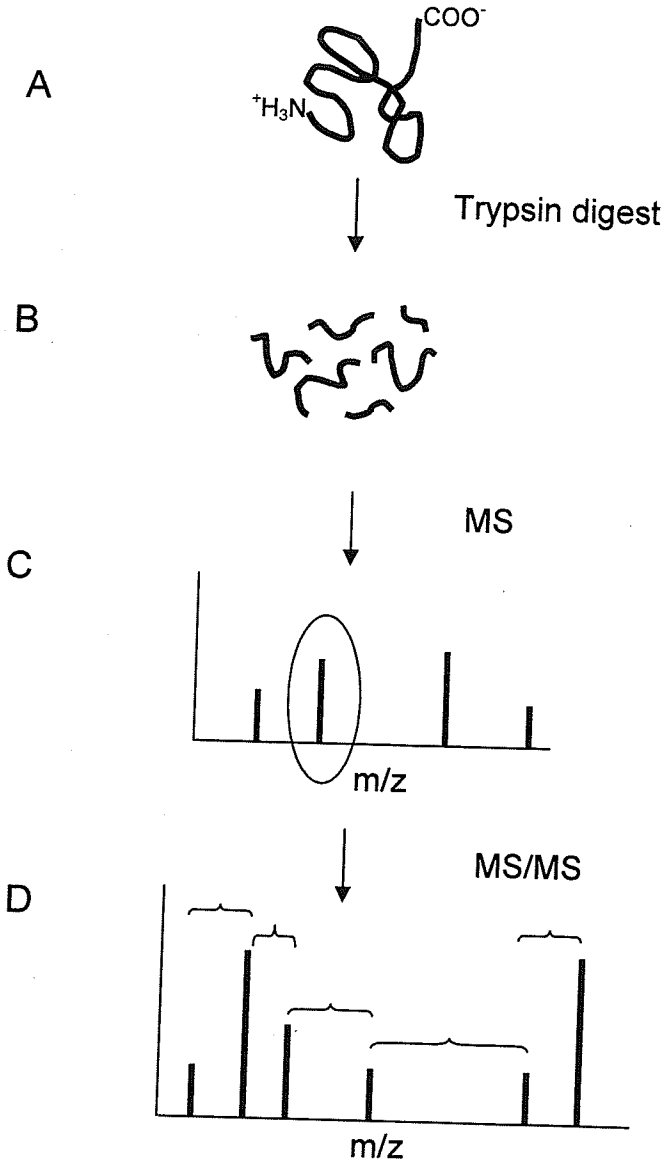
A
COO-
+H3N
Trypsin digest
B
MS
C
m/z
MS/MS
D
m/z

theoretical digests. One caveat is that protein and peptide sequence not currently available in public databases will not match to a given sequence and in this case manual interrogation of MS and MS/MS spectra is essential.

Mass spectrometry-based quantitative proteomics

Although dependant on the mass spectrometer and software employed, mass spectrometry-based methods are able to incorporate protein identification and protein quantification in the same workflow. As depicted in figure 4, there are two main branches of non-gel based methods, label based and label free (Ong and Mann, 2005). Label-based methods rely on the incorporation of labels at either the pre-extraction level through stable isotope labelling of amino acids in cell culture (SILAC) (Ong et al., 2002) or at the post-extraction level as with isotope coded affinity tags (ICAT) (Gygi et al., 1999a) or with iTraq™ (Ross et al., 2004; Chong et al., 2006; Wiese et al., 2007) and $^{16}O/^{18}O$ heavy oxygen labelling. Alternatively, gaining more interest are label free methods which are based on the extraction of relative peptide levels based on either the number of peptides seen for a given protein (emPAI) (Ishihama et al., 2005), or alternatively the extracted ion current for each peptide (Andersen et al., 2003).

Gel-based quantitative proteomics

The gold standard for protein separation and relative quantification for the past three decades has been two-dimensional electrophoresis (2DE). 2DE takes advantage of many characteristics of proteins and allows thousands of proteins

Figure 4. **Proteomic methods**. **(A)** Protein extracts are typically separated into various fractions by 2D electrophoresis or chromatography (shotgun). Protein identification is subsequently performed by mass spectrometry which provides peptide (peptide mass fingerprint, PMF) and amino acid sequence information (tandem mass spectrometry, MS/MS). **(B)** There are two main branches in order to characterize protein abundance differences between experimental conditions, gel-based and mass spectrometry-based. Gel-based methods have relied heavily on image morphing to overlay 2D gels visualized with various stains (i.e. Coomassie Blue, Silver Staining and Sypro Ruby) and use of image analysis software to compare protein staining intensities. The more recent advance of 2D difference-in-gel electrophoresis (DIGE) enables the co-electrophoresis of multiple samples thereby enabling more accurate spot mapping and comparisons. Moreover, the addition of an internal control on all replicate gels allows users to perform statistical analysis of protein abundance differences. Quantitative mass spectrometry based methods can be divided into at least two categories, label-free and label-based methods. emPAI quantification is based on the number of times a peptide is seen for each sample. The more abundant a protein is, the more often, more peptides will be seen. Alternatively, the extracted ion current can also be used to quantify how much protein is present in a sample. Label-based methods are more commonly used and are based on the addition of quantifiable reagents to samples. This can be achieved a three levels, first tissue culture cells can be grown in medium that contains heavy stable isotopes of lysine and/or arginine amino acids and compared to cells grown in normal medium (light isotopes) (SILAC). The second method relies on the labelling of proteins with isotope coded affinity tags with different masses (ICAT). Finally, tags of different masses can be added to peptides at the time of protein cleavage either through the addition of water that contains heavy isotopes of oxygen or addition of isobaric tags for relative and absolute quantification (iTRAQ). The major advantage of label-based methods is similar to the 2D-DIGE methodology which allows multiplexing of experimental samples, thereby reducing inherent standard errors.

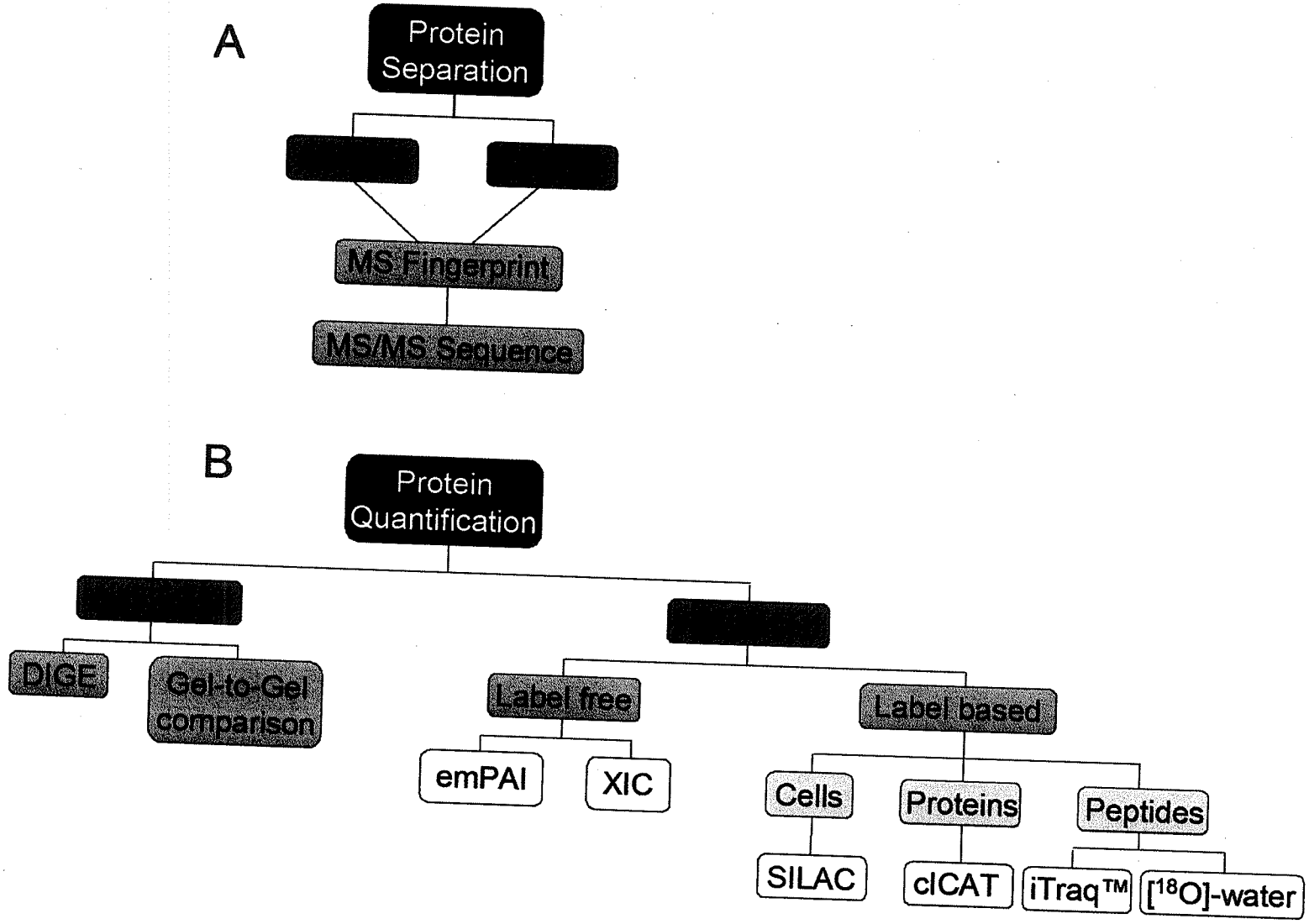
A
Protein Separation
MS Fingerprint
MS/MS Sequence
B
Protein Quantification
DIGE
Gel-to-Gel comparison
Label free
emPAI
XIC
Label based
Cells
SILAC
Proteins
cICAT
Peptides
iTraq™
[18O]-water

to be separated on a single high resolution gel. Separation is based on protein isoelectric point (pI) and molecular weight. First, proteins are separated based on their net charge (pI) using thin strip acrylamide gels containing a pH gradient.

Application of an electric current causes proteins to migrate through the immobilized gel until they reach the point at which their net charge is zero (pI) and therefore are no longer drawn towards either the anode or cathode (O'Farrell, 1975). Commercially available immobilized pH gradients (IPGs) originally described in 1982 (Bjellqvist et al., 1982), have shown excellent reproducibility and resolving power in the 1st dimension. Moreover, the advent of narrow range IPG strips (for example pH 5.0-5.6) have the ability to detect changes in pI of 0.001 allowing for even more detailed investigation of proteins and their associated isoforms (Gorg et al., 2004). Following protein separation in the first dimension, proteins are further separated based on their molecular weight by SDS-PAGE.

Once proteins have been separated, they are detected by various methods including staining (silver, coomassie or fluorescent stains) or radioactivity (via isotope incorporation). In order to obtain statistical information on replicate experiments, gel morphing software is used to match proteins from one gel to another. Although these methods are used extensively, there are problems with the limited dynamic range of some of the dyes typically used (Silver or Coomassie); but more importantly, accurate gel-to-gel matching and protein spot

boundary definition is difficult given inherent variations in running conditions and software interpolation. A more recent advance in the quantitative 2DE methodology is 2D difference-in-gel-electrophoresis (2D DIGE) (Unlu et al., 1997). Two critical components of DIGE are, (i), the ability to co-electrophorese up to three samples on the same gel thereby avoiding artefacts due to gel-to-gel variation and (ii), the ability to include a loading standard (in place of the third sample) that is representative of the entire sample being studied on all gel replicates. This allows for very accurate spot mapping and quantification between gel replicates. Figure 5 details the sequence of sample preparation, detection and quantification for a typical 2D DIGE experiment. It has been documented that 2D DIGE can detect 0.5fmol of an average sized protein based on the fluorescent properties of the cyanine derived protein labels (Cy2, Cy3 and Cy5). In addition, the large linear range of the CyDyes (1000-10,000 fold range) can accurately detect protein differences of as little as +/- 15%. Because the CyDyes are both charge and weight matched, samples that are labelled with any of the dyes will co-resolve on gels thereby ensuring accurate spot mapping (Karp et al., 2004; Shaw et al., 2003).

The ability to distinguish intact proteins from one another becomes especially crucial when investigating post-translational modifications, such as the case with the body of work presented here. Despite the rapidly increasing number of MS-based proteomic methods, to date, there is no single method by which to profile protein isoforms, more specifically isoforms generated by post-translational

Figure 5. **2D Difference-in-gel electrophoresis flowchart**. Protein samples are labelled with spectrally distinct, mass- and charge-matched fluorescent dyes. Sample labelled with Cy2 contains equal amounts of all protein samples used in 2D-DIGE analysis and serves as an internal control. Experimental samples are either Cy3 or Cy5 dye labelled and all three labelled protein samples are mixed together and co-electrophoresed by high resolution 2D-PAGE. Fluorescent protein patterns are visualized using an Imaging platform coupled with lasers (Typhoon Imager). Each channel can be viewed independent from the other and can also be overlaid. Protein maps are imported into the DeCyder software package which determines the protein spot boundaries on all gels within an experiment. Protein abundances are determined based on the fluorescent intensity of each spot and subsequently normalized to the internal control (Cy2 labelled pool). Volume abundances across each experimental condition are accessed and appropriate statistical analysis can be performed to determine if any protein abundances are consistently altered between experimental conditions. After analysis the proteins of interest are excised from gels and identified by mass spectrometry.

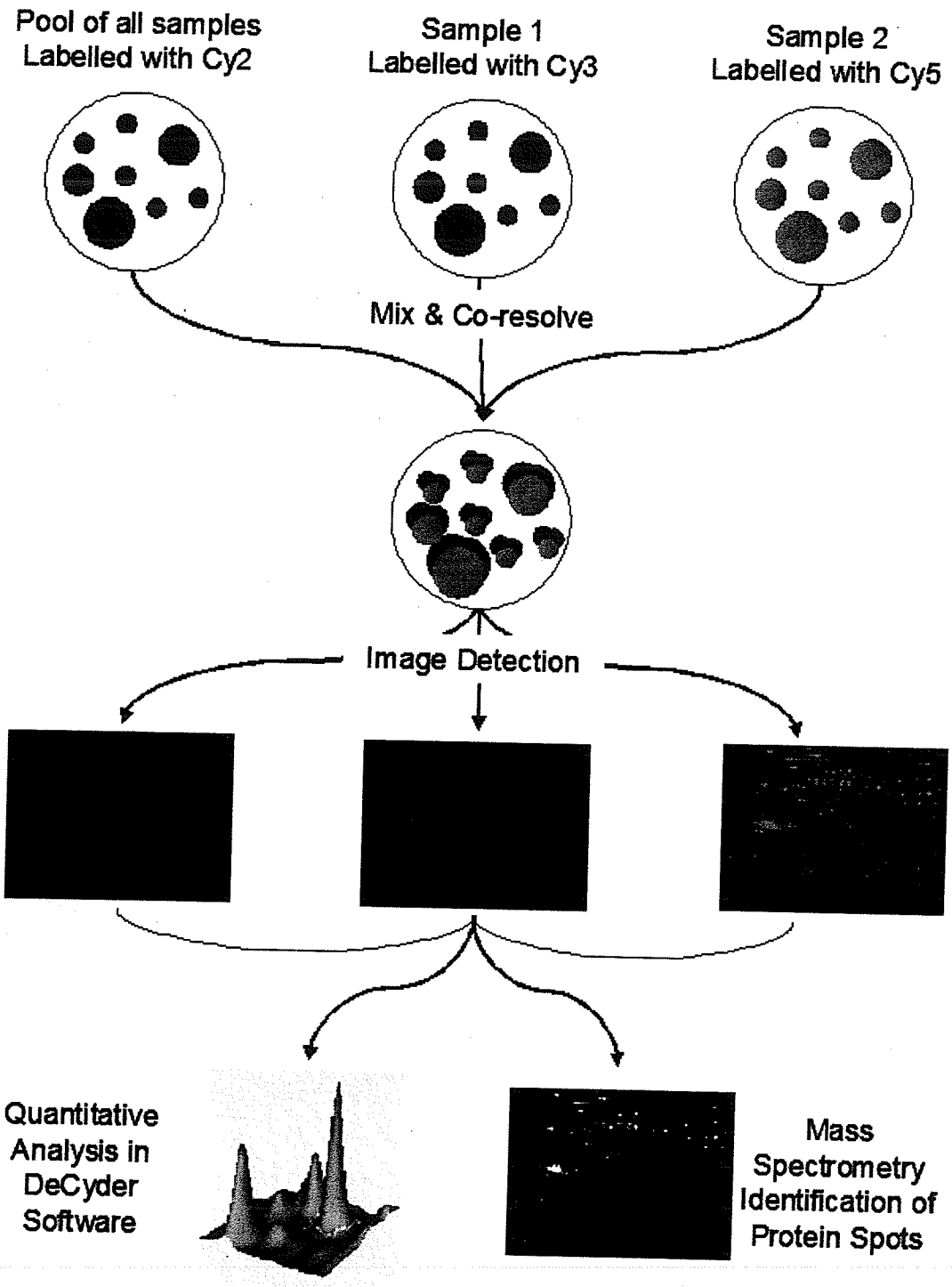
Pool of all samples
Labelled with Cy2
Sample 1
Labelled with Cy3
Sample 2
Labelled with Cy5
Mix & Co-resolve
Image Detection
Quantitative
Analysis in
DeCyder
Software
Mass
Spectrometry
Identification of
Protein Spots

modifications such as phosphorylation (phosphoproteomics) and degradation specific functional changes of proteins (degradomics). It is for these reasons that the analysis performed in this thesis has utilized a gel-based approach to characterize the phosphoproteome changes induced by HCV viral proteins and replication.

Previous HCV proteomic studies

The large majority of studies previously looking at changes in protein levels in HCV infection have focused on potential biomarkers of HCV disease, more specifically, protein expression changes that demarcate transitions from primary fibrosis and hepatocellular carcinoma. A common theme has evolved whereby increases in the HSP70 family of chaperones and impairment of common mitochondrial processes such as fatty acid oxidation and oxidative phosphorylation are linked to disease progression (Takashima et al., 2003; Yokoyama et al., 2004; Jacobs et al., 2005; Diamond et al., 2007). Studies that have investigated the cellular proteome changes due to the expression of single HCV proteins or subgenomic/full length HCV replicons have been more limited. One such study investigated the changes to the lipid raft proteome in cells expressing full-length replicon genotype 1b HCV. Using comparative 2DE (silver staining) and SILAC analysis, Mannova and colleagues (2006) isolated lipid rafts from cells expressing the HCV 1b replicon or a cell line expressing the selectable marker, G418. They found increases in proteins responsible for vesicle transport and protein trafficking including Rab GTPases, TER ATPase and translation

proteins hnRNP K and eIF3. Two potential reasons for these observed changes are; one, virus replication overwhelms the cell and thus the host cell deals with the overabundance of exogenous protein by increasing proteins involved in these pathways presumably to target the viral proteins for degradation, or two, the virus enhances the cellular retrograde transport system for its own use. Although this study used the replicon model, which does not package and release progeny virions, it does not preclude the possibility that the viral proteins subvert trafficking mechanisms of the cell in order to efficiently release virions (Mannova et al., 2006).

Another research group isolated detergent-resistant membrane fractions which have been reported to be the site of virus replication complexes (Yi et al., 2006). In this study which utilized comparative 2DE (silver stained gels), the group found an increase in protein abundance for 60 protein species and a decrease for 14 protein species in cells supporting subgenomic replicon propagation. It should be mentioned that although Yi and colleagues used large format 2DE analysis, the comparison of mock and replicon cell lines was based on differences in silver staining intensities, a stain that has a limited dynamic range of ~10^2. Particular focus in this study was the ras-GTPase-activating protein binding protein 1 (G3BP1) which was shown to be important to efficient HCV genome replication as the authors showed that siRNA mediated inhibition of G3BP1 resulted in a dramatic decrease in HCV replication (Yi et al., 2006). Finally, a more global proteomic approach that used both coomassie and silver staining comparison of

2DE from cells expressing the subgenomic replicon, found 179 differentially expressed proteins. A number of ER-resident proteins were altered, including stress-related proteins such as HSP70, HSP60 and GRP78 (Fang et al., 2006). Unfortunately, as with the study done by Yi and colleagues (2006) previously mentioned, comparative analysis was based on silver staining intensities. To this point, there have been no studies evaluatin the effects of JFH1.

The expression of HCV elements results in changes to host protein phosphorylation. It is highly likely that there are other phosphorylation changes which have not been characterized to this point and using a global quantitative proteomic analysis will reveal novel protein phosphorylation changes. The subsequent sections of this thesis describe the following:

Chapter III:

A Comparison of Immobilized Metal- and Immunoaffinity-based Methods for Capturing the Global Phosphoproteome: Evaluation of methods commonly used for phosphoprotein capture.

Chapter IV:

Alterations to the host cell phosphoproteome induced by a HCV subgenomic replicon: 2D-DIGE analysis of phosphoproteins enriched from parental Huh7.5 cell lines and two independently derived subgenomic replicon cell lines.

Chapter V:

Phosphoproteome alterations to Huh7.5 cells infected with hepatitis C virus: 2D-DIGE analysis of phosphoproteins enriched from HCV- and mock-infected cell lines.

CHAPTER II: MATERIALS AND METHODS

Please refer to Appendix I for detailed product information
Please refer to Appendix II for detailed solution recipe information

Cell culture

Human hepatoma Huh7.5 cells (kindly provided by Dr. Charles Rice, Rockefeller University, NY) were maintained in Dulbecco's modified Eagle's medium supplemented with nonessential amino acids, 10U/mL penicillin + 10ug/mL streptomycin and 10% fetal calf serum. For cell lines containing HCV replicons or the neomycin cassette, 0.5mg/ml Geneticin® (G418) was added to the medium. All cell lines were maintained at 37°C, 5% CO_2

Phosphoprotein enrichment for IMAC and immunoaffinity capture

Cells were seeded 20-24 hours prior to harvest at 8 x 10^6 cells/15cm dishes. Prior to lysis, cells were washed three times with HEPES buffered saline. Cells were harvested with a rubber policeman either before lysis (IMAC, BD Clonetech) or post lysis (immunoaffinity, Qiagen). Phosphoprotein enrichment was performed in pairs using both antibody and IMAC affinity as per manufacturer's protocols. Briefly, for immunoaffinity purification, protein lysates were diluted to 0.1mg/mL and a total of 2.5mg was applied to the resin. Non-specific proteins were washed from the column with 3x2mL phospholysis buffer and phosphoproteins were eluted in 4x1mL fractions. 2.5mg of undiluted protein lysates were added to the IMAC resins and incubated while shaking at 4°C for 20min. Non-specific proteins were removed from the column by 4x4mL washes

with phospholysis buffer and phosphoproteins were collected in 4x1mL fractions using phosphoprotein elution buffer. Purification pairs were performed on four separate occasions (Fig. 6). After phosphoprotein purification, samples were concentrated using Amicon Ultracel columns (MW cut-off 3000Da). Phosphoprotein enriched samples were desalted and concentrated using a 2D Clean-Up Kit (GE Healthcare) and resuspended in lysis buffer (7M Urea, 2M Thiourea, 4% CHAPS, 30mM Tris, pH 8.5). Protein concentrations were determined using the 2D Quant Kit and the pH of the sample was adjusted to be within the range of 8-9 for optimal CyDye labelling by adding 1N NAOH when necessary.

Phosphoprotein purifications performed for the subgenomic replicon (Fig. 7) and HCV-infected (Fig. 9) cell lines were performed as above, but were performed exclusively by immunoaffinity capture.

Immunoblots

Clarified cell lysates or phosphoprotein enriched samples were separated on SDS-PAGE mini-gels (varying percentage acrylamide, 10%, 12%, 10-20% gradient gels, handcast and Invitrogen NuPAGE gels). All samples were concentrated using Amicon Ultracel columns (MW cut-off 3000Da) and quantified by Bradford Dye analysis or 2D Quant. Equal protein loads (typically 0.5-25µg/well) were used for each sample well unless otherwise specified. Western blotting was performed using the iBlot dry transfer system (Invitrogen). Nitrocellulose membranes were blocked overnight at 4°C in blocking solution (5%

Figure 6. **Comparison of phosphoprotein enrichment techniques**. Cells were seeded in 15cm dishes for immobilized metal affinity chromatography (IMAC, BD Clonetech) or immunoaffinity (Qiagen) purification 24 hours prior to cell harvest. Phosphoproteins were purified by IMAC or immunoaffinity according to the manufacturer's protocols. Phosphoprotein enriched samples were precipitated and concentrated using the 2D Clean Up Kit (GE Healthcare) and processed by 2D-DIGE as described in Fig. 5. The entire protocol listed above was performed four independent times and phosphoprotein samples from IMAC and immunoaffinity purification were compared to one another.

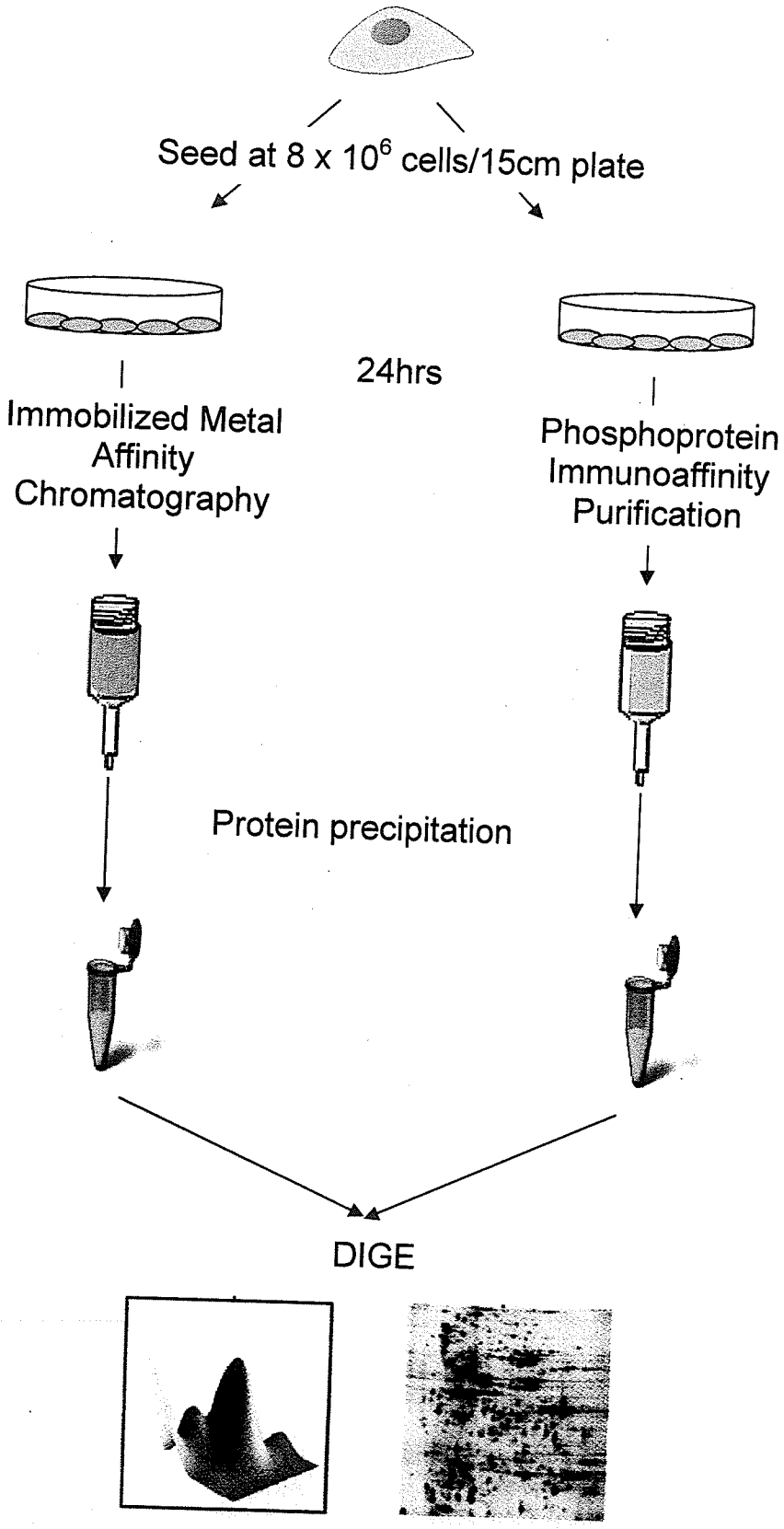
Seed at 8 x 10^6 cells/15cm plate
24hrs
Immobilized Metal Affinity Chromatography
Phosphoprotein Immunoaffinity Purification
Protein precipitation
DIGE

carnation skim milk powder in TBS, 0.1%Tween 20) then incubated with primary and secondary-HRP conjugated antibodies in the same solution. For phosphoprotein Immunoblots, a different blocking solution was employed which contained 5% bovine serum albumin in TBST. Chemiluminescent detection was carried out using Immobilon Western detection as recommended by the manufacturer (Millipore).

Protein labelling with CyDye fluors

Phosphoprotein enriched samples were labelled with Cy2, Cy3, and Cy5 following the protocols in the Ettan DIGE System User Manual (18-1173-17 Edition AA, GE Healthcare). Briefly, 50ug of lysate was labelled with 400pmol of dye. Labelling reactions were carried out for 30min followed by a 10min lysine quench (1uL of 10mM lysine). Samples were then mixed and reduced with 130mM DTT in an equal volume of 2X sample/rehydration buffer for 10min and then sample volume was increased to 450µL with 1X sample/rehydration buffer. All reactions were carried out in the dark on ice. The labelled samples were then used for 2D-DIGE analysis. The pooled standard contained an equal protein amount from each sample in the dataset and served as an internal standard.

Two-dimensional gel electrophoresis

Labelled proteins were separated on an IPGphor isoelectric focusing unit using 24cm pH 4-7 IPG strips in the dark using the following profile: 10hrs passive rehydration, 4hrs 300V, 0.5kVh stepped to 500V, 1.0kVh gradient to 1000V, 13.5kVh gradient to 8000V, 45kVh stepped to 8000V. Prior to the second

dimension run, IPG strips were reduced and alkylated in SDS equilibration buffer (50mM Tris-HCl, pH 8.8, containing 6M Urea, 30% v/v glycerol, 2% w/v SDS and 0.002% w/v bromophenol blue) for 15 min each in 1% w/v DTT followed by 2.5% w/v IAA. Samples were electrophoresed on 26cm x 20cm x 1mm precast 10-20% gradient Optigels (nextgensciences) using the Ettan Dalt 6 Electrophoresis System (GE Healthcare). Gels were run in the dark at 10°C at constant power (2W/gel) overnight. In the morning, the power was increased to 100W and gels were run for 20min following migration of the bromophenol blue dye front off the gel bottom.

2DE image analysis and post-staining

The gels were imaged directly between low fluorescence glass plates on the Typhoon 9400 variable mode imager (GE Healthcare) with the following settings; resolution 100microns, sensitivity 450-600V. The DIGE images were previewed with ImageQuant software to ensure the absence of dye saturation. After image acquisition, the gels were fixed overnight in a solution containing 40% methanol and 10% acetic acid. Gels were then stored at 4°C until further processing. Finally, gels were subjected to mass-spectrometry compatible silver staining as described by Yan *et al.* 2000 (Yan et al., 2000).

DeCyder analysis

DeCyder v.5.02 was used to analyze the DIGE images as described in the Ettan DIGE User Manual (GE Healthcare). DIGE images were cropped in ImageQuant to remove gel boundaries and then each image underwent spot detection in the

differential in-gel analysis (DIA) module without any restrictions set. For each gel an average of 2000 spots were detected. Next, the matched gels from DIA were exported to the biological variation analysis (BVA) module. The Student's t-test was performed to give statistical confidence of the analysis. Only statistically significant spots ($p < 0.05$) were evaluated further.

In-gel tryptic digestion

Proteins of interest identified in DeCyder analysis were manually excised from preparative Coomassie stained gels and silver stained DIGE gels and transferred to siliconized 1.5mL tubes (Diamed). Silver stained samples were destained with a 1:1 ratio of 30mM potassium ferricyanide:100mM sodium thiosulfate as per Gharahdaghi *et al.* (Gharahdaghi et al., 1999). Gel spots were rehydrated in 5ng/uL sequencing grade trypsin gold (Promega) in 50mM ammonium bicarbonate and incubated overnight at 37°C. Digested peptides were extracted with 0.1% formic acid/50% acetonitrile and dried by vacuum centrifugation without heat.

Mass spectrometry and database searching

Peptides were analyzed by LC/MS/MS using nanoflow HPLC (Agilent 1100) system configured with a C_{18} pre column (Agilent) and a C_{18} analytical column, The aqueous mobile phase (solution A) contained 5% acetonitrile and 0.1% formic acid, and the organic mobile phase (solution B) contained 98% acetonitrile and 0.1% formic acid. 5µL of sample were loaded and washed on the pre column

for 5min with solution A at 50μL/min, and then peptides were eluted off the pre column and through the analytical column with a 125min gradient from 1% to 40% solution B, 5min gradient from 40% to 95% solution B and a 5min rinse with 95% at a flow rate if 250nL/min. Elutted peptides were injected via nanospray source into a QStar XL Qq-TOF (Applied Biosystems) coupled with a 50μm inner-diameter, fused silica needle with a 15μm tip (PicoTip Emitter, New Objective). Information-dependent data acquisition was used with a 10sec cycle: 1sec interval for intact peptide signal (MS) and 3x3sec intervals for collision-induced dissociation of the 3 most intense peptide signals in the initial 1sec MS scan (MS/MS). The MS m/z range was 350-1500, and the MS/MS m/z range was 70-2000. Collision energy was automatically determined by the data acquisition software (Analyst QS 1.1). MS/MS data was acquired for the entire LC run. Database searching was performed using Mascot (Matrixscience) on SwissProt database version 55.6 with the following parameters: *homo sapiens*, unrestricted molecular weights and pIs, fixed modification=carbamidomethylation and variable modification=methionine oxidation. One missed trypsin cleavage was allowed.

Generation of stable subgenomic replicon cell lines

The HCV subgenomic replicon pHCVreplicon1b.BB7 plasmid (a gift from Dr. Charles Rice, Rockefeller University, NY) was linearized with ScaI and purified using QIAEXII resin (Qiagen). Plasmid DNA was *in vitro* transcribed using T7 RNA polymerase (RiboMAX large scale RNA, Promega) followed by treatment with 1U/μg RNase-free DNase and purified using QIAEXII resin. Five micrograms

of RNA was transfected into approximately 3 x 10^6 Huh 7.5 cells in 10cm dishes using TransMessenger™ transfection reagent and 24 hours post transfection G418 selection was applied (1mg/ml). Two independent polyclonal cell lines (Huh7.5 RI and Huh7.5 RII) were generated in this manner. Huh7.5 NeoR was generated by transfection of 1µg pSV2Neo (BD Clonetech) with Effectene transfection reagent (Qiagen) followed by G418 selection (1mg/ml) (Fig. 2). Phosphoproteins were enriched from Huh7.5, Huh7.5 RI, Huh7.5 RII and Huh7.5 NeoR cell lines as per Figs. 6 and 7.

HCV propagation

JFH1 coding plasmid (a kind gift from Dr. T. Wakita, TIID, Japan) was linearized with XbaI and purified using QIAEX II resin. Linear DNA was treated with 5U/µg KLENOW followed by *in vitro* transcription using T7 polymerase (T7 RiboMAX express, Promega) as previously described in Wakita *et al.* 2005 (Zhong et al., 2005). *In vitro* transcripts were treated with 1U/µg RNase-free DNase and purified using RNease® MinElute™ Cleanup kit (Qiagen). Ten micrograms of *in vitro* transcribed RNA was electroporated into Huh7.5 cells as per Lindenbach *et al.* 2005 (Lindenbach et al., 2005). In brief, 6.0 x 10^6 cells were washed with ice-cold PBS and mixed with 10µg HCV RNA and electroporated in 0.2cm gap cuvettes for five pulses of 99µsec at 820V over 1.1 seconds on an ECM electroporator (BTX). Following a 10min recovery, transfected cells were seeded into T75 flasks with 20% FBS supplemented DMEM and cells were passaged for three weeks. Culture supernatants were harvested and concentrated by addition of 1/4th volume 40% P.E.G. 8000, followed by end-over-end incubation overnight

Figure 7. **Alterations to the cellular phosphoproteome induced by the expression of a HCV subgenomic replicon.** Two control cells lines (Huh7.5 and Huh7.5 NeoR) were compared to two independently derived HCV subgenomic replicon cell lines (Huh7.5 RI and Huh7.5 RII). Huh7.5 cells are a derivative of human hepatocyte Huh7.0 cells that are highly permissive to HCV infections and replicon propagation. Huh7.5 NeoR cells are Huh7.5 cells that were stably transfected with a neomycin phosphotransferase gene. Huh7.5 RI and RII cell lines were generated by selection for the HCV subgenomic replicon as per Fig. 2. Each cell line was seeded in 15cm plates 24 hours prior to harvest. Phosphoproteins were enriched for by phospho-immunoaffinity chromatography (Qiagen). The purification of phosphoproteins was performed three times independently and then all samples were processed by 2D-DIGE analysis.

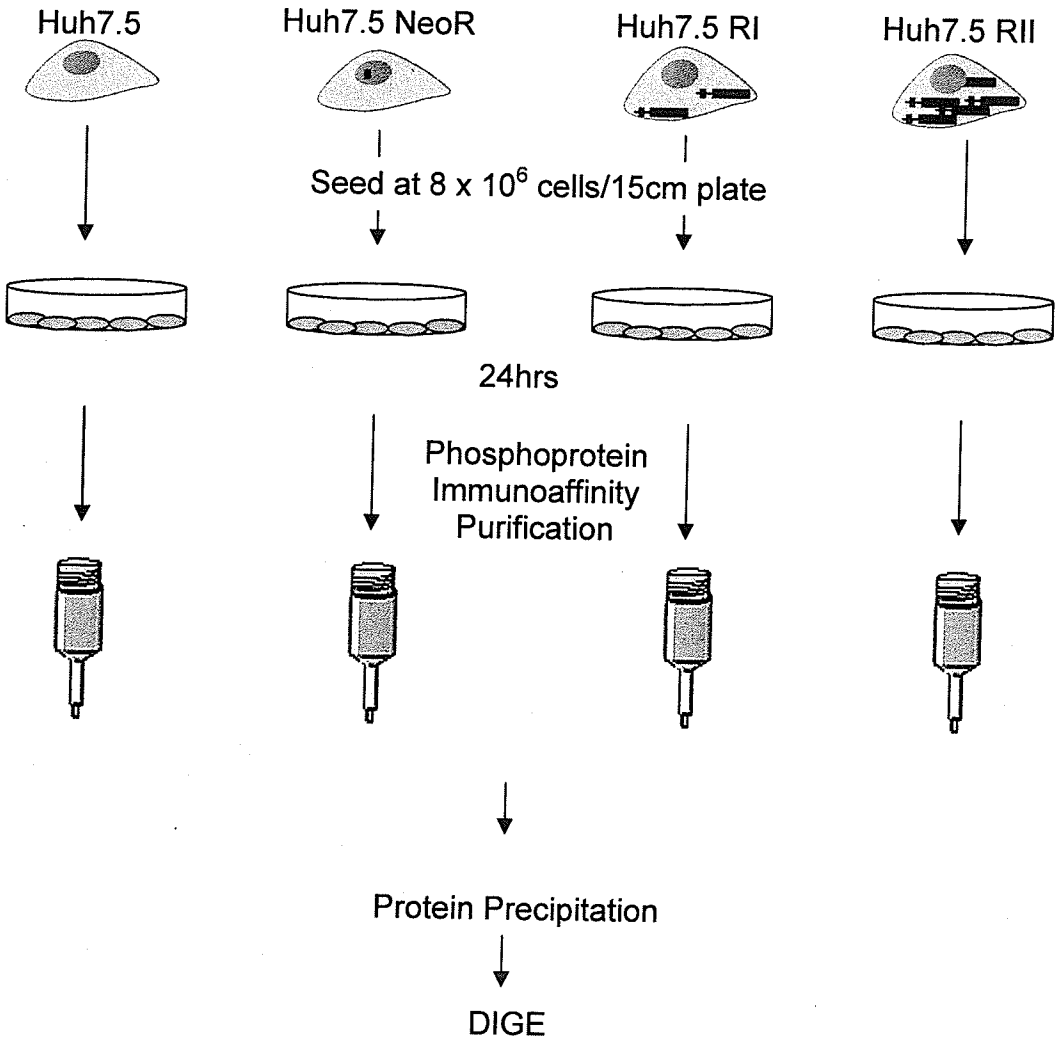
Huh7.5
Huh7.5 NeoR
Huh7.5 RI
Huh7.5 RII
Seed at 8 x 10^6 cells/15cm plate
24hrs
Phosphoprotein
Immunoaffinity
Purification
Protein Precipitation
DIGE

at 4°C and precipitation by centrifugation at 8000xg for 15min, as per (Lindenbach et al., 2005) to create virus stocks. Virus stocks were passaged 5 times to obtain a high titre stock ranging between 1 and 4 x 10^6 focus forming units/mL (ffu/mL) determined by indirect immunofluorescence (Fig. 8). Phosphoproteins were enriched from mock- and HCV-infected Huh7.5 cells as per Figs. 6 and 9.

Virus titre and indirect immunofluorescence

Huh7.5 cells were seeded in 96 well tissue culture plates at 1 x 10^3 cells per well. Four hours post seeding, cells were infected with 100µl dilutions of virus stocks (in serum free culture medium) and incubated for 1hr at 37°C, 5% CO_2. Virus inoculums were replaced with fresh culture medium containing 10% FBS and infection proceeded for four days. After culture medium was removed, cells were washed twice with PBS and then fixed with ice-cold methanol at -20°C for 20min. Cells were permeabilized and blocked for 1hr (in IFA blocking solution), followed by primary antibody (anti-NS5A 9E10) incubation overnight at 4°C as per Lindenbach *et al.* 2005 (Lindenbach et al., 2005). Cells were then incubated with secondary anti-mouse antibody conjugated with Alexa fluor 488 for 1hr and then nuclei were counterstained with DAPI. Cells were imaged on an AxioVert 200M microscope (Zeiss) coupled with the AxioCamMRc camera (Zeiss). Images were processed using AxioVision software version 4.5 (Zeiss). The highest dilution of virus stock which contained between one and ten infection foci per field of view at 100X magnification was used to determine virus. A similar protocol was

Figure 8. **Transfection and propagation of hepatitis C virus, strain JFH1 (genotype 2a).** The cDNA of the JFH1 strain of HCV was cloned into an expression vector containing a T7 promoter and drug selection marker. The JFH1 plasmid was produced and provided by the Wakita lab (Japan) (Wakita, Pietschmann, Kato, Date, Miyamoto, Zhao, Murthy, Habermann, Krausslich, Mizokami, Bartenschlager, & Liang, 2005). **(A)** Purified vector DNA was linearized and *in vitro* transcribed with T7 polymerase. **(B)** HCV RNA was transfected into permissive cells by electroporation. **(C)** Cells transfected with HCV RNA were expanded for approximately 4 weeks. **(D)** Supernatant from transfected cells was collected and virus precipitated and concentrated by centrifugation with polyethalene glycol. **(E)** Naïve cells were incubated with concentrated virus containing supernatant and passaged for 4-5 days and supernatants collected and concentrated as before. Steps **D-E** were repeated five times in order to acquire high titre virus stocks (~10^6 focus forming units/mL based on indirect virus specific immunofluoresence).

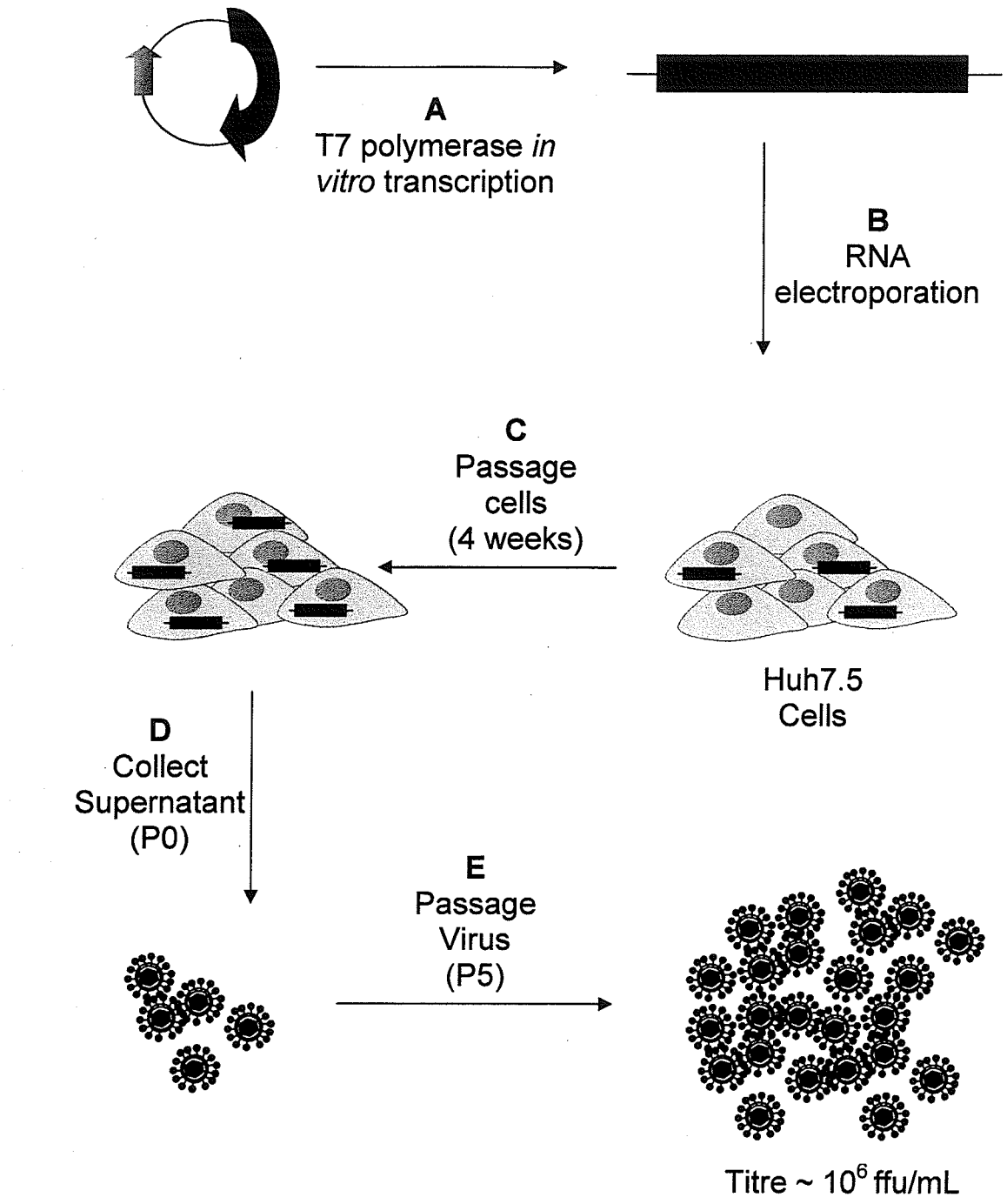
A
T7 polymerase *in vitro* transcription
B
RNA electroporation
C
Passage cells (4 weeks)
Huh7.5 Cells
D
Collect Supernatant (P0)
E
Passage Virus (P5)
Titre ~ 10^6 ffu/mL
Ampicillin Resistance Marker
HCV full coding sequence

Figure 9. **Alterations to the cellular phosphoproteome induced by HCV infection.** Cells were seeded in 15cm plates 24 hours prior to incubation with HCV (multiplicity of infection ~1) or mock purified supernatant. Four days post infection, cells were divided in half and then harvest for phosphoprotein purification by immunoaffinity chromatography the following day. The purification of phosphoproteins from mock- and HCV-infected cells was performed on three separate occasions and then all samples were simultaneously processed by 2D-DIGE analysis.

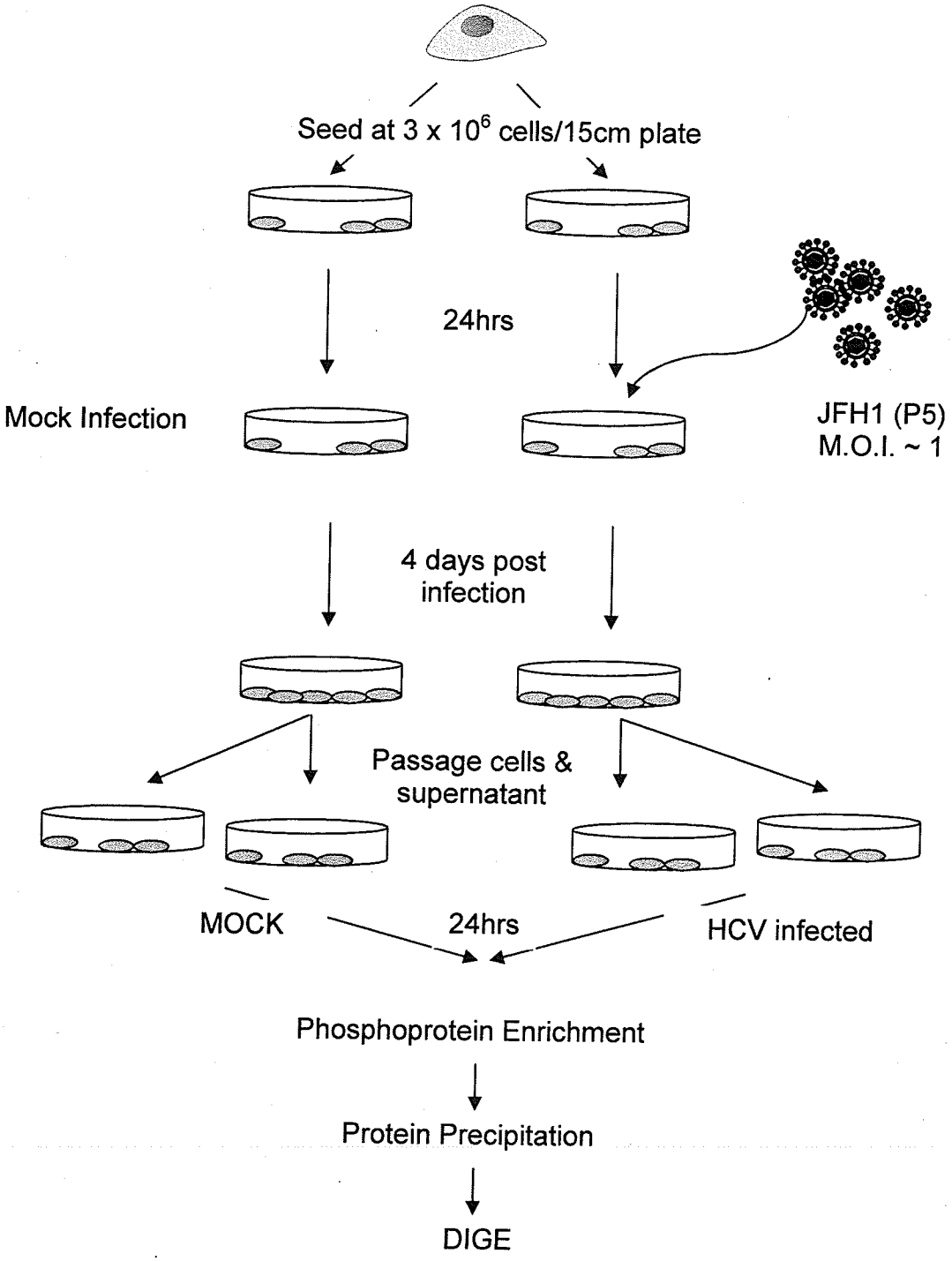
Seed at 3 x 10^6 cells/15cm plate
24hrs
Mock Infection
JFH1 (P5)
M.O.I. ~ 1
4 days post infection
Passage cells & supernatant
MOCK
24hrs
HCV infected
Phosphoprotein Enrichment
Protein Precipitation
DIGE

followed to assess the extent of infection in Chapter V with the exception that infected cells were seeded in 6 well tissue culture plates at 3 x 10^5 cells per well and the infection was halted one day post seeding (which corresponded to 5 days post infection).

HCV infection

3 x 10^8 Huh7.5 cells were plated in 15cm culture dishes and infected with JFH1 at a multiplicity of infection (m.o.i.) of 1 or mock infected with naïve cell supernatant that was precipitated in the same manner as virus stocks (performed in triplicate). Four days post infection; cells were split into two dishes and then harvested at five days post infection and phosphoproteins were immunoaffinity purified as detailed above (Fig. 6).

Additional materials and methods to each chapter are provided in their corresponding sections.

CHAPTER III: A Comparison of Immobilized Metal- and Immunoaffinity-based Methods for Capturing the Global Phosphoproteome

Abstract

Phosphorylation plays a critical role in most biological functions; however, it remains difficult to study given the potentially transient nature of the modification as well as the low abundance phosphorylated proteins represent in the cell. The aim of this work was to characterize two commonly used phosphoprotein purification methods, immobilized metal affinity chromatography (IMAC) and immunoaffinity, employing 2D-DIGE technologies in order to make direct comparisons of the two techniques. Phosphoproteins were purified from human liver cell line lysates and the proteome profiles were compared using DeCyder analysis. On average, 923 protein spots were consistently observed between both methods, of which 31 proteins differed in their relative abundance by at least 3.5 fold between IMAC and immunoaffinity purifications. Twenty-eight of the differentially purified proteins were subsequently identified by LC-MS/MS. Multiple proteins from the heterogeneous nuclear ribonucleoprotein and T-complex protein families were purified to high levels by IMAC but were virtually undetectable following immunoaffinity purification. Furthermore, a marker for non-phosphorylated protein was also purified by IMAC but not immunoaffinity. Although the phosphoproteomes purified by both methods were very similar, use of either purification technique must be dictated by the ability of the technology to capture phospho-species relevant to the study at hand.

Introduction

Phosphorylation is a critical post-translational modification used by eukaryotic cells to regulate many processes including cell cycle progression, signal transduction, transcription, cytoskeletal rearrangement, apoptosis, differentiation, movement and immune function (Raggiaschi et al., 2005). Although phosphorylation is a highly dynamic process due to the opposing actions of protein kinases and phosphatases, it is estimated that at any given time, at least 10% of the proteome is phosphorylated on serine (S), threonine (T) and tyrosine (Y) residues at a ratio of 1000:100:1 (Hunter, 1998). Given the extensive function phosphorylation plays in cell homeostasis, it is not surprising that its deregulation has been implicated in many human diseases including cancer (Clarke, 2003; Emaduddin et al., 2008), neurodegenerative disorders (Geschwind, 2003) and infectious agent pathogenesis (Jakubiec and Jupin, 2007; McDowell and Sacks, 1999; Schulze zur et al., 2003; Deutscher and Saier, Jr., 2005).

Traditionally, phosphoproteins have been detected using phospho-specific antibodies, stains (ProQ Diamond) or by labelling cells with $\gamma^{32}P$. While these techniques are relatively specific and sensitive they can suffer deficiencies when investigating the global phosphoproteome. Although increasing rapidly, the number of phospho-antibodies is incomplete and, while ProQ Diamond staining may be able to detect phosphoproteins regardless of sequence content, a certain degree of non-specificity exists (Gorg et al., 2004; Stasyk et al., 2005). Labelling with $\gamma^{32}P$, which is both extremely sensitive and specific but requires special

containment and disposal facilities and, at least for global proteomic analysis, typically requires *in vivo* labelling. In addition to these problems, subsequent protein identification of phosphoproteins from a complex mixture which is predominantly composed of non-phosphorylated proteins is a daunting task. The identification of phosphorylation sites by tandem mass spectrometry (MS/MS) has aided in addressing many of the issues mentioned above (Beausoleil et al., 2004; Beausoleil et al., 2006; Molina et al., 2007; Olsen et al., 2006). However, given the peptide centric nature of MS/MS analysis, information pertaining to differences in protein isoforms due to multi-site phosphorylation or to phosphorylation in combination with other post translational modifications at different sites in the protein, is typically lost.

Regardless of the detection method used, the separation of phosphorylated species from non-phosphorylated species is warranted in order to increase the sensitivity and specificity of phosphoprotein studies. To this end, different purification techniques have been developed to assist in global phosphoprotein capture based on chemical (metal affinity and strong anion exchange chromatography) or biological (antibody) principles. Anion exchange or immobilized iron (Fe3+), nickel (Ni2+) or titanium (Ti2+) resins selectively enrich for protein or peptide species containing a negative charge. Although simple to implement, the potential lack of specificity towards phosphorylated proteins remains a concern. In contrast, phospho-specific antibodies may be more specific for phosphoprotein enrichment, although, only the phospho-tyrosine (pY)

proteome has been successfully enriched for by using a single antibody capable of global capture (Yeung et al., 1998). To date, no single phospho-serine (pS) or phospho-threonine (pT) antibody has been developed. This is predominantly due to the weak antigenicity of serine and threonine residues and therefore surrounding amino acid motifs are required to obtain stronger antigen-antibody interaction (Kaufmann et al., 2001). Because of this, phosphoproteome enrichment performed by immunoaffinity requires a mixture of antibodies, each capable of recognizing several sequence motifs.

Although reports have been published using either antibody or metal-affinity for global phosphoproteome capture, there has to date been no comparison of the two techniques with respect to their sensitivity, specificity and bias towards the subsets of proteins that are captured. In this study, the phosphoproteome of human liver cell extracts was compared following enrichment by two different capture methods: antibody or immobilized metal affinity chromatography (IMAC). Purified proteins were differentially labelled with CyDyes in order to directly compare the captured proteins by 2D DIGE (Unlu et al., 1997; Karp et al., 2004). Despite the different physiochemical properties of both resins, the two methods captured 95% of the same proteins both qualitatively and quantitatively. Thirty-one proteins were differentially captured by the two resins (>3.5 fold difference), 27 of which were consistently in greater abundance following IMAC purification. Subsequent identification by mass spectrometry did not reveal any particular sequence attribute that could impart the observed differential specificity.

Treatment of the captured proteins with lambda phosphatase indicated that most of the proteins captured by either method were in fact phosphoproteins. However, for at least one of the proteins preferentially captured by IMAC, we were unable to detect phosphorylation consistent with current literature and this may represent inappropriate capture of a non-phosphorylated protein.

Additional Methods

DeCyder Analysis

Proteins that were detected on at least 3/4 gel replicates and differed in abundance (volume ratio $\geq$3.50 fold) between antibody and IMAC purifications based on the difference-in-gel analysis software module (DIA) were excised for identification by mass spectrometry.

Mass spectrometry

The SwissProt database version 55.4 was queried for protein identifications.

Immunoblots

Clarified cell lysates used for phosphoprotein purification (total cell lysate and phospho-enriched samples) were separated on 10% NuPAGE Bis-Tris minigels (Invitrogen). Equal amounts of immunoaffinity- or IMAC-purified protein were loaded into each well unless otherwise noted (typically 0.5ug of protein was loaded per lane for starting lysate samples and 5ug of protein was loaded per lane for phosphoprotein enriched samples). The primary AKT (Ser/Thr) Akt

Substrate antibody was diluted in 5% BSA/TBS, 0.1% Tween 20 and all other antibodies were diluted in blocking solution (5% skim milk/TBS, 0.1% Tween 20).

Results

Due to the critical role phosphorylation plays in most areas of cell biology, methods to enrich for phosphorylated proteins that are both sensitive and specific are extremely important regardless of whether top-down or bottom-up approaches are ultimately used. Although many procedures exist for capturing and validating phosphorylated proteins, the majority of these are performed at the peptide level using MS and MS/MS. Nevertheless, when working with digested samples, information pertaining to protein isoforms is lost and therefore approaches which maintain proteins in an intact state are highly desirable. At a global level, it is not clear which method of enrichment would ensure high yield while still maintaining specificity. Of the two commonly used methodologies, chemical and antibody-based, I hypothesized that phospho-S/T/Y antibody-based resins would provide the highest specificity for phosphoprotein capture but would have lower global capture potential due to the requirements for additional amino acid residues in the context of antibody binding. In contrast, IMAC has capture specificity for the negative charge associated with phosphate groups, and therefore has a greater likelihood to bind a more diverse group of phosphoproteins but with potentially less specificity as other net negatively charged elements may also be bound including highly acidic proteins. The availability of commercially produced kits; IMAC- (BD Clontech) and Ab-based

(Qiagen) simplifies the process of phosphoprotein enrichment allowing for a consistent comparison of the two techniques. Both methodologies were evaluated for their sensitivity and specificity in this article.

Immunoaffinity capture and immobilized metal affinity chromatography enrich for phosphorylated proteins

In order to determine the efficiency and specificity of the two phosphoprotein capture methods human hepatoma cells (Huh7.5) were grown to sub-confluent monolayers (~75%) and proteins were extracted according to the manufacturers' recommended protocols. Both methods enriched for approximately the same amount of protein, representing 8.14% (+/- 1.33%) of total input protein from the IMAC resins and 8.24% (+/- 0.56%) from the immunoaffinity resins.

Starting lysates, column flow-through and purified fractions were evaluated by Western blot analysis with antibodies specific to phosphorylated substrates of the cell signalling molecule Akt or Hsp60. Akt is known to phosphorylate a number of different cellular targets (Manning and Cantley, 2007) and serves as a control for phosphoprotein enrichment. In contrast, while some evidence suggests Hsp60 can be phosphorylated at S70 (Beausoleil et al., 2006) and Y227(Rush et al., 2005), it is considered a rare event and at best tissue specific and therefore serves as a marker for non-phosphorylated protein (Khan et al., 1998). Starting lysates or column flow-through from either immunoaffinity or IMAC methods detected little, if any phospho-Akt substrates (Fig. 10A, lanes 1, 2, 4, 5).

Figure 10. **Detection of phosphorylated and non-phosphorylated proteins following immunoaffinity or IMAC enrichment**. Huh7.5 human liver cell extracts were processed by either immunoaffinity- (lanes 1-3) or IMAC- (lanes 4-6) based chromatography and fractions corresponding to lysate (lanes 1, 4), flow-through (lanes 2,5) and elution (lanes 3,6) were subjected to SDS-PAGE and Western blotting. Blots were probed with either **(A)** anti-phospho- (Ser/Thr) Akt substrates as a marker of phosphorylated proteins or **(B)** anti-Hsp60 as a marker of non-phosphorylated proteins.

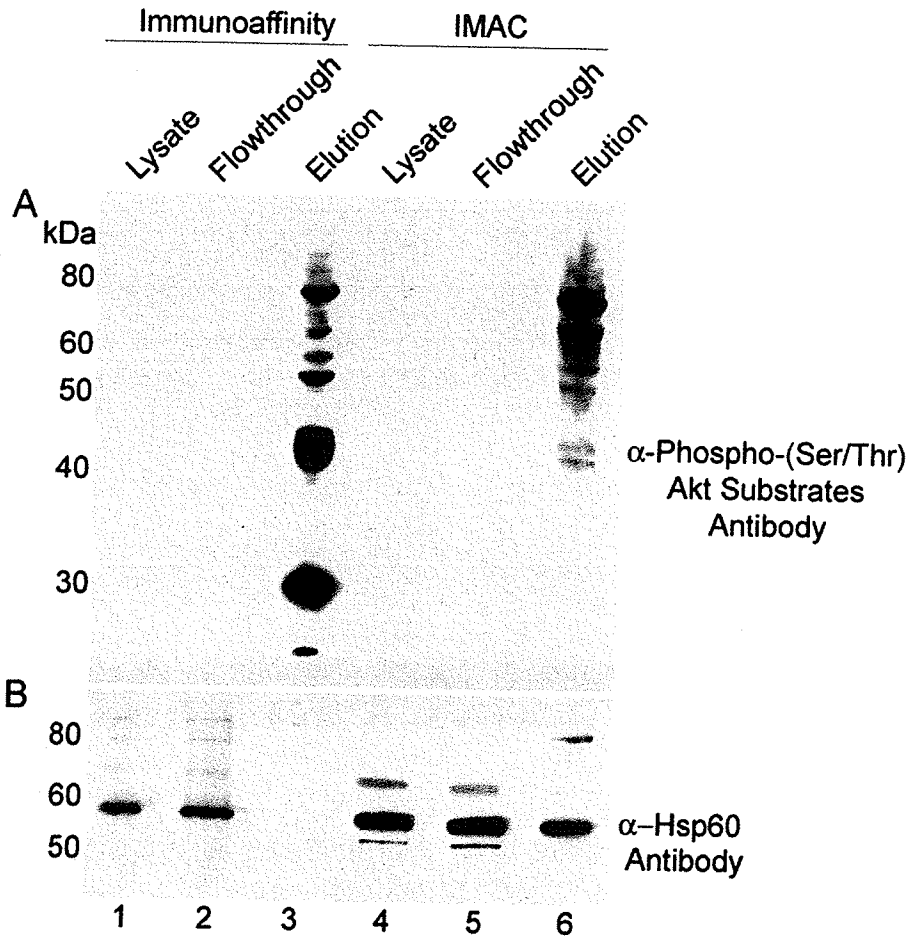
Immunoaffinity
IMAC
Lysate
Flowthrough
Elution
Lysate
Flowthrough
Elution
A
kDa
80
60
50
40
30
α-Phospho-(Ser/Thr)
Akt Substrates
Antibody
B
80
60
50
α–Hsp60
Antibody
1
2
3
4
5
6

However, both procedures significantly enriched for phosphoproteins as demonstrated in the elution fractions (Fig. 10A, lanes 3 and 6). Although both procedures demonstrated enrichment, the phosphoproteins detected and their relative abundances differed between the two techniques. For example, proteins within the molecular weight range of 40-80kDa were purified by both methods, albeit to different extents. Phosphorylated substrates that migrated at 80 and 70kDa species in the eluted fractions (Fig. 10A, lanes 3 and 6) were present at different ratios in the two methods (i.e. the 80kDa species was present in greater quantity compared to the 70kDa species in the immunoaffinity purified samples but were at a more equal ratio when purified by IMAC). Furthermore, one protein species at ~30kDa was only detected in the immunoaffinity enriched sample. This demonstrates that differences in either the initial lysis or capture for certain phosphoproteins exist depending on the procedure used for enrichment.

To evaluate the specificity of the two resins for capturing only phosphorylated proteins, the amount of Hsp60 was monitored. In both the starting lysate material and flow-through, detectable levels of Hsp60 were present irrespective of the technique used (Fig. 10B lanes 1, 2, 4, 5). Hsp60 was not detected in the enriched fraction from immunoaffinity capture but was present in the IMAC eluted fraction (Fig. 10B, compare lanes 3 and 6) raising the possibility that non-phosphorylated proteins are captured by IMAC. This result was not surprising given the well documented fact that metal based affinity resins interact not only with the net negative charge on phosphate groups but also with proteins rich in

acidic amino acids (Dubrovska and Souchelnytskyi, 2005; Collins et al., 2005) thereby allowing for greater capture of highly acidic proteins. Interestingly, Hsp60 is not highly acidic (~14% D/E amino acid content) and does not contain obvious clusters of acidic residues. Although based on only a single protein species, Hsp60, this data suggests that the antibody-based methodology may be more specific for phosphoprotein capture.

Immunoaffinity and IMAC purification methods differ both in their quantitative and qualitative phosphoprotein capture

The results described above demonstrated that antibody and IMAC based phospho-enrichment methods differed in their relative and specific ability to capture certain phosphoproteins. However, Western blot analysis of Akt phosphorylated substrates constitutes only a very small portion of potential phosphoproteins in a cell as this antibody only detects phosphorylated residues in the context of R/K-X-R/K-X-X-S/T (where X equals any amino acid). In order to perform a more global analysis of the cellular phosphoproteins purified, the proteins from both enrichment methods were subjected to 2D-DIGE. A major advantage of the 2D-DIGE technology is the ability to multiplex samples on a single gel thereby making direct comparisons between the proteins captured by the two methods very precise. To address issues of inherent biological variation of the phosphoprotein content of cells, proteins were purified by both techniques in parallel from cells plated and harvested on four separate occasions. Proteins

that were purified from the same batch of cells were co-electrophoresed on single gels. Furthermore, dye swapping was employed in order to account for any differential dye labelling.

Figure 11 depicts a representative gel from the multiplexed 2D-DIGE experiments. On average 923 protein spots +/- 209 (based on co-detection of both fluorescent channels) were detected on the 2D gels (IMAC average spot number 973 +/- 121, immunoaffinity average spot number 920 +/- 291 under individual channel analysis) with virtually the same protein pattern present irrespective of enrichment procedure for any of the four gel sets. Qualitatively, the spot patterns generated from IMAC (Fig. 11A) and immunoaffinity-based (Fig. 11B) purifications were highly concordant in the pI range 4-7 and MW range of 15-150 kDa.

In order to assess the quantitative amounts, the relative abundance of all detected proteins for each gel set was determined using the DIA analysis software package in DeCyder. Proteins exhibiting an average spot volume ratio between replicate gels differing by more than 3.5 fold and present on at least three of the four gels were selected for further investigation. A total of 31 protein spots passed the selection criteria, 27 of which were present in higher abundance in the IMAC purifications (average fold ratio ranging from 6.2 to 38.7), while the remaining four protein spots were elevated in the immunoaffinity fraction (average fold ratio ranging from 3.7 to 5.5). To ensure that the identified

Figure 11. **2D DIGE patterns of phosphoprotein enriched extracts from (A) IMAC or (B) immunoaffinity methodologies.** Each spot map represents individual channels from of the same gel. Protein spots with labels were consistently increased (≥3.5 fold change) in their respective gels when compared to the alternate purification method. Molecular weights and the pI range are indicated.

A

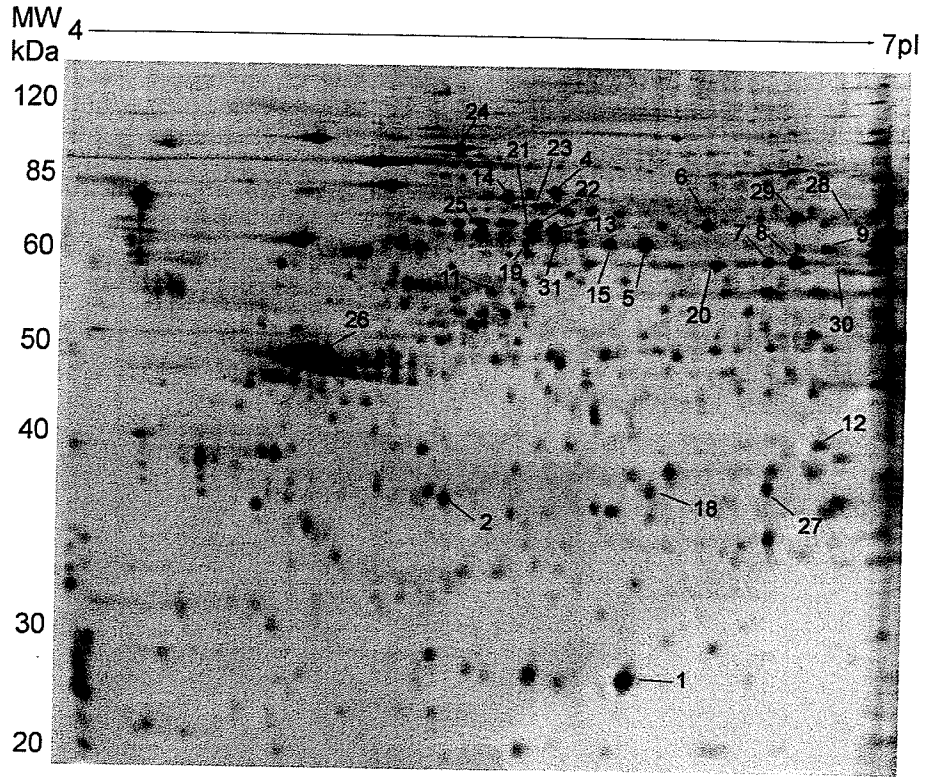
MW
kDa
4
7pI
120
85
60
50
40
30
20
24
21
23
4
14
22
6
29
28
25
13
7
8
9
19
31
11
15
5
20
30
26
12
2
18
27
1

B

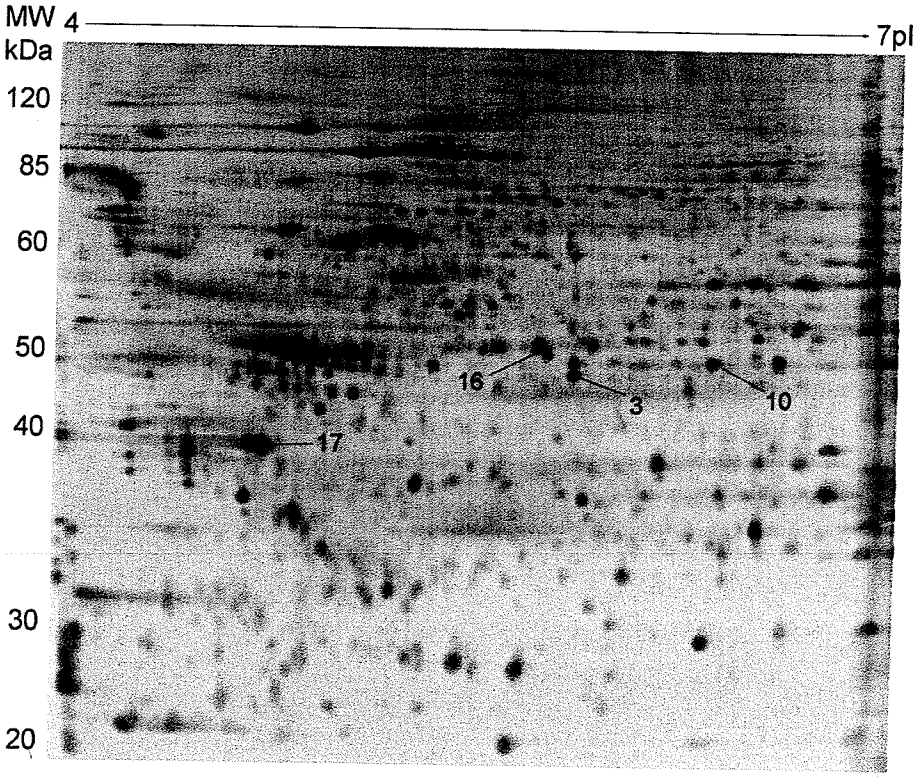
MW
kDa
4
7pI
120
85
60
50
40
30
20
16
3
10
17

changes consistently represented the differential capture affinities of both resins, samples were enriched for on four separate occasions. Volume abundances for all of the differentially purified proteins are plotted in Fig. 12 according to the data set and respective dye-labelling scheme. This figure demonstrates the absence of any inherent bias for any one of the biological replicates. Furthermore, CyDye labelling can not account for any labelling bias as IMAC protein samples labelled with Cy5 (sample sets one and three) do not show any consistently biased abundance ratios when compared to replicates labelled with Cy3 (sets two and four).

Interestingly, a more careful analysis of the DeCyder three dimensional spot volume maps suggested that several of the proteins captured more efficiently by IMAC compared with immunoaffinity were essentially absent from the immunoaffinity purified proteins (spots 6, 7, 8, 11, 15, 19, 21, 23, 25, 26 and 28 were undetectable in immunoaffinity purified samples), while many others which were present in both purification methods were barely detectable. In certain cases where protein spots were negligible, the detected spot intensities across replicates had large standard deviations. The large variation in volume abundances of a single protein over multiple samples was attributed to the poor signal-to-noise resolution of low abundance proteins that ultimately resulted in inaccurate assignment of protein volumes (spots 13 and 20). As shown in figure 13A, the three dimensional representation of spot 17 exhibits a larger peak in the immunoaffinity compared to the IMAC purified sample, while spots 6, 15, (Fig.

Figure 12. **Protein spot volume ratio (IMAC/immunoaffinity) determined from 2D DIGE analysis.** Phosphoprotein enriched IMAC or immunoaffinity samples from four replicate experiments (datasets one to four). Immunoaffinity captured proteins were labelled with Cy3 (dataset one and three) or with Cy5 (dataset two and four). IMAC captured proteins were labelled with Cy5 (dataset one and three) or with Cy3 (dataset two and four).

Protein Spot Volume Ratio
(IMAC/ Immunoaffinity)
60
50
40
30
20
10
0
-10
Dataset One
Dataset Two
Dataset Three
Dataset Four
Average
1 2 4 5 6 7 8 9 11 12 13 14 15 18 19 20 21 22 23 24 25 26 27 28 29 30 31 3 10 16 17
2D Spot Labels

13B), and spot 25 (Fig. 13C) were clearly absent from immunoaffinity enrichments.

Identification of proteins exhibiting the largest and most consistent differential capture was performed by mass spectrometry. Of the 31 protein spots passing the selection criteria, 28 were subsequently identified but due to spot co-migration, the spots contained 34 distinct proteins (Table 1, see Appendix III for detailed MS/MS information). All of the proteins that differed between the two enrichment methods had wide MW and pI range (in keeping with their migration patterns on the gel, Fig. 11). Within the identified proteins, numerous spots collectively belonged to two protein families. These included the heterogeneous nuclear ribonucleoproteins (Table 1, protein spots 5, 11, 20, and 22) and the T-complex protein 1 subunit families (Table 1, protein spots 6-9, 13, 29 and 31).

Of the 34 proteins listed in table 1, it has previously been shown that 21 can exist in a phosphorylated state (Beausoleil et al., 2004; Beausoleil et al., 2006; Molina et al., 2007; Olsen et al., 2006; Rush et al., 2005; Brill et al., 2004; Matsuoka et al., 2007; Yu et al., 2007; Marklund et al., 1993a; Labdon et al., 1992; Salomon et al., 2003; Tourriere et al., 2001; Amanchy et al., 2005; Aboulaich et al., 2004) (Table 1, last column). This does not however prove that the proteins seen for this extract are in a phospho-state. Moreover, since IMAC enrichment may be somewhat less specific than immunoaffinity for phosphorylated proteins, we wondered whether the proteins seen by IMAC but not immunoaffinity purification

Figure 13. **Topographical map of IMAC and immunoaffinity enriched phosphoproteins.** A selection of proteins purified differentially by IMAC compared to immunoaffinity is shown. Protein boundaries outlined in black represent protein spot regions that did not differ between the two purification methods (≥3.5 fold). Proteins that consistently differed in capture efficiency are denoted with their assigned protein spot numbers.

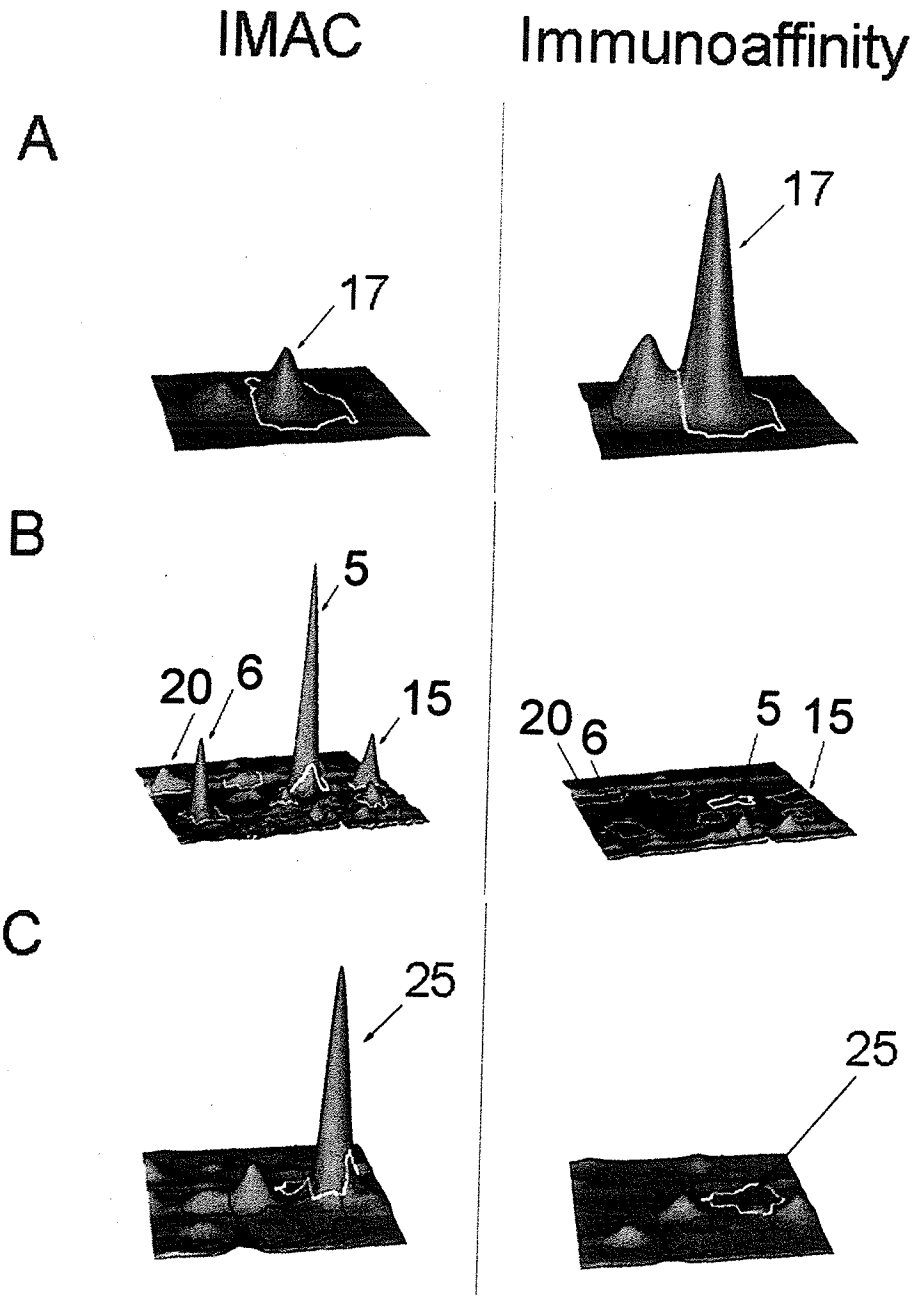
IMAC
Immunoaffinity
A
17
17
B
5
20
6
15
20
6
5
15
C
25
25

Table 1. **Proteins differentially captured by IMAC and immunoaffinity phosphoprotein purification.** In total, 28 protein spots with differential enrichment ($\geq$3.5 fold difference and spot matched on at least found on three of four gels) between immunoaffinity and IMAC capture were identified by LC-MS/MS. Bold text represents the highest scoring protein based on Mascot prediction, a) average volume ratio from DeCyder DIA (difference in gel analysis) run in quadruplicate, b) number of times protein spot was identified versus number of gels run, c) Mascot score, scores >28 are significant ($p<0.05$), d) percent peptide coverage for entire protein sequence, e) number of unique peptide matches, f) references which document phosphorylation evidence, g) all peptides are shared with upper protein due to sequence homology. Details of the peptides identified by MS/MS are provided in the Supplementary Table 1.

Spot #	SwissProt Accession/Protein Name	Expected MW	AVR IMAC/Ab[a]	Gels[b]	Mascot Score[c]	Coverage[d]	Peptides ID[e]	Phosphorylation References[f]
1	**STMN1_HUMAN, Stathmin**	17292	33.61	4/4	475	24%	4	(Labdon et al., 1992; Marklund et al., 1993; Beausoleil et al., 2004)
2	**RANG_HUMAN, Ran-specific GTPase activating protein**	23467	6.93	4/4	170	22%	4	(Molina et al., 2007)
3	**RLA0_HUMAN, 60S acidic ribosomal protein P0**	34423	-5.50	4/4	526	40%	9	(Beausoleil et al., 2004; Olsen et al., 2006; Rush et al., 2005)
4	**GRP75_HUMAN, Stress-70 protein, mitochondrial precursor** ANXA6_HUMAN, Annexin A6	73920 76168	14.15	4/4	1129 104	33% 5%	20 4	(Brill et al., 2004) (Olsen et al., 2006)
5	**PDIA3_HUMAN, Protein disulfide isomerase A3 precursor** HNRPK_HUMAN, Heterogeneous nuclear ribonucleoprotein K	57146 51230	14.93	4/4	444 142	29% 14%	15 5	No evidence No evidence
6	**TCPA_HUMAN, T-complex protein 1 subunit alpha**	60819	17.33	4/4	842	16%	26	(Olsen et al., 2006)
7	**TCPB_HUMAN, T-complex protein 1 subunit beta**	57794	20.55	4/4	1073	41%	19	No evidence
8	**TCPB_HUMAN, T-complex protein 1 subunit beta**	57794	30.86	4/4	1049	47%	21	No evidence
9	**TCPZ_HUMAN, T-complex protein 1 subunit zeta** TCPW_HUMAN, T-complex protein 1 subunit zeta-2[g)]	58444 58299	15.91	4/4	189 66	17% 6%	7 3	No evidence No evidence
11	**HNRPF_HUMAN, Heterogenous nuclear ribonulceoprotein F**	45985	11.85	4/4	301	34%	10	(Beausoleil et al., 2004; Rush et al., 2005; Brill et al., 2004)
12	**HCC1_HUMAN, Nuclear protein HCC-1**	23714	7.11	4/4	165	22%	4	No evidence
13	**TCPE_HUMAN, T-complex protein 1 subunit epsilon**	60089	38.73	4/4	808	46%	28	No evidence
14	**HSP7C_HUMAN, Heat shock 70kDa protein 1**	70052	6.15	4/4	833	30%	21	(Beausoleil et al., 2004; Salomon et al., 2003)
15	**PDIA3_HUMAN, Protein disulfide isomerase A3**	57146	7.94	4/4	325	22%	11	No evidence
16	**CNN3_HUMAN, Calponin-3** TBAK_HUMAN, Tubulin alpha-ubiquitous chain	36562 50804	-3.66	4/4	313 90	25% 11%	6 3	(Olsen et al., 2006) (Molina et al., 2007)
17	**TPM3_HUMAN, Tropomyosin-alpha 3 chain** TPM1_HUMAN, Tropomyosin-alpha 1 chain[g)]	32856 32746	-3.97	4/4	380 245	16% 13%	7 5	(Beausoleil et al., 2004) No evidence
18	**ERP29_HUMAN, Endoplasmic reticulum protein**	29032	8.65	4/4	155	22%	5	No evidence
20	**HNRH1_HUMAN, Heterogeneous nuclear ribonucleoprotein H**	49484	21.50	4/4	208	24%	7	(Beausoleil et al., 2004; Olsen et al., 2006; Rush et al., 2005; Matsuoka et al., 2007)
22	**HNRPK_HUMAN, Heterogeneous nuclear ribonucleoprotein K**	51230	12.90	4/4	382	29%	9	(Beausoleil et al., 2004; Beausoleil et al., 2006; Olsen et al., 2006; Yu et al., 2007)

23	**G3BP1_HUMAN, Ras GTPase-activating protein binding protein**	52189	10.16	4/4	174	15%	5	Yu et al., 2007; Tourriere et al., 2001)
24	**TERA_HUMAN, Transitional endoplasmic reticulum ATPase** SRC8_HUMAN, Src substrate cortactin SAE2_HUMAN, SUMO-activating enzyme subunit 2	89950 61770 71749	8.67	3/4	741 108 65	42% 6% 7%	29 3 4	(Beausoleil et al., 2006; Amanchy et al., 2005) (Beausoleil et al., 2004; Molina et al., 2007; Rush et al., 2005; Salomon et al., 2003; Amanchy et al., 2005) No evidence
25	**CH60_HUMAN, 60 kDa heat shock protein, mitochondrial precursor**	61187	28.59	3/4	1009	39%	18	(Beausoleil et al., 2004; Rush et al., 2005)
26	**RSSA_HUMAN, 40s ribosomal protein SA**	32948	11.33	3/4	220	18%	6	(Rush et al., 2005)
27	**ERP29_HUMAN, Endoplasmic reticulum protein ERp29 precursor**	29032	14.10	3/4	130	19%	4	No evidence
28	**PRP19_HUMAN, Pre-mRNA-processing factor 19**	55602	8.19	4/4	140	21%	8	No evidence
29	**TCPG_HUMAN, T-complex protein 1 subunit gamma** COPD_HUMAN, Coatomer subunit delta	61066 57630	6.43	3/4	653 118	35% 14%	14 7	(Yu et al., 2007) No evidence
30	**RUVB1_HUMAN, RuvB-like 1** SEPT6_HUMAN, Septin-6 SEPT7_HUMAN, Septin-7	50538 50084 50933	7.03	3/4	317 35 30	35% 4% 2%	12 2 1	No evidence (Molina et al., 2007; Brill et al., 2004) (Rush et al., 2005; Molina et al., 2007; Olsen et al., 2006)
31	**TCPQ_HUMAN, T-complex protein 1 subunit theta**	60153	4.37	3/4	362	35%	15	(Rush et al., 2005; Yu et al., 2007)

truly represented phosphorylated species. For each of the proteins identified at least one or more of the reported phosphopeptides were absent from our MS/MS traces. This would be consistent, although certainly not definitive evidence given our sequence coverage that these are phosphorylated proteins. However, in the cases for GRP75, HCC1 and HSP60 all reported phosphopeptides were clearly present in our MS/MS analysis but were present in non-phosphorylated states. For the Hsp60 peptides (GYISPYFIN**T**SK and TVIIEQSWG**S**PK where bold represents the phosphosite) the MS precursor mass and subsequent MS/MS spectra show no evidence for phosphorylation at the threonine or serine residues (Fig.14).

Proteins captured by IMAC and immunoaffinity are predominately phosphoproteins

To address the issue of whether the differentially captured proteins, as well as the entire protein profile examined was representative of phosphorylated proteins, we took advantage of the multiplex nature of 2D-DIGE to compare phospho-enriched proteins to a duplicate sample treated with lambda phosphatase. De-phosphorylated proteins shift in pI towards the cathode after the removal of the negatively charged phosphate moieties post lambda phosphatase treatment. The shift in pI induced by phosphatase treatment of phosphorylated proteins has been used previously to map phosphoproteins in rat fibroblasts (Yamagata et al., 2002) and cortical neurons (Raggiaschi et al., 2006).

Figure 14. **MS/MS analysis of IMAC enriched Hsp60.** **(A)** MS/MS sequence coverage of Hsp60 equalled 39% and is highlighted in grey. The MS/MS traces of the two peptides previously reported to be phosphorylated for Hsp60 are shown in **(B)** and **(C)**. There is no evidence for phosphorylation at either of these sites.

A

MLRLPTVFRQMRPVSRVLAPHLTRAYAKDVKFGADARALMLQGVDLLADAVAVTMGPKGRTVII
EQSWGSPKVTKDGVTVAKSIDLKDKYKNIGAKLVQDVANNTNEEAGDGTTTATVLARSIAKEGFE
KISKGANPVEIRRGVMLAVDAVIAELKKQSKPVTTPEEIAQVATISANGDKEIGNIISDAMKKVGRK
GVITVKDGKTLNDELEIIEGMKFDRGYISPYFINTSKGQKCEFQDAYVLLSEKKISSIQSIVPALEIAN
AHRKPLVIIAEDVDGEALSTLVLNRLKVGLQVVAVKAPGFGDNRKNQLKDMAIATGGAVFGEEGL
TLNLEDVQPHDLGKVGEVIVTKDDAMLLKGKGDKAQIEKRIQEIIEQLDVTTSEYEKEKLNERLAKL
SDGVAVLKVGGTSDVEVNEKKDRVTDALNATRAAVEEGIVLGGGCALLRCIPALDSLTPANEDQ
KIGIEIIKRTLKIPAMTIAKNAGVEGSLIVEKIMQSSSEVGYDAMAGDFVNMVEKGIIDPTKVVRTAL
LDAAGVASLLTTAEVVVTEIPKEEKDPGMGAMGGMGGGMGGGMF

B

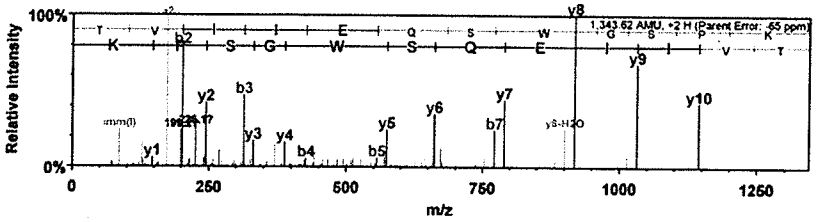

...	B Ions	B+2H	B-NH3	B-H2O	AA	Y Ions	Y+2H	Y-NH3	Y-H2O	...
1	58.0				G	1,389.7	695.4	1,372.7	1,371.7	12
2	221.1				Y	1,332.7	666.8	1,315.7	1,314.7	11
3	334.2				I	1,169.6	585.3	1,152.6	1,151.6	10
4	421.2			403.2	S	1,056.5	528.8	1,039.5	1,038.5	9
5	518.3			500.3	P	969.5	485.3	952.5	951.5	8
6	681.3	341.2		663.3	Y	872.5	436.7	855.4	854.4	7
7	828.4	414.7		810.4	F	709.4	355.2	692.4	691.4	6
8	941.5	471.2		923.5	I	562.3		545.3	544.3	5
9	1,055.5	528.3	1,038.5	1,037.5	N	449.2		432.2	431.2	4
10	1,156.6	578.8	1,139.5	1,138.6	T	335.2		318.2	317.2	3
11	1,243.6	622.3	1,226.6	1,225.6	S	234.1		217.1	216.1	2
12	1,389.7	695.4	1,372.7	1,371.7	K	147.1		130.1		1

C

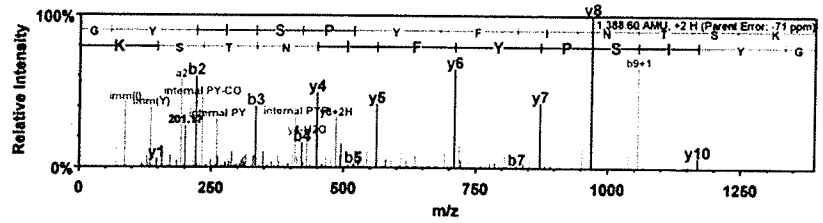

...	B Ions	B+2H	B-NH3	B-H2O	AA	Y Ions	Y+2H	Y-NH3	Y-H2O	...
1	102.1			84.0	T	1,344.7	672.9	1,327.7	1,326.7	12
2	201.1			183.1	V	1,243.7	622.3	1,226.6	1,225.7	11
3	314.2			296.2	I	1,144.6	572.8	1,127.6	1,126.6	10
4	427.3			409.3	I	1,031.5	516.3	1,014.5	1,013.5	9
5	556.3			538.3	E	918.4	459.7	901.4	900.4	8
6	684.4	342.7	667.4	666.4	Q	789.4	395.2	772.4	771.4	7
7	771.4	386.2	754.4	753.4	S	681.3	331.2	644.3	643.3	6
8	957.5	479.3	940.5	939.5	W	574.3		557.3	556.3	5
9	1,014.5	507.8	997.5	996.5	G	388.2		371.2	370.2	4
10	1,101.6	551.3	1,084.5	1,083.5	S	331.2		314.2	313.2	3
11	1,198.6	599.8	1,181.6	1,180.6	P	244.2		227.1		2
12	1,344.7	672.9	1,327.7	1,326.7	K	147.1		130.1		1

Figure 15 shows the results of the lambda phosphatase treatment of IMAC phospho-enriched samples. An overlay of the sample images mock treated and phosphatase treated, is depicted in figure 15A. In this image, red spots represent sample incubated with lambda phosphatase that demonstrated a shift in migration with respect to the mock treated sample depicted in green, while yellow represents the overlap of the two colour channels. Figures 15B and C represent individual CyDye channels corresponding to the phosphatase inhibitor treated sample and the lambda phosphatase treated sample respectively. A clear example of the shift in protein pI following phosphatase treatment is highlighted in figure 15A (asterisk) where a mock treated protein (green) disappears following phosphatase treatment but is replaced by a protein at a similar molecular weight with more basic pI. Of the spots differentially captured by IMAC, clear shifts were seen for spots 7 (TCP-1beta), 20 (hnRNP H) and 24 (TER ATPase). While there was strong discordance between untreated and treated samples (green versus red spots) supporting the hypothesis that most of the enriched proteins were phosphorylated, there was also a significant amount of overlap between the overlaid proteome maps (yellow channel). Explanations for this include: 1) the protein is not in a phosphorylated state, or 2) phoshorylated proteins once treated with lambda phosphatase migrate to the same position on the gel as a protein in the untreated group thereby creating an overlay pattern. All of the other proteins fit into this category and with a notable case being Hsp60. We also performed the same experiment with immunoaffinity purified samples (data not shown) and here, clear shifts were also seen for spots 3 (60S acidic ribosomal protein P0)

Figure 15. **Lambda phosphatase treatment alters the migration pattern of proteins in phosphoprotein enriched samples**. **(A)** Overlay of lambda phosphatase-and mock-treated IMAC samples. Green spots represent proteins not treated with phosphatase, red spots represent samples treated with lambda phosphatase, yellow spots denote proteins that did not change their migration position post treatment (and represent possible non-phosphorylated proteins). Individual CyDye channels of mock-treated **(B)** and lambda phosphatase-treated **(C)** samples illustrate the differential spot pattern of phosphoprotein enriched samples pre- and post-phosphate removal.

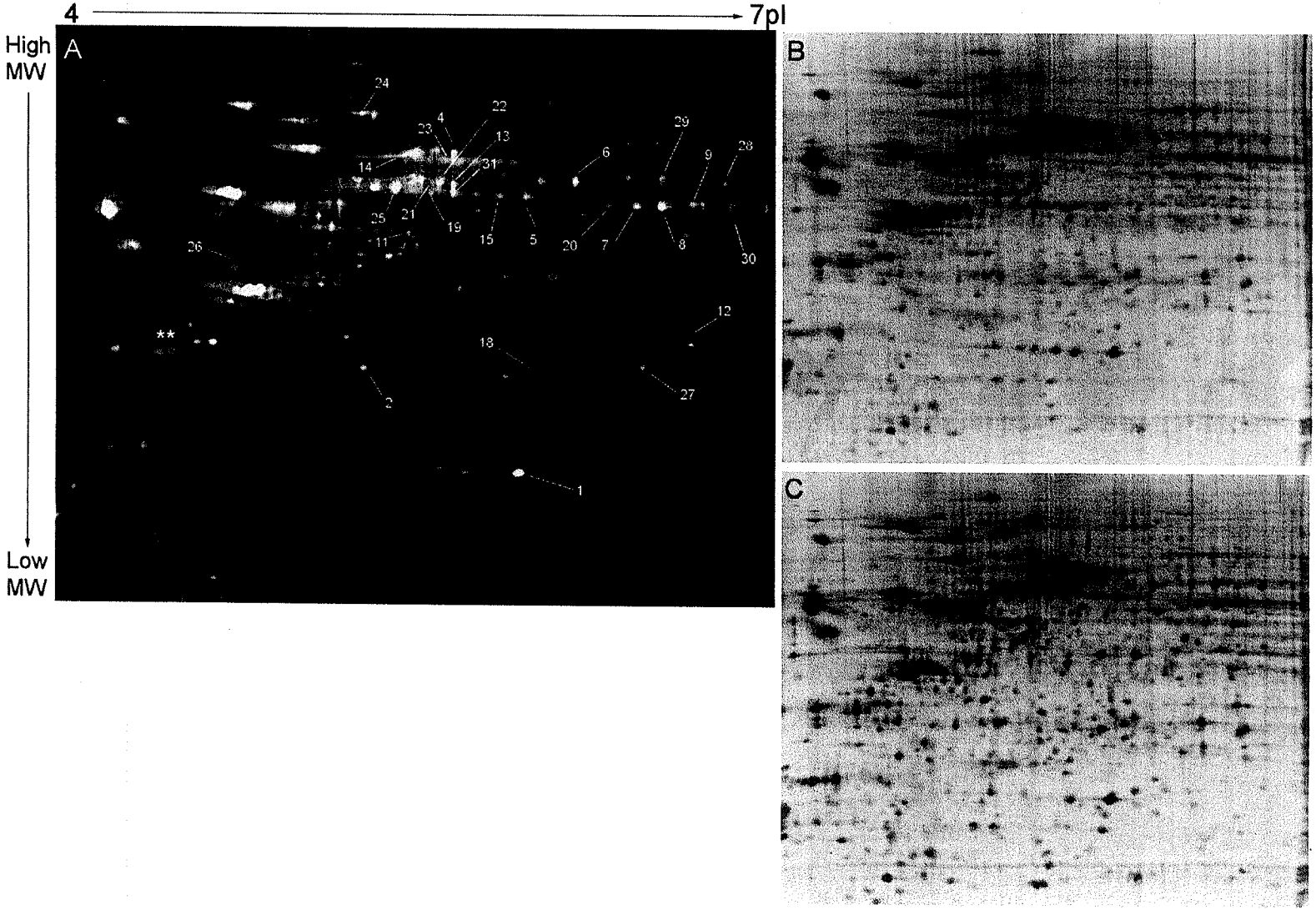
4
7pI
High MW
Low MW
A
B
C
24
22
4
23
13
29
6
9
28
14
31
25
21
19
15
5
20
7
8
30
26
11
12
**
18
27
2
1

and 16 (calponin-3). Given the large number of proteins evaluated in this experiment, it is inevitable that spot overlap for the second reason would occur.

Differences in the relative capture of phosphoproteins between immunoaffinity and IMAC are multifactorial

The results from the 2D-DIGE analysis demonstrated a difference in the capture profile of immunoaffinity and IMAC phosphoprotein capture. This difference is unlikely due to the state of the phosphoproteome at the time of cell lysis as the individual data set samples (one through four) were harvested at the same time from cells that were identically plated. Furthermore, these differences were consistent over the four purifications albeit at different ratios. However, there were other reasons that could contribute to the differential capture: 1) differences in cell lysis conditions that could alter the amount of a specific phosphoprotein solubilized; 2) column saturation – specifically in the case of the immunoaffinity resin, whereby the amount of a specific antibody available to bind certain epitopes may be limited and therefore proteins sharing the same/similar epitope could compete for the antibody, or alternatively; 3) differences in avidity between a specific antibody and similar epitopes could result in a bias towards one particular protein species compared to another; 4) steric interference whereby certain epitopes are blocked or occluded by proximate bound proteins and 5) protein interactions of non-phosphorylated proteins with phosphorylated proteins. Moreover, although 2D gel electrophoresis is a relatively high-resolution technique, as seen from table 1 there was still a certain amount of co-migration

that could affect the spot volume ratios, (evidenced by spot numbers 4, 5, 16, 24, 29 and 30) which contained more than one protein identification by LC-MS/MS.

To address the first issue, a selection of proteins that were differentially purified by IMAC and immunoaffinity resins was subjected to Western blot analysis. TCP-1-alpha, TCP-1-beta and ERp29 were captured with greater efficiency from IMAC purification, while tropomyosin demonstrated the opposite trend. To determine if the differential capture was due to differences in the amount of antigen applied to the resin after protein solubilization, equal amounts of immunoaffinity and IMAC cell lysates and column elutions were analyzed by Western blot analysis (Fig. 16). In the case of TCP-1-alpha, although identical amounts of starting antigen were present in both lysis conditions, (Fig. 16A, lanes 1 and 2), it is clear that little if any protein was captured post immunoaffinity capture while there was clear enrichment for this protein after IMAC purification (Fig. 16A, compare lanes 3 and 4). The same trend could be seen for ERp29 (see Fig. 16B) however there did not appear to be as significant a concentrating effect on this protein as was seen with both T-complex proteins. Interestingly, in the case of TCP-1-beta, although the immunoaffinity lysis conditions resulted in better solubilization of this protein versus the IMAC lysis conditions (Fig. 16C, compare lanes 1 and 2), ultimately, IMAC demonstrated enhanced capture of this protein. The absence of both TCP isoforms in immunoaffinity purifications based on 3D volume analysis (see Fig. 13) is further evidenced by the lack of antigen detection by Western blot

Figure 16. **Western blots confirm differential capture of select proteins as determined by 2D DIGE**. Starting material (lanes 1 and 2) and eluted proteins (lanes 3 and 4) of TCP-1 alpha **(A)**, TCP-1 beta **(B)**, Tropomyosin **(C)** and ERp29.

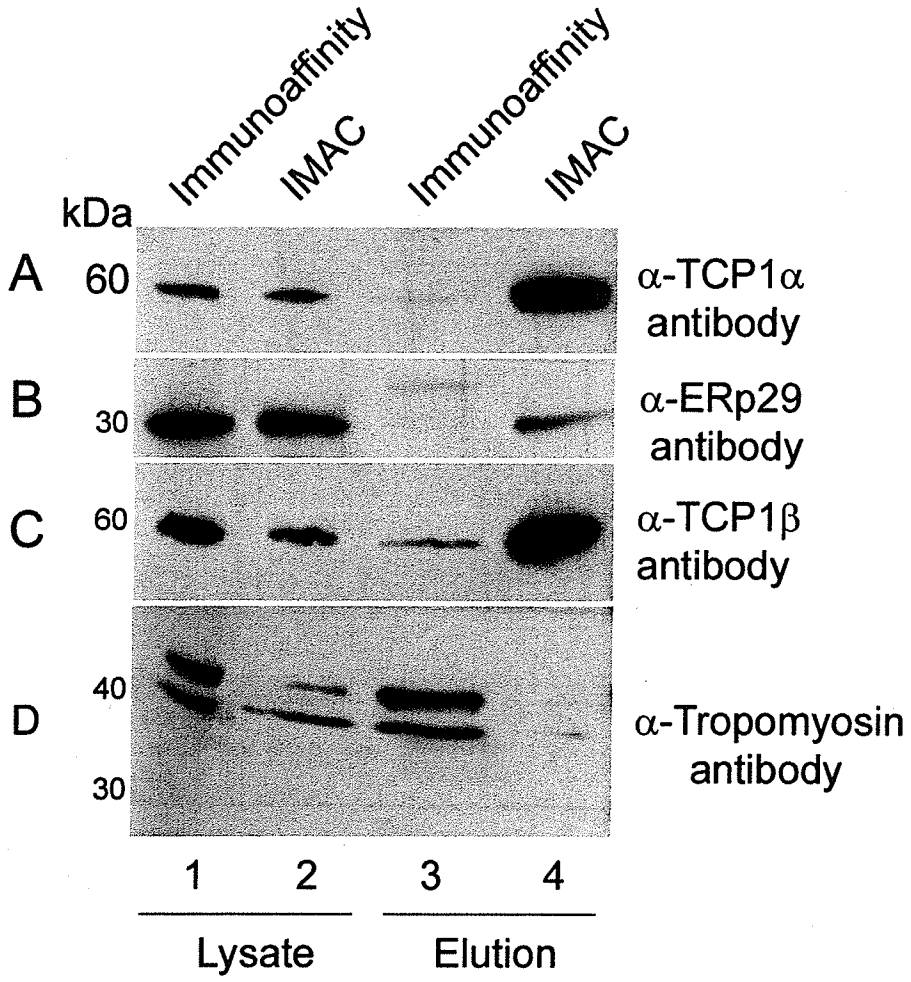
Immunoaffinity
IMAC
Immunoaffinity
IMAC
kDa
A
60
α-TCP1α antibody
B
30
α-ERp29 antibody
C
60
α-TCP1β antibody
D
40
30
α-Tropomyosin antibody
1
2
3
4
Lysate
Elution

(Fig. 16A and C, lane 3) while ERp29 and tropomyosin were present in both eluted fractions, but to different degrees (Fig. 16B and D, lane 3). Finally, in the case of tropomyosin, one of four proteins identified by 2D-DIGE to be purified to a greater extent by immunoaffinity behaved differently. The enhanced capture of tropomyosin by immunoaffnity may in large part be due to enhanced solubilization of this protein during lysis conditions evidenced by the elevated amount of this protein in the starting material (Fig. 16D, compare lanes 1 and 2).

Discussion

Phosphorylation is critical to many biological processes and its deregulation has been shown to play a role in disease pathogenesis. However, several impediments exist to studying the phosphoproteome, including; the comparatively low abundance of these proteins in the cell and the transient nature of the modification due to phosphatase activity. In order to address phosphorylation dynamics on a large-scale, there is a need for selective enrichment methods for phosphoproteome capture. Two commonly employed enrichment methods are IMAC and phospho-specific immunoaffinity enrichment. As there has not yet been a detailed comparison of these two methods in the literature, I employed a quantitative proteomic strategy to assess their enrichment capacities.

Western blot analysis of phospho-Akt substrates showed that both methods were able to enrich for phosphorylated proteins not typically detectable in whole cell lysate preparation (Fig. 10A, lane 1 and 4); a finding consistent with a recent study utilizing IMAC purification from *Arabidopsis* (Laugesen et al., 2006).

However, the differential capture observed for this small subset of proteins and for Hsp60, a marker of non-phosphorylated protein (Fig. 10A) raised questions as to the qualitative and quantitative nature of the two enrichment technologies. To gain a broader evaluation of the proteins enriched by the two purifications, a more global analysis of the phosphoproteome captured by each method was performed using multiplexed 2D-gel electrophoresis (Fig. 11). Overlap between the two profiles was 97% (892/923 proteins were purified to a similar extent by both methods). Of 31 proteins differentially captured ($\geq$3.5 fold), 27 were consistently enriched better by IMAC (Fig. 12) and in many cases appeared to be completely absent from the immunoaffinity capture. Immobilized metal affinity purification is based on the attraction of a positively charged metal ion bound resin to a negatively charged (phosphate) group; therefore, we wondered it these differentially captured elements represented true phosphoproteins or non-phosphorylated proteins that were captured due to their charges or interactions with true phosphoproteins.

Identification of the differentially enriched proteins by LC-MS/MS (Table 1), and evaluation of the literature, suggested that most of the differentially purified proteins could be phosphorylated based on MS/MS phospho-site mapping. Moreover, they also tended to lack highly acidic content (acidic amino acid content ranges from ~12% to 24%) or any obvious clusters of acidic residues within their primary sequences. This does not preclude the possibility of acidic

residue patches within the native structure, since according to the manufacturers' literature (Clontech) proteins purified with this kit are not likely to be denatured.

Two groups of proteins that were captured better by IMAC belong to the heterogeneous nuclear ribonucleoprotein family (Table 1, protein spots 5, 11, 20 and 22) and T-complex protein 1 subunit family (Table 1, protein spots 6-9, 13, 29 and 31). The hnRNP proteins are predominately involved in binding RNA within the nucleus and form complexes with RNA polymerase II transcripts. These proteins are involved in many processes including mRNA stability, transport and turnover, telomere biogenesis, polyadenlyation, oncogenesis, transcription and heat shock response (Krecic and Swanson, 1999). The TCP proteins also form oligomeric complexes but interact with many proteins and act as molecular chaperones upon ATP hydrolysis (Burns and Surridge, 1994). Each of the hnRNP proteins identified in this study have previously been shown to contain phosphorylation sites, however, three of the six TCP proteins identified have no currently described phosphorylation states (TCP-1-beta, TCP-1-epsilon and TCP-1-zeta). It should also be noted that in most cases where proteins were captured better by IMAC than immunoaffinity, a closer evaluation revealed the corresponding proteins to be absent from the immunoaffinity purification (Fig. 12) indicating that large fold differences determined by 2D-DIGE may in fact be much larger than reported due to the contribution of low level noise present in any fluorescent scans. Also, given the differences observed in the enrichment of phosphorylated Akt substrates seen in Figure 10A, we expected to identify some

of these proteins in the global analysis; however among all of the proteins differentially purified by either resin, none represented defined Akt substrates. The disparity between Western and 2D-gel analysis could be due to a number of reasons; including abundance levels below CyDye fluor detection, lack of protein migration from the IPG strip into the second dimension SDS polyacrylamide gel, the pI of the substrates lies outside the range investigated (4-7), or that differences, when evaluated over multiple biological replicate samples, fall outside of the selection criteria used (average spot volume ratios >3.50). Despite the disparity observed pertaining to Akt substrates, Hsp60, one of the proteins preferentially purified by IMAC but not by immunoaffinity was detected by both Western blotting (Fig 10B) and 2D-DIGE (Fig. 11A, spot 25).

Two of the four proteins which showed enhanced protein capture following immunoaffinity purification exhibited a definite shift in pI post lambda phosphatase treatment (spot 3, 60 ribosomal acidic protein and spot 16, calponin), implying they were phosphorylated. In contrast, only three (spots 7, 20,and 24) of the 27 proteins purified to a greater extent by IMAC, demonstrated any obvious shift towards the basic side of the gel following phosphatase treatment although there were increases in the spot volumes at these sites following phosphatase treatment. The increase in spot volume is likely explained by dephosphorylation of other isoforms of the same protein or the dephosphorylation of other protein species that now migrated to the same position. In the case of Hsp60, HCC1 and GRP75, all of the peptides

corresponding to reported phosphorylation sites previously mentioned in the literature were observed by our MS/MS analysis but they lacked any evidence of phosphorylation. In addition, treatment with phosphatase did not alter the migration pattern of this species. Although the proteins could contain phosphorylation sites not previously described, we favour the likelihood that these protein isoforms captured by IMAC but not immunoaffinity represent non-phosphorylated proteins (Fig. 14). It is very possible especially since two of these proteins are chaperonins that co-purification in a complex containing phosphorylated proteins could easily occur. If this is the case, it is intriguing that the immunoaffinity purification did not similarly capture these elements.

In an attempt to establish the underlying reason for differential capture of the two resins, we determined whether the initial lysis conditions resulted in an enhanced solubility of these proteins for purification. In all of the cases where IMAC preferentially enriched for a protein better than immunoaffinity, the amount of protein present in the initial starting lysate was either equal (Fig. 16A and B, TCP-1-alpha, ERp29) or greater than the amount present in the IMAC starting lysate (Fig 16C and D). Therefore in the cases where IMAC captured better than immunoaffinity, this data suggests that starting conditions did not play a major role in the differential capture. Unfortunately, no conclusion could be formed for the differential capture of AKT substrates observed in Figure 10, as the phosphorylated substrates were not detected in the starting lysates prior to IMAC or immunoaffinity cell lysis.

When evaluating the patterns of purified proteins it is noteworthy that TCP1 alpha and TCP1 beta were both concentrated by IMAC enrichment compared to the starting lysate whereas ERp29 was not concentrated. Furthermore, purified tropomyosin was also concentrated by immunoaffinity as the amount loaded of the elution fraction is $1/10^{th}$ the amount loaded of starting lysate sample. The lack of concentration observed for ERp29 could occur if only a portion of the protein was initially present in a phospho-state or if the protein was being inefficiently captured.

In conclusion, this study demonstrates that both IMAC and immunoaffinity technologies enrich for a highly similar subset of phosphoproteins. While it is unknown what percentage of the total cellular proteome is phosphorylated at any given time, our purifications consistently yielded approximately 7-12% of the cellular protein irrespective of the method employed. Ultimately, the decision as to which method to employ depends on the characteristics of the resin to be used, whether or not it allows maximal recovery of the phosphorylated species of interest and finally the concerns over specificity of the capture resin. It should be noted that we consistently had more difficulty concentrating and precipitating phosphoprotein elutions from IMAC capture for our 2D-analysis. This may in part be explained by the elution buffer properties and the greater volumes used for protein elution in the IMAC protocol (4mL per resin compared to 2mL per resin for

IMAC and immunoaffinity respectively). This will also likely play a role in choosing between these two enrichment technologies.

CHAPTER IV: Alterations to the host cell phosphoproteome induced by a HCV subgenomic replicon

Abstract

Infection with HCV often results in a chronic infection that can culminate in liver steatosis, cirrhosis and hepatocellular carcinoma. The mechanism(s) by which HCV causes these manifestations is not clear, however, changes to the host cell proteome must play a role. Host protein phosphorylation in particular has been shown in other virus systems to be affected during viral infection and acts as a molecular switch for cell cycle progression, signal transduction, protein translation and oncogenesis. Here, I have undertaken a global, quantitative phosphoproteome analysis in order to identify differential phosphoprotein abundances between Huh7.5 cells and Huh7.5 cells harbouring a HCV subgenomic replicon. Approximately 1000 distinct protein species were detected by 2D-DIGE of phosphoprotein-enriched lysates. Twenty-two proteins differed in protein abundance by 1.20 to 2.26-fold ($p \leq 0.05$). The differentially abundant phosphoproteins mainly belonged to ER-stress response, protein translation and cytoskeletal protein families.

Introduction

The introduction of exogenous viral RNA and proteins into host cells can often have dramatic effects on host cell functions including cell proliferation, antiviral pathways and cell ultra structure. One mechanism by which host cell functions are altered is through the post-translational modification of phosphorylation.

Protein phosphorylation is a reversible phenomenon controlled by protein kinases and protein phosphatases. In mammals, the most common form of phosphorylation occurs on serine, threonine and tyrosine (Hunter, 1998) residues and is directly involved in metabolism, immune function, transcription, translation, cell cycle progression, movement, apoptosis, cytoskeletal rearrangement and signalling pathways (Raggiaschi et al., 2005). Because phosphorylation is a dynamic process that can often occur at multiple sites within a given protein and often occur on low abundance substrates, the study of a global phosphoproteome has been challenging, particularly when performing "top-down" experiments that require intact proteins for analysis. However, commercially available resins which capture intact phosphoproteins have been used successfully to analyze a number of experimental conditions including the phosphorylated protein complement associated with differentiation of monocytes to macrophages (Metodiev et al., 2004), growth of *S. cervisiae (Makrantoni et al., 2005)* and late-embryogenesis of *Arabidopsis* seeds (Irar et al., 2006).

Prior HCV proteomic studies have investigated the activation of signalling pathways and/or the phosphorylation of specific proteins, with particular emphasis on protein kinases in cells. Typically, these experiments have involved expression of single HCV proteins and in fewer cases replicons. To date, no previous study has addressed the global phosphoproteome content of such cells, nor have they focused on the phosphorylated substrates (Jacobs et al., 2005; Mannova et al., 2006; Fang et al., 2006; Yi et al., 2006). Furthermore, many of

these studies have employed serum starvation/mitogen stimulation in order to monitor changes in either a protein and/or pathway of interest (Macdonald et al., 2003; Street et al., 2004; Borowski et al., 1999a; Borowski et al., 1996; Schulze zur et al., 2003; Fukuda et al., 2001; Tsuchihara et al., 1999; Georgopoulou et al., 2003).

2D electrophoresis is very amendable to phosphoprotein studies due to its ability to separate proteins based on their molecular weight and pI. While phosphate addition has nominal effect on the molecular weight of a protein (~80Da), it changes the charge by -1, a biophysical change which often has a dramatic effect on the protein pI. In this study we have compared the global phosphoproteome of naïve cells and cells harbouring a HCV subgenomic replicon (genotype 1b). A quantitative analysis was performed using 2D-difference-in-gel electrophoresis (2D-DIGE) of immunoaffinity enriched phosphoproteins. In total 22 proteins were found to be differentially abundant in stable subgenomic replicon cells when compared to control cell lines. Although the majority of proteins exhibited only a moderate fold change (1.2 – 1.75), one protein showed a fold change of 2.26. The majority of proteins isolated function in protein folding, particularly during ER-stress and proteins associated with cytoskeleton rearrangement.

Additional Methods

Immunoblots

Western blot transfer was performed for 30minutes using a Bio-Rad SemiDry apparatus with Trans-blot Transfer Medium Nitrocellulose (Bio-Rad) at a constant voltage of 25V with transfer buffer (20% methanol in Tris-glycine buffer). Membranes were blocked overnight at 4°C in 5% skim milk powder (Carnation) and probed with monoclonal anti-NS5A (Virogen, 256-A) and polyclonal anti-GAPDH (abcam, ab9483). Appropriate HRP-conjugated secondary antibodies (Upstate Cell Signaling Technologies) were incubated for 1 hour at room temperature (1:10,000 dilution in 5% skim milk/TBST). Chemiluminescent detection was carried out using Visualizer Western Blot Detection as recommended by the manufacturer (Upstate Cell Signaling Technologies) prior to exposure to Kodak™ X-OMat™ X-ray film for 30sec-5min.

Two-dimensional electrophoresis

Cy-Dye-labelled protein was separated on an IPGphor isoelectric focusing unit using pH 4-7 IPG (24cm) strips (GE Healthcare) in the dark using the following profile: 10hrs passive rehydration, 4hrs 30V, 0.5kVh 500V, 1.0kVh 1000V, 62.5kVh 8000V. The DIGE experimental design for 6 samples pairs is shown in Table 2. Samples were then processed simultaneously on 26cm x 20cm x 1mm 12.5% handcast polyacylamide gels using the Ettan Dalt 6 Electrophoresis System (GE Healthcare). Gels were run in the dark at 2W/gel and kept at 10°C. Preparative gels contained unlabelled protein samples were run with 325ug of protein from each cell line (1300ug protein/strip). These were stained with colloidal Coomassie blue (GelCode Blue, Pierce).

Table 2. **2D-DIGE experimental design**. Phosphoproteins were purified from Huh7.5, Huh7.5 NeoR, Huh7.5 RI and Huh7.5 RII cell lines in triplicate. A total of six multiplexed 2D gels were run with the sample pairs shown above.

GEL	Cy2	Cy3	Cy5
One	Pool	Huh7.5 A	Huh7.5 RI A
Two	Pool	Huh7.5 RII A	Huh7.5 B
Three	Pool	Huh7.5 C	Huh7.5 NeoR A
Four	Pool	Huh7.5 RI B	Huh7.5 RII B
Five	Pool	Huh7.5 NeoR	Huh7.5 RI C
Six	Pool	Huh7.5 RII C	Huh7.5 NeoR C

DeCyder Analysis

Each gel was first assigned to one of 4 groups, Huh7.5, Huh7.5 RI, Huh7.5 RII and Huh7.5 NeoR and compared to one another as per the datasets described in table 3. At least 30 protein landmarks were assigned to each gel followed by spot matching between each gel image. Spot matching accuracy was assessed by confirmation of at least 30 additional spots chosen at random on each gel. Proteins that varied by 1.20 fold with a Students` T-test score of $p < 0.05$ were deemed of interest.

In-gel tryptic digest

Destained gel spots were incubated while rotating in gel wash solution (50% methanol, 5% acetic acid) at room temperature overnight. Gel wash solution was replaced and gel spots incubated for an additional 2-3 hours. Gel spots were washed and dehydrated with 3 washes of 50% acetonitrile/25mM ammonium bicarbonate followed by a 100% acetonitrile wash prior to drying in a vacuum centrifuge. Gel spots were rehydrated in 20ng/uL sequencing grade trypsin (Sigma) in 50mM ammonium bicarbonate and incubated overnight at 30°C. Digested peptides were then extracted in 0.25% trifluoroacetic acid and desalted and concentrated using ZipTips (C18 resin, Millipore).

Mass spectrometry and database searching

Table 3. **Sample datasets used for DeCyder analysis**. Statistical analysis was performed for each dataset listed and protein volume differences greater than 1.20 ($p<0.05$) were further investigated. Each sample group contained at least 3 replicates.

Dataset	Samples		
One	Huh7.5	vs.	Huh7.5 NeoR
Two	Huh7.5 RI	vs.	Huh7.5 RII
Three	Huh7.5	vs.	Huh7.5 RI
Four	Huh7.5	vs.	Huh7.5 RII
Five	Huh7.5	vs.	Huh7.5 RI + Huh7.5 RII
Six	Huh7.5 NeoR	vs.	Huh7.5 RI + Huh7.5 RII
Seven	Huh7.5 + Huh7.5 NeoR	vs.	Huh7.5 RI + Huh7.5 RII

Peptides were analyzed on a MALDI QqTOF mass spectrometer (QSTAR XL, ABI) coupled to a PCI Interface (MALDI, Ciphergen Biosystems). 1uL of digested peptides were co-crystallized with 1uL of freshly prepared CHCA matrix (Sigma) solution (10mg/ml) in 50% acetonitrile in 0.10% trifluoroacetic acid solution on a gold plated array (Ciphergen Biosystems). The TOF tube was calibrated using bradykinin and ACTH and quadropole one (Q1) was calibrated using collision induced fragments of ACTH each day of analysis. The mass range was set between m/z 700 to 3000. Mass spectra were processed using Mascot Distiller. Database searching was performed using Mascot (www.matrixscience.com) with the following parameters: *homo sapiens*, all molecular weights, all pIs, fixed modification=carbamidomethylation and variable modification=methionine oxidation. One missed cleavage was allowed. The SwissProt database was queried (database 55.6). In several cases, duplicate spot samples were also sent to the Institute for Biomolecular Design (University of Alberta) for independent confirmation.

Results

Hepatitis C virus infection is associated with a number of pathologies including liver cirrhosis and hepatocellular carcinoma. In addition, the means by which the virus is able to maintain itself in a persistent fashion remain poorly understood. Although the molecular mechanism(s) by which the virus infection contributes to disease progression are as yet unsolved, one attribute of the host cell that is known to be altered by the expression of individual viral proteins and replicons is

the protein phosphorylation. The aim of this study was to characterize the change in abundance of host cell protein phosphorylation induced by the expression of stable subgenomic replicons employing immunoaffinity-based phosphorylation enrichment and quantitative 2D gel electrophoresis coupled with mass spectrometry.

HCV replicon cell lines

Huh7.5 cells were transfected with HCV1bH77 RNA and following neomycin selection, two independently generated cell populations were selected generating cell lines Huh7.5 RI and Huh7.5 RII. Polyclonal populations rather than clonal cell lines in order to mitigate protein changes specific to one clone that may exhibit abbarently high or low viral expression. It was reasoned that a broader range of levels may be more characteristic of *in vivo* infection. However, upon close analysis of the Huh7.5 RI and Huh7.5 RII cell lines, we discovered that the two polyclonal cell lines did not behave similarly to each other at least with respect to the amount of viral protein that was expressed from each cell line. Figure 17 illustrates the expression level of the viral protein NS5A in the two cell lines. NS5A serves as a surrogate marker of HCV replicon replication. When NS5A expression was compared to an endogenous cellular housekeeping protein, GAPDH, it was apparent that the Huh7.5 RI cell line expressed lower levels of NS5A than the Huh7.5 RII cell line. These results were also consistent when the expression levels of the NS3 viral protein and the neomycin phosphotransferase protein (NPTII) were evaluated (data not shown). It should be noted that the

Figure 17. **Viral protein expression in Huh7.5 RI and Huh7.5 RII HCV subgenomic replicon cell lines differ.** Equal amounts of total cellular extracts from parental Huh7.5 cells and two independently derived HCV replicon cell lines were immunoblotted with NS5A specific antisera. When NS5A protein abundance was normalized to the cellular host keeping protein GAPDH, it is evident that the Huh7.5 RII cell line expressed substantially higher amounts of viral protein than the Huh7.5 RI cell line.

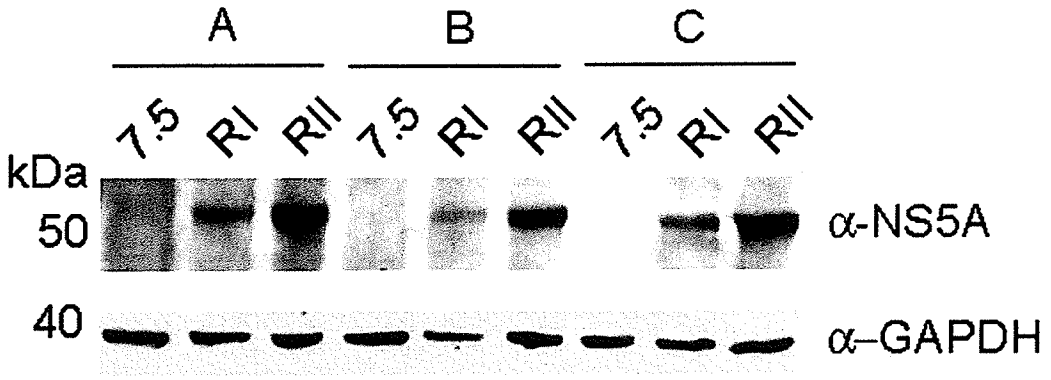
A
B
C
7.5
RI
RII
7.5
RI
RII
7.5
RI
RII
kDa
50
40
α-NS5A
α–GAPDH

translation of NPTII is mediated by the HCV IRES, while the translation of the non-structural proteins is mediated by the EMCV IRES. Given that expression of the viral proteins (mediated through the ECMV IRES) and expression of NPTII (mediated by the HCV IRES) behaved similarly, these results would suggest that the expression differences between the Huh7.5 RI and Huh7.5 RII cell lines was due to differences in the amount of viral RNA present the in the cells rather than differences in translation from one or the other IRES. Due to the expression differences observed between Huh7.5 RI and Huh7.5 RII, the cell lines were analysed both independently and together for subsequent proteomic analyses.

Expression of the HCV NS3-NS5B coding region alters the host phosphoproteome

Sub-confluent monolayers of cells were harvested and processed for phosphoprotein purification by immunoaffinity resin according to the manufacturer's protocol. In order to account for changes in phosphorylation status due to the expression of NPTII, a stable polyclonal cell line was generated containing the NPTII gene under a CMV promoter. This served as alternative control cell line to the naïve Huh7.5 parental cell line. Protein was purified on three separate occasions in order to account for inherent variation in the state of the cell lines that could exist at the time of harvest.

In order to compare all four cell lines to one another, we took advantage of the multiplex nature of 2D-DIGE which has been documented to detect protein

abundance differences as little as 15% with statistical confidence (Unlu et al., 1997). To account for any inherent labelling differences between the CyDyes, dye swapping was employed for all samples and each of the four cell lines were co-detected with each of the alternate sample in order to account for any technical variation that could be due to the sample characteristics (see Table 2). All of the 2D gels qualitatively were essentially the same with regards to the protein pattern resolved and therefore, a single gel image was used to represent all of the datasets. The protein spots of interest are highlighted with their assigned protein numbers (Fig. 18).

Gel images were processed using the biological variation analysis software module (BVA) of DeCyder and protein statistics were determined for seven different datasets (Table 3). Very few protein differences were observed between the two control cell lines, Huh7.5 and Huh7.5 NeoR (dataset one) or the two replicon cell lines, Huh7.5 RI and Huh7.5 RII (dataset two). On average 996 proteins were detected (standard deviation +/- 191). DeCyder has the capacity to define protein abundance differences of 15% or greater. Therefore, we assigned selection criteria of at least 20% average volume ratio (AVR) with a statistically significant student's t-test value of $p \leq 0.05$. Depending on which cell lines were compared to one another (which dataset was investigated), different proteins passed the selection criteria set. In total 22 different proteins were identified to be differentially expressed when one or both of the control cell lines were compared to one or both replicon cell lines. However, in each case the differences were

Figure 18. **Representative 2D gel of Huh7.5 phosphoproteome.** The phosphoproteome of four separate cell lines were compared to one another by 2D-DIGE. Proteins that differed in abundance by at least 1.20 fold ($p<0.05$) that were subsequently identified by mass spectrometry are indicated with their corresponding spot number assignments.

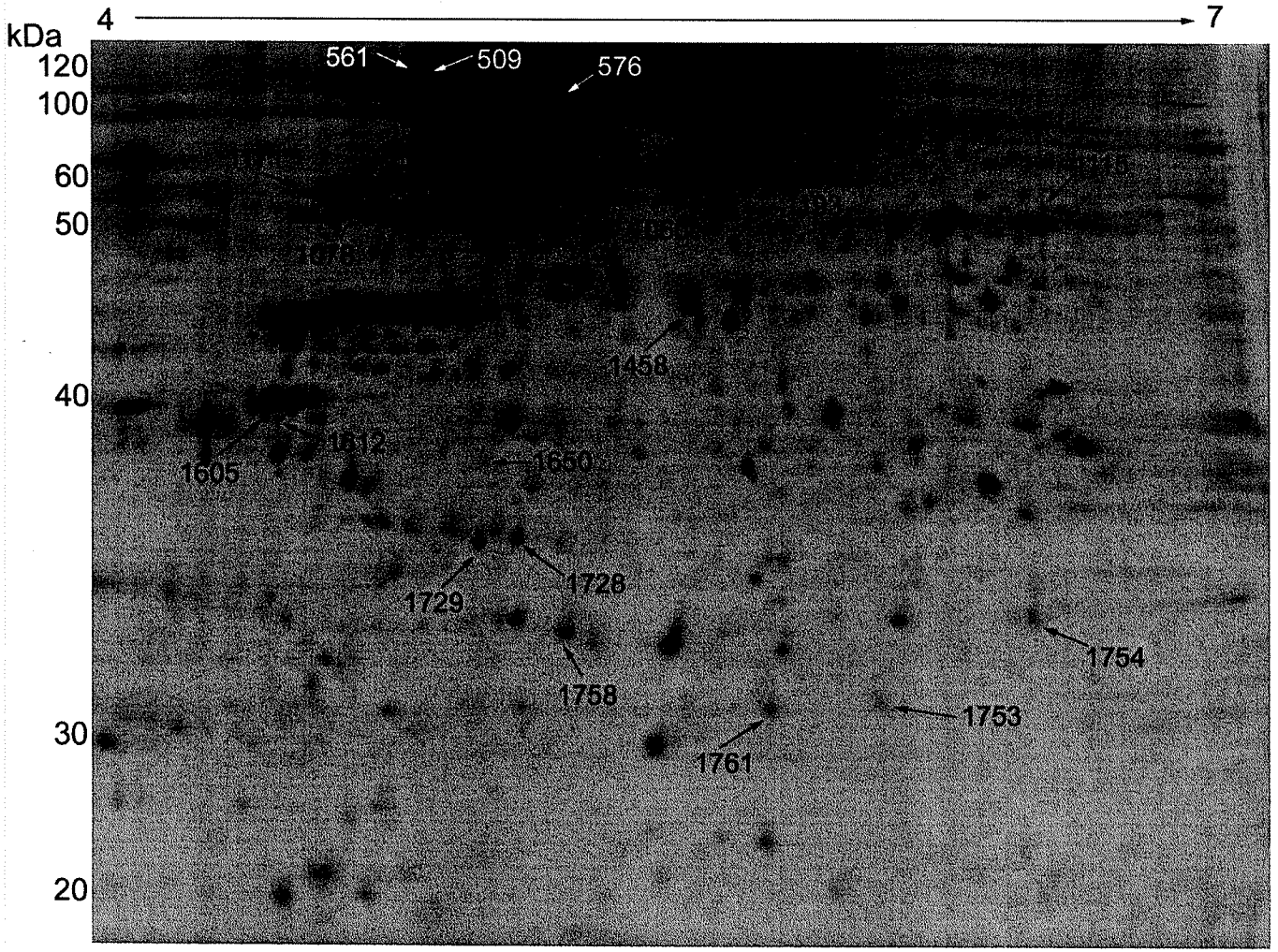
4
7
kDa
120
100
60
50
40
30
20
561
509
576
1458
1612
1605
1650
1729
1728
1754
1758
1753
1761

moderate (1.20 – 1.99 fold, with the exception of two spots with fold differences greater than 2). The proteins deemed of interest for each dataset were subsequently identified by either MALDI-ToF MS and/or ESI-MS/MS. Protein statistics and identifications are detailed in table 4 (see Appendix IV for detailed MS/MS information).

Of the 22 proteins identified, seven of these proteins were present in more than one dataset. Both amphiphysin II (spot 837, 1.75 fold increase, p=0.0073) and Rho GDP dissociation inhibitor alpha (Rho GDI, spot 1650, 1.28 fold increase, p=0.015) were increased in abundance, specifically in Huh7.5 RI versus Huh7.5 or Huh7.5 RI + Huh7.5 RII versus Huh7.5 + Huh7.5NeoR. The five other proteins that were present in multiple datasets demonstrated a decrease in abundance in replicon cells. Elongation initiation factor-2-beta (eIF2β, spot 1193, -1.24 fold, p=0.035), TRF2-interacting telomeric RAP1 (spot 1171, -1.29 fold, p=0.043), RNA-binding motif 8A protein (RBM8A, spot 1729, -1.48 fold, p=0.009), the basic transcription factor 3-like-4 (BTF3L4, spot 1753, -1.28 fold, p=0.039) and stathmin (spot 1758, -1.33 fold, p=0.018) were all decreased in abundance in one or both replicon cell lines.

The resolving capacity of 2DE was highlighted by the identification of three proteins from multiple locations on the 2D gels. Not only was RNA-binding protein 8A differentially expressed in more than one dataset (spot 1729, datasets 4 and 5), it was also present in more than one isoform, at the spot position 1728

Table 4. **Phosphoproteins that differed in volume abundance due to the expression of a subgenomic replicon.** (A) Standardized log abundance average volume ratio of "group 2"/ "group 1" (see Table 3 for groups and corresponding datasets). (B) Mascot probability score of protein identification, where a score >26 is considered significant ($p \leq 0.05$). (C) Percent coverage of protein sequenced and (D) the number of unique peptides seen by the mass spectrometer. (E) Distiller probability score of a protein identified by peptide mass fingerprint from MALDI-ToF data.

Spot #	SwissProt Accession/Protein Name	Predicted MW	AVR[a]	Students' T-test(p)	Mascot Score[b]	Coverage[c]	Peptides ID[d]
Dataset One – Huh7.5 NeoR/Huh 7.5							
954			2.46	0.028			
1425			-1.84	0.009			
1523			-1.24	0.044			
1534			-1.43	0.033			
1772			-1.23	0.040			
Dataset Two – Huh 7.5 RII/ Huh7.5 RI							
575			-1.88	0.025			
1077			-1.75	0.040			
1085			-1.67	0.046			
1324			-1.32	0.040			
1481			1.29	0.044			
1579			-1.99	0.013			
1624			-1.34	0.012			
1735			-1.67	0.022			
Dataset Three – Huh7.5/Huh7.5 RI							
837	**BIN1_HUMAN,** Amphiphysin II/Bin1	64,887	1.75	0.0073	155	5%	3
1193	**IF2B_HUMAN**, eIF2beta	38,388	-1.34	0.013	59.57[f)]	39%	22
1650	**GDIR1_HUMAN**, Rho GDP dissociation inhibitor alpha	23,421	1.28	0.015	182	22%	6
Dataset Four – Huh7.5/Huh7.5 RII							
1171	**TE2IP_HUMAN,** TRF2-interacting telomeric RAP1	44,404	-1.29	0.043	101	5	3
1729	**RBM8A_HUMAN**, RNA-binding motif protein 8A	19,934	-1.48	0.0087	167	27%	6
1753	**BT3L4_HUMAN**, Basic transcription factor 3-like 4	17,260	-1.25	0.016	86	12%	2
1758	**STMN1_HUMAN**, Stathmin/Op18	17,161	-1.43	0.0083	185	29%	4
1761	**STMN1_HUMAN**, Stathmin/Op18	17,161	-1.50	0.012	383	54%	11
Dataset Five – Huh7.5/Huh7.5 RI + Huh7.5 RII							
1060	**HNRPK_HUMAN,** Heterogeneous nuclear RNA binding protein K	50,976	1.22	0.048	111	12%	3
1193	**IF2B_HUMAN**, eIF2beta	38,388	-1.24	0.035	59.57[f)]	39%	22
1458	**CNN3_HUMAN**, Calponin	36,414	-1.33	0.013	52[f)]	31%	10
1729	**RBM8A_HUMAN**, RNA-binding motif protein 8A	19,889	-1.38	0.021	167	27%	6
Dataset Six – Huh7.5 NeoR/Huh7.5 RI + Huh7.5 RII							
509	**HS90B_HUMAN**, Heat shock 90kDa protein alpha	83,264	1.44	0.014	241	13%	8
561	**HS90B_HUMAN**, Heat shock 90kDa protein alpha	83,264	-1.20	0.040	481	14%	9
795	**PDIA4_HUMAN**, Protein disulfide isomerase A4 precursor (Protein Erp)	72,932	1.46	0.011	84	3%	2

935	**EIF3D_HUMAN**, Elongation initiation factor 3 zeta (eIF3 zeta)	63,973	1.63	0.039	58	1%	1
1605	**TPM4_HUMAN,** Tropomyosin-4 (TM30p1)	28,619	-1.46	0.017	330	29%	7
1612	**TPM1_HUMAN,** alpha-Tropomyosin	32,746	-1.64	0.021	483	32%	9
1728	**RBM8A_HUMAN**, RNA binding motif protein 8A	19,889	-1.39	0.024	256	31%	10
Dataset Seven – Huh7.5 + Huh5.7 NeoR/Huh7.5 RI + Huh7.5 RII							
576	**TERA_HUMAN,** Transitional ER ATPase	89,322	2.26	0.027	244	8%	7
815	**GRP78_HUMAN,** Glucose regulated 78kDa protein/BiP	72,402	-1.23	0.045	126	6%	4
837	**BIN1_HUMAN,** Amphiphysin II/Bin1	64.699	1.41	0.038	156	5%	3
884	**GRP75_HUMAN,** Heat shock protein 70B	73,680	1.44	0.020	217	7%	7
1078	**PDIA1_HUMAN,** Protein disulfide isomerase (PDI)	57.116	-1.73	0.037	509	27%	13
1115	**SEP11_HUMAN,** Septin-11	49.398	1.63	0.026	48	6%	2
1171	**TE21P_HUMAN,** TRF2-interacting telomeric RAP1 protein	55,551	-1.33	0.009	101	5%	3
1650	**GDIRI_HUMAN,** Rho GDP dissociation inhibitor alpha	23,421	1.25	0.025	167	22%	6
1753	**BT3L4_HUMAN,** Basic transcription factor 3-like 4	17,271	-1.28	0.039	86	13%	2
1754	**COF1_HUMAN,** Cofilin-1 (18kDa phosphoprotein)	18,502	1.50	0.037	180	35%	4
1758	**STMN_HUMAN**, Stathmin 1	17,161	-1.33	0.018	185	29%	4

(dataset 6). Both RBM8A isoforms were decreased in abundance in replicon cells. Another protein that demonstrated a similar trend to RBM8A was stathmin, which was present in more than one dataset and isoform (spots 1758 and 1761, dataset four). Finally, a somewhat more complicated expression pattern was identified for the heat shock protein 90A (HSP90) which demonstrated a decreased abundance in replicon cells at spot 561 and an increased abundance at spot 509 both in dataset six (two replicon cell lines versus the two control cell lines).

The known phosphorylation sites and protein functions of the proteins are detailed in table 5 according to their increase or decrease in abundance in one or more replicon cell lines. With the exception of six proteins identified, all of the differentially abundant proteins have previously described phosphorylation sites.

Stathmin immunoblotting

Unfortunately, due to the relatively minor alterations described by our 2D analyses (typically <50%), confirmation of the identified changes using alternative experimental strategies such as Western blot is difficult. Not only are phosphospecific antibodies generally not available for these species but the multi-isoform nature of the study increases the difficulty. Shown in figure 19 are the results of immunoblotting for the protein stathmin. Two stathmin isoforms have lower protein abundances in replicon cell lines compared to naïve cell lines (spot 1758 and 1761). There was no obvious difference in the total amount of stathmin seen by standard 1D-PAGE before (lysate) or after (elution)

Table 5. **Protein function and phosphorylation evidence for proteins differentially abundant in subgenomic replicon cell lines**. Proteins are grouped as to whether they were increased in one or both replicon cell lines or decreased in one or both replicon cell lines.

Protein	Function	Phosphorylation References
Increased abundance in replicon cells		
Amphiphysin II/Bin1	Potential tumour suppressor, possibly involved in synaptic vesicle endocytosis	(Beausoleil et al., 2004; Olsen et al., 2006)6)
Cofilin	Reversibly controls actin polymerization and depolymerization	(Olsen et al., 2006; Rush et al., 2005; Beausoleil et al., 2006; Nakano et al., 2003)3)
eIF3 zeta	Promotes binding of methionyl tRNAi and mRNA, phosphorylated upon DNA damage (likely by ATM or ATR)	(Rush et al., 2005; Matsuoka et al., 2007; Zahedi et al., 2008)8)
hnRNP K	Major pre-mRNA-binding protein, binds tenaciously to poly (c) sequences	(Olsen et al., 2006; Beausoleil et al., 2004; Beausoleil et al., 2006; Yu et al., 2007; Kim et al., 2005; Dejgaard et al., 1994)4)
Hsp70B/GRP 75	Implicated in control of cell proliferation and aging, may act as a molecular chaperone, phosphorylated upon DNA damage (likely by ATM or ATR)	(Matsuoka et al., 2007)7)
Hsp90 alpha Hsp90 beta	Molecular chaperone with ATPase activity	(Olsen et al., 2006; Lees-Miller and Anderson, 1989a; Lees-Miller and Anderson, 1989b; DeGiorgis et al., 2005)5) (Olsen et al., 2006; Beausoleil et al., 2004; Beausoleil et al., 2006; Rush et al., 2005; Matsuoka et al., 2007; Lees-Miller and Anderson, 1989b)b)
Protein disulfide isomerase A4	Rearrangement of disulfide bonds	No evidence
Septin 11	Cytokinesis	No evidence
Vasolin containing protein/TER ATPase	Involved in fragmentation and reassembly of Golgi stacks during mitosis and after mitosis, phosphorylated upon DNA damage (likely by ATM or ATR)	(Amanchy et al., 2005; Matsuoka et al., 2007; Imami et al., 2008)8)
Rho GDP dissociation	Inhibits GDP dissociation from Rho proteins	No evidence

inhibitor		
Decrease abundance in replicon cells		
Calponin	Capable of binding actin, calmodulin, troponin and tropomyosin, inhibits the actomyosin Mg-ATPase activity of actin when bound	(Olsen et al., 2006; Molina et al., 2007)
eIF2 beta	Involved in early steps of translation, binds to GTP and initiator tNRA	(Olsen et al., 2006)
GRP78/BiP	Implicated in aiding formation of multimeric complexes in the ER	(Molina et al., 2007)
Hsp90 alpha Hsp90 beta	Molecular chaperone with ATPase activity	(Olsen et al., 2006; Lees-Miller and Anderson, 1989a; Lees-Miller and Anderson, 1989b; DeGiorgis et al., 2005) (Olsen et al., 2006; Beausoleil et al., 2004; Beausoleil et al., 2006; Rush et al., 2005; Matsuoka et al., 2007; Lees-Miller and Anderson, 1989b)
Protein disulfide isomerase	Catalyzes the formation, breakage and rearrangement of disulfide bonds	No evidence
RNA binding protein 8A	mRNA nuclear export and mRNA surveillance	(Beausoleil et al., 2004; Olsen et al., 2006; Kim et al., 2005)41
Stathmin	Disassembly of microtubules	(Labdon et al., 1992; Marklund et al., 1993; Beausoleil et al., 2004)
Transcription factor BTF3L4	Unknown, belongs to NAC family	No evidence
TRF2-interacting telomeric RAP1	Telomere length regulation	(Beausoleil et al., 2004; Beausoleil et al., 2006)
Tropomyosin alpha	Implicated in actin cytoskeleton stabilization in non-muscle cells	No evidence
Tropomyosin 4	Implicated in actin cytoskeleton stabilization in non-muscle cells	(Nousiainen et al., 2006)

Figure 19. **Stathmin immunoblotting by standard 1D-PAGE and 2D-PAGE.** Two protein spots were shown to have a decreased abundance in the Huh7.5 RII cell line when compared to the parental Huh7.5 cell line. **(A)** Immunoblotting for total stathmin (input) and phosphoprotein enriched stathmin (elution) did not reveal any differences in protein abundance between the two cell lines. **(B)** A more complex migration pattern for stathmin was revealed when immunoblotting was performed on phosphoprotein enriched samples separated by 2D-PAGE. At least 8 different stathmin phospho-isoforms were observed. Stathmin isoforms which appeared to be less abundant in Huh7.5 RII cells are highlighted with arrows.

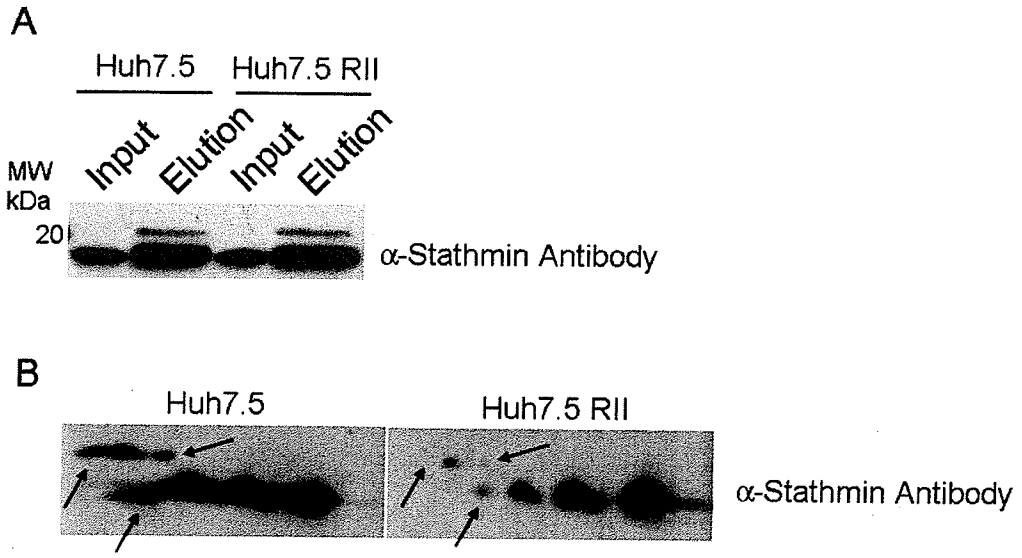
A
Huh7.5
Huh7.5 RII
Input
Elution
Input
Elution
MW
kDa
20
α-Stathmin Antibody
B
Huh7.5
Huh7.5 RII
α-Stathmin Antibody

phosphoprotein enrichment (Fig. 19A). However, when a 2D Western blot was performed, there appeared to be decreased amounts of at least two-three isoforms of stathmin (Fig. 19B, arrows). It has yet to be confirmed whether the stathmin isoforms that differ by Western blot represent the protein spots defined in the 2D DeCyder analysis as initial immunoblotting was performed on mini-SDS-PAGE gels compared to the large format (24cm) used in 2D-DIGE. However, immunoblotting for stathmin on large format 2D gels displayed similar spot patterns as the mini gels (data not shown) and suggested that spots 1758 and 1761 represent stathmin isoforms that contain >2 phosphates based on previously described stathmin migration patterns (Beretta et al., 1993).

Discussion

In order to study the global phosphorylation changes induced by expression of the HCV non-structural proteins (NS3-NS5B) and replication of the viral genome; two independently derived replicon cell lines were created. These replicon cell lines were developed in order to identify changes that are persistently altered in cells, with the intention of identifying changes that mimic those seen in chronic infections. The intention of using clonal pools was that these pools would represent a broad range of replicon expression and thus would be more consistent with an *in vivo* state. Surprisingly, we observed that the two cell lines expressed substantially different levels of viral proteins (Fig. 17, compare lanes 2 and 3). One possible explanation for the differences in the expression levels of the two replicon cell lines is that the subgenomic replicons acquired different cell culture adaptive mutations that influenced the replication fitness of the replicon

constructs differently. Alternatively, those cells which were successfully transfected with the replicon may have been in different cell cycle states that may have influenced which cells were more permissive to the replicon and subsequently a certain cell phenotype was selected for that supports a higher level of replicon expression. Therefore, our subsequent analyses comparing control- to replicon-cell lines were performed under a number of conditions, ensuring that each replicon cell line was studied independent from one another (representing low and high level expression) and also together (thereby representing an average of low and high level expression).

Phosphoproteins were enriched from naïve Huh7.5 cells, both replicon cell lines (Huh7.5 RI and Huh7.5 RII) and a second control cell line was also created that stably expressed the neomycin phosphotransferase (NPTII) gene. When the two control cell lines were compared to one another using DeCyder analyses (dataset one), only five proteins were significantly altered and none of these were found to be differentially expressed in the replicon cell lines compared to the naïve Huh7.5 cell line (fold changes ranged from 1.24 to 2.46 fold). A comparison of the two replicon cell lines (RI and RII) to each other (dataset two) was also performed and seven proteins showed different abundances (fold changes ranged from 1.29 to 1.99). Despite the substantial difference in viral protein expression levels between Huh7.5 RI and Huh7.5 RII, very few cellular phosphoproteome changes were observed by quantitative 2D analysis. Because none of the proteins that were differentially expressed in datasets one and two

were significantly altered when control cells were compared to replicon cells, only protein spots from datasets three through seven were subsequently identified by mass spectrometry (Table four).

Elevations in a number of the phosphoprotein isoforms identified in this study have previously been described to be involved with HCV proteins and/or infection including heat shock protein 90 (VR= 1.44, p=0.014 and VR= -1.20, p=0.04), GRP75 (VR= 1.44, p=0.02), GRP78 (VR= -1.23, p=0.045) and various tropomyosin isoforms (VR= -1.46, p=0.017 and VR= -1.64, p=0.021) (Takashima et al., 2003; Yokoyama et al., 2004). It should be kept in mind however, that these previous studies did not investigate the potential phosphorylation changes that occur in response to HCV but rather addressed global protein amounts and therefore, although previous work may have found elevated protein levels of certain cellular proteins, this does not preclude the possibility that phosphoprotein isoforms of this protein behave differently.

One of the proteins previously described to be involved in HCV infection is amphiphysin II (also referred to as Bin 1). Amphiphysin has been shown to bind to NS5A in a SH3-dependent manner (Zech et al., 2003) which results in the inhibition of NS5A phosphorylation (Masumi et al., 2005). Although the function of amphiphysin II is not fully understood, it is implicated in clathrin-mediated endocytosis (Wigge et al., 1997; McMahon et al., 1997), a process which HCV uses during virus entry (Blanchard et al., 2006). The implications of elevated

amphiphysin phosphorylation in replicon cells is unclear, however, it is known that phosphorylation inhibits amphiphysins' ability to bind to clathrin (Slepnev et al., 1998). Furthermore, clathrin-mediated endocytosis occurs following the rapid dephosphorylation of amphiphysin (Wigge et al., 1997) and therefore, it is plausible that once HCV establishes an infection in the host cell, certain components of the virus induce the phosphorylation of amphiphysin in order to block any further clathrin-mediated endocytosis and thereby inhibit co-infection with additional virions. Alternatively, the inhibition of further endocytosis may be the result of cellular antiviral strategies. The other proteins identified in this study that have been previously associated with HCV are eukaryotic initiation factors 2 and 3 (Hellen and Pestova, 1999), hnRNP K (Hsieh et al., 1998), HSP90 (Okamoto et al., 2006), GRP75 (Kuramitsu and Nakamura, 2005; Yokoyama et al., 2004; Takashima et al., 2003), GRP78 (Takashima et al., 2003; Choukhi et al., 1998) and tropomyosin (Kuramitsu and Nakamura, 2005; Yokoyama et al., 2004).

One of the other goals of this research was to identify common pathways that may be activated in response to HCV replication. Interestingly, three of the elevated phosphoproteins described in this study are known to be phosphorylated in response to cellular DNA damage (Hsp70, eIF3 zeta and TER ATPase). Their phosphorylation is likely mediated by ATR or ATM protein kinases (Matsuoka et al., 2007). These results would suggest that the replicon cell lines maybe experiencing something akin to DNA damage, a process

associated with cellular transformation and progression to cancer, a pathology that HCV is associated with (Seeff, 2002; Alter and Seeff, 2000). Activation of ATR and ATM kinases in these cell lines is being investigated further.

A second group of phosphoproteins described in this work can be functionally classified together as members of cytoskeletal rearrangement, stability and polymerization (cofilin, calponin, stathmin, tropomyosin alpha and tropomyosin 4). In recent years the importance of the cytoskeleton with regards to virus propagation has become more evident. Not only do viruses need to circumnavigate the intracellular network of microtubules and actin, they also utilize these cellular components for protein trafficking and tethering (Cudmore et al., 1997). Of the cytoskeletal proteins described in this study, all were decreased in abundance in replicon cells with the exception of cofilin. Additionally, two distinct isoforms of the oncoprotein stathmin were decreased in Huh7.5 RI and RII cell lines. Stathmin can be phosphorylated on at least four serine residues under a variety of combinations (Beretta et al., 1993). Stathmin phosphorylation/dephosphorylation is tightly coupled to the cell cycle, whereby phosphorylation is critical to the initiation of mitosis (Brattsand et al., 1994; Marklund et al., 1993b). Furthermore, phosphorylation of stathmin leads to the inability of stathmin to depolymerize actin filaments which are required for the formation of the mitotic spindle (Mistry and Atweh, 2001). Upon exit from mitosis, stathmin is subsequently dephosphorylated. Interestingly, it has been documented that the expression of NS5A in liver cell lines leads to aberrations in

mitosis and chromosome content (Baek et al., 2006). It is therefore possible that stathmin dephosphorylation in part contributes to anomalies in chromosome segregation. Moreover, overall stathmin levels have been shown to be altered in HCV-associated hepatocellular carcinoma (Wong et al., 2008) and cells expressing a full length HCV replicon (Jacobs et al., 2005), although, these previous studies described elevations in total stathmin levels. It should therefore be kept in mind that although global protein levels can increase, the functional status of said protein can be diminished depending on the post translational modifications on the protein.

A third and fourth group of protein functional classes can be formed based on proteins involved in protein folding and processing (GRP75, GRP78, HSP90alpha, PDI, PDI A4 and GRP78) and protein translation (eIF3 zeta, Rho GDI, RNBP8A and eIF2 alpha). It is well documented that heat shock proteins and ER chaperone proteins are altered when cells are under duress. Given the production of viral proteins during efficient virus replication, it is not surprising that these proteins change in response to HCV infection. It is well documented that HCV infection and replicon expression induce ER stress (Tardif et al., 2002; Ciccaglione et al., 2005; Fang et al., 2006; Sekine-Osajima et al., 2008). The finding of proteins involved in translation is also consistent with the processes that occur during viral infection. Inherent to virus replication is the subversion of cellular processes for the replication of virus proteins. In the case of the replicon,

a balance must be struck between virus and cellular translation as these represent persistently infected cells.

One of the phosphoproteins shown to be increased in replicon cells was Rho GDP dissociation inhibitor alpha (Rho GDI). Complex formation of the Rho GDIs with Rac1 and Rho1 is regulated in part by the phosphorylation of Rho GDI which leads to the release of Rac1 from the complex. Rho GDI proteins have three known functions which are associated with the inhibition of GTPase activity both through GTP-GDP exchange regulation and sub-cellular distribution, reviewed in (DerMardirossian and Bokoch, 2005). If the increase in abundance observed in replicon cells is due to phosphorylation, it would imply that the Rho GDI complex may be partially inactive and therefore Rho GTPase activity is maintained in replicon cells.

Eukaryotic initiation factor 2-beta combines with three other eIF-2-subunits (alpha, gamma, epsilon), forming the initiation complex for cap-dependent translation, which, HCV does not use for protein translation due to the IRES located in the 5' NTR of the genome. Although there is no documented evidence of HCV-induced phosphorylation changes to eIF-2-beta; an independent research group described a decrease in the phosphorylation of eIF-2-alpha and a closely related translation initiation factor, eIF-4-epsilon in replicon cell lines (Tardif et al., 2002). Therefore, the decrease to eIF2β documented here would be consistent with these observations.

Overall, only minor changes to the phosphoproteome were observed in stable replicon cell lines. The relatively minor alterations observed in this study are consistent with a number of previously performed microarray experiments that compared replicon cell lines to naïve cell lines. Aside from the induction of interferon stimulated genes (after treatment of cells with interferon), only subtle changes were observed (Guo et al., 2001; Zhu et al., 2003b; Aizaki et al., 2002). Moreover, the alterations in gene expression often differed to similar extents regardless of replicon expression (Hayashi et al., 2005). Our findings are not surprising as previous work performed in the Seeger Lab (2005) found when comparing different replicon cell lines by microarray analysis that transcript differences were more often due to individual cell lines differences rather than the presence or absence of a HCV replicon (Hayashi et al., 2005).

Because of the time changes possibly induced due to selection over long periods of time, and the results from microarray studies, we wondered whether an actual HCV infection would identify more robust phosphorylation changes and therefore, future efforts focused on identifying phosphoprotein changes during a robust HCV infection.

CHAPTER V: Phosphoproteome alterations to Huh7.5 cells infected with hepatitis C virus

Abstract

Hepatitis C virus infection is associated with a variety of clinical manifestations including liver cirrhosis and hepatocellular carcinoma. It is now well documented that HCV replication, or the expression of virus open reading frames, has a significant effect on the host cell proteome. Activation and suppression of the innate immune response, rearrangement of the cellular architecture and hijacking of cellular machinery are methods viruses use to create an environment conducive to replication. Not only do virus elements affect the relative abundance of transcripts and proteins, but they also can alter protein cellular localization and post-translational modifications. Protein phosphorylation is a key regulator of many cellular effectors and has previously been show to be altered in the context of HCV expression. Here, a more global approach has been taken to detect changes to the host cell phosphoproteome that occur during HCV infection. Using phosphoprotein immunoaffinity capture and high-resolution quantitative two-dimensional gel electrophoresis, we detected 38 proteins that exhibited at least a 1.5 fold change in relative phosphoprotein abundance levels when comparing mock- to HCV-infected Huh7.5 cells. Of the proteins subsequently identified by mass spectrometry, increased abundance was seen for proteins involved in cytoskeletal regulation (tropomyosin and tubulin), cellular translational (eIF-1-Δ and PCBP1) and molecular chaperones (GRP78). Downregulated phosphoproteins included calponin and deoxyuridine 5'-triphosphate nucleotidohyrolase. These findings impart information on the protein

phosphorylation changes induced by HCV and provide insight regarding the cellular substrates affected during HCV infection.

Introduction

Alteration to cellular proteins during virus infection is necessary in order to generate an environment conducive for virus propagation. This can involve the modification of transcription and translation factor activities that alter protein abundance, changing the subcellular localization or altering the activity of a protein through direct binding or post-translational modifications. As a consequence, this can lead to deregulation of host control pathways leading to cellular pathogenesis.

Protein phosphorylation is a key post-translational modification regulating such diverse functions as cell metabolism, morphology and division, protein translation and antiviral responses. Signalling cascades mediated by phosphorylation of activated kinases are responsible for transmitting extracellular signals from cell surface receptors to the nucleus. Expression of portions or the entirety of the HCV genome have been documented to alter the activation of specific signalling cascades and in some cases the downstream substrates of these pathways. In particular, the viral protein NS5A has been shown to interact with Src kinase family members that ultimately leads to differential inhibition, and in one case, for Fyn, the activation of these kinases, that subsequently lead to downstream effects observed at the substrate level (Macdonald et al., 2004).

Here we characterize changes to the cellular phosphoproteome during HCV infection. Using high-resolution 2D difference-in-gel electrophoresis (2D-DIGE), we detected 38 differentially phosphorylated protein isoforms from HCV-infected cells compared to mock-infected cells. The majority of the proteins demonstrated an elevated abundance in infected cells and belong to a number of different protein families; however, cytoskeletal elements and stress-response pathways represented a large subset of proteins identified. A number of proteins involved in mRNA translation were also identified. These findings describe for the first time the global phosphoproteome changes induced by HCV infection and highlight potential targets for HCV therapies.

Additional Methods

DeCyder Analysis

Spot maps were then exported to the BVA (biological variance analysis) module and each gel was manually land-marked for at least 20 different spots. Landmarks were then used to match all gels to one another and individual spot were assigned numbers that were cross referenced on each gel (three images per CyDye, for a total of nine gel images). Each image was then assigned to one of three groups, standard, mock or JFH1 infected and the standardized log abundance of the spot volumes was compared. Protein spots were considered of interest if their volume abundance between mock and JFH1 infection differed by at least 1.40 fold (student's t-test $p<0.05$).

Mass spectrometry

The SwissProt database version 54.7 was queried for protein identifications.

Immunoblots

Phosphoprotein enriched samples from mock and HCV-infected cells were resolved by standard SDS-PAGE and 2DE as described above with the exception that samples used for tropomyosin-3 immunoblotting were processed in the first dimension on 7cm IPG strips rather than on 24cm IPG strips with the following first dimension profile: at least 8hrs passive rehydration, step to 30V for 30min., step to 300V for 200Vhrs, gradient to 1000V for 300Vhrs, gradient to 5000V for 4500Vhrs and step to 5000V for 3000Vhrs. Protein was transferred to PVDF membrane (Millipore) using the iBlot system (Invitrogen). Membranes were blocked overnight at 4°C in SEA BLOCK (Pierce), and then incubated with appropriate primary antibody overnight, followed by addition of the species-appropriate secondary antibodies. Tropomyosin-3 was detected with secondary antibody conjugated with Cy5-dye for fluorescent detection while PCBP was detected with secondary antibody conjugated to HRP for chemiluminescent detection. Fluorescent detection was performed using the Typhoon Imager 9400 at 200μM normal sensitivity while chemiluminescent detection was performed using Immobilon (Millipore) and Kodak™ X-OMAT™ x-ray film according to the manufacturer's conditions.

Results

Hepatitis C virus (HCV) often persists in the liver of infected individuals. While the mechanisms of viral persistence remain poorly understood, they are certain to involve both immune supression and cellular modifications. Regardless, continuing replication can lead to severe liver complications including cirrhosis, fibrosis and carcinoma. Many of these changes can be mediated through intracellular signalling changes, a process predominantly controlled through the phosphorylation of key regulatory proteins. Although previous studies have investigated the functional status of specific protein kinases and phosphatases with respect to the expression of HCV proteins (Alisi et al., 2005; Borowski et al., 1999a; Borowski et al., 1996; Foy et al., 2003; Fukuda et al., 2001; Francois et al., 2000; Gale, Jr. et al., 1998; Georgopoulou et al., 2003; He et al., 2002; Macdonald et al., 2003; Street et al., 2004; Macdonald et al., 2004; Pavio et al., 2003; Sarcar et al., 2004; Soldaini et al., 2003; Sundstrom et al., 2005; Tan et al., 1999; Tsukiyama-Kohara et al., 2004; Waris et al., 2003; Zhao et al., 2001), in most cases the functional consequences (i.e. change to the phosphorylation status of the substrate) have not been addressed. It was therefore the aim of this work to identify the changes to the host cell phosphoproteome during HCV infection.

JFH1 infection.

A derivative of the Huh7 human hepatocyte cell line, referred to as Huh7.5 (Blight et al., 2002), was infected with passage five of HCV-JFH1 at a multiplicity of infection (m.o.i.) of one. Identically plated Huh7.5 cells were incubated with

supernatant from mock transfected (but similarly treated) samples. When cells approached confluency (four days post infection), they were split into two culture dishes and harvested the following day. This was done in order to ensure adequate protein yields and to acquire cells at an appropriate density to allow for cell proliferation. As a marker for HCV replication, cells were probed for viral protein NS5A expression by indirect immunofluorescence. As shown in figure 20; essentially all cells that were incubated with virus expressed viral NS5A protein at five days post infection. Mock infected samples displayed no immunofluorescent signal.

HCV infection alters the phosphoproteome of Huh7.5 cells.

In an effort to study the potential phosphorylation changes induced during early stages of HCV infection, mock and JFH1 infected cellular lysates were subjected to phosphoprotein immunoaffinity purification. Based on the amount of purified protein obtained from starting lysates, the percentage of phosphorylated protein by weight captured was similar: mock-infected (14% ± 4%) verus HCV-infected (10% ± 1.9%) of total cell lysates (three replicates).

Enriched phosphoprotein samples were then compared in a quantitative manner using high-resolution two-dimensional difference-in-gel electrophoresis (2D-DIGE) (Unlu et al., 1997). 2D-DIGE differs from traditional 2D-gel analysis by having the ability to multiplex protein samples within the same gel by tagging each sample with spectrally distinct fluorochromes prior to separation. In addition,

Figure 20. **Persistent infection of Huh7.5 cells with hepatitis C virus.** Huh7.5 cells were infected (m.o.i = 1) with JFH1 virus and passaged twice into fresh media for a total of five days. Viral protein expression was detected by indirect immunofluorescence of NS5A protein (depicted in green). Nuclei were stained with DAPI (depicted in blue). **(A)** Mock-infected cells, **(B)** HCV-infected cells. Overlay of the two images demonstrates near complete infection of all cells. Images were captured at 100X magnification.

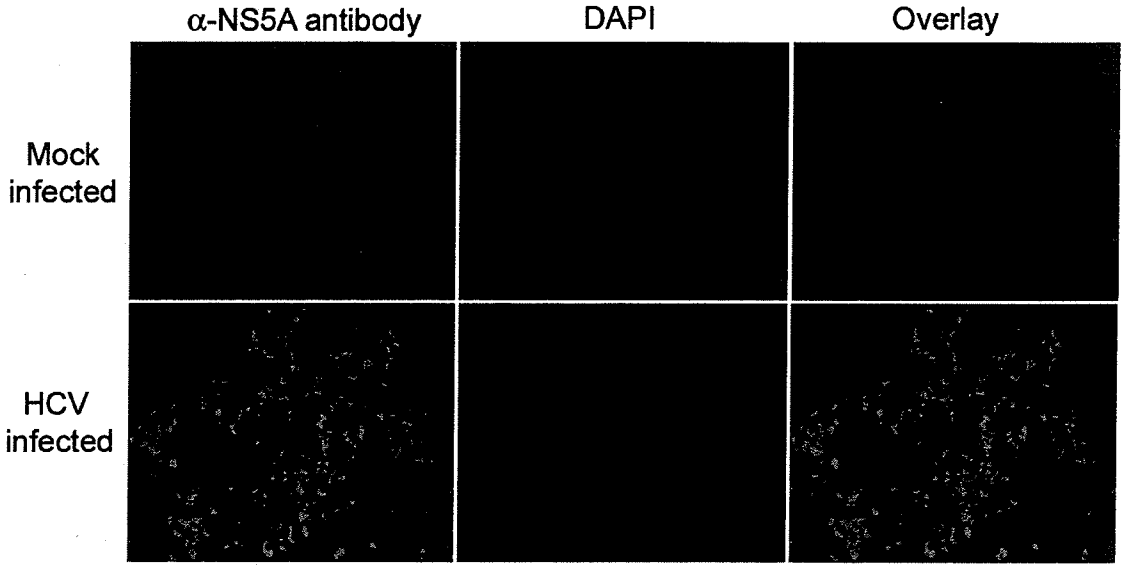
α-NS5A antibody
DAPI
Overlay
Mock infected
HCV infected

it incorporates an internal standard which is generated by pooling equal portions from each sample type. This standard is present on every gel used for the experiment and each individual protein spot volume is then normalized to the internal control spot volume. The standardized log volume ratios are determined and protein spot abundances which differed between mock- and HCV-infected cells by at least 1.50 fold with a student's t-test $p \leq 0.05$ were deemed significant. On average, 2002 proteins (standard deviation=94) were detected and of these, 38 distinct protein spots passed the selection criteria set out above. Thirty protein spots were increased in abundance while eight were decreased in abundance when comparing HCV-infected to mock-infected cells. A representative gel image from HCV-infected cells is depicted in Fig. 21 with spot labels indicating proteins that showed significant differential abundance. The spot pattern for mock infected samples demonstrated essentially the same qualitative protein pattern as for virus infected cells, with the exception of protein spot 1232 which was completely absent from mock-infected cells (Fig. 22).

Of the 38 altered proteins, 16 were subsequently identified by LC-MS/MS and those identifications along with spot volume ratios are presented in table six (see Appendix V for detailed MS/MS information). Although this study used larger format, high resolution 2D analysis, many of the spots appeared to contain more than one protein species. The majority of the co-migrating proteins share common peptide sequences and belong to the same family of proteins, for example, tubulin (spots 853 and 860) and tropomyosin (spots 1537, 1609 and

Figure 21. **Two dimensional DIGE map of JFH1- compared to mock-infected Huh7.5 cellular phosphoproteomes.** Numbered spots indicate proteins exhibiting at least a 1.5 fold spot volume change ($p<0.05$) between mock- and JFH1-infected cells. The JFH1 scan is shown.

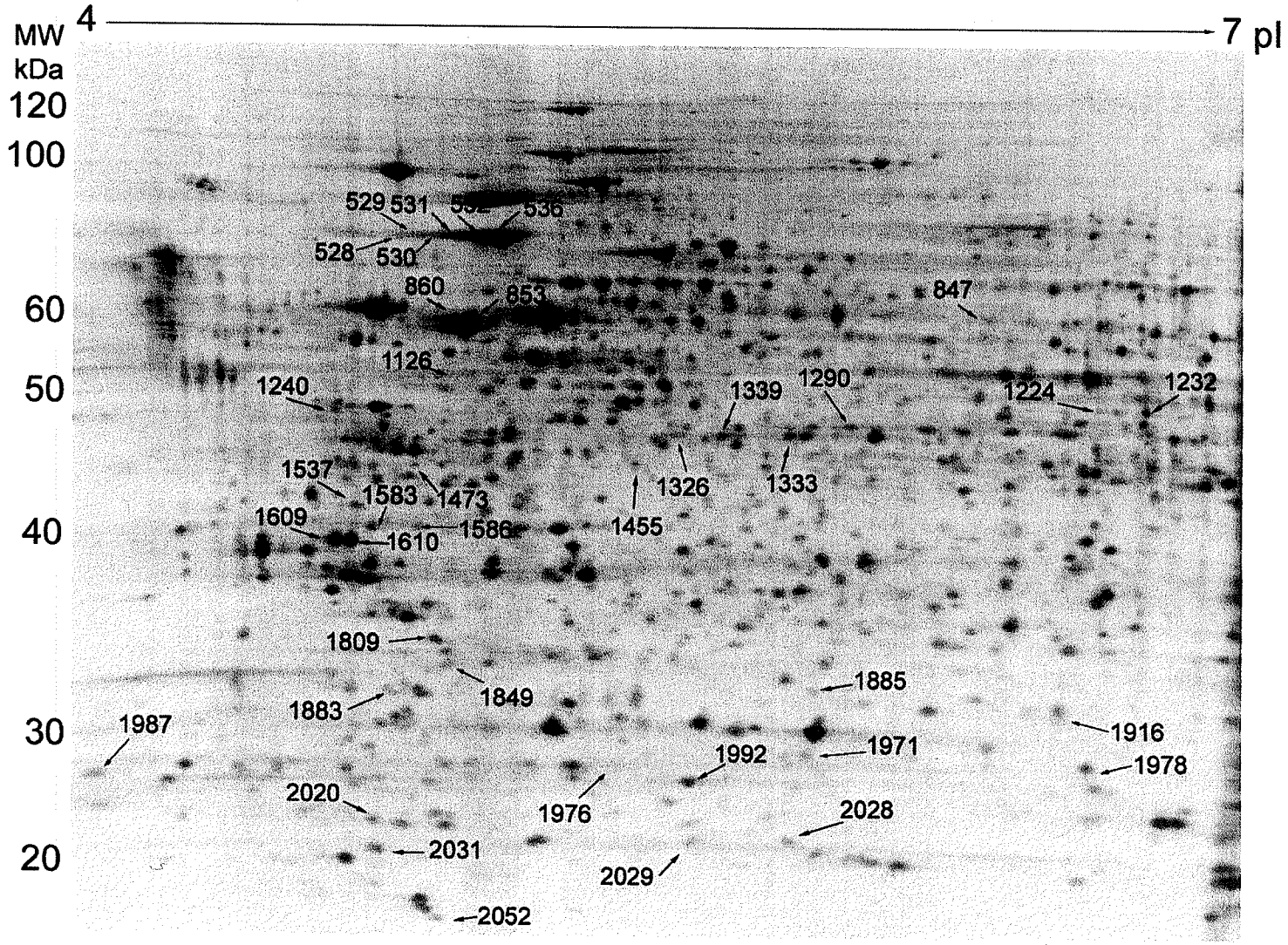
MW
kDa
4
7 pI
120
100
60
50
40
30
20
529
531
536
528
530
860
853
847
1126
1240
1339
1290
1224
1232
1537
1583
1473
1326
1333
1609
1610
1586
1455
1809
1849
1885
1883
1987
1916
1992
1971
1978
2020
1976
2028
2031
2029
2052

Figure 22. **Two-dimensional migration pattern (A) and topographical representation (B) of protein spot 1232.** Of all 36 proteins found to be differentially abundant between mock- and HCV-infected Huh7.5 cells, only spot 1232 was not detected in mock-infected cells (volume ratio=24.5 increased in infected cells).

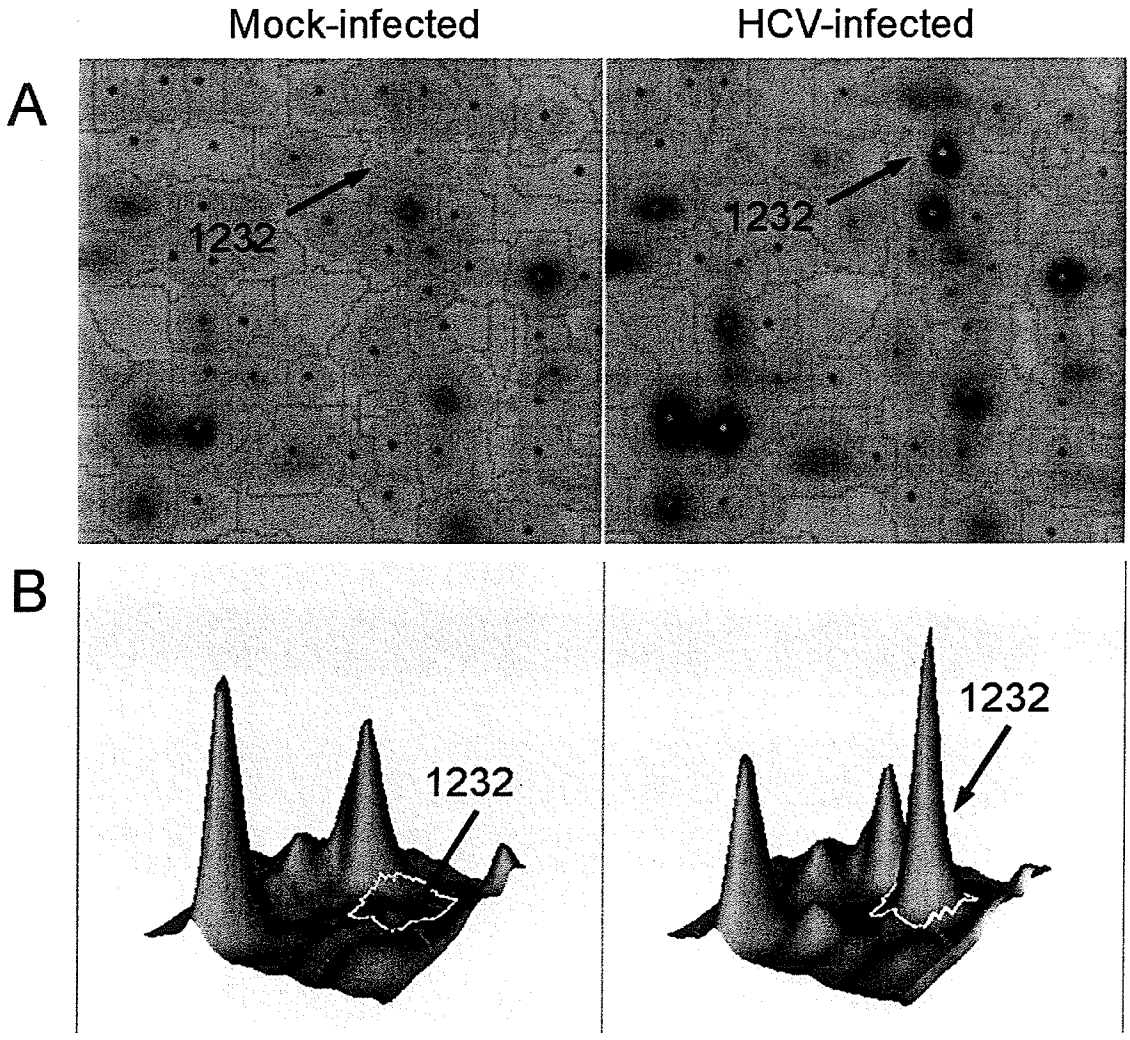
Mock-infected
HCV-infected
A
1232
1232
B
1232
1232

Table 6. **Mass spectrometry based identification of phosphoproteins differentially expressed in HCV infected cell lines.** In cases where more than one protein species was identified from a single protein spot, the highest rankling protein identification based on Mascot score is listed first. (A) Standardized log abundance average volume ratio of HCV infected/mock-infected cells from DeCyder, (B) Mascot probability score of protein identification, where a score >26 is considered significant ($p \leq 0.05$), (C) percent coverage of protein sequenced, and (D) the number of peptides seen by the mass spectrometer followed by the number of unique peptides in brackets.

Spot #	AVR[a]	Students' T-test(p)	SwissProt ID/Protein Name	MW	Score[b]	Coverage[c]	Unique Peptides[d]
Proteins identified with increased abundance in HCV infected cells							
531	3.76	0.0084	GRP78_HUMAN, 78kDa glucose-regulated protein	72402	354	22%	10
536	3.61	0.0043	GRP78_HUMAN, 78kDa glucose-regulated protein	72402	1043	37%	21 (20)
			HSP7C_HUMAN, Heat shock cognate 71kDa	71082	91	5%	1 (0)
853	1.60	0.029	TBB2C_HUMAN, Tubulin beta-2C chain	50255	718	33%	11 (0)
			TBB4_HUMAN, Tubulin beta-4 chain	50010	646	29%	10 (1)
			TBB2A_HUMAN, Tubulin beta-2A chain	50274	627	33%	11 (2)
			TBB5_HUMAN, Tubulin beta chain	50095	578	29%	10 (1)
			TBB3_HUMAN, Tubulin beta-3 chain	50856	488	22%	8 (1)
			TBB6_HUMANm Tubulin beta-6 chain	50281	355	12%	5 (1)
			TBB1_HUMAN, Tubulin beta-1 chain	50865	174	5%	2 (0)
			TBA1A_Tubulin alpha-1A chain	50788	44	5%	2 (2)
860	1.60	0.036	TBB2C_HUMAN, Tubulin beta 2C-chain	50255	819	38%	13 (0)
			TBB5_HUMAN, Tubulin beta chain	50095	808	38%	13 (1)
			TBB2A_HUMAN, Tubulin beta-2A chain	50274	699	34%	11 (0)
			TBB4_HUMAN, Tubulin	50010	677	34%	12 (1)
			TBB3_HUMAN, Tubulin beta-3 chain	50856	546	24%	10 (0)
			TBB6_HUMAN, Tubulin beta-6 chain	50281	405	20%	8 (3)
1232	24.45	0.00054	PCBP1_HUMAN, Poly (rC)-binding protein 1	37987	166	19%	4
1473	2.48	0.029	EF1D_HUMAN, Elongation factor 1-delta	31217	171	29%	7
1537	3.46	0.022	TPM1_HUMAN, Tropomyosin alpha-1 chain	32746	99	15%	4 (1)
			TPM3_HUMAN, Tropomyosin alpha-3 chain	32856	53	11%	3 (0)
1583	2.98	0.017	CHM4A_HUMAN, Charge multivesicular body protein 4A	25083	149	22%	3
1609	4.43	0.0067	TPM4_HUMAN, Tropomyosin alpha-4 chain	28619	209	35%	6 (0)
			TPM2_HUMAN, Tropomyosin beta chain	32945	209	12%	6 (1)
			TPM1_HUMAN, Tropomyosin alpha-1 chain	32746	116	9%	3 (0)
			TPM3_HUMAN, Tropomyosin alpha-3 chain	32856	116	9%	3 (0)
1610	3.05	0.021	TPM3_HUMAN, Tropomyosin alpha-3 chain	32856	318	16%	6 (2)
			TPM1_HUMAN, Tropomyosin alpha-1 chain	32746	159	13%	4 (0)
			TPM4_HUMAN, Tropomyosin alpha-4 chain	28619	120	10%	3 (0)
1992	1.83	0.012	PDCD5_HUMAN, Programmed cell death protein 5	14276	371	37%	4 (4)
			H2B1A_HUMAN, Histone H2B type 1-A	14159	46	7%	1 (1)
			TPD54_HUMAN, Tumor protein D54	22281	37	4%	1 (1)

2031	2.63	0.0035	MOFA1_HUMAN, MORF4 family-associated protein 1 TBA1B_HUMAN, Tubulin alpha-1B chain	14697 50804	93 67	18% 6%	1 2	(1) (2)
528	2.91	0.0099						
529	4.09	0.016						
530	2.94	0.031						
532	5.28	0.019						
847	1.96	0.025						
1126	1.46	0.043						
1224	4.52	0.0088						
1240	4.13	0.0022						
1290	1.42	0.048						
1455	1.40	0.025						
1586	2.30	0.039						
1849	3.95	0.0093						
1883	2.71	0.035						
1987	2.27	0.030						
2020	3.63	0.0019						
2028	4.45	0.030						
2029	2.70	0.037						
2052	7.20	0.041						
Phosphoproteins identified with decreased abudance in HCV infected cells								
1333	-1.61	0.034	CNN3_HUMAN, Calponin-3 MYG1_HUMAN, UPF0160 protein MYG1	36562 42761	271 37	34% 13%	7 3	(7) (3)
1339	-2.15	0.025	CNN3_HUMAN, Calponin-3	36562	114	21%	5	
1885	-1.57	0.038	DUT_HUMAN, Deoxyuridine 5'-triphosphate nucleotidohydrolase	26975	204	21%	4	
1971	-4.85	0.0017	MGN_HUMAN, Protein mago nashi homolog RL22_HUMAN, 60S ribosomal protein L22 H2B1A_HUMAN, Histone 2B type 1-A	17210 14835 14159	125 73 49	32% 8% 7%	3 1 1	(3) (1) (1)
1326	-1.61	0.012						
1809	-1.53	0.029						
1916	-2.02	0.037						
1978	-3.08	0.0034						

1610) proteins. It should be noted that despite the high sequence identity for most of the co-migrating proteins, each protein detailed in table 6 was represented by at least one unique peptide not found in the other protein family members and because of this, we are not in a position to definitively exclude these proteins from the list.

Phosphoproteins increased during HCV infection were tubulin-beta chain family members (1, 2A, 2B, 3, 4, 5 and 6), tropomyosin alpha and beta chain family members (α1, α3, α4), stress response proteins (GRP78 and programmed cell death protein 5) as well as regulators of translation (elongation factor 1-delta and poly (rC)-binding protein). Fold increases varied from 1.6 to 24.5. The most dramatic change in protein abundance was seen for poly (rC)-binding protein (spot 1232) which had an average standardized log volume ratio of HCV/mock=24.5 (p= 0.00054). Poly (rC)-binding protein 1 (PCBP1) shares significant homology with PCBP2 and the heterogeneous nuclear ribonucleoprotein K (hnRNP K) which are both involved in the stabilization and control of cellular mRNA translation (Leffers et al., 1995) and translation of some viral RNAs including poliovirus (Silvera et al., 1999). Table 7 details each of the identified proteins function(s) and their documented phosphorylation sites.

Substantially fewer phosphoproteins demonstrated a decrease in abundance in infected cells. Fold decreases were from -1.6 to -4.9. One protein, calponin, was found at two of the decreased spot locations (1.6 (spot 1333) and 2.2 (spot 1339)

Table 7. **Known phosphorylation sites and protein functions of identified proteins from HCV infected cells.** Proteins which share extensive homology (tubulin and tropomyosin proteins) are characterized to have the same protein function; however, each individual protein family member exhibited different phosphorylation patterns as indicated.

Protein	Phosphorylation	Function
Increased abundance in HCV infected cells		
Charge multivesicular body protein 4A	No evidence	Mediates formation and sorting endosomal cargo protein into multivesicular bodies
Elongation factor 1-delta	(Gevaert et al., 2005; Molina et al., 2007; Olsen et al., 2006)	Stimulates exchange of GDP for GTP bound to EF-1-alpha, phosphorylated upon DNA damage (likely by ATM or ATR)
GRP78	(Molina et al., 2007)	Implicated in aiding formation of multimeric complexes in the ER
Histone H2B type 1-A	No evidence	Core component of nucleosome
MORF-4 family associated protein 1	No evidence	Forms a complex with MORF4L1, MRFAP1 and RB1, implicated in inducing senescence in tumour cell lines
Poly (rC)-binding protein 1	(Beausoleil et al., 2004; Beausoleil et al., 2006; Olsen et al., 2006; Olsen et al., 2006)	Binds single stranded nucleic acid, preferentially to oligo dC via 3 KH domains, phosphorylation decreases nucleic acid binding ability
Programmed cell death protein 5	(Beausoleil et al., 2004)	Activated in cells undergoing apoptosis
Tubulin alpha-1A chain Tubulin alpha-1B chain	(Olsen et al., 2006) (Rush et al., 2005)	Major constituent of microtubules, forms heterodimers of alpha and beta chains

Tubulin beta chain Tubulin beta-1 chain Tubulin beta-2A chain Tubulin beta-2C chain Tubulin beta-3 chain Tubulin beta-4 chain Tubulin beta-6 chain	(Rush et al., 2005) No evidence No evidence (Olsen et al., 2006) No evidence (Nousiainen et al., 2006) (Matsuoka et al., 2007)	Major constituent of microtubules, forms heterodimers of alpha and beta chains
Tropomyosin alpha-1 chain Tropomyosin alpha-3 chain Tropomyosin alpha-4 chain	No evidence (Beausoleil et al., 2004) No evidence	Implicated in stabilization of actin cytoskeleton in non-muscle cells
Decreased abundance in HCV infected cells		
Calponin-3	(Molina et al., 2007; Olsen et al., 2006)	Capable of binding actin, calmodulin, troponin and tropomyosin, inhibits the actomyosin Mg-ATPase activity of actin when bound
Deoxyuridine 5'-triphosphate nucleotidohydrolase	(Olsen et al., 2006)	Nucleotide metabolism, decreases intracellular pools of dUTP in order to avoid uracil incorporation into DNA, phosphorylated form is inactive
Protein mago nashi	No evidence	Involved in mRNA splicing and non-sense mediated decay

fold decreased). The remaining decreased abundance phosphoproteins were identified as deoxyuridine 5'-trisphosphate nucleotidohydrolase (VR= -1.6), a protein involved in nucleotide metabolism (Ladner et al., 1996b; McIntosh et al., 1992) and protein mago nashi homolog (VR= -4.9).

Immunoblot confirmation of 2D-DIGE results

In order to confirm the differences detected by 2D-DIGE for select proteins, we performed 1DE and 2DE immunoblotting. Phosphoprotein-enriched samples from mock- and JFH1-infected cells were separated by either standard SDS-PAGE (1DE) or 2DE and processed for immuno-detection. Standard 1D minigel immunoblotting for two of the elevated proteins, tropomyosin-3 (Fig. 23A) and PCBP1 (Fig. 23B), did not corroborate the findings seen by 2D-DIGE analyses. In fact, the levels of tropomyosin-3 were lower in HCV-infected cells than mock-infected cells (compare lanes 1-3 to lanes 4-6 in Fig. 23A). The lower amount of tropomyosin in HCV-infected cells is consistent with previous findings that the global amount of tropomyosin is lower in both HCV infected cells and HCV-related hepatocellular carcinoma (Mannova et al., 2006; Yokoyama et al., 2004).

Alternatively, high resolution 2DE immunoblotting specific for tropomyosin-3 revealed that one of the isoforms detected by the antibody was essentially undetectable in mock-infected samples (Fig. 23C arrowhead) by 2DE blotting. These findings confirmed that tropomyosin-3 was in fact one of the isoforms of

Figure 23. **Confirmation of tropomyosin-3 and PCBP1 by immunoblotting.** 1D SDS-PAGE immunoblotting for total protein did not corroborate changes characterized by 2D-DeCyder analysis. Equal amounts of phospho-enriched samples were purified in triplicate (mock lanes 1-3, HCV-infected lanes 4-6) and probed for **(A)** tropomyosin-3 (TPM3) and **(B)** PCBP1. Immunoblotting of proteins separated by 2DE revealed significant differences in protein spot patterns for both tropomyosin-3 **(C)** and PCBP1 **(D)**. Protein isoforms that differed in expression are highlighted with arrowheads. Additional PCBP1 isoforms are indicated with arrows.

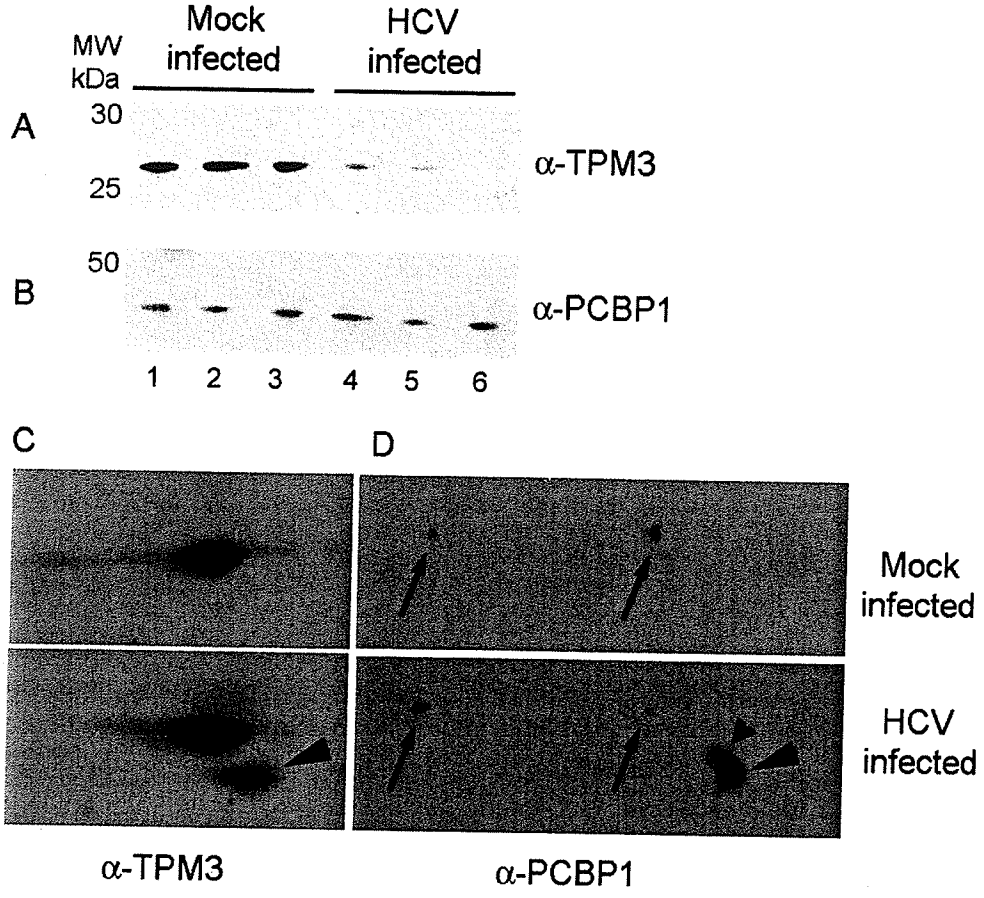
Mock infected
HCV infected
MW kDa
A
30
25
α-TPM3
B
50
α-PCBP1
1 2 3 4 5 6
C
D
Mock infected
HCV infected
α-TPM3
α-PCBP1

tropomyosin which was elevated during infection and represents almost a plus/minus change in abundance. It is likely that this greater degree of difference was obscured in our 2D-DIGE analysis by additional proteins of the tropomyosin family which did not differ in abundance but which comigrated to the same position as tropomyosin 3. Furthermore, these findings suggest that the differences seen by our 2D DeCyder analysis represented changes specific to phospho-isoforms and was tropomyosin-3 specific. In other words, not all tropomyosin 3 phospho-isoforms were altered, only one of the two isoforms seen in the 2D immunoblot was significantly increased in HCV-infected cells (compare Fig. 23A to C). It is also noteworthy to mention that when 1D-immunoblotting was performed with a pan-tropomyosin family antibody on phospho-enriched mock and HCV-infected samples no significant differences were observed (data not shown). This reinforces the specific nature of phospho changes seen during HCV infection (data not shown and Fig. 23C).

The second protein change evaluated by immunoblotting was poly-rC-binding protein 1 (PCBP1), which showed the largest change in abundance, by 24.5 fold. Shown in Fig. 23D are the 2D-PAGE western blots for PCBP1 from mock- and HCV-infected phosphoprotein enriched samples. Despite the presence of at least two higher MW PCBP1 isoforms in both samples (arrows), the absence of the lower isoform (arrowhead) from mock-infected samples confirms the dramatic abundance difference observed for PCBP1 between mock- and HCV-infected phosphoproteomes. This high resolution Western blot also raises the possibility

that a second PCBP1 protein (small arrowhead) is up-regulated in HCV infected cells.

Discussion

Hepatitis C virus (HCV) often leads to severe liver complications in chronically infected patients. Although the mechanism(s) of virus persistence and associated diseases are poorly understood, viruses do alter the homeostasis of infected cells in order to generate a cellular environment conducive to virus propagation. These changes can lead to alterations in cascade events such as those observed in intracellular signalling pathways mediated by protein phosphorylation. These changes can ultimately modify the functional status of downstream substrate proteins and alter gene transcription and protein expression levels of specific targets.

Previous studies have attempted to address both the genomic and proteomic changes induced by the expression of HCV proteins, genome replication and infection in a number of models. Large scale microarray analyses of chimpanzee liver biopsies revealed only subtle changes mostly associated with the interferon response to infection (Bigger et al., 2001; Bigger et al., 2004). These alterations have not been directly associated with changes induced in HCV-infected cells as the changes may have been due to co-purified immune cells. Furthermore, even in detailed analyses of cell lines harbouring self replicating HCV subgenomic and full length genomes (replicon cell lines), very few, if any, significant changes in mRNA levels were observed between parental cell lines and those in which the

HCV genome was present (Geiss et al., 2003; Hayashi et al., 2000; Scholle et al., 2004). It is conceivable that few differences were seen in replicon containing cell lines for several reasons including the level of HCV expression and replicon attenuation. The lack of transcriptome changes here does not exclude the possibility of proteome changes as expression levels of proteins can occur even in the absence of changes to the cognate mRNA levels. Furthermore, protein function can be altered by post-translational modification, cleavage and subcellular localization; all issues that would only be revealved at the protein level.

With regards to proteomic changes induced by HCV, prior studies have focused on the differences in non-cancerous and cancerous liver biopsies from HCV afflicted patients. A number of groups have described elevations in stress response proteins in tumour tissues with heat shock proteins; GRP75, GRP78 and HSC70 (Takashima et al., 2003; Yokoyama et al., 2004). There have also been multiple studies that demonstrated decreases in various tropomyosin proteins in HCV related carcinoma (Takashima et al., 2003; Yokoyama et al., 2004; Diamond et al., 2007). Proteomic analyses of replicon cell lines have also characterized changes in fatty acid oxidation pathways, mitochondrial function, apoptosis, vesicle transport/cytoskeleton and stress response related proteins (Mannova et al., 2006; Fang et al., 2006; Jacobs et al., 2005). However in all previous HCV proteomic studies, information pertaining to isoform specific changes with valid quantitative analyses had been lacking. Furthermore, no study

has yet addressed the phosphorylation changes that occur during HCV infection, particularly in the absence of mitogen stimulation. It was therefore the goal of this research to characterize the phosphorylation alterations that occur in HCV-infected cells using high-resolution, quantitative 2D electrophoresis.

In order to identify the potential phosphorylation changes induced by hepatitis C virus infection, we infected Huh7.5 liver cell lines with high titre HCV (JFH1 strain, genotype 2) and passaged the infected cells for five days. Although it is not definitively known what proportion of the liver is infected in chronic individuals, it has been postulated that approximately 10% of hepatocytes are infected (Chang et al., 2003) and that these infected cells produce roughly 1×10^{12} virions per day (Neumann et al., 1998). From Figure 20 it is clear that approximately 100% of the cells were infected. Such a high level of infection was used in order to more clearly detect virus-induced effects and although the proportion of cells infected in this study may be large with regards to a clinical chronic infection, it nevertheless addresses differences in phosphoproteins relevant to HCV infection.

Both mock-infected and HCV-infected Huh7.5 liver cell lines were harvested and processed for phosphoprotein enrichment by immunoaffinity resin followed by multiplexed, quantitative two-dimensional electrophoresis (Fig. 21). Thirty-eight phosphoprotein species were found to be differentially represented in infected cells versus mock-infected cells. Of these, 16 protein spots were subsequently

identified but our analysis suggested the possibility of more than one protein in several spots. The detection of multiple proteins within one spot is likely due to spot co-migration and could potentially be resolved by using alternate strategies including narrower pH range IPG strips. Multiple protein identifications were assigned to certain protein spots, specifically spots identified as tubulin or tropomyosin. Each of the tubulin or tropomyosin isoforms identified in this study have very little difference in isoelectric points and molecular weights, hence co-migration is likely. Moreover, they share substantial sequence homology. Because we can not exclude the presence of multiple tubulin or tropomyosin isoforms in certain protein spots, we have included them in table 6. Further work is underway to definitively assign identifications to these proteins.

The most dramatically altered phosphoprotein isoform identified in this study was poly-rC nucleic acid binding protein (PCBP1). Interestingly, the isoform which was increased in viral infection was not even detectable by 2D-DIGE analysis in mock-infected cells (Fig. 22). PCBP1 is present in phospho-enriched samples from both mock-infected and HCV-infected cells, however, it appears that at least one phosphorylated isoform of PCBP1, denoted as spot 1232, is much more abundant in HCV infected cells (DeCyder volume ratio=24.5). As phosphorylated PCBP1 shows decreased affinity for binding nucleic acid (Leffers et al., 1995), it suggests that PCBP1 may have a significant proportion as an inactive form in HCV-infected cells. Previous work has described the ability of PCBP1 and the highly homologous PCBP2 protein to bind the 5' non-translated regions of HCV

(Spangberg and Schwartz, 1999), and PCBP2 also binds to the 3' NTR of HCV (Tingting et al., 2006). Although little is known with regards to the involvement of PCBP1 in HCV translation, it has been shown that HCV IRES mediated translation is not inhibited in PCBP2 immunodepleted rabbit reticulolystes (Fukushi et al., 2001) or in *Sacchromyces cerevisiae (Rosenfeld and Racaniello, 2005)* in which the PCBP2 gene is absent. These results are in contrast to what is known with regards to poliovirus IRES translation which requires the co-operation of PCBP2 (Blyn et al., 1996; Blyn et al., 1997; Silvera et al., 1999). Therefore it is possible that HCV IRES translation relies on PCBP1 much in the same manner that poliovirus IRES translation requires PCBP2. Additionally, the functional role that PCBP1 plays in infected cells may be altered due to the prescence of phospho-PCBP1. In either case, the role of post-translational modification remains unknown and we are examining this issue further.

Elongation factor 1 delta (EF-1 Δ), another protein associated with translation, was found to be elevated in phosphoprotein-enriched HCV infected cell lysates. EF-1-Δ combines in a complex with three other elongation factor subunits (alpha, beta and gamma) (Ejiri et al., 1983). The delta subunit is responsible for the exchange of GDP for GTP that is bound to the alpha subunit, a function essential for efficient cellular mRNA translation (Carvalho et al., 1984b; Carvalho et al., 1984a; van Damme et al., 1990) but not necessarily for viral RNA translation. For example, it has been shown that HIV-1 expresses a protein that binds and inhibits EF-1-Δ (Xiao et al., 1998). EF-1-Δ has is also involved in the

oncogenic transformation of cells (Kolettas et al., 1998; Sinha et al., 2000; Lei et al., 2002) and is elevated in oesophageal carcinoma (Ogawa et al., 2004). EF-1-Δ is believed to be phosphorylated upon DNA damage of the host genomic material by either ATM or ATR kinases (Matsuoka et al., 2007). The increase in the phospho-isoform of EF-1- Δ in HCV infected cells suggests that these cells may be responding to a stress akin to DNA damage. Given that damage to genomic material is an inherent feature of cellular transformation with progression to cancer, it is possible that these factors may contribute to a transformation phenotype since HCV has been implicated in hepatocellular carcinoma (Saito et al., 1990).

A number of the proteins that were increased in HCV-infected cells were identified as cytoskeletal elements (tropomyosin and tubulin). Although the functional consequences of increased tubulin and tropomyosin protein phosphorylation are not fully understood, numerous publications have described cytoskeleton requirements for virus propagation, reviewed in, (Radtke et al., 2006; Greber and Way, 2006). Tubulin forms heterodimers of alpha and beta chains and constitutes a major component of microtubules, however phosphorylation specific to beta tubulin has been associated with impairing tubulin dimer formation (Fourest-Lieuvin et al., 2006). Previous work examining the cytoskeletal requirements of HCV infection determined that actin and microtubule polymerization is essential for proper viral RNA synthesis (Bost et al., 2003), however, in cells supporting subgenomic replicon propagation, tubulin

alpha-1 and 6 as well as tubulin beta-5 were shown to be decreased compared to naïve cells (Fang et al., 2006). It should be emphasized that these previous findings evaluated total protein amount while our studies have focused on changes in phosphorylated protein isoforms. As shown for two proteins, tropomyosin-3 and PCBP1 (Fig. 23), there are clear differences between total and phosphoprotein contents.

Regulation of the cellular cytoskeleton has also been described for minute virus of mouse (MVM) whereby in early infection, microtubule stability is associated with MVM mediated phosphorylation of alpha and beta tubulin, while at later stages of infection, disassembly of actin filaments is observed (Nuesch et al., 2005). Aberrant distribution of tubulin has been associated with the HCV frameshift protein (F) due to its association with the cellular protein, prefoldin-2 (Tsao et al., 2006), setting the precedent for HCV mediated cytoskeleton regulation.

The other cytoskeletal-associated proteins elevated in the HCV phosphoproteome belong to the tropomyosin family of proteins. Tropomyosin alpha and beta chains are implicated in the stabilization of the actin cytoskeleton in non-muscle cells. Tropomyosin has been implicated in cellular transformation; however, a decrease in tropomyosin levels correlates with cancer (Bhattacharya et al., 1990; Mahadev et al., 2002; Bharadwaj and Prasad, 2002). This is the case with HCV-associated hepatocellular carcinoma, whereby tropomyosin beta

chains have been found to exist in decreased amount in patients (Kuramitsu and Nakamura, 2005; Yokoyama et al., 2004) and also subgenomic replicon cell lines (Mannova et al., 2006). Although each of the above mentioned studies observed a decrease in total tropomyosin levels, our study describes an increase in multiple phospho-tropomyosin isoforms from infected cells. At present, the functional consequences of this modification on tropomyosin are currently unknown.

Another protein shown to increase during HCV infection was programmed cell death protein 5 (PDCD5), which has also been shown to be elevated in tumour cell lines and activated when cells are under stress and undergoing apoptosis (Liu et al., 1999; Cecconi et al., 2003). Of note, a recent plaque assay based method for JFH1 infection quantification is based on the induction of ER-stress induced apoptosis of infected cells and their resulting cell death (Sekine-Osajima et al., 2008). It is plausible that one of the mechanisms responsible for this phenotype is the activation of PDCD5.

The remaining proteins found to be increased in abundance from the infected cells belong to protein chaperone families (GRP78 and charge multvesicular body protein 4A) and are involved in mediating proper folding of proteins. Given that viruses often overwhelm the host cellular translational machinery due to the extensive amount of protein production, it is a reasonable observation that cellular proteins responsible for handling protein processing and folding would be

up-regulated upon viral infection. It has been previously documented that the heat shock proteins 90 (HSP90), HSP71 and GRP78 are all involved in some manner with HCV infection and hepatocellular carcinoma. These associations are most likely due to the ER-stress induced by excess protein production (Takashima et al., 2003; Sekine-Osajima et al., 2008; Ciccaglione et al., 2005; Ciccaglione et al., 2007; Nakagawa et al., 2005; Benali-Furet et al., 2005; Tardif et al., 2002; Choukhi et al., 1998). When cells undergo ER stress associated with excess protein processing, GRP78 (also known as BiP), releases from two transmembrane proteins, PERK and IRE-1 which allows these two proteins to transmit signals in response to errors in protein folding that ultimately culminate in translation inhibition (Bertolotti et al., 2000). Freed GRP78 then exists as either unmodified monomers or aggregates that are phosphorylated. In its phosphorylated form, GRP78 is likely inactive (Freiden et al., 1992). In this study we found two isoforms of GRP78 to be increased in phosphoprotein-enriched HCV-infected cells (spot 531 by 3.8-fold and spot 536 by 3.6 fold). Moreover, it is very likely given the migration pattern in Fig. 21, that unidentified spots 528-530 and 532 also represent different GRP78 isoforms. Although total GRP78 levels are elevated during HCV infection thus leading to the inhibition of PERK, it is possible that these effects are balanced by phosphorylation of GRP78 thereby inactivating it. Interestingly, the HCV E2 glycoprotein binds to both PERK (Pavio et al., 2003) and eIF2 alpha (Taylor et al., 1999) which inhibits the ability of both proteins to suppress translation. Based on these findings and previous work, it would seem that HCV infection modulates many stages of the unfolded

protein response likely to ensure that translation is not halted during the ER stress induced by viral infection.

Of the four phosphoprotein isoforms decreased during HCV infection, no clear trend in pathway activation or protein function can be made. Two of the protein species were identified as calponin. In non-muscle cells such as hepatocytes, calponin is capable of binding to actin (Takahashi et al., 1986), calmodulin, troponin and tropomyosin (Nakamura et al., 1993). Furthermore, calponin is thought to function similarly to the smooth muscle isoforms of calponin which inhibit cell motility and actin redistribution (Shirinsky et al., 1992; Haeberle, 1994) due to the inhibition of the Mg-ATPase activity of actin. Protein kinase C (PKC) mediated phosphorylation of calponin inhibits the proteins ability to bind both actin and tropomyosin (Winder and Walsh, 1990; Jin et al., 2000) however, both actin and tropomyosin can decrease the rate of calponin phosphorylation (Nakamura et al., 1993). Interestingly, tropomyosin has been shown to inhibit the phosphorylation of calponin (Nakamura et al., 1993) and therefore the decrease in calponin phosphorylation observed in this study may be a reflection of the elevated phosphorylation of multiple tropomyosin isoforms from HCV-infected cells.

The identification of deoxyuridine 5'-trisphosphate nucleotidohydrolase (DUT) as one of the decreased proteins is curious. DUT produces dUMP from dUTP thereby decreasing intracellular pools of dUTP. This process reduces the

possibility of uracil incorporation into DNA. Both herpes viruses and HIV encode their own DUT enzyme(Priet et al., 2006), but given that HCV is an RNA virus, maintenance of DUT function would not seem to be essential. However, it should be kept in mind that the species of DUT found in this study represents a phosphorylated isoform and the significance of decreased phosphorylation to the proteins' function is not currently known, however phosphorylation of DUT has been linked with the cell cycle, in particular, to cyclin dependent protein kinase p34 (cdc2) (Ladner et al., 1996a).

Overall, a general theme of phosphoproteome changes induced by HCV can be formed that predominantly involves the modulation of cytoskeletal elements and translational machinery during infection. As with all virus replication, the ability to circumnavigate the intracellular network of cytoskeletal proteins is essential for successful virus propagation. These changes may be a reflection of the required transport of viral components to a specific subcellular compartment of the cell for efficient replication, the tethering of viral replication complexes to membranous structures, the assembly of virus particles and/or providing a path free of obstructions. Additionally, viruses are known to commandeer cellular translation mediators in order to generate large quantities of viral protein. This must of course be balanced in the case of HCV with the requirement associated with a persistent infection.

The majority of previous HCV-related phosphorylation studies have investigated the changes that occur upon serum starvation or mitogen stimulation of cells. To our knowledge that is the first work to have characterized the global quantitiatve phosphoproteome alterations induced by HCV and can serve as a comparative model for other viral studies.

Our future research efforts will entail the identification of the specific residues that are differentially phosphorylated and what kinase/phosphatase combinations cause these changes.

CHAPTER VI: Concluding Remarks

Overall conclusions

Given the intimate relationship viruses have with their host cells, understanding the delicate balance between cell survival and virus propagation represents a significant area of study. Studies based on the cellular changes induced by hepatitis C virus are of no exception. Examination of HCV pathogenesis often takes a reductionist approach, whereby alterations induced by the expression of a single viral gene are analysed.

Here, changes to the host cell phosphoproteome induced by hepatitis C virus proteins and infection were addressed in a quantitative proteomic analysis. This is the first characterization of global phosphorylation patterns of both stable subgenomic replicon cell lines and cells infected with replication competent HCV.

In order to characterize the phosphorylation changes that occur in subgenomic replicon cells or HCV-infected cells, there was the requirement for a method to enrich for phosphorylated proteins both efficiently and specifically. Phosphoprotein enrichment is accomplished using immobilized metal affinity chromatography (IMAC) whereby proteins containing negatively charged phosphate moieties are bound by a positively charged metal coupled to a support. The major advantage of this technique lies in the ability to bind phosphorylated residues, irrespective of the amino acid modified. However, it raises a potential pitfall of IMAC resins, in that metal ions do not discriminate the

origin of the negative charge, and therefore, proteins that contain extensive acidic amino acids can also be captured thereby reducing the phosphoprotein capture specificity. It has been postulated that phosphoprotein capture by immunoaffinity is more specific for phosphorylated residues; however, due to the intrinsic specificity of antibody recognition sites, greater than one form of antibody is required to capture all phosphorylated residues (serine, threonine and tyrosine). In this thesis, these hypotheses were tested by comparing the phosphoproteomes captured by IMAC and immunoaffinity. Overall, the proteins enriched for by either method were highly concordant at a qualitative level. We chose to examine protein that exhibited a substantive quantitative difference in capture (>3.5 fold) in an attempt to understand the nature of the quantitative difference. The largest proportion of proteins captured differentially were heavily enriched for by IMAC but were limited in immunoaffinity purifications. For at least one of the proteins captured by IMAC and not immunoaffinity (Hsp60), reported phosphorylation sites were not modified and therefore, the conclusion was drawn that immunoaffinity capture was more specific for phosphorylated protein isoforms over IMAC. One other issue to consider is that some of the proteins may be carried along with truly phosphorylation forms, but in this case it is hard to understand how one buffer left these interactions intact but the other buffer did not. In all subsequent phosphoproteome studies, immunoaffinity capture was utilized, because, in addition to the enhanced phosphoprotein specificity mentioned herein, the resulting samples were more amendable to the proteomic platform used to perform quantitative analyses. The ease of sample manipulation

following immunoaffinity was likely due to the inherent greater protein concentration after immunoaffinity elution as the volume generated was half of the IMAC eluted fractions. The greater the initial protein concentration was, the more likely the proteins could co-precipitate. This was of critical importance for downstream 2D-DIGE analysis as the CyDye labelling reactions are preferentially performed with protein concentrations ranging between 5-10mg/mL.

In order to address the phosphorylation changes that occur during HCV replication and polyprotein expression, two separate replication models were used. First, the prototypical subgenomic replicon, genotype 1b and second the recently isolated infectious JFH1 HCV clone, genotype 2a. There are two major differences between the subgenomic replicon and infectious clone studies. First, the genomes from which each construct was originally designed are from two distinct genotypes. The subgenomic replicon encodes one of the most predominant genotypes worldwide, 1b. Furthermore, the 1b replicon used in these studies has undergone cell-culture adaptive mutations that enhance its replication competence *ex vivo*, but are less pathogenic *in vivo* (in chimpanzee animal models). Although many researchers have developed replicons based on practically all genotypes, the classic model remains the 1b genotype most likely due to the high global incidence of this genotype. The only efficient replication competent genotype of HCV isolated to date is genotype 2a, isolate JFH1. As mentioned, this isolate demonstrates very different clinical manifestations from the prototypical HCV genotypes whereby the infected patient exhibited an extra-

hepatic disease associated with inflammation of the brain. Genotype 2a viral infections also generally respond successfully to standard therapies whereas the 1a and 1b genotypes do not. As is the case with the replicon systems, many researchers have developed other infectious genomes; however, the critical difference is the non-structural region of the genome must remain genotype 2a coding sequence in order to maintain highly efficient replication of the virus.

The second major difference between the replicon and full length studies presented herein is that although the replicon recapitulates the molecular process of virus infection (genome replication and protein expression) it does not undergo a full lifecycle of virus replication, particularly virus entry, uncoating, assembly and release. Therefore, one would not necessarily suspect that the phosphorylation changes identified to be differentially abundant in replicon cells are of the same phenotype observed in JFH1 "persistently" infected cells. However, there were a number of functional trends that were consistently observed between both systems relating to cytoskeleton alterations, ER-Golgi stress pathways and translation regulation which can be seen in figure 24. A more detailed comparison of the altered phosphoproteins is listed in table 8. Moreover, phosphorylated isoforms of calponin, a cytoskeletal regulator were decreased in abundance in HCV replicon cell lines and HCV infected cell lines, although at this time it is unknown if the proteins from each study represent the same isoform. Interestingly, the calponin isoform that demonstrated altered abundance due to HCV was also the same isoform that immunoaffinity

Figure 24. **Gene ontology of proteins differentially abundant in HCV replicon cell lines and cells infected with HCV.** Category assignment based on NcBI database.

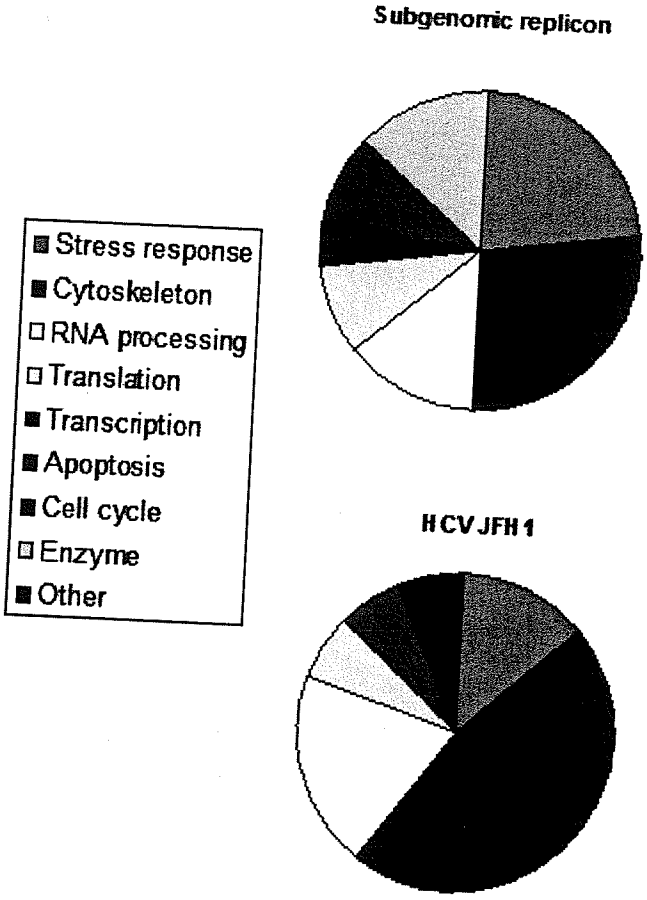
Subgenomic replicon
Stress response
Cytoskeleton
RNA processing
Translation
Transcription
Apoptosis
Cell cycle
Enzyme
Other
HCV JFH 1

Table 8. **Comparative analysis of altered phosphoproteins in HCV subgenomic replicon- and HCV infected-Huh7.5 cells**. Phosphoproteins that exhibited an increase in abundance are indicated with ↑ while proteins that exhibited a decrease in abundance are indicated with ↓. ND, not determined.

Protein	Subgenomic Replicon	JFH1 Infection
Amphiphysin II	↑	ND
Basic transcription factor 3L4	↓	ND
Calponin	↓	↓
Charged multivesicular body 4A	ND	↑
Cofilin	↑	ND
DUT	ND	↓
GRP75	↑	ND
GRP78	↓	↑
hnRNP K	↑	ND
HSP90alpha	↓	ND
HSP90beta	↑/↓	ND
EF – 1 – delta	ND	↑
eIF2 beta	↓	ND
eIF3 zeta	↑	ND
MORF4 family-associated protein	ND	↑
PDI	↓	ND
PDI isomerase A4	↑	ND
Poly-rC binding protein 1	ND	↑
Programmed cell death protein 5	ND	↑
Protein mago nashi	ND	↓
RBMA8A	↓	NA
Rho GDP dissociation inhibitor	↑	ND
Septin 11	↑	ND
Stathmin	↓	ND
Transitional ER ATPase	↑	ND
Tropomyosin 1	↓	↑
Tropomyosin 3	ND	↑
Tropomyosin 4	↓	↑
TRF2 interacting telomeric RAP1	↓	ND
Tubulin alpha	ND	↑
Tubulin beta	ND	↑

purification captured more efficiently than IMAC and therefore, the differences in calponin may not have been observed if IMAC purification has been used.

Two other proteins were characterized to be differentially abundant in both the replicon and infectious systems however, in both cases, the abundance changes were opposite from one another when comparing infected cells to replicon cell lines. For example, GRP78 and tropomyosin alpha isoforms were more abundant in HCV-infected cells compared to control cells but less abundant in replicon cell lines when compared to control cell lines. The contrary differences observed for GRP78 and tropomyosin may by explained in part by the differing pathologies of the replicon system compared to a true HCV infection. As alluded to in Chapter IV, a necessary balance must be achieved between replicon persistence and cell survival and therefore, the level of cellular stress and resulting phosphoproteome alterations are substantially different between the replicon model and infection. If for instance, the decrease in stathmin phosphorylation is considered for both the replicon and infectious virus studies, one might contribute the difference in results to the chronic state of the replicon system which is more likely to mimic persistent infection that can lead to hepatocellular carcinoma. For example, in replicon cell lines, an aberration in stathmin phosphorylation could lead to errors in mitotic spindle formation and cell division, two complications associated with cell transformation, while in the infectious system, the infected cells are not under selective pressure to maintain the virus and therefore robust infection leads to

cell death and therefore there would be a decreased chance for cellular transformation.

Given that global proteomic methodologies are still in their infancy, studies addressing the global protein changes induced by HCV components are limited. The vast majority of proteomic analyses with regards to HCV have focused on chronic HCV cases, with particular emphasis on the identification of HCV-specific biological markers involved in the development of hepatocellular carcinoma (HCC) or liver fibrosis. Two separate studies observed protein abundance elevations in the HSP70 family members, GRP78, HSC70, GRP75 and HSP70.1 (Kuramitsu and Nakamura, 2005; Takashima et al., 2003), suggesting that ER-stress pathways involved in the unfolded protein response are induced during HCC. These findings are consistent with hypotheses that the ER-proteome is altered in many different cancers (Moenner et al., 2007; Ma and Hendershot, 2004; Li and Lee, 2006). Proteins previously observed to be decreased in HCC tended to have a broader spread in functionalities and included various tropomyosin isoforms, arginase 1 and enoyl-CoA to name a few (Yokoyama et al., 2004; Kuramitsu and Nakamura, 2005).

Not only have HCV specific proteome studies been limited, so too have proteomic studies pertaining to other viral infections. Moreover, studies of the phosphoproteome are even still more limited. Nevertheless, phosphoproteome studies of Rous sarcoma virus and pichinde virus were performed in the past few years. In order to study phospho-tyrosine changes that are possibly responsible

for maintenance of Rous sarcoma virus cellular transformation, Yamaoka and colleagues (2006) examined the proteome content of transformed cells using 2DE and mass spectrometry following immunoblotting specific for phospho-tyrosine (Yamaoka et al., 2006). As mentioned in Chapter III, generation of antibodies specific to phosphorylated tyrosine residues has been more successful compared to phospho-serine and threonine residues. This is somewhat unfortunate given that substantially greater amounts of serine and threonine residues are phosphorylated in the cell compared to tyrosine, nonetheless, phosphorylation at tyrosine residues often initiates signal cascades that result in the downstream phosphorylation of serine and threonine residues. With the exception of changes to RNA binding proteins (hnRNP A2 and hnRNP A3), there were limited similarities between those proteins identified in the above mentioned study and the one presented in this thesis. However, as with this study, the Rous sarcoma virus study also emphasized the importance of "top-down" methodologies in order to compare multiple phosphorylated isoforms of the same protein. Multiple isoforms of the hnRNP proteins were shown to be differentially phosphorylated in virus transformed cells and these differences would be difficult to characterize if a "bottom-up" approach would have been used as mass spectrometry characterization relies on peptide information versus intact protein. The same is true for the changes identified in this thesis with particular emphasis on stathmin, hsp90, tubulin and tropomyosin isoforms. However, the trade-off is that bottom-up MS-based approaches can detect protein not available to 2DE due to protein hydrophobicity, or proteins with extreme MW or pI.

A more focused study of the kinases altered during pichinde virus infection was performed by profiling with the aid of protein chip arrays. When an attenuated strain was compared to the virulent strain, the researchers found substantially fewer kinase or phosphoprotein changes in virulent infected cells which were attributed to the blockage of antiviral signalling cascades that would typically lead to the clearance of the virus. An important finding in this study was that although there were changes to the phosphorylation/activation of specific proteins in response to infection, the amount of total protein did not vary (Bowick et al., 2007). This is in keeping with the findings pertaining to stathmin, tropomyosin and PCBP1 in the data presented in this body of work, which did not differ markedly in their total protein amount, but did demonstrate statistically significant changes of phosphorylated forms of the protein, thereby further validating both the phosphoprotein enrichment and 2DE methods used in these studies.

Virus-induced total proteome changes have also been evaluated for dengue virus (Pattanakitsakul et al., 2007), bovine viral diarrhea virus (BVDV) (Pinchuk et al., 2008), HIV-1 (Ringrose et al., 2008; Burgener et al., 2008), influenza virus (Liu et al., 2008) and SARS CoV (Jiang et al., 2005) using a variety of different methods. Both dengue and BVDV are members of the virus family *Flaviviridae*, to which HCV also belongs. Using 2D-LC MS/MS, Pinchuk and colleagues identified more than 375 protein kinases, of which 18 were considered to be present in different amounts between mock and BVDV-infected cow monocytes. Of these, there

were increases in proteins responsible for cell differentiation and cell migration and decreases in proteins responsible for inducing an anti-viral state (Pinchuk et al., 2008). It is anticipated that the changes identified in the above study may in part explain the mechanisms of virus-induced transformation seen in cattle, and although BVDV infects cattle, it is used heavily as a model for HCV infection. Dengue virus is less related to HCV than BVDV however, similar protein families were altered in abundance between dengue-infected Vero cells and HCV infection, including increases in proteins involved in RNA processing (pre-mRNA processing factor 4), translation (EF-Tu, elongin C), ER-stress proteins (HspB7) and oxidative stress markers (ERO-1) (Pattanakitsakul et al., 2007).

Presumably, as more data is presented pertaining to the proteome and phosphoproteome changes induced by a variety of viral infections, researchers will be able to identify those changes that are associated with viral infection in general versus those that are specific to individual virus infection and specific pathologies observed.

Future work

The findings presented in this body of work detail both the qualitative and quantitative changes to the host cellular phosphoproteome in the presence of HCV replication and protein expression. The phosphorylated proteins which demonstrated altered abundance due to the prescence of HCV elements belonged to numerous protein families and consequently their phosphorylation

state is regulated by a variety of different mechanisms. Moreover, the majority of altered phosphoproteins in this study have multiple phosphorylation sites that can be phosphorylated in combination with one another or independently. Identifying which site is altered in phosphorylation may provide a clue as to which protein kinase is responsible for the changes observed. For example, the oncoprotein stathmin, which was found to be less abundant in replicon cells in two isoforms is a good test case. Stathmin contains four highly characterized phosphorylation sites which can be phosphorylated in a variety of combinations to generate upwards of 12 distinct phospho-isoforms. It may be possible to map which sites are differentially phosphorylated on the stathmin isoforms of this study using MS/MS with more protein, or in the negative ion scan mode because these are phosphopeptides. There are antibodies available which are specific to each of the four well-characterized sites, however, it is possible and likely that the two isoforms that have decreased abundance in replicon cells are actually a mixture of different phosphorylation sites as a stathmin isoform which contains two phosphorylated residues can actually be generated by the phosphorylation of any two of the known residues.

Not only are there multiple sites on stathmin that may be differentially phosphorylated, there are also multiple proteins upstream of stathmin that are responsible for the phosphorylation and dephosphorylation of each site. Given that phosphorylation is a transient, reversible post-translational modification, the observed lower abundance of the two isoforms described in this study could be

the result of decreased levels and/or activation of kinases responsible for the phosphorylation of a specific site or alternatively, the increased activity of the phosphatase responsible for the removal of the specific phosphate. Therefore, it is also of interest to identify the underlying reasons for the observed phosphorylated differences. As the kinases and phosphatases for many proteins are known, it may be possible to hinder their activity in order to alter the observed phenotypes described. This may be achieved by over expression of the kinases/phosphatases, or alternatively the silencing of their cognate mRNA transcripts. However, it bears mentioning that since the changes in this study are due to post-translational modification, the activity of the kinases/phosphatases of study may have to be specifically altered in order to delineate which are responsible for our findings. Ultimately, even a limited number of protein changes could identify the pathways responsible for the altered protein phosphorylation.

Ultimately, the significance of these findings with regards to virus propagation, pathogenesis and the cellular antiviral response are of utmost interest. Determining whether the changes observed are due to the cellular response to infection or alternatively are due to specific actions of the viral components is crucial. For instance, the observed increase in stathmin observed in HCC (Wong et al., 2008) and replicon cells (Jacobs et al., 2005) may be a result of the microtubule aggregation that occurs during replication and the cellular response to inhibit this action, as a main function of stathmin is the depolymerization of

tubulin. In contrast, the altered phosphorylation of stathmin may occur due to the action of viral components that ensures infected cells rest in a certain stage of the cell cycle as stathmin phosphorylation is tightly coupled to entry into mitosis and the subsequent rearrangement of tubulin into mitotic spindles. Maintaining infected cells in a certain cell state may enable the production of necessary cellular co-factors for infection but may also be related to the transformation phenotype of HCV and the observed chromosome abnormalities observed by NS5A expressing cells (Baek et al., 2006).

Finally, determining what significance these changes have on the fitness of viral infection/pathogenesis and cellular homeostasis should be investigated. By inhibiting the phosphorylation alterations described, cell survival, transformation and virus replication can be monitored to establish whether these changes are essential to the cells survival during infection or alternatively to increase the replication capacity of the virus.

Reference List

Abe,K., Ikeda,M., Dansako,H., Naka,K., Shimotohno,K., and Kato,N. (2005). cDNA microarray analysis to compare HCV subgenomic replicon cells with their cured cells. Virus Res. *107*, 73-81.

Aboulaich,N., Vainonen,J.P., Stralfors,P., and Vener,A.V. (2004). Vectorial proteomics reveal targeting, phosphorylation and specific fragmentation of polymerase I and transcript release factor (PTRF) at the surface of caveolae in human adipocytes. Biochem. J. *383*, 237-248.

Aizaki,H., Harada,T., Otsuka,M., Seki,N., Matsuda,M., Li,Y.W., Kawakami,H., Matsuura,Y., Miyamura,T., and Suzuki,T. (2002). Expression profiling of liver cell lines expressing entire or parts of hepatitis C virus open reading frame. Hepatology *36*, 1431-1438.

Ali,S., Pellerin,C., Lamarre,D., and Kukolj,G. (2004). Hepatitis C virus subgenomic replicons in the human embryonic kidney 293 cell line. J. Virol. *78*, 491-501.

Alisi,A., Mele,R., Spaziani,A., Tavolaro,S., Palescandolo,E., and Balsano,C. (2005). Thr 446 phosphorylation of PKR by HCV core protein deregulates G2/M phase in HCC cells. J. Cell Physiol *205*, 25-31.

Alter,H.J. and Seeff,L.B. (2000). Recovery, persistence, and sequelae in hepatitis C virus infection: a perspective on long-term outcome. Semin. Liver Dis. *20*, 17-35.

Amanchy,R., Kalume,D.E., Iwahori,A., Zhong,J., and Pandey,A. (2005). Phosphoproteome analysis of HeLa cells using stable isotope labeling with amino acids in cell culture (SILAC). J. Proteome. Res. *4*, 1661-1671.

Andersen,J.S., Wilkinson,C.J., Mayor,T., Mortensen,P., Nigg,E.A., and Mann,M. (2003). Proteomic characterization of the human centrosome by protein correlation profiling. Nature *426*, 570-574.

Anderson,L. and Seilhamer,J. (1997). A comparison of selected mRNA and protein abundances in human liver. Electrophoresis *18*, 533-537.

Andre,P., Perlemuter,G., Budkowska,A., Brechot,C., and Lotteau,V. (2005). Hepatitis C virus particles and lipoprotein metabolism. Semin. Liver Dis. *25*, 93-104.

Andriulli,A., Mangia,A., Iacobellis,A., Ippolito,A., Leandro,G., and Zeuzem,S. (2008). Meta-analysis: the outcome of anti-viral therapy in HCV genotype 2 and genotype 3 infected patients with chronic hepatitis. Aliment. Pharmacol. Ther. *28*, 397-404.

Appel,N., Pietschmann,T., and Bartenschlager,R. (2005). Mutational analysis of hepatitis C virus nonstructural protein 5A: potential role of differential phosphorylation in RNA replication and identification of a genetically flexible domain. J. Virol. *79*, 3187-3194.

Appel,N., Schaller,T., Penin,F., and Bartenschlager,R. (2006). From structure to function: new insights into hepatitis C virus RNA replication. J. Biol. Chem. *281*, 9833-9836.

Authier,F.J., Bassez,G., Payan,C., Guillevin,L., Pawlotsky,J.M., Degos,J.D., Gherardi,R.K., and Belec,L. (2003). Detection of genomic viral RNA in nerve and muscle of patients with HCV neuropathy. Neurology *60*, 808-812.

Bacon,B.R. and McHutchison,J.G. (2007). Into the light: strategies for battling hepatitis C. Am. J. Manag. Care *13 Suppl 12*, S319-S326.

Baek,K.H., Park,H.Y., Kang,C.M., Kim,S.J., Jeong,S.J., Hong,E.K., Park,J.W., Sung,Y.C., Suzuki,T., Kim,C.M., and Lee,C.W. (2006). Overexpression of hepatitis C virus NS5A protein induces chromosome instability via mitotic cell cycle dysregulation. J. Mol. Biol. *359*, 22-34.

Bagaglio,S., De Mitri,M.S., Lodrini,S., Paties,C., Cassini,R., Bianchi,G., Bernardi,M., Lazzarin,A., and Morsica,G. (2005). Mutations in the E2-PePHD region of hepatitis C virus type 1b in patients with hepatocellular carcinoma. J. Viral Hepat. *12*, 243-250.

Bare,P., Massud,I., Parodi,C., Belmonte,L., Garcia,G., Nebel,M.C., Corti,M., Pinto,M.T., Bianco,R.P., Bracco,M.M., Campos,R., and Ares,B.R. (2005). Continuous release of hepatitis C virus (HCV) by peripheral blood mononuclear cells and B-lymphoblastoid cell-line cultures derived from HCV-infected patients. J. Gen. Virol. *86*, 1717-1727.

Bartenschlager,R. (1999). The NS3/4A proteinase of the hepatitis C virus: unravelling structure and function of an unusual enzyme and a prime target for antiviral therapy. J. Viral Hepat. *6*, 165-181.

Bartenschlager,R., Frese,M., and Pietschmann,T. (2004). Novel insights into hepatitis C virus replication and persistence. Adv. Virus Res. *63*, 71-180.

Bartenschlager,R., Kaul,A., and Sparacio,S. (2003). Replication of the hepatitis C virus in cell culture. Antiviral Res. *60*, 91-102.

Bartenschlager,R. and Lohmann,V. (2001). Novel cell culture systems for the hepatitis C virus. Antiviral Res. *52*, 1-17.

Bartenschlager,R., Lohmann,V., Wilkinson,T., and Koch,J.O. (1995). Complex formation between the NS3 serine-type proteinase of the hepatitis C virus and NS4A and its importance for polyprotein maturation. J. Virol. *69*, 7519-7528.

Bartosch,B. and Cosset,F.L. (2006). Cell entry of hepatitis C virus. Virology *348*, 1-12.

Bartosch,B., Vitelli,A., Granier,C., Goujon,C., Dubuisson,J., Pascale,S., Scarselli,E., Cortese,R., Nicosia,A., and Cosset,F.L. (2003). Cell entry of hepatitis C virus requires a set of co-receptors that include the CD81 tetraspanin and the SR-B1 scavenger receptor. J. Biol. Chem. *278*, 41624-41630.

Beausoleil,S.A., Jedrychowski,M., Schwartz,D., Elias,J.E., Villen,J., Li,J., Cohn,M.A., Cantley,L.C., and Gygi,S.P. (2004). Large-scale characterization of HeLa cell nuclear phosphoproteins. Proc. Natl. Acad. Sci. U. S. A *101*, 12130-12135.

Beausoleil,S.A., Villen,J., Gerber,S.A., Rush,J., and Gygi,S.P. (2006). A probability-based approach for high-throughput protein phosphorylation analysis and site localization. Nat. Biotechnol. *24*, 1285-1292.

Benali-Furet,N.L., Chami,M., Houel,L., De Giorgi,F., Vernejoul,F., Lagorce,D., Buscail,L., Bartenschlager,R., Ichas,F., Rizzuto,R., and Paterlini-Brechot,P. (2005). Hepatitis C virus core triggers apoptosis in liver cells by inducing ER stress and ER calcium depletion. Oncogene *24*, 4921-4933.

Beretta,L., Dobransky,T., and Sobel,A. (1993). Multiple phosphorylation of stathmin. Identification of four sites phosphorylated in intact cells and in vitro by cyclic AMP-dependent protein kinase and p34cdc2. J. Biol. Chem. *268*, 20076-20084.

Berg,T., Mas,M.A., Hohne,M., Wiedenmann,B., Hopf,U., and Schreier,E. (2000). Mutations in the E2-PePHD and NS5A region of hepatitis C virus type 1 and the dynamics of hepatitis C viremia decline during interferon alfa treatment. Hepatology *32*, 1386-1395.

Bertolotti,A., Zhang,Y., Hendershot,L.M., Harding,H.P., and Ron,D. (2000). Dynamic interaction of BiP and ER stress transducers in the unfolded-protein response. Nat. Cell Biol. *2*, 326-332.

Bharadwaj,S. and Prasad,G.L. (2002). Tropomyosin-1, a novel suppressor of cellular transformation is downregulated by promoter methylation in cancer cells. Cancer Lett. *183*, 205-213.

Bhattacharya,B., Prasad,G.L., Valverius,E.M., Salomon,D.S., and Cooper,H.L. (1990). Tropomyosins of human mammary epithelial cells: consistent defects of expression in mammary carcinoma cell lines. Cancer Res. *50*, 2105-2112.

Bigger,C.B., Brasky,K.M., and Lanford,R.E. (2001). DNA microarray analysis of chimpanzee liver during acute resolving hepatitis C virus infection. J. Virol. *75*, 7059-7066.

Bigger,C.B., Guerra,B., Brasky,K.M., Hubbard,G., Beard,M.R., Luxon,B.A., Lemon,S.M., and Lanford,R.E. (2004). Intrahepatic gene expression during chronic hepatitis C virus infection in chimpanzees. J. Virol. *78*, 13779-13792.

Bjellqvist,B., Ek,K., Righetti,P.G., Gianazza,E., Gorg,A., Westermeier,R., and Postel,W. (1982). Isoelectric focusing in immobilized pH gradients: principle, methodology and some applications. J. Biochem. Biophys. Methods *6*, 317-339.

Blanchard,E., Belouzard,S., Goueslain,L., Wakita,T., Dubuisson,J., Wychowski,C., and Rouille,Y. (2006). Hepatitis C virus entry depends on clathrin-mediated endocytosis. J. Virol. *80*, 6964-6972.

Blanchard,E., Brand,D., Trassard,S., Goudeau,A., and Roingeard,P. (2002). Hepatitis C virus-like particle morphogenesis. J. Virol. *76*, 4073-4079.

Blight,K.J., Kolykhalov,A.A., and Rice,C.M. (2000). Efficient initiation of HCV RNA replication in cell culture. Science *290*, 1972-1974.

Blight,K.J., McKeating,J.A., Marcotrigiano,J., and Rice,C.M. (2003). Efficient replication of hepatitis C virus genotype 1a RNAs in cell culture. J. Virol. *77*, 3181-3190.

Blight,K.J., McKeating,J.A., and Rice,C.M. (2002). Highly permissive cell lines for subgenomic and genomic hepatitis C virus RNA replication. J. Virol. *76*, 13001-13014.

Blyn,L.B., Swiderek,K.M., Richards,O., Stahl,D.C., Semler,B.L., and Ehrenfeld,E. (1996). Poly(rC) binding protein 2 binds to stem-loop IV of the poliovirus RNA 5' noncoding region: identification by automated liquid chromatography-tandem mass spectrometry. Proc. Natl. Acad. Sci. U. S. A *93*, 11115-11120.

Blyn,L.B., Towner,J.S., Semler,B.L., and Ehrenfeld,E. (1997). Requirement of poly(rC) binding protein 2 for translation of poliovirus RNA. J. Virol. *71*, 6243-6246.

Borowski,P., Heiland,M., Feucht,H., and Laufs,R. (1999a). Characterisation of non-structural protein 3 of hepatitis C virus as modulator of protein phosphorylation mediated by PKA and PKC: evidences for action on the level of substrate and enzyme. Arch. Virol. *144*, 687-701.

Borowski,P., Heiland,M., Oehlmann,K., Becker,B., Kornetzky,L., Feucht,H., and Laufs,R. (1996). Non-structural protein 3 of hepatitis C virus inhibits phosphorylation mediated by cAMP-dependent protein kinase. Eur. J. Biochem. *237*, 611-618.

Borowski,P., Oehlmann,K., Heiland,M., and Laufs,R. (1997). Nonstructural protein 3 of hepatitis C virus blocks the distribution of the free catalytic subunit of cyclic AMP-dependent protein kinase. J. Virol. *71*, 2838-2843.

Borowski,P., zur Wiesch,J.S., Resch,K., Feucht,H., Laufs,R., and Schmitz,H. (1999b). Protein kinase C recognizes the protein kinase A-binding motif of nonstructural protein 3 of hepatitis C virus. J. Biol. Chem. *274*, 30722-30728.

Bost,A.G., Venable,D., Liu,L., and Heinz,B.A. (2003). Cytoskeletal requirements for hepatitis C virus (HCV) RNA synthesis in the HCV replicon cell culture system. J. Virol. *77*, 4401-4408.

Boulant,S., Becchi,M., Penin,F., and Lavergne,J.P. (2003). Unusual multiple recoding events leading to alternative forms of hepatitis C virus core protein from genotype 1b. J. Biol. Chem. *278*, 45785-45792.

Boulestin,A., Sandres-Saune,K., Payen,J.L., Alric,L., Dubois,M., Pasquier,C., Vinel,J.P., Pascal,J.P., Puel,J., and Izopet,J. (2002). Genetic heterogeneity of the envelope 2 gene and eradication of hepatitis C virus after a second course of interferon-alpha. J. Med. Virol. *68*, 221-228.

Bowick,G.C., Fennewald,S.M., Scott,E.P., Zhang,L., Elsom,B.L., Aronson,J.F., Spratt,H.M., Luxon,B.A., Gorenstein,D.G., and Herzog,N.K. (2007). Identification of differentially activated cell-signaling networks associated with pichinde virus pathogenesis by using systems kinomics. J. Virol. *81*, 1923-1933.

Brattsand,G., Marklund,U., Nylander,K., Roos,G., and Gullberg,M. (1994). Cell-cycle-regulated phosphorylation of oncoprotein 18 on Ser16, Ser25 and Ser38. Eur. J. Biochem. *220*, 359-368.

Brill,L.M., Salomon,A.R., Ficarro,S.B., Mukherji,M., Stettler-Gill,M., and Peters,E.C. (2004). Robust phosphoproteomic profiling of tyrosine phosphorylation sites from human T cells using immobilized metal affinity chromatography and tandem mass spectrometry. Anal. Chem. *76*, 2763-2772.

Bukh,J., Pietschmann,T., Lohmann,V., Krieger,N., Faulk,K., Engle,R.E., Govindarajan,S., Shapiro,M., St Claire,M., and Bartenschlager,R. (2002). Mutations that permit efficient replication of hepatitis C virus RNA in Huh-7 cells prevent productive replication in chimpanzees. Proc. Natl. Acad. Sci. U. S. A *99*, 14416-14421.

Burgener,A., Boutilier,J., Wachihi,C., Kimani,J., Carpenter,M., Westmacott,G., Cheng,K., Ball,T.B., and Plummer,F. (2008). Identification of Differentially Expressed Proteins in the Cervical Mucosa of HIV-1-Resistant Sex Workers. J. Proteome. Res.

Burns,R.G. and Surridge,C.D. (1994). Functional role of a consensus peptide which is common to alpha-, beta-, and gamma-tubulin, to actin and centractin, to phytochrome A, and to the TCP1 alpha chaperonin protein. FEBS Lett. *347*, 105-111.

Carvalho,J.F., Carvalho,M.D., and Merrick,W.C. (1984a). Purification of various forms of elongation factor 1 from rabbit reticulocytes. Arch. Biochem. Biophys. *234*, 591-602.

Carvalho,M.D., Carvalho,J.F., and Merrick,W.C. (1984b). Biological characterization of various forms of elongation factor 1 from rabbit reticulocytes. Arch. Biochem. Biophys. *234*, 603-611.

Cecconi,D., Scarpa,A., Donadelli,M., Palmieri,M., Hamdan,M., Astner,H., and Righetti,P.G. (2003). Proteomic profiling of pancreatic ductal carcinoma cell lines treated with trichostatin-A. Electrophoresis *24*, 1871-1878.

Chang,M., Williams,O., Mittler,J., Quintanilla,A., Carithers,R.L., Jr., Perkins,J., Corey,L., and Gretch,D.R. (2003). Dynamics of hepatitis C virus replication in human liver. Am. J. Pathol. *163*, 433-444.

Chayama,K., Suzuki,F., Tsubota,A., Kobayashi,M., Arase,Y., Saitoh,S., Suzuki,Y., Murashima,N., Ikeda,K., Takahashi,N., Kinoshita,M., and Kumada,H. (2000). Association of amino acid sequence in the PKR-eIF2 phosphorylation homology domain and response to interferon therapy. Hepatology *32*, 1138-1144.

Chen,G., Gharib,T.G., Huang,C.C., Taylor,J.M., Misek,D.E., Kardia,S.L., Giordano,T.J., Iannettoni,M.D., Orringer,M.B., Hanash,S.M., and Beer,D.G. (2002). Discordant protein and mRNA expression in lung adenocarcinomas. Mol. Cell Proteomics. *1*, 304-313.

Chong,P.K., Gan,C.S., Pham,T.K., and Wright,P.C. (2006). Isobaric tags for relative and absolute quantitation (iTRAQ) reproducibility: Implication of multiple injections. J. Proteome. Res. *5*, 1232-1240.

Choo,Q.L., Kuo,G., Weiner,A.J., Overby,L.R., Bradley,D.W., and Houghton,M. (1989). Isolation of a cDNA clone derived from a blood-borne non-A, non-B viral hepatitis genome. Science *244*, 359-362.

Choukhi,A., Ung,S., Wychowski,C., and Dubuisson,J. (1998). Involvement of endoplasmic reticulum chaperones in the folding of hepatitis C virus glycoproteins. J. Virol. *72*, 3851-3858.

Ciccaglione,A.R., Costantino,A., Tritarelli,E., Marcantonio,C., Equestre,M., Marziliano,N., and Rapicetta,M. (2005). Activation of endoplasmic reticulum stress response by hepatitis C virus proteins. Arch. Virol. *150*, 1339-1356.

Ciccaglione,A.R., Marcantonio,C., Tritarelli,E., Equestre,M., Venditteli,F., Costantino,A., Geraci,A., and Rapicetta,M. (2007). Activation of the ER stress gene gadd153 by hepatitis C virus sensitizes cells to oxidant injury. Virus Res. *126*, 128-138.

Clarke,R.B. (2003). p27KIP1 phosphorylation by PKB/Akt leads to poor breast cancer prognosis. Breast Cancer Res. *5*, 162-163.

Cochrane,A., Orr,A., Shaw,M.L., Mills,P.R., and McCruden,E.A. (2000). The amino acid sequence of the PKR-eIF2alpha phosphorylation homology domain of hepatitis C virus envelope 2 protein and response to interferon-alpha. J. Infect. Dis. *182*, 1515-1518.

Cocquerel,L., Op,d.B., Lambot,M., Roussel,J., Delgrange,D., Pillez,A., Wychowski,C., Penin,F., and Dubuisson,J. (2002). Topological changes in the transmembrane domains of hepatitis C virus envelope glycoproteins. EMBO J. *21*, 2893-2902.

Cocquerel,L., Voisset,C., and Dubuisson,J. (2006). Hepatitis C virus entry: potential receptors and their biological functions. J. Gen. Virol. *87*, 1075-1084.

Codran,A., Royer,C., Jaeck,D., Bastien-Valle,M., Baumert,T.F., Kieny,M.P., Pereira,C.A., and Martin,J.P. (2006). Entry of hepatitis C virus pseudotypes into primary human hepatocytes by clathrin-dependent endocytosis. J. Gen. Virol. *87*, 2583-2593.

Collins,M.O., Yu,L., Coba,M.P., Husi,H., Campuzano,I., Blackstock,W.P., Choudhary,J.S., and Grant,S.G. (2005). Proteomic analysis of in vivo phosphorylated synaptic proteins. J. Biol. Chem. *280*, 5972-5982.

Cross,T.J., Antoniades,C.G., and Harrison,P.M. (2008). Current and future management of chronic hepatitis C infection. Postgrad. Med. J. *84*, 172-176.

Cudmore,S., Reckmann,I., and Way,M. (1997). Viral manipulations of the actin cytoskeleton. Trends Microbiol. *5*, 142-148.

Date,T., Kato,T., Miyamoto,M., Zhao,Z., Yasui,K., Mizokami,M., and Wakita,T. (2004). Genotype 2a hepatitis C virus subgenomic replicon can replicate in HepG2 and IMY-N9 cells. J. Biol. Chem. *279*, 22371-22376.

Deforges,S., Evlashev,A., Perret,M., Sodoyer,M., Pouzol,S., Scoazec,J.Y., Bonnaud,B., Diaz,O., Paranhos-Baccala,G., Lotteau,V., and Andre,P. (2004). Expression of hepatitis C virus proteins in epithelial intestinal cells in vivo. J. Gen. Virol. *85*, 2515-2523.

Deleersnyder,V., Pillez,A., Wychowski,C., Blight,K., Xu,J., Hahn,Y.S., Rice,C.M., and Dubuisson,J. (1997). Formation of native hepatitis C virus glycoprotein complexes. J. Virol. *71*, 697-704.

DerMardirossian,C. and Bokoch,G.M. (2005). GDIs: central regulatory molecules in Rho GTPase activation. Trends Cell Biol. *15*, 356-363.

Deutscher,J. and Saier,M.H., Jr. (2005). Ser/Thr/Tyr protein phosphorylation in bacteria - for long time neglected, now well established. J. Mol. Microbiol. Biotechnol. *9*, 125-131.

Diamond,D.L., Jacobs,J.M., Paeper,B., Proll,S.C., Gritsenko,M.A., Carithers,R.L., Jr., Larson,A.M., Yeh,M.M., Camp,D.G., Smith,R.D., and Katze,M.G. (2007). Proteomic profiling of human liver biopsies: hepatitis C virus-induced fibrosis and mitochondrial dysfunction. Hepatology *46*, 649-657.

Dubrovska,A. and Souchelnytskyi,S. (2005). Efficient enrichment of intact phosphorylated proteins by modified immobilized metal-affinity chromatography. Proteomics. *5*, 4678-4683.

Dubuisson,J., Helle,F., and Cocquerel,L. (2008). Early steps of the hepatitis C virus life cycle. Cell Microbiol. *10*, 821-827.

Dumoulin,F.L., von dem,B.A., Li,J., Khamzina,L., Wands,J.R., Sauerbruch,T., and Spengler,U. (2003). Hepatitis C virus NS2 protein inhibits gene expression from different cellular and viral promoters in hepatic and nonhepatic cell lines. Virology *305*, 260-266.

Egger,D., Wolk,B., Gosert,R., Bianchi,L., Blum,H.E., Moradpour,D., and Bienz,K. (2002). Expression of hepatitis C virus proteins induces distinct membrane alterations including a candidate viral replication complex. J. Virol. *76*, 5974-5984.

Einav,S., Elazar,M., Danieli,T., and Glenn,J.S. (2004). A nucleotide binding motif in hepatitis C virus (HCV) NS4B mediates HCV RNA replication. J. Virol. *78*, 11288-11295.

Einav,S., Sklan,E.H., Moon,H.M., Gehrig,E., Liu,P., Hao,Y., Lowe,A.W., and Glenn,J.S. (2008). The nucleotide binding motif of hepatitis C virus NS4B can mediate cellular transformation and tumor formation without Ha-ras co-transfection. Hepatology *47*, 827-835.

Ejiri,S., Ebata,N., Kawamura,R., and Katsumata,T. (1983). Occurrence of four subunits in high molecular weight forms of polypeptide chain elongation factor 1 from wheat embryo. J. Biochem. *94*, 319-322.

Elazar,M., Liu,P., Rice,C.M., and Glenn,J.S. (2004). An N-terminal amphipathic helix in hepatitis C virus (HCV) NS4B mediates membrane association, correct localization of replication complex proteins, and HCV RNA replication. J. Virol. *78*, 11393-11400.

Emaduddin,M., Bicknell,D.C., Bodmer,W.F., and Feller,S.M. (2008). Cell growth, global phosphotyrosine elevation, and c-Met phosphorylation through Src family kinases in colorectal cancer cells. Proc. Natl. Acad. Sci. U. S. A *105*, 2358-2362.

Enomoto,N., Sakuma,I., Asahina,Y., Kurosaki,M., Murakami,T., Yamamoto,C., Izumi,N., Marumo,F., and Sato,C. (1995). Comparison of full-length sequences of interferon-sensitive and resistant hepatitis C virus 1b. Sensitivity to interferon is conferred by amino acid substitutions in the NS5A region. J. Clin. Invest *96*, 224-230.

Enomoto,N., Sakuma,I., Asahina,Y., Kurosaki,M., Murakami,T., Yamamoto,C., Ogura,Y., Izumi,N., Marumo,F., and Sato,C. (1996). Mutations in the nonstructural protein 5A gene and response to interferon in patients with chronic hepatitis C virus 1b infection. N. Engl. J. Med. *334*, 77-81.

Erdtmann,L., Franck,N., Lerat,H., Le Seyec,J., Gilot,D., Cannie,I., Gripon,P., Hibner,U., and Guguen-Guillouzo,C. (2003). The hepatitis C virus NS2 protein is an inhibitor of CIDE-B-induced apoptosis. J. Biol. Chem. *278*, 18256-18264.

Evans,M.J., Rice,C.M., and Goff,S.P. (2004). Phosphorylation of hepatitis C virus nonstructural protein 5A modulates its protein interactions and viral RNA replication. Proc. Natl. Acad. Sci. U. S. A *101*, 13038-13043.

Evans,M.J., von Hahn,T., Tscherne,D.M., Syder,A.J., Panis,M., Wolk,B., Hatziioannou,T., McKeating,J.A., Bieniasz,P.D., and Rice,C.M. (2007). Claudin-1 is a hepatitis C virus co-receptor required for a late step in entry. Nature *446*, 801-805.

Fang,C., Yi,Z., Liu,F., Lan,S., Wang,J., Lu,H., Yang,P., and Yuan,Z. (2006). Proteome analysis of human liver carcinoma Huh7 cells harboring hepatitis C virus subgenomic replicon. Proteomics. *6*, 519-527.

Farci,P., Alter,H.J., Shimoda,A., Govindarajan,S., Cheung,L.C., Melpolder,J.C., Sacher,R.A., Shih,J.W., and Purcell,R.H. (1996). Hepatitis C virus-associated fulminant hepatic failure. N. Engl. J. Med. *335*, 631-634.

Fourest-Lieuvin,A., Peris,L., Gache,V., Garcia-Saez,I., Juillan-Binard,C., Lantez,V., and Job,D. (2006). Microtubule regulation in mitosis: tubulin phosphorylation by the cyclin-dependent kinase Cdk1. Mol. Biol. Cell *17*, 1041-1050.

Foy,E., Li,K., Sumpter,R., Jr., Loo,Y.M., Johnson,C.L., Wang,C., Fish,P.M., Yoneyama,M., Fujita,T., Lemon,S.M., and Gale,M., Jr. (2005). Control of antiviral defenses through hepatitis C virus disruption of retinoic acid-inducible gene-I signaling. Proc. Natl. Acad. Sci. U. S. A *102*, 2986-2991.

Foy,E., Li,K., Wang,C., Sumpter,R., Jr., Ikeda,M., Lemon,S.M., and Gale,M., Jr. (2003). Regulation of interferon regulatory factor-3 by the hepatitis C virus serine protease. Science *300*, 1145-1148.

Francois,C., Duverlie,G., Rebouillat,D., Khorsi,H., Castelain,S., Blum,H.E., Gatignol,A., Wychowski,C., Moradpour,D., and Meurs,E.F. (2000). Expression of

hepatitis C virus proteins interferes with the antiviral action of interferon independently of PKR-mediated control of protein synthesis. J. Virol. *74*, 5587-5596.

Freiden,P.J., Gaut,J.R., and Hendershot,L.M. (1992). Interconversion of three differentially modified and assembled forms of BiP. EMBO J. *11*, 63-70.

Friebe,P., Boudet,J., Simorre,J.P., and Bartenschlager,R. (2005). Kissing-loop interaction in the 3' end of the hepatitis C virus genome essential for RNA replication. J. Virol. *79*, 380-392.

Friebe,P., Lohmann,V., Krieger,N., and Bartenschlager,R. (2001). Sequences in the 5' nontranslated region of hepatitis C virus required for RNA replication. J. Virol. *75*, 12047-12057.

Fukuda,K., Tsuchihara,K., Hijikata,M., Nishiguchi,S., Kuroki,T., and Shimotohno,K. (2001). Hepatitis C virus core protein enhances the activation of the transcription factor, Elk1, in response to mitogenic stimuli. Hepatology *33*, 159-165.

Fukushi,S., Okada,M., Kageyama,T., Hoshino,F.B., Nagai,K., and Katayama,K. (2001). Interaction of poly(rC)-binding protein 2 with the 5'-terminal stem loop of the hepatitis C-virus genome. Virus Res. *73*, 67-79.

Gale,M., Jr., Blakely,C.M., Kwieciszewski,B., Tan,S.L., Dossett,M., Tang,N.M., Korth,M.J., Polyak,S.J., Gretch,D.R., and Katze,M.G. (1998). Control of PKR protein kinase by hepatitis C virus nonstructural 5A protein: molecular mechanisms of kinase regulation. Mol. Cell Biol. *18*, 5208-5218.

Gale,M., Jr., Kwieciszewski,B., Dossett,M., Nakao,H., and Katze,M.G. (1999). Antiapoptotic and oncogenic potentials of hepatitis C virus are linked to interferon resistance by viral repression of the PKR protein kinase. J. Virol. *73*, 6506-6516.

Garry,R.F. and Dash,S. (2003). Proteomics computational analyses suggest that hepatitis C virus E1 and pestivirus E2 envelope glycoproteins are truncated class II fusion proteins. Virology *307*, 255-265.

Gastaminza,P., Cheng,G., Wieland,S., Zhong,J., Liao,W., and Chisari,F.V. (2008). Cellular determinants of hepatitis C virus assembly, maturation, degradation, and secretion. J. Virol. *82*, 2120-2129.

Geiss,G.K., Carter,V.S., He,Y., Kwieciszewski,B.K., Holzman,T., Korth,M.J., Lazaro,C.A., Fausto,N., Bumgarner,R.E., and Katze,M.G. (2003). Gene expression profiling of the cellular transcriptional network regulated by alpha/beta interferon and its partial attenuation by the hepatitis C virus nonstructural 5A protein. J. Virol. *77*, 6367-6375.

Georgopoulou,U., Caravokiri,K., and Mavromara,P. (2003). Suppression of the ERK1/2 signaling pathway from HCV NS5A protein expressed by herpes simplex recombinant viruses. Arch. Virol. *148*, 237-251.

Geschwind,D.H. (2003). Tau phosphorylation, tangles, and neurodegeneration: the chicken or the egg? Neuron *40*, 457-460.

Gharahdaghi,F., Weinberg,C.R., Meagher,D.A., Imai,B.S., and Mische,S.M. (1999). Mass spectrometric identification of proteins from silver-stained polyacrylamide gel: a method for the removal of silver ions to enhance sensitivity. Electrophoresis *20*, 601-605.

Gordon,F.D., Anastopoulos,H., Khettry,U., Loda,M., Jenkins,R.L., Lewis,W.D., and Trey,C. (1995). Hepatitis C infection: a rare cause of fulminant hepatic failure. Am. J. Gastroenterol. *90*, 117-120.

Gorg,A., Weiss,W., and Dunn,M.J. (2004). Current two-dimensional electrophoresis technology for proteomics. Proteomics. *4*, 3665-3685.

Gosert,R., Egger,D., Lohmann,V., Bartenschlager,R., Blum,H.E., Bienz,K., and Moradpour,D. (2003). Identification of the hepatitis C virus RNA replication complex in Huh-7 cells harboring subgenomic replicons. J. Virol. *77*, 5487-5492.

Grakoui,A., Wychowski,C., Lin,C., Feinstone,S.M., and Rice,C.M. (1993). Expression and identification of hepatitis C virus polyprotein cleavage products. J. Virol. *67*, 1385-1395.

Greber,U.F. and Way,M. (2006). A superhighway to virus infection. Cell *124*, 741-754.

Griffin,S.D., Beales,L.P., Clarke,D.S., Worsfold,O., Evans,S.D., Jaeger,J., Harris,M.P., and Rowlands,D.J. (2003). The p7 protein of hepatitis C virus forms an ion channel that is blocked by the antiviral drug, Amantadine. FEBS Lett. *535*, 34-38.

Guo,J.T., Bichko,V.V., and Seeger,C. (2001). Effect of alpha interferon on the hepatitis C virus replicon. J. Virol. *75*, 8516-8523.

Gygi,S.P., Rist,B., Gerber,S.A., Turecek,F., Gelb,M.H., and Aebersold,R. (1999a). Quantitative analysis of complex protein mixtures using isotope-coded affinity tags. Nat. Biotechnol. *17*, 994-999.

Gygi,S.P., Rochon,Y., Franza,B.R., and Aebersold,R. (1999b). Correlation between protein and mRNA abundance in yeast. Mol. Cell Biol. *19*, 1720-1730.

Haeberle,J.R. (1994). Calponin decreases the rate of cross-bridge cycling and increases maximum force production by smooth muscle myosin in an in vitro motility assay. J. Biol. Chem. *269*, 12424-12431.

Hayashi,J., Aoki,H., Kajino,K., Moriyama,M., Arakawa,Y., and Hino,O. (2000). Hepatitis C virus core protein activates the MAPK/ERK cascade synergistically with tumor promoter TPA, but not with epidermal growth factor or transforming growth factor alpha. Hepatology *32*, 958-961.

Hayashi,J., Stoyanova,R., and Seeger,C. (2005). The transcriptome of HCV replicon expressing cell lines in the presence of alpha interferon. Virology *335*, 264-275.

He,Y., Nakao,H., Tan,S.L., Polyak,S.J., Neddermann,P., Vijaysri,S., Jacobs,B.L., and Katze,M.G. (2002). Subversion of cell signaling pathways by hepatitis C virus nonstructural 5A protein via interaction with Grb2 and P85 phosphatidylinositol 3-kinase. J. Virol. *76*, 9207-9217.

He,Y., Tan,S.L., Tareen,S.U., Vijaysri,S., Langland,J.O., Jacobs,B.L., and Katze,M.G. (2001). Regulation of mRNA translation and cellular signaling by hepatitis C virus nonstructural protein NS5A. J. Virol. *75*, 5090-5098.

Hellen,C.U. and Pestova,T.V. (1999). Translation of hepatitis C virus RNA. J. Viral Hepat. *6*, 79-87.

Hijikata,M., Mizushima,H., Akagi,T., Mori,S., Kakiuchi,N., Kato,N., Tanaka,T., Kimura,K., and Shimotohno,K. (1993a). Two distinct proteinase activities required for the processing of a putative nonstructural precursor protein of hepatitis C virus. J. Virol. *67*, 4665-4675.

Hijikata,M., Mizushima,H., Tanji,Y., Komoda,Y., Hirowatari,Y., Akagi,T., Kato,N., Kimura,K., and Shimotohno,K. (1993b). Proteolytic processing and membrane association of putative nonstructural proteins of hepatitis C virus. Proc. Natl. Acad. Sci. U. S. A *90*, 10773-10777.

Hoofnagle,J.H. (2002). Course and outcome of hepatitis C. Hepatology *36*, S21-S29.

Hsieh,T.Y., Matsumoto,M., Chou,H.C., Schneider,R., Hwang,S.B., Lee,A.S., and Lai,M.M. (1998). Hepatitis C virus core protein interacts with heterogeneous nuclear ribonucleoprotein K. J. Biol. Chem. *273*, 17651-17659.

Hunter,T. (1998). The Croonian Lecture 1997. The phosphorylation of proteins on tyrosine: its role in cell growth and disease. Philos. Trans. R. Soc. Lond B Biol. Sci. *353*, 583-605.

Ikeda,M., Yi,M., Li,K., and Lemon,S.M. (2002). Selectable subgenomic and genome-length dicistronic RNAs derived from an infectious molecular clone of the HCV-N strain of hepatitis C virus replicate efficiently in cultured Huh7 cells. J. Virol. *76*, 2997-3006.

Irar,S., Oliveira,E., Pages,M., and Goday,A. (2006). Towards the identification of late-embryogenic-abundant phosphoproteome in Arabidopsis by 2-DE and MS. Proteomics. *6 Suppl 1*, S175-S185.

Ishihama,Y., Oda,Y., Tabata,T., Sato,T., Nagasu,T., Rappsilber,J., and Mann,M. (2005). Exponentially modified protein abundance index (emPAI) for estimation of absolute protein amount in proteomics by the number of sequenced peptides per protein. Mol. Cell Proteomics. *4*, 1265-1272.

Jacobs,J.M., Diamond,D.L., Chan,E.Y., Gritsenko,M.A., Qian,W., Stastna,M., Baas,T., Camp,D.G., Carithers,R.L., Jr., Smith,R.D., and Katze,M.G. (2005). Proteome analysis of liver cells expressing a full-length hepatitis C virus (HCV) replicon and biopsy specimens of posttransplantation liver from HCV-infected patients. J. Virol. *79*, 7558-7569.

Jakubiec,A. and Jupin,I. (2007). Regulation of positive-strand RNA virus replication: the emerging role of phosphorylation. Virus Res. *129*, 73-79.

Jiang,X.S., Tang,L.Y., Dai,J., Zhou,H., Li,S.J., Xia,Q.C., Wu,J.R., and Zeng,R. (2005). Quantitative analysis of severe acute respiratory syndrome (SARS)-associated coronavirus-infected cells using proteomic approaches: implications for cellular responses to virus infection. Mol. Cell Proteomics. *4*, 902-913.

Jin,J.P., Walsh,M.P., Sutherland,C., and Chen,W. (2000). A role for serine-175 in modulating the molecular conformation of calponin. Biochem. J. *350 Pt 2*, 579-588.

Johnson,R.J., Willson,R., Yamabe,H., Couser,W., Alpers,C.E., Wener,M.H., Davis,C., and Gretch,D.R. (1994). Renal manifestations of hepatitis C virus infection. Kidney Int. *46*, 1255-1263.

Jones,C.T., Murray,C.L., Eastman,D.K., Tassello,J., and Rice,C.M. (2007a). Hepatitis C virus p7 and NS2 proteins are essential for production of infectious virus. J. Virol. *81*, 8374-8383.

Jones,D.M., Gretton,S.N., McLauchlan,J., and Targett-Adams,P. (2007b). Mobility analysis of an NS5A-GFP fusion protein in cells actively replicating hepatitis C virus subgenomic RNA. J. Gen. Virol. *88*, 470-475.

Kalliampakou,K.I., Kalamvoki,M., and Mavromara,P. (2005). Hepatitis C virus (HCV) NS5A protein downregulates HCV IRES-dependent translation. J. Gen. Virol. *86*, 1015-1025.

Kaneko,T., Tanji,Y., Satoh,S., Hijikata,M., Asabe,S., Kimura,K., and Shimotohno,K. (1994). Production of two phosphoproteins from the NS5A region of the hepatitis C viral genome. Biochem. Biophys. Res. Commun. *205*, 320-326.

Karp,N.A., Kreil,D.P., and Lilley,K.S. (2004). Determining a significant change in protein expression with DeCyder during a pair-wise comparison using two-dimensional difference gel electrophoresis. Proteomics. *4*, 1421-1432.

Kato,J., Kato,N., Yoshida,H., Ono-Nita,S.K., Shiratori,Y., and Omata,M. (2002). Hepatitis C virus NS4A and NS4B proteins suppress translation in vivo. J. Med. Virol. *66*, 187-199.

Kato,T., Furusaka,A., Miyamoto,M., Date,T., Yasui,K., Hiramoto,J., Nagayama,K., Tanaka,T., and Wakita,T. (2001). Sequence analysis of hepatitis C virus isolated from a fulminant hepatitis patient. J. Med. Virol. *64*, 334-339.

Kato,T., Matsumura,T., Heller,T., Saito,S., Sapp,R.K., Murthy,K., Wakita,T., and Liang,T.J. (2007). Production of infectious hepatitis C virus of various genotypes in cell cultures. J. Virol. *81*, 4405-4411.

Kaufmann,H., Bailey,J.E., and Fussenegger,M. (2001). Use of antibodies for detection of phosphorylated proteins separated by two-dimensional gel electrophoresis. Proteomics. *1*, 194-199.

Kaul,A., Woerz,I., Meuleman,P., Leroux-Roels,G., and Bartenschlager,R. (2007). Cell culture adaptation of hepatitis C virus and in vivo viability of an adapted variant. J. Virol. *81*, 13168-13179.

Khan,I.U., Wallin,R., Gupta,R.S., and Kammer,G.M. (1998). Protein kinase A-catalyzed phosphorylation of heat shock protein 60 chaperone regulates its attachment to histone 2B in the T lymphocyte plasma membrane. Proc. Natl. Acad. Sci. U. S. A *95*, 10425-10430.

Kim,Y.K., Kim,C.S., Lee,S.H., and Jang,S.K. (2002). Domains I and II in the 5' nontranslated region of the HCV genome are required for RNA replication. Biochem. Biophys. Res. Commun. *290*, 105-112.

Ko,Y.C., Ho,M.S., Chiang,T.A., Chang,S.J., and Chang,P.Y. (1992). Tattooing as a risk of hepatitis C virus infection. J. Med. Virol. *38*, 288-291.

Kolettas,E., Lymboura,M., Khazaie,K., and Luqmani,Y. (1998). Modulation of elongation factor-1 delta (EF-1 delta) expression by oncogenes in human epithelial cells. Anticancer Res. *18*, 385-392.

Kolykhalov,A.A., Feinstone,S.M., and Rice,C.M. (1996). Identification of a highly conserved sequence element at the 3' terminus of hepatitis C virus genome RNA. J. Virol. *70*, 3363-3371.

Kou,Y.H., Chou,S.M., Wang,Y.M., Chang,Y.T., Huang,S.Y., Jung,M.Y., Huang,Y.H., Chen,M.R., Chang,M.F., and Chang,S.C. (2006). Hepatitis C virus NS4A inhibits cap-dependent and the viral IRES-mediated translation through interacting with eukaryotic elongation factor 1A. J. Biomed. Sci. *13*, 861-874.

Krecic,A.M. and Swanson,M.S. (1999). hnRNP complexes: composition, structure, and function. Curr. Opin. Cell Biol. *11*, 363-371.

Krieger,N., Lohmann,V., and Bartenschlager,R. (2001). Enhancement of hepatitis C virus RNA replication by cell culture-adaptive mutations. J. Virol. *75*, 4614-4624.

Kuramitsu,Y. and Nakamura,K. (2005). Current progress in proteomic study of hepatitis C virus-related human hepatocellular carcinoma. Expert. Rev. Proteomics. *2*, 589-601.

Labdon,J.E., Nieves,E., and Schubart,U.K. (1992). Analysis of phosphoprotein p19 by liquid chromatography/mass spectrometry. Identification of two proline-directed serine phosphorylation sites and a blocked amino terminus. J. Biol. Chem. *267*, 3506-3513.

Ladner,R.D., Carr,S.A., Huddleston,M.J., McNulty,D.E., and Caradonna,S.J. (1996a). Identification of a consensus cyclin-dependent kinase phosphorylation site unique to the nuclear form of human deoxyuridine triphosphate nucleotidohydrolase. J. Biol. Chem. *271*, 7752-7757.

Ladner,R.D., McNulty,D.E., Carr,S.A., Roberts,G.D., and Caradonna,S.J. (1996b). Characterization of distinct nuclear and mitochondrial forms of human deoxyuridine triphosphate nucleotidohydrolase. J. Biol. Chem. *271*, 7745-7751.

Lauer,G.M. and Walker,B.D. (2001). Hepatitis C virus infection. N. Engl. J. Med. *345*, 41-52.

Laugesen,S., Messinese,E., Hem,S., Pichereaux,C., Grat,S., Ranjeva,R., Rossignol,M., and Bono,J.J. (2006). Phosphoproteins analysis in plants: a proteomic approach. Phytochemistry *67*, 2208-2214.

Lavie,M., Goffard,A., and Dubuisson,J. (2007). Assembly of a functional HCV glycoprotein heterodimer. Curr. Issues Mol. Biol. *9*, 71-86.

Lavillette,D., Pecheur,E.I., Donot,P., Fresquet,J., Molle,J., Corbau,R., Dreux,M., Penin,F., and Cosset,F.L. (2007). Characterization of fusion determinants points to the involvement of three discrete regions of both E1 and E2 glycoproteins in the membrane fusion process of hepatitis C virus. J. Virol. *81*, 8752-8765.

Leffers,H., Dejgaard,K., and Celis,J.E. (1995). Characterisation of two major cellular poly(rC)-binding human proteins, each containing three K-homologous (KH) domains. Eur. J. Biochem. *230*, 447-453.

Lei,Y.X., Chen,J.K., and Wu,Z.L. (2002). Blocking the translation elongation factor-1 delta with its antisense mRNA results in a significant reversal of its oncogenic potential. Teratog. Carcinog. Mutagen. *22*, 377-383.

Li,J. and Lee,A.S. (2006). Stress induction of GRP78/BiP and its role in cancer. Curr. Mol. Med. *6*, 45-54.

Lindenbach,B.D., Evans,M.J., Syder,A.J., Wolk,B., Tellinghuisen,T.L., Liu,C.C., Maruyama,T., Hynes,R.O., Burton,D.R., McKeating,J.A., and Rice,C.M. (2005). Complete replication of hepatitis C virus in cell culture. Science *309*, 623-626.

Lindenbach,B.D. and Rice,C.M. (2005). Unravelling hepatitis C virus replication from genome to function. Nature *436*, 933-938.

Liu,H., Wang,Y., Zhang,Y., Song,Q., Di,C., Chen,G., Tang,J., and Ma,D. (1999). TFAR19, a novel apoptosis-related gene cloned from human leukemia cell line TF-1, could enhance apoptosis of some tumor cells induced by growth factor withdrawal. Biochem. Biophys. Res. Commun. *254*, 203-210.

Liu,N., Song,W., Wang,P., Lee,K., Chan,W., Chen,H., and Cai,Z. (2008). Proteomics analysis of differential expression of cellular proteins in response to avian H9N2 virus infection in human cells. Proteomics. *8*, 1851-1858.

Liu,S., Ansari,I.H., Das,S.C., and Pattnaik,A.K. (2006). Insertion and deletion analyses identify regions of non-structural protein 5A of Hepatitis C virus that are dispensable for viral genome replication. J. Gen. Virol. *87*, 323-327.

Lohmann,V., Hoffmann,S., Herian,U., Penin,F., and Bartenschlager,R. (2003). Viral and cellular determinants of hepatitis C virus RNA replication in cell culture. J. Virol. *77*, 3007-3019.

Lohmann,V., Korner,F., Dobierzewska,A., and Bartenschlager,R. (2001). Mutations in hepatitis C virus RNAs conferring cell culture adaptation. J. Virol. *75*, 1437-1449.

Lohmann,V., Korner,F., Koch,J., Herian,U., Theilmann,L., and Bartenschlager,R. (1999). Replication of subgenomic hepatitis C virus RNAs in a hepatoma cell line. Science *285*, 110-113.

Lohmann,V., Roos,A., Korner,F., Koch,J.O., and Bartenschlager,R. (2000). Biochemical and structural analysis of the NS5B RNA-dependent RNA polymerase of the hepatitis C virus. J. Viral Hepat. *7*, 167-174.

Lorenzo,L.J., Duenas-Carrera,S., Falcon,V., Acosta-Rivero,N., Gonzalez,E., de la Rosa,M.C., Menendez,I., and Morales,J. (2001). Assembly of truncated HCV core antigen into virus-like particles in Escherichia coli. Biochem. Biophys. Res. Commun. *281*, 962-965.

Lozach,P.Y., Lortat-Jacob,H., de Lacroix,d.L., Staropoli,I., Foung,S., Amara,A., Houles,C., Fieschi,F., Schwartz,O., Virelizier,J.L., Arenzana-Seisdedos,F., and Altmeyer,R. (2003). DC-SIGN and L-SIGN are high affinity binding receptors for hepatitis C virus glycoprotein E2. J. Biol. Chem. *278*, 20358-20366.

Lyle,J.M., Bullitt,E., Bienz,K., and Kirkegaard,K. (2002). Visualization and functional analysis of RNA-dependent RNA polymerase lattices. Science *296*, 2218-2222.

Lyles,D.S. (2000). Cytopathogenesis and inhibition of host gene expression by RNA viruses. Microbiol. Mol. Biol. Rev. *64*, 709-724.

Ma,Y. and Hendershot,L.M. (2004). The role of the unfolded protein response in tumour development: friend or foe? Nat. Rev. Cancer *4*, 966-977.

Macdonald,A., Crowder,K., Street,A., McCormick,C., and Harris,M. (2004). The hepatitis C virus NS5A protein binds to members of the Src family of tyrosine kinases and regulates kinase activity. J. Gen. Virol. *85*, 721-729.

Macdonald,A., Crowder,K., Street,A., McCormick,C., Saksela,K., and Harris,M. (2003). The hepatitis C virus non-structural NS5A protein inhibits activating protein-1 function by perturbing ras-ERK pathway signaling. J. Biol. Chem. *278*, 17775-17784.

MacParland,S.A., Pham,T.N., Gujar,S.A., and Michalak,T.I. (2006). De novo infection and propagation of wild-type Hepatitis C virus in human T lymphocytes in vitro. J. Gen. Virol. *87*, 3577-3586.

Mahadev,K., Raval,G., Bharadwaj,S., Willingham,M.C., Lange,E.M., Vonderhaar,B., Salomon,D., and Prasad,G.L. (2002). Suppression of the transformed phenotype of breast cancer by tropomyosin-1. Exp. Cell Res. *279*, 40-51.

Maheshwari,A., Ray,S., and Thuluvath,P.J. (2008). Acute hepatitis C. Lancet *372*, 321-332.

Majeau,N., Gagne,V., Boivin,A., Bolduc,M., Majeau,J.A., Ouellet,D., and Leclerc,D. (2004). The N-terminal half of the core protein of hepatitis C virus is sufficient for nucleocapsid formation. J. Gen. Virol. *85*, 971-981.

Makrantoni,V., Antrobus,R., Botting,C.H., and Coote,P.J. (2005). Rapid enrichment and analysis of yeast phosphoproteins using affinity chromatography, 2D-PAGE and peptide mass fingerprinting. Yeast *22*, 401-414.

Manning,B.D. and Cantley,L.C. (2007). AKT/PKB signaling: navigating downstream. Cell *129*, 1261-1274.

Mannova,P., Fang,R., Wang,H., Deng,B., McIntosh,M.W., Hanash,S.M., and Beretta,L. (2006). Modification of host lipid raft proteome upon hepatitis C virus replication. Mol. Cell Proteomics. *5*, 2319-2325.

Marklund,U., Brattsand,G., Osterman,O., Ohlsson,P.I., and Gullberg,M. (1993a). Multiple signal transduction pathways induce phosphorylation of serines 16, 25, and 38 of oncoprotein 18 in T lymphocytes. J. Biol. Chem. *268*, 25671-25680.

Marklund,U., Brattsand,G., Shingler,V., and Gullberg,M. (1993b). Serine 25 of oncoprotein 18 is a major cytosolic target for the mitogen-activated protein kinase. J. Biol. Chem. *268*, 15039-15047.

Masaki,T., Suzuki,R., Murakami,K., Aizaki,H., Ishii,K., Murayama,A., Date,T., Matsuura,Y., Miyamura,T., Wakita,T., and Suzuki,T. (2008). Interaction of hepatitis C virus nonstructural protein 5A with core protein is critical for the production of infectious virus particles. J. Virol.

Masarone,M., La,M., V, Bruno,S., Gaeta,G.B., Vecchione,R., Carrino,F., Moschella,F., Torella,R., and Persico,M. (2007). Steatohepatitis is associated with diabetes and fibrosis in genotype 1b HCV-related chronic liver disease. J. Viral Hepat. *14*, 714-720.

Mason,A. and Nair,S. (2003). Is type II diabetes another extrahepatic manifestation of HCV infection? Am. J. Gastroenterol. *98*, 243-246.

Masumi,A., Aizaki,H., Suzuki,T., DuHadaway,J.B., Prendergast,G.C., Komuro,K., and Fukazawa,H. (2005). Reduction of hepatitis C virus NS5A phosphorylation through its interaction with amphiphysin II. Biochem. Biophys. Res. Commun. *336*, 572-578.

Matsuoka,S., Ballif,B.A., Smogorzewska,A., McDonald,E.R., III, Hurov,K.E., Luo,J., Bakalarski,C.E., Zhao,Z., Solimini,N., Lerenthal,Y., Shiloh,Y., Gygi,S.P., and Elledge,S.J. (2007). ATM and ATR substrate analysis reveals extensive protein networks responsive to DNA damage. Science *316*, 1160-1166.

Mayo,M.J. (2003). Extrahepatic manifestations of hepatitis C infection. Am. J. Med. Sci. *325*, 135-148.

McDowell,M.A. and Sacks,D.L. (1999). Inhibition of host cell signal transduction by Leishmania: observations relevant to the selective impairment of IL-12 responses. Curr. Opin. Microbiol. *2*, 438-443.

McHutchison,J.G. and Fried,M.W. (2003). Current therapy for hepatitis C: pegylated interferon and ribavirin. Clin. Liver Dis. *7*, 149-161.

McIntosh,E.M., Ager,D.D., Gadsden,M.H., and Haynes,R.H. (1992). Human dUTP pyrophosphatase: cDNA sequence and potential biological importance of the enzyme. Proc. Natl. Acad. Sci. U. S. A *89*, 8020-8024.

McLauchlan,J., Lemberg,M.K., Hope,G., and Martoglio,B. (2002). Intramembrane proteolysis promotes trafficking of hepatitis C virus core protein to lipid droplets. EMBO J. *21*, 3980-3988.

McMahon,H.T., Wigge,P., and Smith,C. (1997). Clathrin interacts specifically with amphiphysin and is displaced by dynamin. FEBS Lett. *413*, 319-322.

Meertens,L., Bertaux,C., and Dragic,T. (2006). Hepatitis C virus entry requires a critical postinternalization step and delivery to early endosomes via clathrin-coated vesicles. J. Virol. *80*, 11571-11578.

Metodiev,M.V., Timanova,A., and Stone,D.E. (2004). Differential phosphoproteome profiling by affinity capture and tandem matrix-assisted laser desorption/ionization mass spectrometry. Proteomics. *4*, 1433-1438.

Meyers,G. and Thiel,H.J. (1996). Molecular characterization of pestiviruses. Adv. Virus Res. *47*, 53-118.

Mistry,S.J. and Atweh,G.F. (2001). Stathmin inhibition enhances okadaic acid-induced mitotic arrest: a potential role for stathmin in mitotic exit. J. Biol. Chem. *276*, 31209-31215.

Moenner,M., Pluquet,O., Bouchecareilh,M., and Chevet,E. (2007). Integrated endoplasmic reticulum stress responses in cancer. Cancer Res. *67*, 10631-10634.

Molina,H., Horn,D.M., Tang,N., Mathivanan,S., and Pandey,A. (2007). Global proteomic profiling of phosphopeptides using electron transfer dissociation tandem mass spectrometry. Proc. Natl. Acad. Sci. U. S. A *104*, 2199-2204.

Moradpour,D., Gosert,R., Egger,D., Penin,F., Blum,H.E., and Bienz,K. (2003). Membrane association of hepatitis C virus nonstructural proteins and identification of the membrane alteration that harbors the viral replication complex. Antiviral Res. *60*, 103-109.

Moradpour,D., Penin,F., and Rice,C.M. (2007). Replication of hepatitis C virus. Nat. Rev. Microbiol. *5*, 453-463.

Morgello,S. (2005). The nervous system and hepatitis C virus. Semin. Liver Dis. *25*, 118-121.

Muerhoff,A.S., Leary,T.P., Simons,J.N., Pilot-Matias,T.J., Dawson,G.J., Erker,J.C., Chalmers,M.L., Schlauder,G.G., Desai,S.M., and Mushahwar,I.K. (1995). Genomic organization of GB viruses A and B: two new members of the Flaviviridae associated with GB agent hepatitis. J. Virol. *69*, 5621-5630.

Munoz-Fernandez,S., Barbado,F.J., Martin,M.E., Gijon-Banos,J., Martinez,Z.R., Quevedo,E., Arribas,J.R., Gonzalez,A., I, and Vazquez,J.J. (1994). Evidence of hepatitis C virus antibodies in the cryoprecipitate of patients with mixed cryoglobulinemia. J. Rheumatol. *21*, 229-233.

Murayama,A., Date,T., Morikawa,K., Akazawa,D., Miyamoto,M., Kaga,M., Ishii,K., Suzuki,T., Kato,T., Mizokami,M., and Wakita,T. (2007). The NS3 helicase and NS5B-to-3'X regions are important for efficient hepatitis C virus strain JFH-1 replication in Huh7 cells. J. Virol. *81*, 8030-8040.

Murphy,M.D., Rosen,H.R., Marousek,G.I., and Chou,S. (2002). Analysis of sequence configurations of the ISDR, PKR-binding domain, and V3 region as predictors of response to induction interferon-alpha and ribavirin therapy in chronic hepatitis C infection. Dig. Dis. Sci. *47*, 1195-1205.

Murray,C.L., Jones,C.T., Tassello,J., and Rice,C.M. (2007). Alanine scanning of the hepatitis C virus core protein reveals numerous residues essential for production of infectious virus. J. Virol. *81*, 10220-10231.

Nakagawa,M., Sakamoto,N., Tanabe,Y., Koyama,T., Itsui,Y., Takeda,Y., Chen,C.H., Kakinuma,S., Oooka,S., Maekawa,S., Enomoto,N., and Watanabe,M. (2005). Suppression of hepatitis C virus replication by cyclosporin a is mediated by blockade of cyclophilins. Gastroenterology *129*, 1031-1041.

Nakamura,F., Mino,T., Yamamoto,J., Naka,M., and Tanaka,T. (1993). Identification of the regulatory site in smooth muscle calponin that is phosphorylated by protein kinase C. J. Biol. Chem. *268*, 6194-6201.

Neddermann,P., Clementi,A., and De Francesco,R. (1999). Hyperphosphorylation of the hepatitis C virus NS5A protein requires an active NS3 protease, NS4A, NS4B, and NS5A encoded on the same polyprotein. J. Virol. *73*, 9984-9991.

Nelson,H.B. and Tang,H. (2006). Effect of cell growth on hepatitis C virus (HCV) replication and a mechanism of cell confluence-based inhibition of HCV RNA and protein expression. J. Virol. *80*, 1181-1190.

Neumann,A.U., Lam,N.P., Dahari,H., Gretch,D.R., Wiley,T.E., Layden,T.J., and Perelson,A.S. (1998). Hepatitis C viral dynamics in vivo and the antiviral efficacy of interferon-alpha therapy. Science *282*, 103-107.

Nguyen,M.H. and Keeffe,E.B. (2005). Prevalence and treatment of hepatitis C virus genotypes 4, 5, and 6. Clin. Gastroenterol. Hepatol. *3*, S97-S101.

Nuesch,J.P., Lachmann,S., and Rommelaere,J. (2005). Selective alterations of the host cell architecture upon infection with parvovirus minute virus of mice. Virology *331*, 159-174.

O'Farrell,P.H. (1975). High resolution two-dimensional electrophoresis of proteins. J. Biol. Chem. *250*, 4007-4021.

Ogawa,K., Utsunomiya,T., Mimori,K., Tanaka,Y., Tanaka,F., Inoue,H., Murayama,S., and Mori,M. (2004). Clinical significance of elongation factor-1 delta mRNA expression in oesophageal carcinoma. Br. J. Cancer *91*, 282-286.

Ohba,K., Mizokami,M., Lau,J.Y., Orito,E., Ikeo,K., and Gojobori,T. (1996). Evolutionary relationship of hepatitis C, pesti-, flavi-, plantviruses, and newly discovered GB hepatitis agents. FEBS Lett. *378*, 232-234.

Okamoto,K., Moriishi,K., Miyamura,T., and Matsuura,Y. (2004). Intramembrane proteolysis and endoplasmic reticulum retention of hepatitis C virus core protein. J. Virol. *78*, 6370-6380.

Okamoto,T., Nishimura,Y., Ichimura,T., Suzuki,K., Miyamura,T., Suzuki,T., Moriishi,K., and Matsuura,Y. (2006). Hepatitis C virus RNA replication is regulated by FKBP8 and Hsp90. EMBO J. *25*, 5015-5025.

Olsen,J.V., Blagoev,B., Gnad,F., Macek,B., Kumar,C., Mortensen,P., and Mann,M. (2006). Global, in vivo, and site-specific phosphorylation dynamics in signaling networks. Cell *127*, 635-648.

Ong,S.E., Blagoev,B., Kratchmarova,I., Kristensen,D.B., Steen,H., Pandey,A., and Mann,M. (2002). Stable isotope labeling by amino acids in cell culture, SILAC, as a simple and accurate approach to expression proteomics. Mol. Cell Proteomics. *1*, 376-386.

Ong,S.E. and Mann,M. (2005). Mass spectrometry-based proteomics turns quantitative. Nat. Chem. Biol. *1*, 252-262.

Park,J.S., Yang,J.M., and Min,M.K. (2000). Hepatitis C virus nonstructural protein NS4B transforms NIH3T3 cells in cooperation with the Ha-ras oncogene. Biochem. Biophys. Res. Commun. *267*, 581-587.

Pattanakitsakul,S.N., Rungrojcharoenkit,K., Kanlaya,R., Sinchaikul,S., Noisakran,S., Chen,S.T., Malasit,P., and Thongboonkerd,V. (2007). Proteomic analysis of host responses in HepG2 cells during dengue virus infection. J. Proteome. Res. *6*, 4592-4600.

Pavio,N., Romano,P.R., Graczyk,T.M., Feinstone,S.M., and Taylor,D.R. (2003). Protein synthesis and endoplasmic reticulum stress can be modulated by the hepatitis C virus envelope protein E2 through the eukaryotic initiation factor 2alpha kinase PERK. J. Virol. *77*, 3578-3585.

Pawlotsky,J.M., Germanidis,G., Neumann,A.U., Pellerin,M., Frainais,P.O., and Dhumeaux,D. (1998). Interferon resistance of hepatitis C virus genotype 1b: relationship to nonstructural 5A gene quasispecies mutations. J. Virol. *72*, 2795-2805.

Penin,F., Dubuisson,J., Rey,F.A., Moradpour,D., and Pawlotsky,J.M. (2004). Structural biology of hepatitis C virus. Hepatology *39*, 5-19.

Pietschmann,T. and Bartenschlager,R. (2003). Tissue culture and animal models for hepatitis C virus. Clin. Liver Dis. *7*, 23-43.

Pietschmann,T., Kaul,A., Koutsoudakis,G., Shavinskaya,A., Kallis,S., Steinmann,E., Abid,K., Negro,F., Dreux,M., Cosset,F.L., and Bartenschlager,R. (2006). Construction and characterization of infectious intragenotypic and intergenotypic hepatitis C virus chimeras. Proc. Natl. Acad. Sci. U. S. A *103*, 7408-7413.

Pietschmann,T., Lohmann,V., Kaul,A., Krieger,N., Rinck,G., Rutter,G., Strand,D., and Bartenschlager,R. (2002). Persistent and transient replication of full-length hepatitis C virus genomes in cell culture. J. Virol. *76*, 4008-4021.

Pinchuk,G.V., Lee,S.R., Nanduri,B., Honsinger,K.L., Stokes,J.V., and Pinchuk,L.M. (2008). Bovine viral diarrhea viruses differentially alter the expression of the protein kinases and related proteins affecting the development of infection and anti-viral mechanisms in bovine monocytes. Biochim. Biophys. Acta *1784*, 1234-1247.

Pohlmann,S., Zhang,J., Baribaud,F., Chen,Z., Leslie,G.J., Lin,G., Granelli-Piperno,A., Doms,R.W., Rice,C.M., and McKeating,J.A. (2003). Hepatitis C virus glycoproteins interact with DC-SIGN and DC-SIGNR. J. Virol. *77*, 4070-4080.

Polyak,S.J., Nousbaum,J.B., Larson,A.M., Cotler,S., Carithers,R.L., Jr., and Gretch,D.R. (2000). The protein kinase-interacting domain in the hepatitis C virus envelope glycoprotein-2 gene is highly conserved in genotype 1-infected patients treated with interferon. J. Infect. Dis. *182*, 397-404.

Poynard,T., Yuen,M.F., Ratziu,V., and Lai,C.L. (2003). Viral hepatitis C. Lancet *362*, 2095-2100.

Priet,S., Sire,J., and Querat,G. (2006). Uracils as a cellular weapon against viruses and mechanisms of viral escape. Curr. HIV. Res. *4*, 31-42.

Puig-Basagoiti,F., Saiz,J.C., Forns,X., Ampurdanes,S., Gimenez-Barcons,M., Franco,S., Sanchez-Fueyo,A., Costa,J., Sanchez-Tapias,J.M., and Rodes,J. (2001). Influence of the genetic heterogeneity of the ISDR and PePHD regions of hepatitis C virus on the response to interferon therapy in chronic hepatitis C. J. Med. Virol. *65*, 35-44.

Radtke,K., Dohner,K., and Sodeik,B. (2006). Viral interactions with the cytoskeleton: a hitchhiker's guide to the cell. Cell Microbiol. *8*, 387-400.

Raggiaschi,R., Gotta,S., and Terstappen,G.C. (2005). Phosphoproteome analysis. Biosci. Rep. *25*, 33-44.

Raggiaschi,R., Lorenzetto,C., Diodato,E., Caricasole,A., Gotta,S., and Terstappen,G.C. (2006). Detection of phosphorylation patterns in rat cortical neurons by combining phosphatase treatment and DIGE technology. Proteomics. *6*, 748-756.

Ringrose,J.H., Jeeninga,R.E., Berkhout,B., and Speijer,D. (2008). Proteomic studies reveal coordinated changes in T-cell expression patterns upon infection with human immunodeficiency virus type 1. J. Virol. *82*, 4320-4330.

Robertson,B., Myers,G., Howard,C., Brettin,T., Bukh,J., Gaschen,B., Gojobori,T., Maertens,G., Mizokami,M., Nainan,O., Netesov,S., Nishioka,K., Shin i T, Simmonds,P., Smith,D., Stuyver,L., and Weiner,A. (1998). Classification, nomenclature, and database development for hepatitis C virus (HCV) and related viruses: proposals for standardization. International Committee on Virus Taxonomy. Arch. Virol. *143*, 2493-2503.

Rosenfeld,A.B. and Racaniello,V.R. (2005). Hepatitis C virus internal ribosome entry site-dependent translation in Saccharomyces cerevisiae is independent of polypyrimidine tract-binding protein, poly(rC)-binding protein 2, and La protein. J. Virol. *79*, 10126-10137.

Ross,P.L., Huang,Y.N., Marchese,J.N., Williamson,B., Parker,K., Hattan,S., Khainovski,N., Pillai,S., Dey,S., Daniels,S., Purkayastha,S., Juhasz,P., Martin,S., Bartlet-Jones,M., He,F., Jacobson,A., and Pappin,D.J. (2004). Multiplexed protein quantitation in Saccharomyces cerevisiae using amine-reactive isobaric tagging reagents. Mol. Cell Proteomics. *3*, 1154-1169.

Rush,J., Moritz,A., Lee,K.A., Guo,A., Goss,V.L., Spek,E.J., Zhang,H., Zha,X.M., Polakiewicz,R.D., and Comb,M.J. (2005). Immunoaffinity profiling of tyrosine phosphorylation in cancer cells. Nat. Biotechnol. *23*, 94-101.

Saito,I., Miyamura,T., Ohbayashi,A., Harada,H., Katayama,T., Kikuchi,S., Watanabe,Y., Koi,S., Onji,M., Ohta,Y., and . (1990). Hepatitis C virus infection is associated with the development of hepatocellular carcinoma. Proc. Natl. Acad. Sci. U. S. A *87*, 6547-6549.

Salomon,A.R., Ficarro,S.B., Brill,L.M., Brinker,A., Phung,Q.T., Ericson,C., Sauer,K., Brock,A., Horn,D.M., Schultz,P.G., and Peters,E.C. (2003). Profiling of tyrosine phosphorylation pathways in human cells using mass spectrometry. Proc. Natl. Acad. Sci. U. S. A *100*, 443-448.

Sandrin,V. and Cosset,F.L. (2006). Intracellular versus cell surface assembly of retroviral pseudotypes is determined by the cellular localization of the viral glycoprotein, its capacity to interact with Gag, and the expression of the Nef protein. J. Biol. Chem. *281*, 528-542.

Sarcar,B., Ghosh,A.K., Steele,R., Ray,R., and Ray,R.B. (2004). Hepatitis C virus NS5A mediated STAT3 activation requires co-operation of Jak1 kinase. Virology *322*, 51-60.

Sarrazin,C., Bruckner,M., Herrmann,E., Ruster,B., Bruch,K., Roth,W.K., and Zeuzem,S. (2001). Quasispecies heterogeneity of the carboxy-terminal part of the E2 gene including the PePHD and sensitivity of hepatitis C virus 1b isolates to antiviral therapy. Virology *289*, 150-163.

Scarselli,E., Ansuini,H., Cerino,R., Roccasecca,R.M., Acali,S., Filocamo,G., Traboni,C., Nicosia,A., Cortese,R., and Vitelli,A. (2002). The human scavenger receptor class B type I is a novel candidate receptor for the hepatitis C virus. EMBO J. *21*, 5017-5025.

Scholle,F., Li,K., Bodola,F., Ikeda,M., Luxon,B.A., and Lemon,S.M. (2004). Virus-host cell interactions during hepatitis C virus RNA replication: impact of polyprotein expression on the cellular transcriptome and cell cycle association with viral RNA synthesis. J. Virol. *78*, 1513-1524.

Schulze zur,W.J., Schmitz,H., Borowski,E., and Borowski,P. (2003). The proteins of the Hepatitis C virus: their features and interactions with intracellular protein phosphorylation. Arch. Virol. *148*, 1247-1267.

Schwartz,M., Chen,J., Janda,M., Sullivan,M., den Boon,J., and Ahlquist,P. (2002). A positive-strand RNA virus replication complex parallels form and function of retrovirus capsids. Mol. Cell *9*, 505-514.

Seeff,L.B. (2002). Natural history of chronic hepatitis C. Hepatology *36*, S35-S46.

Seifert,F., Struffert,T., Hildebrandt,M., Blumcke,I., Bruck,W., Staykov,D., Huttner,H.B., Hilz,M.J., Schwab,S., and Bardutzky,J. (2008). In vivo detection of hepatitis C virus (HCV) RNA in the brain in a case of encephalitis: evidence for HCV neuroinvasion. Eur. J. Neurol. *15*, 214-218.

Sekine-Osajima,Y., Sakamoto,N., Mishima,K., Nakagawa,M., Itsui,Y., Tasaka,M., Nishimura-Sakurai,Y., Chen,C.H., Kanai,T., Tsuchiya,K., Wakita,T., Enomoto,N., and Watanabe,M. (2008). Development of plaque assays for hepatitis C virus-JFH1 strain and isolation of mutants with enhanced cytopathogenicity and replication capacity. Virology *371*, 71-85.

Shavinskaya,A., Boulant,S., Penin,F., McLauchlan,J., and Bartenschlager,R. (2007). The lipid droplet binding domain of hepatitis C virus core protein is a major determinant for efficient virus assembly. J. Biol. Chem. *282*, 37158-37169.

Shaw,J., Rowlinson,R., Nickson,J., Stone,T., Sweet,A., Williams,K., and Tonge,R. (2003). Evaluation of saturation labelling two-dimensional difference gel electrophoresis fluorescent dyes. Proteomics. *3*, 1181-1195.

Shimizu,Y.K., Feinstone,S.M., Kohara,M., Purcell,R.H., and Yoshikura,H. (1996). Hepatitis C virus: detection of intracellular virus particles by electron microscopy. Hepatology *23*, 205-209.

Shimotohno,K., Hijikata,M., Tanji,Y., Kaneko,T., Satoh,S., Tanaka,T., and Kato,N. (1995). Processing of hepatitis C virus precursor polyprotein. Princess Takamatsu Symp. *25*, 121-128.

Shirinsky,V.P., Biryukov,K.G., Hettasch,J.M., and Sellers,J.R. (1992). Inhibition of the relative movement of actin and myosin by caldesmon and calponin. J. Biol. Chem. *267*, 15886-15892.

Silvera,D., Gamarnik,A.V., and Andino,R. (1999). The N-terminal K homology domain of the poly(rC)-binding protein is a major determinant for binding to the poliovirus 5'-untranslated region and acts as an inhibitor of viral translation. J. Biol. Chem. *274*, 38163-38170.

Simmonds,P., Bukh,J., Combet,C., Deleage,G., Enomoto,N., Feinstone,S., Halfon,P., Inchauspe,G., Kuiken,C., Maertens,G., Mizokami,M., Murphy,D.G., Okamoto,H., Pawlotsky,J.M., Penin,F., Sablon,E., Shin,I., Stuyver,L.J., Thiel,H.J., Viazov,S., Weiner,A.J., and Widell,A. (2005). Consensus proposals for a unified system of nomenclature of hepatitis C virus genotypes. Hepatology *42*, 962-973.

Simmonds,P., Holmes,E.C., Cha,T.A., Chan,S.W., McOmish,F., Irvine,B., Beall,E., Yap,P.L., Kolberg,J., and Urdea,M.S. (1993). Classification of hepatitis C virus into six major genotypes and a series of subtypes by phylogenetic analysis of the NS-5 region. J. Gen. Virol. *74 (Pt 11)*, 2391-2399.

Sinha,P., Kohl,S., Fischer,J., Hutter,G., Kern,M., Kottgen,E., Dietel,M., Lage,H., Schnolzer,M., and Schadendorf,D. (2000). Identification of novel proteins associated with the development of chemoresistance in malignant melanoma using two-dimensional electrophoresis. Electrophoresis *21*, 3048-3057.

Slepnev,V.I., Ochoa,G.C., Butler,M.H., Grabs,D., and De Camilli,P. (1998). Role of phosphorylation in regulation of the assembly of endocytic coat complexes. Science *281*, 821-824.

Smith,M.W., Yue,Z.N., Korth,M.J., Do,H.A., Boix,L., Fausto,N., Bruix,J., Carithers,R.L., Jr., and Katze,M.G. (2003). Hepatitis C virus and liver disease: global transcriptional profiling and identification of potential markers. Hepatology *38*, 1458-1467.

Soldaini,E., Wack,A., D'Oro,U., Nuti,S., Ulivieri,C., Baldari,C.T., and Abrignani,S. (2003). T cell costimulation by the hepatitis C virus envelope protein E2 binding to CD81 is mediated by Lck. Eur. J. Immunol. *33*, 455-464.

Spangberg,K. and Schwartz,S. (1999). Poly(C)-binding protein interacts with the hepatitis C virus 5' untranslated region. J. Gen. Virol. *80 (Pt 6)*, 1371-1376.

Stasyk,T., Morandell,S., Bakry,R., Feuerstein,I., Huck,C.W., Stecher,G., Bonn,G.K., and Huber,L.A. (2005). Quantitative detection of phosphoproteins by combination of two-dimensional difference gel electrophoresis and phosphospecific fluorescent staining. Electrophoresis *26*, 2850-2854.

Steinmann,E., Penin,F., Kallis,S., Patel,A.H., Bartenschlager,R., and Pietschmann,T. (2007). Hepatitis C virus p7 protein is crucial for assembly and release of infectious virions. PLoS. Pathog. *3*, e103.

Street,A., Macdonald,A., Crowder,K., and Harris,M. (2004). The Hepatitis C virus NS5A protein activates a phosphoinositide 3-kinase-dependent survival signaling cascade. J. Biol. Chem. *279*, 12232-12241.

Street,A., Macdonald,A., McCormick,C., and Harris,M. (2005). Hepatitis C virus NS5A-mediated activation of phosphoinositide 3-kinase results in stabilization of cellular beta-catenin and stimulation of beta-catenin-responsive transcription. J. Virol. *79*, 5006-5016.

Su,A.I., Pezacki,J.P., Wodicka,L., Brideau,A.D., Supekova,L., Thimme,R., Wieland,S., Bukh,J., Purcell,R.H., Schultz,P.G., and Chisari,F.V. (2002). Genomic analysis of the host response to hepatitis C virus infection. Proc. Natl. Acad. Sci. U. S. A *99*, 15669-15674.

Sumpter,R., Jr., Loo,Y.M., Foy,E., Li,K., Yoneyama,M., Fujita,T., Lemon,S.M., and Gale,M., Jr. (2005). Regulating intracellular antiviral defense and permissiveness to hepatitis C virus RNA replication through a cellular RNA helicase, RIG-I. J. Virol. *79*, 2689-2699.

Sundstrom,S., Ota,S., Dimberg,L.Y., Masucci,M.G., and Bergqvist,A. (2005). Hepatitis C virus core protein induces an anergic state characterized by decreased interleukin-2 production and perturbation of mitogen-activated protein kinase responses. J. Virol. *79*, 2230-2239.

Sung,V.M., Shimodaira,S., Doughty,A.L., Picchio,G.R., Can,H., Yen,T.S., Lindsay,K.L., Levine,A.M., and Lai,M.M. (2003). Establishment of B-cell lymphoma cell lines persistently infected with hepatitis C virus in vivo and in vitro: the apoptotic effects of virus infection. J. Virol. *77*, 2134-2146.

Takahashi,K., Hiwada,K., and Kokubu,T. (1986). Isolation and characterization of a 34,000-dalton calmodulin- and F-actin-binding protein from chicken gizzard smooth muscle. Biochem. Biophys. Res. Commun. *141*, 20-26.

Takashima,M., Kuramitsu,Y., Yokoyama,Y., Iizuka,N., Toda,T., Sakaida,I., Okita,K., Oka,M., and Nakamura,K. (2003). Proteomic profiling of heat shock protein 70 family members as biomarkers for hepatitis C virus-related hepatocellular carcinoma. Proteomics. *3*, 2487-2493.

Takikawa,S., Ishii,K., Aizaki,H., Suzuki,T., Asakura,H., Matsuura,Y., and Miyamura,T. (2000). Cell fusion activity of hepatitis C virus envelope proteins. J. Virol. *74*, 5066-5074.

Tan,S.L., Nakao,H., He,Y., Vijaysri,S., Neddermann,P., Jacobs,B.L., Mayer,B.J., and Katze,M.G. (1999). NS5A, a nonstructural protein of hepatitis C virus, binds growth factor receptor-bound protein 2 adaptor protein in a Src homology 3 domain/ligand-dependent manner and perturbs mitogenic signaling. Proc. Natl. Acad. Sci. U. S. A *96*, 5533-5538.

Tanaka,T., Kato,N., Cho,M.J., and Shimotohno,K. (1995). A novel sequence found at the 3' terminus of hepatitis C virus genome. Biochem. Biophys. Res. Commun. *215*, 744-749.

Tanaka,T., Kato,N., Cho,M.J., Sugiyama,K., and Shimotohno,K. (1996). Structure of the 3' terminus of the hepatitis C virus genome. J. Virol. *70*, 3307-3312.

Tang,G. (2005). siRNA and miRNA: an insight into RISCs. Trends Biochem. Sci. *30*, 106-114.

Tardif,K.D., Mori,K., and Siddiqui,A. (2002). Hepatitis C virus subgenomic replicons induce endoplasmic reticulum stress activating an intracellular signaling pathway. J. Virol. *76*, 7453-7459.

Taylor,D.R., Shi,S.T., Romano,P.R., Barber,G.N., and Lai,M.M. (1999). Inhibition of the interferon-inducible protein kinase PKR by HCV E2 protein. Science *285*, 107-110.

Tingting,P., Caiyun,F., Zhigang,Y., Pengyuan,Y., and Zhenghong,Y. (2006). Subproteomic analysis of the cellular proteins associated with the 3' untranslated region of the hepatitis C virus genome in human liver cells. Biochem. Biophys. Res. Commun. *347*, 683-691.

Tourriere,H., Gallouzi,I.E., Chebli,K., Capony,J.P., Mouaikel,J., van der,G.P., and Tazi,J. (2001). RasGAP-associated endoribonuclease G3Bp: selective RNA degradation and phosphorylation-dependent localization. Mol. Cell Biol. *21*, 7747-7760.

Tsao,M.L., Chao,C.H., and Yeh,C.T. (2006). Interaction of hepatitis C virus F protein with prefoldin 2 perturbs tubulin cytoskeleton organization. Biochem. Biophys. Res. Commun. *348*, 271-277.

Tscherne,D.M., Jones,C.T., Evans,M.J., Lindenbach,B.D., McKeating,J.A., and Rice,C.M. (2006). Time- and temperature-dependent activation of hepatitis C virus for low-pH-triggered entry. J. Virol. *80*, 1734-1741.

Tsuchihara,K., Hijikata,M., Fukuda,K., Kuroki,T., Yamamoto,N., and Shimotohno,K. (1999). Hepatitis C virus core protein regulates cell growth and signal transduction pathway transmitting growth stimuli. Virology *258*, 100-107.

Tsukiyama-Kohara,K., Iizuka,N., Kohara,M., and Nomoto,A. (1992). Internal ribosome entry site within hepatitis C virus RNA. J. Virol. *66*, 1476-1483.

Tsukiyama-Kohara,K., Tone,S., Maruyama,I., Inoue,K., Katsume,A., Nuriya,H., Ohmori,H., Ohkawa,J., Taira,K., Hoshikawa,Y., Shibasaki,F., Reth,M., Minatogawa,Y., and Kohara,M. (2004). Activation of the CKI-CDK-Rb-E2F pathway in full genome hepatitis C virus-expressing cells. J. Biol. Chem. *279*, 14531-14541.

Unlu,M., Morgan,M.E., and Minden,J.S. (1997). Difference gel electrophoresis: a single gel method for detecting changes in protein extracts. Electrophoresis *18*, 2071-2077.

van Damme,H.T., Amons,R., Karssies,R., Timmers,C.J., Janssen,G.M., and Moller,W. (1990). Elongation factor 1 beta of artemia: localization of functional sites and homology to elongation factor 1 delta. Biochim. Biophys. Acta *1050*, 241-247.

Varaklioti,A., Vassilaki,N., Georgopoulou,U., and Mavromara,P. (2002). Alternate translation occurs within the core coding region of the hepatitis C viral genome. J. Biol. Chem. *277*, 17713-17721.

Wakita,T., Pietschmann,T., Kato,T., Date,T., Miyamoto,M., Zhao,Z., Murthy,K., Habermann,A., Krausslich,H.G., Mizokami,M., Bartenschlager,R., and Liang,T.J. (2005). Production of infectious hepatitis C virus in tissue culture from a cloned viral genome. Nat. Med. *11*, 791-796.

Walewski,J.L., Keller,T.R., Stump,D.D., and Branch,A.D. (2001). Evidence for a new hepatitis C virus antigen encoded in an overlapping reading frame. RNA. *7*, 710-721.

Wang,C., Sarnow,P., and Siddiqui,A. (1993). Translation of human hepatitis C virus RNA in cultured cells is mediated by an internal ribosome-binding mechanism. J. Virol. *67*, 3338-3344.

Waris,G., Livolsi,A., Imbert,V., Peyron,J.F., and Siddiqui,A. (2003). Hepatitis C virus NS5A and subgenomic replicon activate NF-kappaB via tyrosine phosphorylation of IkappaBalpha and its degradation by calpain protease. J. Biol. Chem. *278*, 40778-40787.

Watanabe,H., Nagayama,K., Enomoto,N., Itakura,J., Tanabe,Y., Sato,C., Izumi,N., and Watanabe,M. (2003). Amino acid substitutions in PKR-eIF2 phosphorylation homology domain (PePHD) of hepatitis C virus E2 protein in

genotype 2a/2b and 1b in Japan and interferon efficacy. Hepatol. Res. *26*, 268-274.

Whitlow,Z.W., Connor,J.H., and Lyles,D.S. (2006). Preferential translation of vesicular stomatitis virus mRNAs is conferred by transcription from the viral genome. J. Virol. *80*, 11733-11742.

Wiese,S., Reidegeld,K.A., Meyer,H.E., and Warscheid,B. (2007). Protein labeling by iTRAQ: a new tool for quantitative mass spectrometry in proteome research. Proteomics. *7*, 340-350.

Wigge,P., Kohler,K., Vallis,Y., Doyle,C.A., Owen,D., Hunt,S.P., and McMahon,H.T. (1997). Amphiphysin heterodimers: potential role in clathrin-mediated endocytosis. Mol. Biol. Cell *8*, 2003-2015.

Willems,M., Metselaar,H.J., Tilanus,H.W., Schalm,S.W., and de Man,R.A. (2002). Liver transplantation and hepatitis C. Transpl. Int. *15*, 61-72.

Winder,S.J. and Walsh,M.P. (1990). Smooth muscle calponin. Inhibition of actomyosin MgATPase and regulation by phosphorylation. J. Biol. Chem. *265*, 10148-10155.

Wong,Q.W., Lung,R.W., Law,P.T., Lai,P.B., Chan,K.Y., To,K.F., and Wong,N. (2008). MicroRNA-223 is commonly repressed in hepatocellular carcinoma and potentiates expression of Stathmin1. Gastroenterology *135*, 257-269.

Wunschmann,S., Medh,J.D., Klinzmann,D., Schmidt,W.N., and Stapleton,J.T. (2000). Characterization of hepatitis C virus (HCV) and HCV E2 interactions with CD81 and the low-density lipoprotein receptor. J. Virol. *74*, 10055-10062.

Xiao,H., Neuveut,C., Benkirane,M., and Jeang,K.T. (1998). Interaction of the second coding exon of Tat with human EF-1 delta delineates a mechanism for HIV-1-mediated shut-off of host mRNA translation. Biochem. Biophys. Res. Commun. *244*, 384-389.

Xu,Z., Choi,J., Lu,W., and Ou,J.H. (2003). Hepatitis C virus f protein is a short-lived protein associated with the endoplasmic reticulum. J. Virol. *77*, 1578-1583.

Xu,Z., Choi,J., Yen,T.S., Lu,W., Strohecker,A., Govindarajan,S., Chien,D., Selby,M.J., and Ou,J. (2001). Synthesis of a novel hepatitis C virus protein by ribosomal frameshift. EMBO J. *20*, 3840-3848.

Yamagata,A., Kristensen,D.B., Takeda,Y., Miyamoto,Y., Okada,K., Inamatsu,M., and Yoshizato,K. (2002). Mapping of phosphorylated proteins on two-dimensional polyacrylamide gels using protein phosphatase. Proteomics. *2*, 1267-1276.

Yamaoka,K., Imajoh-Ohmi,S., Fukuda,H., Akita,Y., Kurosawa,K., Yamamoto,Y., and Sanai,Y. (2006). Identification of phosphoproteins associated with maintenance of transformed state in temperature-sensitive Rous sarcoma-virus infected cells by proteomic analysis. Biochem. Biophys. Res. Commun. *345*, 1240-1246.

Yan,J.X., Wait,R., Berkelman,T., Harry,R.A., Westbrook,J.A., Wheeler,C.H., and Dunn,M.J. (2000). A modified silver staining protocol for visualization of proteins compatible with matrix-assisted laser desorption/ionization and electrospray ionization-mass spectrometry. Electrophoresis *21*, 3666-3672.

Yang,X.J., Liu,J., Ye,L., Liao,Q.J., Wu,J.G., Gao,J.R., She,Y.L., Wu,Z.H., and Ye,L.B. (2006). HCV NS2 protein inhibits cell proliferation and induces cell cycle arrest in the S-phase in mammalian cells through down-regulation of cyclin A expression. Virus Res. *121*, 134-143.

Yao,Z.Q., Eisen-Vandervelde,A., Ray,S., and Hahn,Y.S. (2003). HCV core/gC1qR interaction arrests T cell cycle progression through stabilization of the cell cycle inhibitor p27Kip1. Virology *314*, 271-282.

Yao,Z.Q., Nguyen,D.T., Hiotellis,A.I., and Hahn,Y.S. (2001). Hepatitis C virus core protein inhibits human T lymphocyte responses by a complement-dependent regulatory pathway. J. Immunol. *167*, 5264-5272.

Yen,T., Keeffe,E.B., and Ahmed,A. (2003). The epidemiology of hepatitis C virus infection. J. Clin. Gastroenterol. *36*, 47-53.

Yeung,Y.G., Wang,Y., Einstein,D.B., Lee,P.S., and Stanley,E.R. (1998). Colony-stimulating factor-1 stimulates the formation of multimeric cytosolic complexes of signaling proteins and cytoskeletal components in macrophages. J. Biol. Chem. *273*, 17128-17137.

Yi,M. and Lemon,S.M. (2003a). 3' nontranslated RNA signals required for replication of hepatitis C virus RNA. J. Virol. *77*, 3557-3568.

Yi,M. and Lemon,S.M. (2003b). Structure-function analysis of the 3' stem-loop of hepatitis C virus genomic RNA and its role in viral RNA replication. RNA. *9*, 331-345.

Yi,M., Ma,Y., Yates,J., and Lemon,S.M. (2007). Compensatory mutations in E1, p7, NS2, and NS3 enhance yields of cell culture-infectious intergenotypic chimeric hepatitis C virus. J. Virol. *81*, 629-638.

Yi,Z., Fang,C., Pan,T., Wang,J., Yang,P., and Yuan,Z. (2006). Subproteomic study of hepatitis C virus replicon reveals Ras-GTPase-activating protein binding protein 1 as potential HCV RC component. Biochem. Biophys. Res. Commun. *350*, 174-178.

Yokoyama,Y., Kuramitsu,Y., Takashima,M., Iizuka,N., Toda,T., Terai,S., Sakaida,I., Oka,M., Nakamura,K., and Okita,K. (2004). Proteomic profiling of proteins decreased in hepatocellular carcinoma from patients infected with hepatitis C virus. Proteomics. *4*, 2111-2116.

Yoshida,T., Hanada,T., Tokuhisa,T., Kosai,K., Sata,M., Kohara,M., and Yoshimura,A. (2002). Activation of STAT3 by the hepatitis C virus core protein leads to cellular transformation. J. Exp. Med. *196*, 641-653.

Yu,L.R., Zhu,Z., Chan,K.C., Issaq,H.J., Dimitrov,D.S., and Veenstra,T.D. (2007). Improved titanium dioxide enrichment of phosphopeptides from HeLa cells and high confident phosphopeptide identification by cross-validation of MS/MS and MS/MS/MS spectra. J. Proteome. Res. *6*, 4150-4162.

Zech,B., Kurtenbach,A., Krieger,N., Strand,D., Blencke,S., Morbitzer,M., Salassidis,K., Cotten,M., Wissing,J., Obert,S., Bartenschlager,R., Herget,T., and Daub,H. (2003). Identification and characterization of amphiphysin II as a novel cellular interaction partner of the hepatitis C virus NS5A protein. J. Gen. Virol. *84*, 555-560.

Zemel,R., Gerechet,S., Greif,H., Bachmatove,L., Birk,Y., Golan-Goldhirsh,A., Kunin,M., Berdichevsky,Y., Benhar,I., and Tur-Kaspa,R. (2001). Cell transformation induced by hepatitis C virus NS3 serine protease. J. Viral Hepat. *8*, 96-102.

Zhao,L.J., Liu,H.Q., Cao,J., Feng,G.S., and Qi,Z.T. (2001). Activation of Intracellular MAPK/ERK Initiated by Hepatitis C Virus Envelope Protein E2 in HepG2 Cells. Sheng Wu Hua Xue. Yu Sheng Wu Wu Li Xue. Bao. (Shanghai) *33*, 691-695.

Zhong,J., Gastaminza,P., Cheng,G., Kapadia,S., Kato,T., Burton,D.R., Wieland,S.F., Uprichard,S.L., Wakita,T., and Chisari,F.V. (2005). Robust hepatitis C virus infection in vitro. Proc. Natl. Acad. Sci. U. S. A *102*, 9294-9299.

Zhu,H., Zhao,H., Collins,C.D., Eckenrode,S.E., Run,Q., McIndoe,R.A., Crawford,J.M., Nelson,D.R., She,J.X., and Liu,C. (2003a). Gene expression associated with interferon alfa antiviral activity in an HCV replicon cell line. Hepatology *37*, 1180-1188.

Zhu,Q., Guo,J.T., and Seeger,C. (2003b). Replication of hepatitis C virus subgenomes in nonhepatic epithelial and mouse hepatoma cells. J. Virol. *77*, 9204-9210.

APPENDICES

APPENDIX I – DETAILED MATERIALS

Materials	Company	Catalogue Number
Antibodies		
Alexa Fluor® 488 goat anti-mouse IgG	Molecular Probes	A11029
Anti-actin *(used at 1:1000 dilution)*	Sigma	A 2066
Anti-NPTII *(used at 1:1000 dilution)*	Sigma	N 6537
Anti-Op18/stathmin *(used at 1:10 000 dilution)*	Sigma	O 0138
Anti-Hepatitis C NS5A monoclonal antibody *(used at 1:1000 dilution)*	Virogen	256-A
Cy™3-conjugated AffiniPure goat anti-rabbit IgG *(used at 1:100 dilution)*	Jackson Immunoresearch	111-165-144
Cy™5-conjugated AffiniPure goat anti-mouse *(used at 1:100 dilution)*	Jackson Immunoresearch	115-175-146
Goat anti-mouse IgG HRP conjugated *(used at 1:10 000 dilution)*	Upstate	12-349
Goat anti-rabbit IgG HRP conjugated *(used at 1:10 000 dilution)*	Upstate	12-348
Goat polyclonal to GAPDH *(used at 1:1000 dilution)*	Abcam	ab9483
Monoclonal anti-heat shock protein 60 clone LK1 *(used at 1:400 dilution)*	Sigma	H 4149
Monoclonal anti-TCP-1β clone F39P7F11 *(used at 1:1000 dilution)*	Sigma	T 9076
Monoclonal anti-tropomyosin clone TM311 *(used at 1:1000 dilution)*	Sigma	T 2780
PCBP1 polyclonal antibody (A01) *(used at 1:2500 dilution)*	Abnova Corporation	H00005093
Phospho-(Ser/Thr) Akt substrate antibody *(used at 1:1000 dilution)*	Cell Signaling	9611
Rabbit anti-goat IgG-HRP *(used at 1:10 000 dilution)*	Santa Cruz	sc-2922
Rabbit polyclonal to ERp29 *(used at 1:1000 dilution)*	Novus Biologicals	NB300-523
Rat anti-TCP-1α (CCT) monoclonal *(used at 1:1000 dilution)*	Stressgen Bioreagents	CTA-191
TPM3 polyclonal antibody (A01) *(used at 1:2500 dilution)*	Abnova Corportation	H0007170
Cell Culture Reagents		
Effectene® transfection reagent	Qiagen	301425
Dulbecco's modified Eagle medium	Gibco	11995
Geneticin®	Gibco	10131-027
Heat-inactivated fetal bovine serum	Gibco	10082
MEM non-essential amino acid solution (100x)	Sigma	M 7145
Penicillin/Streptomycin	Gibco	15140

TransMessenger™ transfection reagent	Qiagen	301525
0.25% Trypsin-EDTA	Gibco	25200
Electrophoresis Reagents		
Acrylamide PAGE 40% solution	GE Healthcare	17-1303-01
BenchMark™ prestained protein ladder	Invitrogen	10748-010
Bovine serum albumin	Sigma	B-4287
CHAPS	Sigma	226947
DIGE Fluor Labelling Kit	GE Healthcare	25-8010-65
DL-Dithiothrietol	Fluka	43815
GelCode® Blue (colloidal coomassie stain)	Pierce	24590
Glycerol	Fisher Bioreagents	BP229-01
iBlot™ Gel Transfer Stacks, nitrocellulose	Invitrogen	IB3010
iBlot™ Gel Transfer Stacks, PVDF	Invitrogen	
Immobiline™ DryStrip, 7cm pI 4-7	GE Healthcare	17-6001-10
Immobiline™ DryStrip, 24cm pI 4-7	GE Healthcare	17-6002-46
Immobilon™ Western HRP Chemiluminecence	Millipore	WBKLS0500
Immobilon-FL Transfer Membrane	Millipore	IPFL10100
Iodoacetamide	GE Healthcare	RPN63020LIAF
IPG buffer, pH 4-7	GE Healthcare	17-6000-86
Kodak™ X-OMAT™ x-ray film	Perkin Elmer	NEF596001EA
L-Lysine	Sigma	L 5501
MagicMark™ XP western standard	Invitrogen	LC5602
N'N'-dimethyl formamide	Usb	14862-250
NuPAGE® 12% Bis-Tris Gel	Invitrogen	NP0341BOX
NuPAGE® 4-12% Bis-Tris Gel	Invitrogen	NP0321BOX
Optigels, 10-20% gradient	Nextgensciences	A11622
PlusOne ammonium persulphate	GE Healthcare	17-1311-01
PlusOne bromophenol blue	GE Healthcare	17-1329-01
PlusOne glycine	GE Healthcare	17-1323-01
PlusOne N',N'-methylene-bisacrylamide 2% sol'n	GE Healthcare	17-1306-01
PlusOne tris	GE Healthcare	17-1321-01
PlusOne SDS	GE Healthcare	17-1313-01
PlusOne silver staining kit	GE Healthcare	17-6002-46
PlusOne TEMED	GE Healthcare	17-1312-01
PlusOne urea	GE Healthcare	17-1319-01
Re-Blot Plus strong solution (10x)	Chemicon	VR1369971
Sea Block blocking buffer	Pierce	37527
Thiourea	GE Healthcare	RPN6301V
2-D Clean-Up kit	GE Healthcare	80-6484-51
2-D Quant Kit	GE Healthcare	80-6483-56
Visualizer™ western blot detection kit, mouse	Upstate	64-201SP
Mass spectrometry reagents		
Acetonitrile	Sigma	360457
Ammonium bicarbonate	Sigma	A6141
C18 pre column- Zorbax 300SB-C18, 5µm,	Agilent	

5mmx0.3mm		
C18 analytical column- Zorbax 300SB-C18, 3.5µm, 15cmx75µm	Agilent	
CHCA (a-Cyano040hydroxycinnamic acid)	Sigma	C 8982
Potassium ferricyanide	Fluka	60299
ProteoMass™ peptide and protein MALDI-MS calibration kit	Sigma	MS-CAL1
Sodium thiosulfate	Sigma	217263
Trifluoroacetic acid	Sigma	T 6508
Trypsin Gold, MS grade	Promega	TB309
Trypsin proteomics grade	Sigma	T 6567
Other reagents		
Bradford dye reagent	Bio-Rad	500-0006
DAPI	Molecular Probes	
Lambda protein phosphatase	New England Biolabs	P0753S
PhosphoProtein purification kit	Qiagen	37101
ProLong® Gold antifade reagent	Invitrogen	P36934
pSV2neo (GenBank #U02434)	Clonetech	6172-1
QIAEX II	Qiagen	20902
Restriction enzymes and KLENOW	Qiagen	
RiboMAX™ large scale RNA production systems	Promega	P1300
RNase-Free DNase	Qiagen	79254
RNease® MinElute™ Cleanup kit	Qiagen	74204
Saponin	Acros	41923-1000
Sodium fluoride	Sigma	S7920
Sodium orthovanadate	Sigma	S6508
TALON PMAC Phosphoprotein enrichment kit	Clonetech	635624
T7 RiboMAX™ express large scale RNA production kit	Promega	P1320
Software and equipment		
Amicon Ultra-4, 3kDa filter	Millipore	UFC800396
AxioCamMRc Zeiss	Zeiss	
AxioVert 200M	Zeiss	
AxioVision 4.5 SP1 (03/2006)	Zeiss	
DeCyder	GE Healthcare	
ECM 830 Electroporation System	BTX	45-0002
Ettan™ DALTsix Electrophoresis Unit, 115V	GE Healthcare	
Ettan™ IPGphorII™	GE Healthcare	
ImageQuant 5.2	GE Healthcare	
ImageQuant TL v2002.01	GE Healthcare	
MultiTemp III water circulator	GE Healthcare	
Typhoon 9410 variable mode imager	GE Healthcare	
$ZipTip_{C18}$	Millipore	ZTC18S960

APPENDIX II – DETAILED RECIPES

Solutions

- 1X sample/rehydration buffer
  - 7M urea, 2M thiourea, 4% CHAPS, 0.5% IPG buffer, 65mM DTT
- 2X sample/rehydration buffer
  - 7M urea, 2M thiourea, 4% CHAPS, 1% IPG buffer, 130mM DTT
- 5X SDS running buffer
  - 125mM Tris-base, 120mM glycine, 0.5% SDS
- HEPES, pH 7.1
  - 70mM NaCl, 25mM HEPES
- IFA blocking solution
  - 0.5%w/v saponin, 1.0%w/v BSA, 0.2%w/v skim milk powder in PBS
- PBS (10X), pH 7.2
  - 137mM NaCl, 100mM Na_2HPO_4 $12H_2O$, 25mM KCl, 18mM KH_2PO_4
- 2D cell lysis buffer/Cy labelling buffer
  - 30mM Tris-HCl, 7M urea, 2M Thiourea, 4% CHAPS, pH 8.5
- SDS equilibration buffer stock solution
  - 50mM Tris-HCl, pH 8.8, containing 6M Urea, 30% v/v glycerol, 2% w/v SDS and 0.002% w/v bromophenol blue
- TBS (10X), pH 7.4
  - 685mM NaCl, 125mM Tris-HCl, 12.5mM KCl

APPENDIX III – Identified peptides and corresponding Mascot scores for Chapter III

SwissProt 55.4 (scores >28, p<0.05)

Spot 1

STMN1_HUMAN Score: 475 Queries matched: 16

K.DLSLEEIQK.K	47
K.ESVPEFPLSPPK.K	60
R.ASGQAFELILSPR.S	98
R.SKESVPEFPLSPPK.K	79

Spot 2

RANG_HUMAN Score: 170 Queries matched: 9

R.FASENDLPEWK.E	66
K.TLEEDEEELFK.M	61
R.FASENDLPEWKER.G	42
K.ICANHYITPMMELKPNAGSDR.A + 2 Oxidation (M)	32

Spot 3

RLA0_HUMAN Score: 526 Queries matched: 42

R.GNVGFVFTK.E	46
K.IIQLLDDYPK.C	76
K.TSFFQALGITTK.I	81
R.GTIEILSDVQLIK.T	47
K.EDLTEIRDMLLANK.V + Oxidation (M)	24
R.GNVGFVFTKEDLTEIR.D	45
R.VLALSVETDYTFPLAEK.V	18
R.AGAIAPCEVTVPAQNTGLGPEK.T	55
K.AFLADPSAFVAAAPVAAATTAAPAAAAAPAK.V	72

Spot 4

GRP75_HUMAN Score: 1129 Queries matched: 36

K.LFEMAYK.K	31
R.QAASSLQQASLK.L	46
K.DAGQISGLNVLR.V	24
K.VQQTVQDLFGR.A	68
R.AQFEGIVTDLIR.R	71
K.SDIGEVILVGGMTR.M	71
R.TTPSVVAFTADGER.L	61
R.EQQIVIQSSGGLSK.D	12
R.AQFEGIVTDLIRR.T	4
K.LYSPSQIGAFVLMK.M	51
R.QAVTNPNNTFYATK.R	35
K.MKETAENYLGHTAK.N	37
K.LLGQFTLIGIPPAPR.G	80
R.VINEPTAAALAYGLDK.S	71
K.NAVITVPAYFNDSQR.Q	74
K.SQVFSTAADGQTQVEIK.V	86
R.VEAVNMAEGIIHDTETK.M	84
K.KSQVFSTAADGQTQVEIK.V	103
R.VINEPTAAALAYGLDKSEDK.V	78
K.ERVEAVNMAEGIIHDTETK.M	76

ANXA6_HUMAN Score: 104 Queries matched: 4

K.ALIEILATR.T	47
R.LVFDEYLK.T	31
R.SEIDLLNIR.R	50
K.EAILDIITSR.S	57

Spot 5

PDIA3_HUMAN Score: 444 Queries matched: 23

K.YGVSGYPTLK.I	55
K.FVMQEEFSR.D	42
R.LAPEYEAAATR.L	31
K.LSKDPNIVIAK.M	60
R.GFPTIYFSPANK.K	70
R.FLQDYFDGNLK.R	41
K.SEPIPESNDGPVK.V	14
R.ELSDFISYLQR.E	31
R.GFPTIYFSPANKK.L	47
R.FLQDYFDGNLKR.Y	57
R.EATNPPVIQEEKPK.K	10
K.DLLIAYYDVDYEK.N	41
K.IFRDGEEAGAYDGPR.T	55
K.QAGPASVPLRTEEEFK.K	38
R.YLKSEPIPESNDGPVK.V	12

HNRPK_HUMAN Score: 142 Queries matched: 7

K.DLAGSIIGK.G	16
R.NLPLPPPPPPR.G	33
K.IILDLISESPIK.G	37
R.TDYNASVSVPDSSGPER.I	65
R.GSYGDLGGPIITTQVTIPK.D	24

Spot 6

TCPA_HUMAN Score: 842 Queries matched: 36

K.NTKAR.T	8
R.TSASIILR.G	29
K.SSLGPVGLDK.M	88
M.EGPLSVFGDR.S	36
K.LLEVEHPAAK.V	55
R.SLHDALCVVK.R	61
R.YPVNSVNILK.A	17
K.QAGVFEPTIVK.V	69
K.FATEAAITILR.I	56
K.YFVEAGAMAVR.R	45
K.IHPTSVISGYR.L	22
R.ICDDELILIK.N	51
R.SLHDALCVVKR.V	45
K.LGVQVVITDPEK.L	77
K.VLCELADLQDK.E	67
K.YFVEAGAMAVRR.V + Oxidation (M)	9
K.QKIHPTSVISGYR.L	32
R.GANDFMCDEMER.S + Oxidation (M)	27

R.SQNVMAAASIANIVK.S + Oxidation (M)	99
R.DNKQAGVFEPTIVK.V	41
K.EVGDGTTSVVIIAAELLK.N	49
K.LGVQVVITDPEKLDQIR.Q	72
K.DDKHGSYEDAVHSGALND.-	41
K.ILATGANVILTTGGIDDMCLK.Y	76
R.SQMESMLISGYALNCVVGSQGMPK.R + 2 Oxidation (M)	42
R.YINENLIVNTDELGRDCLINAAK.T	21

Spot 7

TCPB_HUMAN Score: 1073 Queries matched: 37

K.LAVEAVLR.L	44
K.HGINCFINR.Q	25
K.GSGNLEAIHIIK.K	63
K.LIEEVMIGEDK.L	71
K.ILIANTGMDTDK.I	61
K.IHPQTIIAGWR.E	31
R.GATQQILDEAER.S	78
R.LKGSGNLEAIHIIK.K	53
R.QDLMNIAGTTLSSK.L + Oxidation (M)	80
K.ILIANTGMDTDKIK.I + Oxidation (M)	69
R.SLHDALCVLAQTVK.D	45
R.DASLMVTNDGATILK.N + Oxidation (M)	82
R.EALLSSAVDHGSDEVK.F	83
K.FRQDLMNIAGTTLSSK.L + Oxidation (M)	41
R.EALLSSAVDHGSDEVKFR.Q	51
K.LGGSLADSYLDEGFLLDKK.I	49
R.LALVTGGEIASTFDHPELVK.L	34
R.VQDDEVGDGTTSVTVLAAELLR.E	43
R.TVYGGGCSEMLMAHAVTQLANR.T + 2 Oxidation (M)	19

Spot 8

TCPB_HUMAN Score: Queries matched:

K.LAVEAVLR.L	35
K.HGINCFINR.Q	29
K.GSGNLEAIHIIK.K	76
K.LIEEVMIGEDK.L	82
K.ILIANTGMDTDK.I	91
K.IHPQTIIAGWR.E	42
R.GATQQILDEAER.S	87
K.KIHPQTIIAGWR.E	35
R.TPGKEAVAMESYAK.A	53
R.LKGSGNLEAIHIIK.K	45
R.QDLMNIAGTTLSSK.L + Oxidation (M)	84
R.LTSFIGAIAIGDLVK.S	41
K.ILIANTGMDTDKIK.I + Oxidation (M)	53
R.SLHDALCVLAQTVK.D	69
R.EALLSSAVDHGSDEVK.F	70
K.FRQDLMNIAGTTLSSK.L + Oxidation (M)	57
R.EALLSSAVDHGSDEVKFR.Q	65
K.LGGSLADSYLDEGFLLDKK.I	29
R.LALVTGGEIASTFDHPELVK.L	28
R.VQDDEVGDGTTSVTVLAAELLR.E	41
R.TVYGGGCSEMLMAHAVTQLANR.T + 2 Oxidation (M)	30

Spot 9

TCPZ_HUMAN Score: 189 Queries matched: 7

K.ALQFLEEVK.V	49
K.TEVNSGFFYK.S	21
R.AQAALAVNISAAR.G	74
K.GIDPFSLDALSK.E	71
K.QADLYISEGLHPR.I	47
K.VLAQNSGFDLQETLVK.I	43
K.DGNVLLHEMQIQHPTASLIAK.V + Oxidation (M)	19

TCPW_HUMAN Score: 66 Queries matched: 3

K.TEVNSGFFYK.T	*21*
K.GIDPFSLDSLAK.H	*42*
K.QADLYISEGLHPR.I	*47*

Spot 11

HNRPF_HUMAN Score: 301 Queries matched: 17

R.YIEVFK.S	27
R.TEMDWVLK.H	30
R.VHIEIGPDGR.V	37
R.DLSYCLSGMYDHR.Y	53
R.QSGEAFVELGSEDDVK.M	81
K.ITGEAFVQFASQELAEK.A	52
K.FMSVQRPGPYDRPGTAR.R	9
K.ATENDIYNFFSPLNPVR.V	23
R.VTGEADVEFATHEEAVAAMSK.D + Oxidation (M)	72
R.YGDSEFTVQSTTGHCVHMR.G	57

Spot 12

HCC1_HUMAN Score: 165 Queries matched: 4

R.FGISSVPTK.G	68
R.FGLNVSSISR.K	60
R.FNVPVSLESK.K	48
R.FGIVTSSAGTGTTEDTEAK.K	66

Spot 13

TCPE_HUMAN Score: 808 Queries matched: 39

R.AVTIFIR.G	36
K.LMVELSK.S + Oxidation (M)	38
R.LMGLEALK.S + Oxidation (M)	30
R.FSELTAEK.L	21
K.MLVIEQCK.N	48
K.ISDSVLVDIK.D	81
R.IADGYEQAAR.V	47
R.RDVDFELIK.V	46
K.FEEMIQQIK.E	45
K.LDVTSVEDYK.A	75
R.SLHDALCVIR.N	9
K.QQHVIETLIGK.K	48
K.CPTLEQYAMR.A + Oxidation (M)	64
K.QQISLATQMVR.M + Oxidation (M)	48
K.RSLHDALCVIR.N	34
R.DVDFELIKVEGK.V	61

K.QQHVIETLIGKK.Q	56
K.KQQISLATQMVR.M	73
K.HKLDVTSVEDYK.A	81
K.EKFEEMIQQIK.E + Oxidation (M)	56
K.EMNPALGIDCLHK.G	51
K.IAILTCPFEPPKPK.T	67
K.LGFAGLVQEISFGTTK.D	52
K.GVIVDKDFSHPQMPK.K	55
R.WVGGPEIELIAIATGGR.I	41
K.GTNDMKQQHVIETLIGK.K + Oxidation (M)	41
K.ISDSVLVDIKDTEPLIQTAK.T	41
R.VVYGGGAAEISCALAVSQEADK.C	31

Spot 14

HSP7C_HUMAN Score: 833 Queries matched: 35

K.FELTGIPPAPR.G	37
K.DAGTIAGLNVLR.I	33
R.MVNHFIAEFK.R + Oxidation (M)	46
K.MKEIAEAYLGK.T	68
R.FEELNADLFR.G	70
K.CNEIINWLDK.N	63
K.NSLESYAFNMK.A + Oxidation (M)	50
R.MVNHFIAEFKR.K + Oxidation (M)	32
R.RFDDAVVQSDMK.H	30
K.ELEKVCNPIITK.L	27
R.ARFEELNADLFR.G	31
K.SQIHDIVLVGGSTR.I	65
R.TTPSYVAFTDTER.L	66
R.QATKDAGTIAGLNVLR.I	35
K.SFYPEEVSSMVLTK.M + Oxidation (M)	48
R.IINEPTAAAIAYGLDK.K	79
K.NQVAMNPTNTVFDAK.R + Oxidation (M)	80
K.STAGDTHLGGEDFDNR.M	24
R.IINEPTAAAIAYGLDKK.V	76
K.NQVAMNPTNTVFDAKR.L	67
K.LDKSQIHDIVLVGGSTR.I	47

Spot 15

PDIA3_HUMAN Score: 325 Queries matched: 16

K.YGVSGYPTLK.I	58
K.FVMQEEFSR.D	48
R.GFPTIYFSPANK.K	54
R.FLQDYFDGNLK.R	40
R.ELSDFISYLQR.E	39
R.GFPTIYFSPANKK.L	40
R.FLQDYFDGNLKR.Y	34
K.DLLIAYYDVDYEK.N	23
K.IFRDGEEAGAYDGPR.T	46
K.MDATANDVPSPYEVR.G + Oxidation (M)	51
R.YLKSEPIPESNDGPVK.V	17

Spot 16

CNN3_HUMAN Score: 313 Queries matched: 17

K.GFHTTIDIGVK.Y	39
K.DGIILCELINK.L	52

K.TKGFHTTIDIGVK.Y	61
K.LTLQPVDNSTISLQMGTNK.V	110
K.MQTDKPFDQTTISLQMGTNK.G + Oxidation (M)	70
K.KVNESSLNWPQLENIGNFIK.A	8

TBAK_HUMAN Score: 90 Queries matched: 3

R.AVFVDLEPTVIDEVR.T	85
R.IHFPLATYAPVISAEK.A	4
K.TIGGGDDSFNTFFSETGAGK.H	28

Spot 17

TPM3_HUMAN Score: 380 Queries matched: 23

K.MELQEIQLK.E	48
K.LVIIEGDLER.T	71
R.IQLVEEELDR.A	39
R.KLVIIEGDLER.T	64
R.RIQLVEEELDR.A	87
R.LATALQKLEEAEK.A	96
R.IQLVEEELDRAQER.L	29

TPM1_HUMAN Score: 245 Queries matched: 16

K.MEIQEIQLK.E	*48*
R.IQLVEEELDR.A	*39*
R.RIQLVEEELDR.A	*87*
R.LATALQKLEEAEK.A	*96*
R.IQLVEEELDRAQER.L	*29*

Spot 18

ERP29_HUMAN Score: 155 Queries matched: 8

K.WAEQYLK.I	34
K.SLNILTAFQK.K	40
K.GALPLDTVTFYK.V	44
R.DGDFENPVPYTGAVK.V	43
K.ILDQGEDFPASEMTR.I + Oxidation (M)	50

Spot 20

HNRH1_HUMAN Score: 208 Queries matched: 8

K.SNNVEMDWVLK.H	47
R.GLPWSCSADEVQR.F	85
R.DLNYCFSGMSDHR.Y	19
R.STGEAFVQFASQEIAEK.A	52
R.ATENDIYNFFSPLNPVR.V	45
R.EGRPSGEAFVELESEDEVK.L	48
R.VTGEADVEFATHEDAVAAMSK.D + Oxidation (M)	11

Spot 22

HNRPK_HUMAN Score: 382 Queries matched: 26

R.NLPLPPPPPPR.G	49
K.IILDLISESPIK.G	94
R.LLIHQSLAGGIIGVK.G	56
K.IILDLISESPIKGR.A	45
R.TDYNASVSVPDSSGPER.I	58
R.ILSISADIETIGEILKK.I	15

R.GSYGDLGGPIITTQVTIPK.D	19
R.HESGASIKIDEPLEGSEDR.I	68
R.IITITGTQDQIQNAQYLLQNSVK.Q	13

Spot 23

G3BP1_HUMAN Score: 174 Queries matched: 9

R.TFSWASVTSK.N	53
K.FYVHNDIFR.Y	38
R.FMQTFVLAPEGSVANK.F	67
K.NLPPSGAVPVTGIPPHVVK.V	28
K.LPNFGFVVFDDSEPVQK.V	8

Spot 24

TERA_HUMAN Score: 741 Queries matched: 51

K.DVDLEFLAK.M	24
K.MDELQLFR.G + Oxidation (M)	53
R.LEILQIHTK.N	60
R.GILLYGPPGTGK.T	56
R.EVDIGIPDATGR.L	63
K.GVLFYGPPGCGK.T	56
R.WALSQSNPSALR.E	71
R.IVSQLLTLMDGLK.Q + Oxidation (M)	67
R.LGDVISIQPCPDVK.Y	74
R.LDQLIYIPLPDEK.S	37
K.AIANECQANFISIK.G	101
R.KYEMFAQTLQQSR.G + Oxidation (M)	76
R.VINQILTEMDGMSTK.K + Oxidation (M)	14
K.EMVELPLRHPALFK.A + Oxidation (M)	19
R.IVSQLLTLMDGLKQR.A + Oxidation (M)	53
R.VRLGDVISIQPCPDVK.Y	52
K.NAPAIIFIDELDAIAPK.R	35
R.ELQELVQYPVEHPDK.F	14
R.EAVCIVLSDDTCSDEK.I	34
R.QAAPCVLFFDELDSIAK.A	29
K.GPELLTMWFGESEANVR.E + Oxidation (M)	53
K.NAPAIIFIDELDAIAPKR.E	24
R.EAVCIVLSDDTCSDEKIR.M	32
R.AHVIVMAATNRPNSIDPALR.R + Oxidation (M)	14
R.QTNPSAMEVEEDDPVPEIRR.D	28
R.EVDIGIPDATGRLEILQIHTK.N	35
R.ERQTNPSAMEVEEDDPVPEIR.R + Oxidation (M)	41
R.ETVVEVPQVTWEDIGGLEDVKR.E	21
K.NVFIIGATNRPDIIDPAILRPGR.L	11

SRC8_HUMAN Score: 108 Queries matched: 3

R.YGLFPANYVELR.Q	48
R.YGLFPANYVELRQ.-	71
R.GPVSGTEPEPVYSMEAADYR.E + Oxidation (M)	29

SAE2_HUMAN Score: 65 Queries matched: 5

K.ESVLQFYPK.A	53
K.STGYDPVKLFTK.L	5
R.QFILVMNALDNR.A + Oxidation (M)	14
R.VLVVGAGGIGCELLK.N	32

Spot 25

CH60_HUMAN Score: 1009 Queries matched: 64

R.TLKIPAMTIAK.N	44
K.NAGVEGSLIVEK.I	21
R.TVIIEQSWGSPK.V	77
R.GYISPYFINTSK.G	45
K.TLNDELEIIEGMK.F	47
R.GVMLAVDAVIAELKK.Q + Oxidation (M)	78
K.VGEVIVTKDDAMLLK.G	65
R.AAVEEGIVLGGGCALLR.C	69
K.CEFQDAYVLLSEKK.I	60
R.CIPALDSLTPANEDQK.I	64
K.FDRGYISPYFINTSK.G	28
K.DGKTLNDELEIIEGMK.F + Oxidation (M)	2
K.ISSIQSIVPALEIANAHR.K	60
K.TLNDELEIIEGMKFDR.G + Oxidation (M)	61
K.KISSIQSIVPALEIANAHR.K	75
R.ALMLQGVDLLADAVAVTMGPK.G + 2 Oxidation (M)	78
R.IQEIIEQLDVTTSEYEKEK.L	53
K.IMQSSSEVGYDAMAGDFVNMVEK.G + 3 Oxidation (M)	62

Spot 26

RSSA_HUMAN Score: 220 Queries matched: 7

K.SDGIYIINLK.R	47
R.KSDGIYIINLK.R	68
K.SDGUYIINLKR.T	47
R.YVDIAIPCNNK.G	49
R.FTPGTFTNQIQAAFR.E	71
R.AIVAIENPADVSVISSR.N	71

Spot 27

ERP29_HUMAN Score: 130 Queries matched: 6

K.SLNILTAFQK.K	62
K.GALPLDTVTFYK.V	39
R.DGDFENPVPYTGAVK.V	45
K.ILDQGENFPASEMTR.I + Oxidation (M)	33

Spot 28

PRP19_HUMAN Score: 140 Queries matched: 9

K.SSEQILATLK.G	30
K.TLQLDNNFEVK.S	36
K.ILTGGADKNVVVFDK.S	29
K.TVPEELVKPEELSK.Y	68
R.IWSVPNASCVQVVR.A	64
K.VAHPIRPKPPSATSIPAILK.A	19
K.VTSVVFHPSQDLVFSASPDATIR.I	27
K.KVTSVVFHPSQDLVFSASPDATIR.I	14

Spot 29

TCPG_HUMAN Score: 653 Queries matched: 40

R.AVAQALEVIPR.T	70
K.TAVETAVLLLR.I	60

K.ALDDMISTLKK.I	27
K.ELGIWEPLAVK.L	53
R.IVLLDSSLEYK.K	82
K.AMTGVEQWPYR.A + Oxidation (M)	47
K.GISDLAQHYLMR.A + Oxidation (M)	48
K.IPGGIIEDSCVLR.G	85
R.WSSLACNIALDAVK.M	95
R.VEKIPGGIIEDSCVLR.G	36
K.IGDEYFTFITDCKDPK.A	2
K.MLLDPMGGIVMTNDGNAILR.E + 3 Oxidation (M)	21
R.IVSRPEELREDDVGTGAGLLEIK.K	26
R.NVLLDPQLVPGGGASEMAVAHALTEK.S + Oxidation (M)	11

COPD_HUMAN Score: 118 Queries matched: 8

R.IEGLLAAFPK.L	19
K.LYMVLITTK.N	38
K.LFTAESLIGLK.N	49
K.SFPVNSDVGVLK.W	41
R.TRIEGLLAAFPK.L	44
K.NSNILEDLETLR.L	51
R.DGGLQNMELHGMIMLR.I + 3 Oxidation (M)	12

Spot 30

RUVB1_HUMAN Score: 317 Queries matched: 17

K.TISHVIIGLK.T	73
K.TEVLMENFR.R	27
R.EACGVIVELIK.S	46
K.LDPSIFESLQK.E	62
K.TALALAIAQELGSK.V	39
R.YSVQLLTPANLLAK.I	51
R.ALESSIAPIVIFASNR.G	74
R.VEAGDVIYIEANSGAVKR.Q	43
R.GTEDITSPHGIPLDLLDR.V	38
K.VPFCPMVGSEVYSTEIK.K	42
K.VPFCPMVGSEVYSTEIKK.T + Oxidation (M)	10
K.EVYEGEVTELTPCETENPMGGYGK.T + Oxidation (M)	15

SEPT6_HUMAN Score: 35 Queries matched: 2

K.VNIIPIIAK.A	30
K.STLMDTLFNTK.F + Oxidation (M)	25

SEPT7_HUMAN Score: 30 Queries matched: 1

K.VNIIPIIAK.A	*30*

Spot 31

TCPQ_HUMAN Score: 362 Queries matched: 17

K.LATNAAVTVLR.V	39
R.DIDEVSSLLR.T	22
K.EDGAISTIVLR.G	68

K.KFAEAFEAIPR.A	64
K.HFSGLEEAVYR.N	73
R.LVPGGGATEIELAK.Q	68
R.GSTDNLMDDIER.A	17
K.NVGLDIEAEVPAVK.D	68
K.DMLEAGILDTYLGK.Y + Oxidation (M)	67
K.AHEILPNLVCCSAK.N	29
R.KAHEILPNLVCCSAK.N	22
K.ILGSGISSSSVLHGMVFK.K + Oxidation (M)	50
K.IAVYSCPFDGMITETK.G + Oxidation (M)	47
K.QITSYGETCPGLEQYAIKK.F	7
K.TAEELMNFSKGEENLMDAQVK.A + 2 Oxidation (M)	16

APPENDIX IV – Identified peptides and corresponding Mascot scores for Chapter IV

SwissProt 55.6 (score >29, p<0.05)

Spot 509

HS90B_HUMAN Score: 106 Queries matched: 8

K.LGIHEDSTNR.R	22
K.YIDQEELNK.T	22
R.ELISNASDALDK.I	45
R.DNSTMGYMMAK.K + 3 Oxidation (M)	18
R.TLTLVDTGIGMTK.A + Oxidation (M)	35
R.GVVDSEDLPLNISR.E	31
K.HLEINPDHPIVETLR.Q	59
K.HSQFIGYPITLYLEK.E	8

Spot 561

HS90B_HUMAN Score: 290 Queries matched: 10

K.FYEAFSK.N	16
R.APFDLFENK.K	45
K.IDIIPNPQER.T	7
K.ADLINNLGTIAK.S	15
R.ELISNASDALDK.I	83
R.DNSTMGYMMAK.K + 3 Oxidation (M)	50
K.EDQTEYLEER.R	90
R.TLTLVDTGIGMTK.A + Oxidation (M)	65
R.GVVDSEDLPLNISR.E	62
R.NPDDITQEEYGEFYK.S	4

HS90A_HUMAN Score: 245 Queries matched: 8

R.TDTGEPMGR.G	44
R.APFDLFENR.K	32
K.LGIHEDSQNR.K	41
R.DNSTMGYMAAK.K + 2 Oxidation (M)	56
K.ADLINNLGTIAK.S	15
K.EDQTEYLEER.R	90
R.TLTIVDTGIGMTK.A + Oxidation (M)	65
R.GVVDSEDLPLNISR.E	62

Spot 576

TERA_HUMAN Score: 138 Queries matched: 7

R.SVSDNDIR.K	28
R.KGDIFLVR.G	7
K.EMVELPLR.H + Oxidation (M)	7
K.GDDLSTAILK.Q	10
K.MDELQLFR.G + Oxidation (M)	44
K.LAGESESNLR.K	88
R.GGNIGDGGGAADR.V	62

Spot 795

PDIA4_HUMAN Score: 63 Queries matched: 2

K.IDATSASVLASR.F	36
K.MDATANDVPSDR.Y + Oxidation (M)	48

Spot 815

GRP78_HUMAN Score: 482 Queries matched: 15

K.VLEDSDLK.K	44
K.VYEGERPLTK.D	30
R.VEIIANDQGNR.I	70
K.DAGTIAGLNVMR.I + Oxidation (M)	46
K.MKETAEAYLGK.K + Oxidation (M)	43
K.FEELNMDLFR.S + Oxidation (M)	81
K.ELEEIVQPIISK.L	57
K.SDIDEIVLVGGSTR.I	54
K.TFAPEEISAMVLTK.M + Oxidation (M)	51
R.IINEPTAAAIAYGLDK.R	47
K.NQLTSNPENTVFDAK.R	42
K.SQIFSTASDNQPTVTIK.V	13
K.VTHAVVTVPAYFNDAQR.Q	55
K.DNHLLGTFDLTGIPPAPR.G	14
R.IEIESFYEGEDFSETLTR.A	87

Spot 837

BIN1_HUMAN Score: 106 Queries matched: 3

R.GVFPENFTER.V	26
R.HHYESLQTAK.K	23
K.LNQNLNDVLVGLEK.Q	106

Spot 884

GRP75_HUMAN Score: 117 Queries matched: 7

K.VLENAEGAR.T	62
R.YDDPEVQK.D	3
K.DSETGENIR.Q	39
R.RYDDPEVQK.D	63
K.DQLPADECNK.L	42
K.LLGQFTLIGIPPAPR.G	7
K.MEEFKDQLPADECNK.L + Oxidation (M)	7

Spot 935

EIF3D_HUMAN Score: 58 Queries matched: 1

K.LGDDIDLIVR.C	58

FBP1L_HUMAN Score: 37 Queries matched: 1

K.LAETMNNIDR.L + Oxidation (M)	37

SDC10_HUMAN Score: 32 Queries matched: 2

K.VTGDTVYNMLR.L + Oxidation (M)	36
R.SEEEEAPPDGAVAEYR.R	20

Spot 1060

HNRPK_HUMAN Score: 55 Queries matched: 4

K.GSDFDCELR.L	33
R.NLPLPPPPPPR.G	39
K.RPAEDMEEEQAFKR.S + Oxidation (M)	31
-.METEQPEETFPNTETNGEFGKRPAEDMEEEQAFK.R + 2 Oxidation (M)	10

Spot 1078

PDIA1_HUMAN Score: 221 Queries matched: 13

K.ALAPEYAK.A	36
K.FFPASADR.T	28
R.ITEFCHR.F	51
K.QLAPIWDK.L	20
K.KEECPAVR.L	13
R.NNFEGEVTK.E	34
R.EADDIVNWLK.K	70
K.NFEDVAFDEK.K	52
K.MDSTANEVEAVK.V + Oxidation (M)	108
K.YKPESEELTAER.I	27
K.LGETYKDHENIVIAK.M	21
K.VDATEESDLAQQYGVR.G	16
K.HNQLPLVIEFTEQTAPK.I	28

Spot 1115

SEP11_HUMAN Score: 49 Queries matched: 2

K.ELEEEVNNFQK.K	49
K.AAAQLLQSQAQQSGAQQTK.K	2

Spot 1171

TE2IP_HUMAN Score: 58 Queries matched: 3

K.MLVEATR.E + Oxidation (M)	30
K.FGAQNVAR.R	56
R.LELEAYR.L	15

Spot 1605

TPM4_HUMAN Score: 170 Queries matched: 7

K.TIDDLEEK.L	35
K.AEGDVAALNR.R	69
K.CGDLEEELK.N	24
K.MEIQEMQLK.E + 2 Oxidation (M)	26
R.IQLVEEELDR.A	77
R.KLVILEGELER.A	75
R.KIQALQQQADEAEDR.A	29

Spot 1612

TPM1_HUMAN Score: 154 Queries matched: 5

K.MEIQEIQLK.E + Oxidation (M)	35
K.LVIIESDLER.A	67
K.EDRYEEEIK.V	17
R.IQLVEEELDR.A	75
R.KLVIIESDLER.A	65

MKL2_HUMAN Score: 32 Queries matched: 1

K.QIEELKR.K	32

Spot 1650

GDIR1_HUMAN Score: 111 Queries matched: 5

K.YIQHTYR.K	43
K.SIQEIQELDK.D	24
K.TDYMVGSYGPR.A + Oxidation (M)	75
K.IDKTDYMVGSYGPR.A + Oxidation (M)	18
R.AEEYEFLTPVEEAPK.G	23

Spot 1728

RBM8A_HUMAN Score: 181 Queries matched: 6

R.GFGSEEGSR.A	53
K.FAEYGEIK.N	41
K.NIHLNLDR.R	22
K.GYTLVEYETYK.E	58
R.EDYDSVEQDGDEPGPQR.S	29
R.MREDYDSVEQDGDEPGPQR.S + Oxidation (M)	57

Spot 1729

RBM8A_HUMAN Score: 79 Queries matched: 5

R.GFGSEEGSR.A	61
K.FAEYGEIK.N	24
K.GYTLVEYETYK.E	30
R.EDYDSVEQDGDEPGPQR.S	16
R.MREDYDSVEQDGDEPGPQR.S	36

Spot 1753

BT3L4_HUMAN Score: 86 Queries matched: 2

R.KLAEQFPR.Q	39
K.DDGTVIHFNNPK.V	46

Spot 1754

COF1_HUMAN Score: 123 Queries matched: 4

R.YALYDATYETK.E	56
K.LGGSAVISLEGKPL.-	52

K.HELQANCYEEVKDR.C	67
K.EILVGDVGQTVDDPYATFVK.M	5

Spot 1758

STMN1_HUMAN Score: 105 Queries matched: 4

K.DLSLEEIQK.K	39
K.AIEENNNFSK.M	56
K.ESKDPADETEAD.-	19
R.ASGQAFELILSPR.S	71

Spot 1761

STMN1_HUMAN Score: 237 Queries matched: 8

K.SHEAEVLK.Q	58
K.KLEAAEER.R	55
K.DKHIEEVR.K	32
K.DLSLEEIQK.K	38
K.AIEENNNFSK.M	17
K.ESKDPADETEAD.-	41
K.ESVPEFPLSPPK.K	48
R.ASGQAFELILSPR.S	94

Peptide Mass fingerprint

Spot 1193

IF2_HUMAN Score: 59.57

871.49	QIENVLR
891.545	LLHRQPK
1027.586	QIENVLRR
1064.569	TGFQAVTGKR
1200.65	FVMKPPQVVR
1216.682	FVMKPPQVVR
1225.527	EYVTCHTCR
1273.653	SPDTILQKDTR
1315.622	DYTYEELLNR
1320.594	DLEADEEDTRK
1331.639	TSFVNFTDICK
1344.763	KFVMKPPQVVR
1364.662	IFDIDEAEEGVK
1459.723	KTSFVNFTDICK
1556.722	LYFLQCETCHSR
1613.726	LYFLQCETCHSR
1629.749	YIKEYVTCHTCR
1720.871	IFDIDEAEEGVKDLK
1756.781	DASDDLDDLNFFNQK
1884.875	KDASDDLDDLNFFNQK
2631.234	IESDVQEPTEPEDDLDIMLGNKK
2859.339	DLKIESDVQEPTEPEDDLDIMLGNK

Spot 1458

CNN3_HUMAN	Score: 52	Queries matched: 6
939.535	K.GMSVYGLGR.Q	
1107.634	K.GPSYGLSAECK.N	
1187.662	K.GFHTTIDIGVK.Y	
1287.68	K.DGIILCELINK.L	
1375.692	R.HLYDPKMQTDK.P	
2076.96	K.LTLQPVDNSTISLQMGTNK.V + Oxidation (M)	

APPENDIX V – Identified peptides and corresponding Mascot scores for Chapter V

SwissProt 54.7 (score >29, p<0.05)

Spot 531

GRP78_HUMAN Score: 354 Queries matched: 10

K.DAGTIAGLNVMR.I	10
R.NELESYAYSLK.N	53
K.ELEEIVQPIISK.L	33
K.TFAPEEISAMVLTK.M + Oxidation (M)	46
R.ITPSYVAFTPEGER.L	60
K.KSDIDEIVLVGGSTR.I	71
K.NQLTSNPENTVFDAK.R	48
R.IINEPTAAAIAYGLDKR.E	74
K.SQIFSTASDNQPTVTIK.V	64
K.VTHAVVTVPAYFNDAQR.Q	80

Spot 536

GRP78_HUMAN Score: 1043 Queries matched: 21

K.DAGTIAGLNVMR.I	62
K.FEELNMDLFR.S	79
R.NELESYAYSLK.N	56
K.ELEEIVQPIISK.L	54
R.TWNDPSVQQDIK.F	37
K.SDIDEIVLVGGSTR.I	67
R.AKFEELNMDLFR.S + Oxidation (M)	67
K.TFAPEEISAMVLTK.M	81
R.ITPSYVAFTPEGER.L	69
K.KSDIDEIVLVGGSTR.I	51
R.IINEPTAAAIAYGLDK.R	91
K.NQLTSNPENTVFDAK.R	87
R.IINEPTAAAIAYGLDKR.E	86
K.SQIFSTASDNQPTVTIK.V	78
K.VTHAVVTVPAYFNDAQR.Q	67
K.DNHLLGTFDLTGIPPAPR.G	81
K.KSQIFSTASDNQPTVTIK.V	68
K.IEWLESHQDADIEDFK.A	63
K.KVTHAVVTVPAYFNDAQR.Q	48
R.IEIESFYEGEDFSETLTR.A	98
K.LYGSAGPPPTGEEDTAEKDEL.-	37

Spot 853

TBB2C_HUMAN Score: 718 Queries matched: 11

R.YLTVAAVFR.G	*42*
K.LAVNMVPFPR.L + Oxidation (M)	*70*
R.ISEQFTAMFR.R	*76*
R.KLAVNMVPFPR.L	*65*
R.AVLVDLEPGTMDSVR.S	*76*
R.LHFFMPGFAPLTSR.G	*68*
R.ALTVPELTQQMFDAK.N	*68*
K.NSSYFVEWIPNNVK.T	*72*

K.MSATFIGNSTAIQELFK.R + Oxidation (M)	*74*
K.GHYTEGAELVDSVLDVVR.K	*44*
K.LTTPTYGDLNHLVSATMSGVTTCLR.F	*81*

TBB4_HUMAN Score: 646 Queries matched: 10

R.YLTVAAVFR.G	*42*
K.LAVNMVPFPR.L + Oxidation (M)	*70*
R.ISEQFTAMFR.R	*76*
R.KLAVNMVPFPR.L	*65*
R.AVLVDLEPGTMDSVR.S	*76*
R.LHFFMPGFAPLTSR.G	*68*
K.NSSYFVEWIPNNVK.T	*68*
K.NSSYFVEWIPNNVK.T	*72*
K.MAATFIGNSTAIQELFK.R + Oxidation (M)	*34*
K.LTTPTYGDLNHLVSATMSGVTTCLR.F	*81*

TBB2A_HUMAN Score: 627 Queries matched: 11

R.YLTVAAIFR.G	**40**
K.LAVNMVPFPR.L + Oxidation (M)	*70*
R.ISEQFTAMFR.R	*76*
R.KLAVNMVPFPR.L	*65*
R.LHFFMPGFAPLTSR.G	*68*
R.AILVDLEPGTMDSVR.S + Oxidation (M)	*56*
K.NSSYFVEWIPNNVK.T	*72*
R.ALTVPELTQQMFDSK.N	*38*
K.MSATFIGNSTAIQELFK.R + Oxidation (M)	*74*
K.GHYTEGAELVDSVLDVVR.K	*44*
K.LTTPTYGDLNHLVSATMSGVTTCLR.F	*81*

TBB5_HUMAN Score: 578 Queries matched: 10

R.YLTVAAVFR.G	**42**
K.LAVNMVPFPR.L + Oxidation (M)	*70*
R.ISEQFTAMFR.R	*76*
R.KLAVNMVPFPR.L	*65*
R.LHFFMPGFAPLTSR.G	*68*
R.AILVDLEPGTMDSVR.S + Oxidation (M)	*56*
R.ALTVPELTQQVFDAK.N	**36**
K.NSSYFVEWIPNNVK.T	*72*
K.GHYTEGAELVDSVLDVVR.K	*44*
K.LTTPTYGDLNHLVSATMSGVTTCLR.F	*81*

TBB3_HUMAN Score: 488 Queries matched: 8

K.LAVNMVPFPR.L + Oxidation (M)	*70*
R.ISEQFTAMFR.R	*76*
R.KLAVNMVPFPR.L	*65*
R.AILVDLEPGTMDSVR.S + Oxidation (M)	*56*
R.ALTVPELTQQMFDAK.N	*68*
K.NSSYFVEWIPNNVK.T	*72*
K.MSSTFIGNSTAIQELFK.R	*61*
K.GHYTEGAELVDSVLDVVR.K	*44*

TBB6_HUMAN Score: 355 Queries matched: 5

K.LAVNMVPFPR.L + Oxidation (M)	*70*
R.KLAVNMVPFPR.L	*65*
R.LHFFMPGFAPLTSR.G	*68*
K.NSSYFVEWIPNNVK.T	*72*
K.MASTFIGNSTAIQELFK.R + Oxidation (M)	*68*

TBB1_HUMAN Score: 174 Queries matched: 3

K.LAVNMVPFPR.L + Oxidation (M)	*70*
R.KLAVNMVPFPR.L	*65*
R.IMNSFSVMPSPK.V	**13**

TBB1A_HUMAN Score: 44 Queries matched: 2

K.EIIDLVLDR.I	**37**
R.AVFVDLEPTVIDEVR.T	**31**

Spot 860

TBB2C_HUMAN Score: 819 Queries matched: 13

R.YLTVAAVFR.G	43
K.LAVNMVPFPR.L + Oxidation (M)	62
R.ISEQFTAMFR.R	90
R.KLAVNMVPFPR.L	78
R.IMNTFSVVPSPK.V + Oxidation (M)	68
K.RISEQFTAMFR.R + Oxidation (M)	37
R.AVLVDLEPGTMDSVR.S	79
R.LHFFMPGFAPLTSR.G	71
R.ALTVPELTQQMFDAK.N	74
K.MSATFIGNSTAIQELFK.R + Oxidation (M)	96
K.GHYTEGAELVDSVLDVVR.K	100
K.LTTPTYGDLNHLVSATMSGVTTCLR.F	79
R.SGPFGQIFRPDNFVFGQSGAGNNWAK.G	54

TBB5_HUMAN Score: 808 Queries matched: 13

R.YLTVAAVFR.G	*43*
K.LAVNMVPFPR.L + Oxidation (M)	*62*
R.ISEQFTAMFR.R	*90*
R.KLAVNMVPFPR.L	*78*
R.IMNTFSVVPSPK.V + Oxidation (M)	*68*
K.RISEQFTAMFR.R + Oxidation (M)	*37*
R.AILVDLEPGTMDSVR.S	*74*
R.LHFFMPGFAPLTSR.G	*71*
R.ALTVPELTQQVFDAK.N	**72**
K.MAVTFIGNSTAIQELFK.R + Oxidation (M)	**85**
K.GHYTEGAELVDSVLDVVR.K	*100*
K.LTTPTYGDLNHLVSATMSGVTTCLR.F	*79*
R.SGPFGQIFRPDNFVFGQSGAGNNWAK.G	*54*

TBB2A_HUMAN Score: 699 Queries matched: 11

K.LAVNMVPFPR.L + Oxidation (M) *62*
R.ISEQFTAMFR.R *90*
R.KLAVNMVPFPR.L *78*
K.RISEQFTAMFR.R + Oxidation (M) *37*
R.AILVDLEPGTMDSVR.S *74*
R.LHFFMPGFAPLTSR.G *71*
R.ALTVPELTQQMFDSK.N *46*
K.MSATFIGNSTAIQELFK.R + Oxidation (M) *96*
K.GHYTEGAELVDSVLDVVR.K *100*
K.LTTPTYGDLNHLVSATMSGVTTCLR.F *79*
R.SGPFGQIFRPDNFVFGQSGAGNNWAK.G *54*

TBB4_HUMAN Score: 677 Queries matched: 12

R.YLTVAAVFR.G *43*
K.LAVNMVPFPR.L + Oxidation (M) *62*
R.ISEQFTAMFR.R *90*
R.KLAVNMVPFPR.L *78*
R.IMNTFSVVPSPK.V + Oxidation (M) *68*
K.RISEQFTAMFR.R + Oxidation (M) *37*
R.AVLVDLEPGTMDSVR.S *79*
R.LHFFMPGFAPLTSR.G *71*
R.ALTVPELTQQMFDAK.N *74*
K.MAATFIGNSTAIQELFK.R + Oxidation (M) *53*
K.LTTPTYGDLNHLVSATMSGVTTCLR.F *79*
R.SGPFGQIFRPDNFVFGQSGAGNNWAK.G *54*

TBB3_HUMAN Score: 546 Queries matched: 10

R.YLTVATVFR.G *21*
K.LAVNMVPFPR.L + Oxidation (M) *62*
R.ISEQFTAMFR.R *90*
R.KLAVNMVPFPR.L *78*
R.IMNTFSVVPSPK.V + Oxidation (M) *68*
K.RISEQFTAMFR.R + Oxidation (M) *37*
R.AILVDLEPGTMDSVR.S *74*
R.ALTVPELTQQMFDAK.N *74*
K.MSSTFIGNSTAIQELFK.R + Oxidation (M) *84*
K.GHYTEGAELVDSVLDVVR.K *100*

TBB6_HUMAN Score: 405 Queries matched: 8

R.YLTVATVFR.G *21*
K.LAVNMVPFPR.L + Oxidation (M) *62*
R.ISEQFSAMFR.R + Oxidation (M) **35**
R.KLAVNMVPFPR.L *78*
R.AALVDLEPGTMDSVR.S **34**
R.LHFFMPGFAPLTSR.G *71*
R.ALTVPELTQQMFDAR.N **63**
K.MASTFIGNSTAIQELFK.R + Oxidation (M) *91*

Spot 1232

PCBP1_HUMAN Score: 166 Queries matched: 4

R.LVVPATQCGSLIGK.G 39

R.AITIAGVPQSVTECVK.Q	36
R.ESTGAQVQVAGDMLPNSTER.A	71
R.QVTITGSAASISLAQYLINAR.L	84

Spot 1333

CNN3_HUMAN Score: 271 Queries matched: 8

K.GFHTTIDIGVK.Y	50
K.DGIILCELINK.L	53
R.DYQYSDQGIDY.-	2
K.LTLQPVDNSTISLQMGTNK.V + Oxidation (M)	71
K.VNESSLNWPQLENIGNFIK.A	35
R.NWIEEVTGMSIGPNFQLGLK.D + Oxidation (M)	114
K.MQTDKPFDQTTISLQMGTNK.G + Oxidation (M)	37
K.KVNESSLNWPQLENIGNFIK.A	51

Spot 1339

CNN3_HUMAN Score: 114 Queries matched: 5

K.GFHTTIDIGVK.Y	49
K.DGIILCELINK.L	39
R.DYQYSDQGIDY.-	15
K.LTLQPVDNSTISLQMGTNK.V + Oxidation (M)	75
K.VNESSLNWPQLENIGNFIK.A	27

Spot 1473

EF1D_HUMAN Score: 171 Queries matched: 7

K.IWFDKFK.Y	9
R.GVVQELQQAISK.L	36
K.LQIQCVVEDDK.V	28
K.VGTDLLEEEITK.F	53
R.IASLEVENQSLR.G	78
R.SIQLDGLVWGASK.L	79
K.FEEHVQSVDIAAFNK.I	24

Spot 1537

TPM1_HUMAN Score: 99 Queries matched: 5

K.MEIQEIQLK.E	*35*
R.IQLVEEELDR.A	*14*
R.KLVIIESDLER.A	**73**
R.RIQLVEEELDR.A	*32*
K.GTEDELDKYSEALK.D	*43*

TPM3_HUMAN Score: 53 Queries matched: 4

K.MEIQEIQLK.E	*35*
R.IQLVEEELDR.A	*14*
R.RIQLVEEELDR.A	*32*
K.GTEDELDKYSEALK.D	*43*

Spot 1583

CHM4A_HUMAN Score: 149 Queries matched: 3

R.EAIENATTNAEVLR.T	95
K.LPSVPSTHLPAGPAPK.V	53

R.FEQQLAQTDGTLSTLEFQR.E 42

Spot 1609

TPM4_HUMAN Score: 209 Queries matched: 8

K.MEIQEMQLK.E	*36*
K.LVILEGELER.A	*75*
R.IQLVEEELDR.A	*70*
R.KLVILEGELER.A	*63*
K.YEEEIKLLSDK.L	**1**
R.RIQLVEEELDR.A	*65*
R.IQLVEEELDRAQER.L	*33*
K.CGDLEEELKNVTNNLK.S	**16**

TPM2_HUMAN Score: 209 Queries matched: 6

K.MEIQEMQLK.E	*36*
K.LVILEGELER.A	*75*
R.IQLVEEELDR.A	*70*
R.KLVILEGELER.A	*63*
R.RIQLVEEELDR.A	*65*
R.IQLVEEELDRAQER.L	*33*

TPM1_HUMAN Score: 116 Queries matched: 4

R.IQLVEEELDR.A	*70*
R.RIQLVEEELDR.A	*65*
K.MEIQEIQLKEAK.H	*13*
R.IQLVEEELDRAQER.L	*33*

TPM3_HUMAN Score: 116 Queries matched: 4

R.IQLVEEELDR.A	*70*
R.RIQLVEEELDR.A	*65*
K.MELQEIQLKEAK.H	*13*
R.IQLVEEELDRAQER.L	*33*

Spot 1610

TPM3_HUMAN Score: 318 Queries matched: 7

K.MELQEIQLK.E + Oxidation (M)	*53*
K.LVIIEGDLER.T	**58**
R.IQLVEEELDR.A	*70*
K.QLEDELAAMQK.K	**3**
R.KLVIIEGDLER.T	**76**
R.RIQLVEEELDR.A	*50*
R.IQLVEEELDRAQER.L	*42*

TPM1_HUMAN Score: 159 Queries matched: 5

R.AQKDEEK.M	**2**
K.MELQEIQLK.E + Oxidation (M)	*53*
R.IQLVEEELDR.A	*70*
R.RIQLVEEELDR.A	*50*
R.IQLVEEELDRAQER.L	*42*

TPM4_HUMAN Score: 120 Queries matched: 4

R.IQLVEEELDR.A *70*
K.YEEEIKLLSDK.L **8**
R.RIQLVEEELDR.A *50*
R.IQLVEEELDRAQER.L *42*

Spot 1885

DUT_HUMAN Score: 204 Queries matched: 4

R.GASTVGAAGWK.G 4
R.GNVGVVLFNFGK.E 85
K.TDIQIALPSGCYGR.V 43
R.IFYPEIEEVQALDDTER.G 124

Spot 1971

MGN_HUMAN Score: 125 Queries matched: 4

R.VFYYLVQDLK.C 57
K.EDDALWPPPDR.V 28
K.IGSLIDVNQSKDPEGLR.V 54
R.IIDDSEITKEDDALWPPPDR.V 46

RL22_HUMAN Score: 73 Queries matched: 1

K.ITVTSEVPFSK.R 73

H2B1A_HUMAN Score: 49 Queries matched: 1

R.LLLPGELAK.H 49

Spot 1992

PDCD5_HUMAN Score: 371 Queries matched: 5

R.LSNLALVKPEK.T 28
K.VSEQGLIEILK.K 64
K.AVENYLIQMAR.Y + Oxidation (M) 53
K.VSEQGLIEILKK.V 75
R.NSILAQVLDQSAR.A 89

H2B1A_HUMAN Score: 46 Queries matched: 1

R.LLLPGELAK.H 46

Spot 2031

MOFA1_HUMAN Score: 93 Queries matched: 1

K.TQVEASEESALNHLQNPGDAAEGR.A 93

TBA1B_HUMAN Score: 67 Queries matched: 2

R.SIQFVDWCPTGFK.V 56
K.VGINYQPPTVVPGGDLAK.V 3